



**INSA**



**SAPIENZA**  
UNIVERSITÀ DI ROMA

N°d'ordre NNT : TH1076

Ph.D. Thesis  
Jointly awarded by

**Institut National des Sciences Appliquées de Lyon**  
**membre de l'UNIVERSITE DE LYON**

**Ecole Doctorale N° 162**

**Mécanique, Energétique, Génie Civil, Acoustique (MEGA)**

Specialité: Génie Mécanique

**Sapienza Università di Roma**

**Dipartimento di Ingegneria Meccanica ed Aerospaziale (DIMA)**

Dottorato di Ricerca in Meccanica Teorica e Applicata

(XXXVI Ciclo)

Defended on February 19th, 2024, by

**Livia Felicetti**

---

# **Analysis and rendering of contact vibrational stimuli for tactile perception**

---

Ph.D. committee:

Bueno Marie-Ange  
Koç Ilker Murat  
Meziane Anissa  
Fregolent Annalisa  
Mouchnino Laurence  
Chatelet Eric  
Bou-Saïd Benyebka  
Massi Francesco  
Akay Adnan

Professeure des Universités  
Full Professor  
Professeure des Universités  
Full Professor  
Professeure des Universités  
Maître de Conférences HDR  
Professeur des Universités  
Full Professor  
Full Professor, Emeritus

Université de Haute-Alsace  
Istanbul Technical University  
Université de Bordeaux  
Sapienza Università di Roma  
Aix-Marseille Université  
INSA de Lyon  
INSA de Lyon  
Sapienza Università di Roma  
Carnegie Mellon University

Reviewer  
Reviewer  
President  
Examiner  
Examiner  
Examiner  
PhD Director  
PhD Director  
Invited



Référence : TH1076\_FELICETTI Livia

L'INSA Lyon a mis en place une procédure de contrôle systématique via un outil de détection de similitudes (logiciel Compilatio). Après le dépôt du manuscrit de thèse, celui-ci est analysé par l'outil. Pour tout taux de similarité supérieur à 10%, le manuscrit est vérifié par l'équipe de FEDORA. Il s'agit notamment d'exclure les auto-citations, à condition qu'elles soient correctement référencées avec citation expresse dans le manuscrit.

Par ce document, il est attesté que ce manuscrit, dans la forme communiquée par la personne doctorante à l'INSA Lyon, satisfait aux exigences de l'Établissement concernant le taux maximal de similitude admissible.

## Département FEDORA – INSA Lyon - Ecoles Doctorales

SIGLE	ECOLE DOCTORALE	NOM ET COORDONNEES DU RESPONSABLE
<b>CHIMIE</b>	<b>CHIMIE DE LYON</b> <a href="https://www.edchimie-lyon.fr">https://www.edchimie-lyon.fr</a> Sec. : Renée EL MELHEM Bât. Blaise PASCAL, 3e étage secretariat@edchimie-lyon.fr	<b>M. Stéphane DANIELE</b> C2P2-CPE LYON-UMR 5265 Bâtiment F308, BP 2077 43 Boulevard du 11 novembre 1918 69616 Villeurbanne <a href="mailto:directeur@edchimie-lyon.fr">directeur@edchimie-lyon.fr</a>
<b>E.E.A.</b>	<b>ÉLECTRONIQUE, ÉLECTROTECHNIQUE, AUTOMATIQUE</b> <a href="https://edeea.universite-lyon.fr">https://edeea.universite-lyon.fr</a> Sec. : Stéphanie CAUVIN Bâtiment Direction INSA Lyon Tél : 04.72.43.71.70 secretariat.edeea@insa-lyon.fr	<b>M. Philippe DELACHARTRE</b> INSA LYON Laboratoire CREATIS Bâtiment Blaise Pascal, 7 avenue Jean Capelle 69621 Villeurbanne CEDEX Tél : 04.72.43.88.63 <a href="mailto:philippe.delachartre@insa-lyon.fr">philippe.delachartre@insa-lyon.fr</a>
<b>E2M2</b>	<b>ÉVOLUTION, ÉCOSYSTÈME, MICROBIOLOGIE, MODÉLISATION</b> <a href="http://e2m2.universite-lyon.fr">http://e2m2.universite-lyon.fr</a> Sec. : Bénédicte LANZA Bât. Atrium, UCB Lyon 1 Tél : 04.72.44.83.62 secretariat.e2m2@univ-lyon1.fr	<b>Mme Sandrine CHARLES</b> Université Claude Bernard Lyon 1 UFR Biosciences Bâtiment Mendel 43, boulevard du 11 Novembre 1918 69622 Villeurbanne CEDEX <a href="mailto:sandrine.charles@univ-lyon1.fr">sandrine.charles@univ-lyon1.fr</a>
<b>EDISS</b>	<b>INTERDISCIPLINAIRE SCIENCES-SANTÉ</b> <a href="http://ediss.universite-lyon.fr">http://ediss.universite-lyon.fr</a> Sec. : Bénédicte LANZA Bât. Atrium, UCB Lyon 1 Tél : 04.72.44.83.62 secretariat.ediss@univ-lyon1.fr	<b>Mme Sylvie RICARD-BLUM</b> Institut de Chimie et Biochimie Moléculaires et Supramoléculaires (ICBMS) - UMR 5246 CNRS - Université Lyon 1 Bâtiment Raulin - 2ème étage Nord 43 Boulevard du 11 novembre 1918 69622 Villeurbanne Cedex Tél : +33(0)4 72 44 82 32 <a href="mailto:sylvie.ricard-blum@univ-lyon1.fr">sylvie.ricard-blum@univ-lyon1.fr</a>
<b>INFOMATHS</b>	<b>INFORMATIQUE ET MATHÉMATIQUES</b> <a href="http://edinfomaths.universite-lyon.fr">http://edinfomaths.universite-lyon.fr</a> Sec. : Renée EL MELHEM Bât. Blaise PASCAL, 3e étage Tél : 04.72.43.80.46 infomaths@univ-lyon1.fr	<b>M. Hamamache KHEDDOUCI</b> Université Claude Bernard Lyon 1 Bât. Nautibus 43, Boulevard du 11 novembre 1918 69 622 Villeurbanne Cedex France Tél : 04.72.44.83.69 <a href="mailto:hamamache.kheddouci@univ-lyon1.fr">hamamache.kheddouci@univ-lyon1.fr</a>
<b>Matériaux</b>	<b>MATÉRIAUX DE LYON</b> <a href="http://ed34.universite-lyon.fr">http://ed34.universite-lyon.fr</a> Sec. : Yann DE ORDENANA Tél : 04.72.18.62.44 yann.de-ordenana@ec-lyon.fr	<b>M. Stéphane BENAYOUN</b> Ecole Centrale de Lyon Laboratoire LTDS 36 avenue Guy de Collongue 69134 Ecully CEDEX Tél : 04.72.18.64.37 <a href="mailto:stephane.benayoun@ec-lyon.fr">stephane.benayoun@ec-lyon.fr</a>
<b>MEGA</b>	<b>MÉCANIQUE, ÉNERGÉTIQUE, GÉNIE CIVIL, ACOUSTIQUE</b> <a href="http://edmega.universite-lyon.fr">http://edmega.universite-lyon.fr</a> Sec. : Stéphanie CAUVIN Tél : 04.72.43.71.70 Bâtiment Direction INSA Lyon mega@insa-lyon.fr	<b>M. Jocelyn BONJOUR</b> INSA Lyon Laboratoire CETHIL Bâtiment Sadi-Carnot 9, rue de la Physique 69621 Villeurbanne CEDEX <a href="mailto:jocelyn.bonjour@insa-lyon.fr">jocelyn.bonjour@insa-lyon.fr</a>
<b>ScSo</b>	<b>ScSo*</b> <a href="https://edsciencessociales.universite-lyon.fr">https://edsciencessociales.universite-lyon.fr</a> Sec. : Mélina FAVETON INSA : J.Y. TOUSSAINT Tél : 04.78.69.77.79 melina.faveton@univ-lyon2.fr	<b>M. Bruno MILLY</b> Université Lumière Lyon 2 86 Rue Pasteur 69365 Lyon CEDEX 07 <a href="mailto:bruno.milly@univ-lyon2.fr">bruno.milly@univ-lyon2.fr</a>

\*ScSo : Histoire, Géographie, Aménagement, Urbanisme, Archéologie, Science politique, Sociologie, Anthropologie

# ACCORD DE COTUTELLE

---

## ACCORD DE COOPERATION POUR LA MISE EN ŒUVRE D'UNE COTUTELLE DE THESE

L'Université de Rome "La Sapienza" ayant son siège à Rome (Italie), Piazzale Aldo Moro 5, représentée par sa Rectrice Professeur Antonella POLIMENI agissant en-qualité et en vertu des pouvoirs qui lui sont conférés d'une part,

ET

L'INSA de LYON, représenté par Monsieur Frédéric FOTIADU, Directeur de l'établissement, agissant en-qualités et en vertu des pouvoirs qui lui sont conférés, d'autre part,

Pour la partie italienne :

- Vue la délibération du Sénat Académique du 2 octobre 2003 ;
- Vue la Loi 240/2010 art. 19 – dottorato di ricerca;
- Vu le D.M. 45/2013 relatif aux normes en matière de doctorat de recherche ;
- Vu le Règlement de l'Université en matière de doctorat de recherche ;

ET

Pour la partie française :

- Vu le code de l'éducation, notamment ses articles L.612-7, L. 613-1, D. 613-3, D. 613-6, D613-18 et D613-19 ;
- Vu le code de la recherche, notamment son article L.412-1 ;
- Vu le décret n° 2015-127 du 5 février 2015 portant approbation des statuts de la communauté d'universités et établissements « Université de Lyon »
- Vu l'arrêté du 25 mai 2016 fixant le cadre national de la formation et les modalités conduisant à la délivrance du diplôme national de doctorat
- Vu la charte du doctorat de l'Université de Lyon avec avenant INSA Lyon
- La convention cadre franco-italienne entre la Conférence des Présidents d'Université (CPU) et la Conferenza dei Rettori delle Università Italiane (CRUI) sur la reconnaissance des diplômes et validation des titres universitaires signée en date 18 janvier 1996;
- La convention cadre franco-italienne entre la Conférence des Présidents d'Université (CPU) e la Conferenza dei Rettori delle Università Italiane (CRUI) sur la co-tutelle de thèse signée le 13 février 1998;

désireux de contribuer à l'instauration et/ou au développement de la coopération scientifique entre équipes de recherche italiennes et étrangères en favorisant la mobilité des doctorants, sont convenu(e)s des dispositions suivantes :

### Titre I – Modalités administratives

Art. 1 – L'Université de Rome "La Sapienza" et l'INSA de Lyon désignées ci-après "les établissements", décident dans le respect des lois et des règlements en vigueur dans chacun des pays et/ou établissements, d'organiser conjointement une cotutelle de thèse au bénéfice de l'étudiante désignée ci-après:

Prénom et nom : **Livia FELICETTI**

Spécialité : Ingénieur Mécanique – Doctorat en Meccanica Teorica ed Applicata

Sujet de thèse : **Analyse et restitution de stimuli mécaniques à l'origine de la perception tactile**

*La perception tactile des surfaces est arbitrée par les stimuli mécaniques (générés lors de l'interaction du doigt et de la surface explorée) captés par les récepteurs tactiles et décodés par le cerveau. Pourtant Les mécanismes sous-jacents au sens du toucher demeurent encore en partie inconnus et font l'objet de recherches dans différents champs disciplinaires, tant dans les domaines du médical, de la biologie, de la psychologie que celui de l'ingénierie. Ainsi, force est de constater que la compréhension et la reproduction de la sensation tactile ont des applications technologiques et sociales importantes.*

*Les stimuli mécaniques statiques et dynamiques impliqués lors de la perception tactile représentent un sujet d'intérêt majeur aux interactions de la tribologie et de la mécanique vibratoire. En particulier, un rôle fondamental dans la perception et la discrimination des textures de surfaces semble être joué par les vibrations induites par frottement, c'est-à-dire les vibrations qui sont générées dans le contact « glissant » entre le doigt et la surface explorée.*

*Le but majeur de la thèse proposée consiste à analyser de tels stimuli mécaniques et à identifier leurs caractéristiques principales en corrélation avec la perception des propriétés de surfaces. De plus, le développement d'un simulateur tactile apte à restituer artificiellement la perception tactile générée par les surfaces se révèle un véritable challenge scientifique. Utilisant des outils technologiques innovants et interagissant avec des laboratoires de recherche issus de différentes disciplines associées, le travail de thèse vise donc à l'analyse, la compréhension et la reproduction des stimuli à l'origine de la perception.*

➤ Contexte de l'étude :

o Conditions de financement :

*La doctorante est salariée au travers d'une bourse ministérielle à la Sapienza Université de Rome (Italie) pour un montant de 15.343,28 €/ans brut. Le montant est augmenté jusqu'à 50% pour toute période de séjour autorisée à l'étranger pour un maximum de 18 mois.*

o Calendrier préliminaire du projet de recherche est indiqué pour les trois années :

*La première année est consacrée à un état de l'art détaillé de la littérature liée aux différents thématiques du projet (perception tactile, vibrations induites par frottement, simulateurs tactiles, ...). Une première analyse expérimentale sera développée par ailleurs pour la prise en main de l'instrumentation adéquate et des diverses méthodologies d'analyses et de post traitements de signaux associées.*

*Au cours de la deuxième année, une partie substantielle du travail de thèse portera sur le développement des protocoles spécifiques appropriés pour mesurer et analyser les vibrations induites par frottement, et les signaux associés, pour les différentes conditions d'analyse. De plus, la simulation de la perception tactile des surfaces à l'aide d'actionneurs polymères électro-actifs sera investiguée et optimisée. Ainsi différentes campagnes de tests seront conduites pour la mesure, l'analyse et la reproduction des vibrations induites par frottement tant en mode de toucher passif qu'actif. De plus, parallèlement aux signaux tribologiques et dynamiques, la mesure des signaux électroencéphalographiques sera également mise en œuvre pour évaluer l'activité cérébrale lors du toucher de surfaces réelles e/ou simulées.*

*Enfin lors de la troisième année, des campagnes de discrimination sur un ou plusieurs panels de volontaires seront menées pour valider la méthodologie de simulation tactile. Le retour d'expérience du simulateur tactile sera lié à la perception des caractéristiques des textures, à la sensation hédoniste des surfaces et à l'activité cérébrale. La synthèse, la rédaction du manuscrit et la soutenance de la thèse clôtureront les 3 années du projet de recherche.*

*Les périodes de séjour dans les deux établissements (minimum 12 mois dans chaque établissement) seront, à titre indicatif, réparties comme suivi:*

Périodes à l'INSA Lyon : du 01/05/2021 au 30/09/2021, du 01/10/2022 au 31/10/2023 (*au moins 12 mois*)

Périodes à l'Université de Rome La Sapienza : du 01/11/2020 au 30/04/2021, du 01/10/2021 au 30/09/2022 (*au moins 12 mois*)

o Les modalités d'encadrement, de suivi de la formation et d'avancement du doctorant : *Les rencontres avec les directeurs de thèse (Francesco MASSI et Benyebka BOU-SAID) auront une périodicité d'une fois toutes les deux semaines minimum. Tout le long de la durée de la thèse la doctorante produira des rapports et présentations intermédiaires pour le suivi du travail. Chaque année, une présentation en face du collège des professeurs du doctorat en « Meccanica Teorica ed Applicata » est obligatoire pour l'inscription à l'année suivante. La doctorante satisfera également aux exigences de l'ED MEGA en ce qui concerne la réunion annuelle du Comité de Suivi Individuel, dont l'avis est requis pour l'inscription en année suivante à l'INSA de Lyon.*

o Conditions matérielles de réalisation du projet :

*Le projet sera développé principalement sur les sites du département DIMA de la Sapienza Université de Rome et du LaMCoS de l'INSA de Lyon. Les bancs d'essais, déjà présents dans les locaux des deux établissements, seront dédiés à l'exécution des campagnes expérimentales. Un ordinateur et les licences des codes numériques nécessaires seront mises à disposition de la doctorante.*

Les principes et les modalités administratives et pédagogiques de cette cotutelle sont définis par le présent accord.

Art. 2 - La durée de préparation de la thèse est normalement de trois ans. Le cas échéant, cette durée peut être prolongée conformément à la réglementation en vigueur dans les deux institutions.

Un avenant sera rédigé au moins 6 mois avant la date de fin prévue initialement. Des périodes de recherche alternées auront lieu dans chacun des établissements. Le calendrier et la durée des séjours seront détaillés à l'article 1 de la présente convention. La durée minimale de préparation effectuée dans un établissement ne peut normalement être inférieure à une année. La durée prévue pour la préparation de la thèse en cotutelle est de 3 ans, à partir de l'année scolaire 2020/2021.

Art. 3 - La préparation de la thèse s'effectue par périodes alternées, à peu près équivalentes, dans chacun des deux établissements partenaires. La durée de ces périodes sera déterminée de commun accord par les deux directeurs de thèse.

Art. 4 – La doctorante est inscrite en thèse dans chacun des deux établissements co-contractants sous le régime de la collaboration internationale à partir de l'année universitaire **2020-2021**.

La doctorante sera inscrite administrativement dans chacun des deux établissements dès que toutes les conditions nécessaires à son inscription seront réunies. La doctorante est inscrite en thèse de doctorat de l'Université de Rome "La Sapienza" à compter de la rentrée universitaire 2020-2021.



Art. 5 – La doctorante acquitte, chaque année, ses droits d'inscription dans un des établissements. Elle est exemptée de ces droits dans l'autre établissement. Sur la durée de la thèse, la doctorante doit obligatoirement s'acquitter de ses droits d'inscription au moins une fois dans chaque établissement; l'acquiescement desdits droits est une condition de validité de la cotutelle internationale. La doctorante doit fournir chaque année les justificatifs d'inscription, s'ils existent, en doctorat à l'établissement pour lequel elle en est exonérée. Si la doctorante ne fréquente pas l'établissement français pendant une année universitaire complète, elle est reconnue non-assujettie à la Contribution Vie Étudiante et de Campus.

Art.6 – La doctorante est soumise à la réglementation en vigueur sur la couverture sociale dans le pays où elle acquitte les droits d'inscription. Dans celui où elle est exonérée, elle doit justifier également d'une couverture analogue, et doit en produire les justificatifs au moment de son inscription administrative dans chaque établissement. Elle s'engage par ailleurs à souscrire une « responsabilité civile vie privée » obligatoire en France. Ces assurances conditionnent l'inscription administrative.

Une assurance couvrant ses déplacements entre les deux pays est par ailleurs vivement conseillée.

Art.7 – Lors de son inscription, la doctorante devra fournir les justificatifs relatifs à ses ressources, à sa couverture sociale ainsi qu'à son assurance relative aux accidents du travail, dans chacun des pays,

Conformément à la Charte du Doctorat de l'UdL avec avenant INSA, un revenu minimum pendant les périodes de séjour en France, conforme à celui mentionné dans la Charte du doctorat conditionne l'inscription en doctorat à l'INSA Lyon. Ce revenu doit être au moins équivalent au SMIC.

Dans le cas où la doctorante serait dans l'incapacité de présenter les justificatifs de financement nécessaires à son inscription, l'INSA Lyon pourra prononcer de plein droit la résiliation de la présente convention.

Art. 8 –Pour les périodes d'études effectuées en France et pour la soutenance, le doctorant bénéficie de l'ensemble des dispositions de l'arrêté du 25 mai 2016 susvisé, et de la charte des thèses de l'INSA de Lyon.

## **Titre II – Modalités pédagogiques**

Art. 1 – Le travail de thèse de la doctorante sera réalisé sous la supervision commune de deux directeurs de thèse :

- Francesco MASSI (Professeur au Dipartimento di Ingegneria Meccanica e Aerospaziale), directeur de thèse à l'Université "La Sapienza" ;
- Benyebka BOU-SAID (Professeur au Laboratoire de Mécanique des Contacts et des Structures), directeur de thèse à l' INSA de Lyon ;

qui s'engagent à exercer pleinement la fonction de tuteurs de la candidate ainsi qu'à formuler chacun un avis écrit sur la thèse de Doctorat.

L'avis favorable des deux Directeurs de Thèse est une condition nécessaire à l'admission à l'examen final.

Art. 2- La thèse donnera lieu à une soutenance unique, reconnue par les deux établissements concernés. La soutenance aura lieu à **l'Université Sapienza de Rome**. Le jury de soutenance est composé sur la base d'une proportion équilibrée de membres de chaque établissement désigné conjointement par les établissements contractants et comprend, en outre, des

personnalités extérieures à ces établissements. Il comprendra au moins quatre membres et au maximum huit, dont la moitié au moins sont des personnalités extérieures aux établissements signataires de la cotutelle. Les autres membres sont désignés sur la base d'une proportion équilibrée de membre de chaque établissement désigné conjointement par les établissements contractants. La parité homme/femme devra se conformer aux conditions requises par les deux établissements contractants. Conformément à l'arrêté du 25 mai 2016, "le directeur de thèse participe au jury, mais ne prend pas part à la décision". Le directeur de thèse, comme les co-encadrants, n'ont pas à sortir pendant les délibérations, ils peuvent prendre part aux discussions préliminaires mais doivent s'abstenir lors de la délibération et du vote final.

Art. 3 - La thèse sera rédigée et discutée en Anglais. Elle comportera un résumé substantiel rédigé en Français et en Italien.

Art. 4 – En cas de rapport favorable du jury, chacun des deux établissements s'engage à conférer le titre de docteur de recherche pour la même thèse.

L'Université de Rome "La Sapienza" s'engage à conférer le grade de docteur de recherche en en Meccanica Teorica e Applicata.

L'INSA de Lyon s'engage à conférer le grade de docteur de l'Université de Lyon opéré au sein de l'INSA Lyon en cotutelle internationale avec l'Université de Rome "La Sapienza".

Art. 5- Les obligations de formation pour l'ED MEGA, telles que définies dans son règlement intérieur, sont au prorata de la durée des séjours prévus dans chaque pays, avec au minimum : au moins 12 heures de formation scientifique et au moins 13 heures de formation transversale à l'insertion professionnelle (dont au moins un cours consacré à l'éthique en recherche) et au moins 2 séminaires.

Les formations effectuées dans l'établissement partenaire ne peuvent pas être admises en équivalence pour satisfaire aux exigences pédagogiques de l'ED MEGA.

### **Titre III – Conclusions**

Art. 1 – L'étudiante est tenue de respecter les règlements et les usages de l'établissement d'accueil.

Art. 2 – Par l'intermédiaire de leurs directeurs de thèses respectifs, les établissements signataires s'engagent à se communiquer toutes les informations et la documentation utiles à l'organisation de la cotutelle de thèse faisant l'objet du présent accord.

Art. 3 – Les modalités de présentation, de dépôt et de reproduction de la thèse seront établies dans chaque pays dans le respect de la réglementation en vigueur.

La protection du sujet de thèse, ainsi que la publication, l'exploitation et la protection des résultats issus des travaux de recherche du doctorant dans les deux établissements signataires seront assujetties à la réglementation en vigueur et assurées conformément aux procédures spécifiques à chacun des pays impliqués dans la cotutelle.

Sur demande, les dispositions concernant la protection des droits de propriété intellectuelle pourront faire l'objet de protocoles ou de documents spécifiques.

Art. 4 – Le présent accord entre en vigueur à partir de la date de signature du représentant légal de chaque établissement signataire et le reste jusqu'à la fin de l'année universitaire au cours de laquelle la thèse ou les travaux seront soutenus. Dans le cas où l'étudiante ne serait

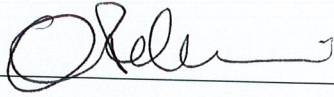
pas inscrite dans l'un et/ou l'autre des établissements signataires, ou bien renoncerait par écrit à poursuivre, ou bien n'est pas autorisée à poursuivre la préparation de sa thèse en vertu de la décision de l'un au moins des deux directeurs de thèse, les deux établissements signataires mettront fin conjointement et sans délai, aux dispositions du présent accord.

Art. 5 – Le présent accord est rédigé en six exemplaires originaux, dont trois en italien et trois en française, faisant également foi.

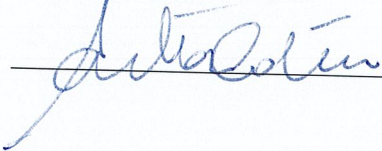
Art. 6 - En cas de différend sur l'interprétation ou l'application de la présente convention, les parties s'engagent à engager des échanges constructifs, réels et sincères, en vue d'un règlement à l'amiable.

Roma, li \_\_\_\_\_

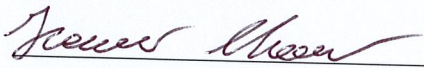
Pour la Rectrice de l'Université  
La Sapienza de Rome

  
\_\_\_\_\_

Il Coordinatore del Dottorato di Ricerca  
Antonio CARCATERRA

  
\_\_\_\_\_

Co-directeur de thèse  
Francesco MASSI

  
\_\_\_\_\_

Le Doctorant  
Livia FELICETTI

  
\_\_\_\_\_

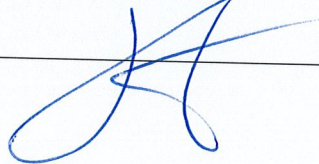
Villeurbanne, li 23.03.2021

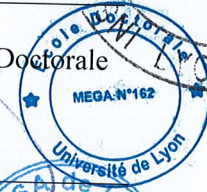
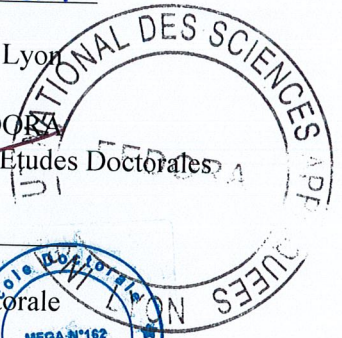
Pour le directeur de l'INSA de Lyon  
Florence POPOWYCZ  
Directrice du département FEDORA  
Formation par la Recherche et Etudes Doctorales

Le Responsable de l'Ecole Doctorale  
Jocelyn BONJOUR

Le Directeur du laboratoire  
Daniel NELIAS

Co-directeur (s) de thèse  
Benyebka BOU-SAID

  
\_\_\_\_\_





# Abstract

---

Among the 5 senses, which connect us with the surrounding world, the sense of touch is between the most articulated and the least understood. While we are able to master the signals that underlie sight and hearing, rendering them using loudspeakers and visual interfaces, the mechanisms underlying the sense of touch are still largely unknown. Touch, originating by the contact between the skin and the explored surface and involving several types of stimuli, requires a strongly multidisciplinary approach and involves a wide range of disciplines, such as Medicine, Neurosciences, Psychology, Dynamics, Tribology, Materials Sciences, and beyond. Tribology and Dynamics are involved in the study of all those complex phenomena that occur at the contact and that generate mechanical stimuli such as Friction-Induced Vibrations and contact forces, at the origin of the stimulation of skin's mechanoreceptors. This Ph.D. thesis is collocated into a research line closely dedicated to the investigation of the role of different features (amplitude, frequency distribution) of Friction-Induced Vibrations (FIV) in mediating between the characteristics of surface textures and the way in which textures are perceived and discriminated. Analyses of vibrational stimuli originating from the exploration of rigid periodic and isotropic textures have been carried out in the present work, revealing different key features in the discrimination of such textures: respectively the amplitude for isotropic textures, and the frequency distribution for periodic ones. At the same time, a tactile rendering device, named PIEZOTACT, has been developed to reproduce/mimic the FIV previously measured during the exploration of real surfaces. The developed vibrotactile device has been used to simulate periodic and isotropic textures and then to conduct campaigns on groups of volunteers, in order to evaluate their ability to discriminate real and simulated textures starting from the sole vibrational tactile stimuli. The good performances achieved by the volunteers in the discrimination campaigns made it possible to validate the device for rendering the tested textures and to correlate the different characteristics of amplitude and frequency distribution of FIV with perception of textures. Because the rendering methodology underlying the device is based on the characterization of the Transfer Function of the overall electromechanical system (consisting of the device and the user's finger), parametric analyses have been carried out on the Transfer Function of the human finger and the device as the participant and the contact conditions vary. Since the analysis revealed a slight deviation between the Transfer Function for different volunteers under the same contact conditions, the possibility of using an averaged Transfer Function to simulate textures using the PIEZOTACT device has been then validated by discrimination campaigns. Finally, as part of a multidisciplinary collaboration, a joint investigation, with laboratories from Neurosciences and Psychology, has been performed to evaluate the brain's response to the mechanical stimuli generated by the exploration of real and simulated surfaces, dealing as well with the role of signal attenuation during the touch motion.



# Résumé

---

Les 5 sens nous permettent de percevoir le monde qui nous entoure et d'interagir avec lui. Parmi les 5 sens, le sens du toucher demeure encore le moins compris. Alors que nous sommes capables de maîtriser les signaux à la base de la vue et de l'ouïe (ondes électromagnétiques et de pression), alors que nous sommes capables de les reproduire à l'aide d'appareils et d'interfaces graphiques et visuelles qui font désormais partie de notre vie quotidienne, les mécanismes sous-jacents au sens du toucher sont encore largement méconnus. Le toucher provient du contact entre la peau et la surface explorée et implique des stimuli mécaniques qui proviennent de l'ensemble du système musculosquelettique, ainsi que de la proprioception et des mécanismes qui lui sont associés. Diverses classes de mécanorécepteurs se situent dans la peau, les tendons et les ligaments. Ceux-ci sont capables de changer chimiquement et structurellement lorsqu'ils sont soumis à des stimuli mécaniques, générant un flux de courant qui est transmis à travers les nerfs au système nerveux central pour être décodé par le cerveau.

L'étude des mécanismes de perception tactile nécessite donc une approche hautement multidisciplinaire qui regroupe un large éventail de disciplines telles que la Médecine, les Neurosciences, la Psychologie, la Dynamique, la Tribologie, la Science des Matériaux, ... Ainsi la Tribologie et la Dynamique sont impliquées dans l'étude de tous les phénomènes complexes qui se produisent au contact et génèrent des stimuli mécaniques, tels que les vibrations induites par frottement (Friction-Induced Vibrations, FIV) et les forces de contact, à la base de la stimulation des mécanorécepteurs de la peau. De nombreux axes de recherche investiguent le rôle de différents stimuli mécaniques générés lors du toucher, qui sont fondamentaux pour une compréhension plus approfondie des mécanismes à l'origine de la perception tactile.

Cette thèse s'inscrit dans un axe de recherche plus étroitement consacré à l'étude du rôle des différentes caractéristiques (amplitude, distribution de fréquence) des vibrations induites par frottement, dans la médiation entre les caractéristiques de surface et la façon dont elles sont perçues et discriminées.

Tout d'abord, dans le présent travail, nous avons effectué des analyses de stimuli vibrationnels issus de l'exploration de textures rigides périodiques et isotropes, révélant plusieurs caractéristiques clés dans leur discrimination : respectivement l'amplitude pour les textures isotropes et la distribution en fréquences pour les textures périodiques.

Dans le même temps, un dispositif de rendu tactile, appelé PIEZOTACT, a été développé afin de reproduire/imiter les vibrations induites préalablement mesurées à partir de l'exploration de surfaces réelles. Le développement de dispositifs tactiles a trouvé une large place dans la recherche au cours de la dernière décennie, exploitant différents types de simulateurs tactiles basés sur différents stimuli mécaniques, tels que les vibrations, le frottement, les forces de contact. Les applications technologiques et l'impact social du rendu tactile sont immenses et couvrent de nombreux domaines de notre vie quotidienne, du commerce en ligne à la rééducation tactile, en passant par les technologies médicales telles que la chirurgie à distance et la télé-opération, les environnements virtuels et la réalité augmentée, le divertissement, l'apprentissage, l'art et bien plus encore... Malgré les efforts déployés par la recherche, le



chemin à parcourir est encore long. Dans la présente thèse, le dispositif vibrotactile développé a été utilisé pour simuler des textures périodiques et isotropes ; après validation appropriée, il a ensuite été exploité pour conduire des campagnes sur des groupes de volontaires, visant à évaluer leur capacité à discriminer des textures réelles et simulées à partir de seuls stimuli tactiles vibratoires. Les bonnes performances réalisées par les volontaires dans les campagnes de discrimination ont permis de valider le dispositif pour les textures testées et de corréler les différentes caractéristiques de distribution d'amplitude et de fréquence de la FIV avec la perception. L'un des points forts de l'appareil est en effet sa capacité à isoler et à découpler les stimuli vibratoires des autres stimuli tactiles ; ce qui en fait un outil de recherche efficace pour étudier encore plus en profondeur le rôle des stimuli mécaniques vibratoires et leurs principales caractéristiques (telles que la distribution d'amplitude et de fréquences) dans la perception et la discrimination des textures. À cette fin, le dispositif a également été utilisé pour mener des campagnes de discrimination dans lesquelles les amplitudes FIV ont été modifiées pour évaluer leur impact sur la perception des textures isotropes, confirmant ainsi le rôle prépondérant de l'amplitude FIV dans la discrimination de telles textures.

Étant donné que le toucher est basé sur l'interaction directe entre le doigt et la surface explorée, les conditions de contact et la réponse dynamique des corps en contact jouent un rôle crucial. Cela est également vrai lorsque le contact se produit entre le doigt et la surface d'un dispositif haptique. La méthodologie de rendu du dispositif PIEZOTACT est donc basée sur la caractérisation de la fonction de transfert de l'ensemble du système électromécanique constitué de l'appareil électromécanique et du doigt de l'utilisateur. Des analyses paramétriques ont été effectuées sur la fonction de transfert du doigt humain et de l'appareil en fonction du sujet et des conditions de contact (force et angle entre le doigt et la surface). L'analyse ayant révélé une légère variation de la fonction de transfert pour différents volontaires dans les mêmes conditions de contact, la possibilité d'utiliser une fonction de transfert moyenne pour simuler des textures à l'aide du dispositif PIEZOTACT. Les résultats obtenus lors de campagnes de discrimination permettent de valider l'utilisation d'une fonction de transfert moyenne, évitant ainsi d'avoir à caractériser la réponse dynamique du doigt de l'utilisateur individuel de l'appareil.

Plusieurs groupes de recherche travaillent en combinant l'expertise de laboratoires liés à différents champs disciplinaires pour étudier en synergie la chaîne globale de la perception tactile, depuis la caractérisation de surface, en passant par les stimuli mécaniques, jusqu'à la réponse et la perception cérébrales. Dans cette thèse, dans un cadre collaboratif pluridisciplinaire, le dispositif PIEZOTACT a été exploité pour fournir un retour tactile dans une étude visant à évaluer la réponse cérébrale aux stimuli mécaniques générés par l'exploration de surfaces réelles et simulées, tout en tenant compte des mécanismes d'atténuation des signaux tactiles dus aux mouvements effectués par le sujet pendant l'exploration des surfaces. L'utilisation du dispositif haptique a permis de mettre en évidence les similitudes et les différences dans la réponse cérébrale dans des conditions tactile réelles et simulées.

D'une manière générale, les résultats obtenus ont fourni des informations importantes sur le rôle des vibrations induites par frottement dans la perception tactile. Ces travaux ont permis le design d'un outil fiable pour la reproduction des stimuli mécaniques associés à ces vibrations. Il sera utilisé à l'avenir pour étudier plus en détail les phénomènes sous-jacents à la perception tactile.

Cette thèse a été développée dans le cadre de la cotutelle de thèses entre le DIMA (Département de Génie Mécanique et Aérospatial) de l'Université La Sapienza de Rome, Italie et le LaMCoS (Laboratoire de Mécanique des Contacts et des Structures) de l'INSA (Institut National des Sciences Appliquées) de Lyon, France.

# Riassunto

---

I 5 sensi ci permettono di percepire il mondo circostante e di interagire con esso. Tra i 5 sensi, il senso del tatto è il più articolato e tutt'ora il meno compreso. Laddove siamo in grado di gestire i segnali che sono alla base della vista e dell'udito (onde elettromagnetiche e di pressione), e siamo in grado di riprodurli utilizzando dispositivi e interfacce grafiche e visive che fanno ormai parte della nostra vita quotidiana, i meccanismi alla base del senso del tatto sono ancora in gran parte sconosciuti. Il tatto ha origine dal contatto tra la pelle e la superficie esplorata, e coinvolge stimoli meccanici che provengono dall'intero sistema muscolo-scheletrico, insieme alla propriocezione e ai meccanismi ad essa associati. Varie classi di recettori tattili si trovano nella pelle, nei tendini e nei legamenti. Questi sono in grado di modificarsi chimicamente e strutturalmente quando sottoposti a stimoli meccanici, generando un flusso di corrente che viene trasmesso tramite i nervi al sistema nervoso centrale, dove gli stimoli sono decodificati dal cervello.

Lo studio dei meccanismi di percezione tattile richiede quindi un approccio fortemente multidisciplinare, e coinvolge una vasta gamma di discipline, come la Medicina, le Neuroscienze, la Psicologia, la Dinamica, la Tribologia, le Scienze dei Materiali, e molte altre. La Tribologia e la Dinamica sono coinvolte nello studio di tutti quei complessi fenomeni che avvengono al contatto e che generano stimoli meccanici, come le vibrazioni indotte dall'attrito (Friction-Induced Vibrations, FIV) e le forze di contatto, che sono alla base della stimolazione dei meccanorecettori. Molte linee di ricerca indagano il ruolo dei diversi stimoli meccanici nella percezione tattile, tutti fondamentali per una comprensione più profonda dei meccanismi all'origine della stessa.

Questa tesi di Dottorato si colloca all'interno della linea di ricerca più strettamente dedicata allo studio del ruolo delle diverse caratteristiche (ampiezza, distribuzione di frequenza) delle vibrazioni indotte dall'attrito, nel mediare tra le caratteristiche topografiche superficiali e il modo in cui sono percepite e discriminate.

In primo luogo, nel presente lavoro sono state condotte analisi di stimoli vibrazionali originati dall'esplorazione di "textures" rigide periodiche e isotrope, rivelando diverse caratteristiche chiave nella loro discriminazione: rispettivamente l'ampiezza per le textures isotrope, e la distribuzione in frequenza per quelle periodiche.

Allo stesso tempo, è stato sviluppato un dispositivo di rendering tattile, denominato PIEZOTACT, al fine di simulare le textures, riproducendo le vibrazioni indotte precedentemente misurate a partire dall'esplorazione di superfici reali. Lo sviluppo di dispositivi tattili ha trovato ampio spazio nella ricerca nell'ultimo decennio, sfruttando diversi tipi di simulatori tattili basati su diversi stimoli meccanici, come vibrazioni, attrito, forze di contatto. Le applicazioni tecnologiche e l'impatto sociale del rendering tattile sono immensi e spaziano in molti campi della nostra vita quotidiana, dal commercio online, alla riabilitazione tattile, alle tecnologie mediche come la chirurgia a distanza e le teleoperazioni, agli ambienti virtuali e alla realtà aumentata, all'intrattenimento, all'apprendimento, all'arte e molto altro. Nonostante gli sforzi che la ricerca sta compiendo, la strada da percorrere è ancora costellata di complessità. Nella presente tesi, il dispositivo vibrotattile sviluppato è stato utilizzato per

simulare textures periodiche e isotrope; dopo opportuna validazione, è stato successivamente sfruttato altresì per condurre campagne su gruppi di volontari, volte a valutare la capacità di discriminare textures reali e simulate a partire dai soli stimoli tattili vibrazionali. Le buone performance raggiunte dai volontari nelle campagne di discriminazione hanno permesso di validare il dispositivo per le textures testate e di correlare le diverse caratteristiche di ampiezza e di distribuzione in frequenza delle FIV con la percezione. Uno dei punti di forza del dispositivo è infatti la capacità di isolare e disaccoppiare gli stimoli vibrazionali dagli altri stimoli tattili, rendendolo un efficace strumento di ricerca per indagare ancor più profondamente il ruolo degli stimoli meccanici e delle loro principali caratteristiche (come ampiezza e distribuzione frequenziale delle FIV) nella percezione e discriminazione delle textures. A questo scopo il dispositivo è stato anche utilizzato per condurre campagne di discriminazione in cui le ampiezze delle FIV sono state alterate per valutarne l'impatto sulla percezione delle textures isotrope, confermando l'importante ruolo dell'ampiezza delle FIV nella discriminazione di tali textures.

Poiché il tatto si basa sull'interazione diretta tra il dito e la superficie esplorata, le condizioni di contatto e la risposta dinamica dei corpi in contatto giocano un ruolo cruciale. Questo vale anche quando il contatto avviene tra il dito e la superficie di un dispositivo tattile. La metodologia di rendering alla base del dispositivo PIEZOTACT si basa quindi sulla caratterizzazione della Funzione di Trasferimento dell'intero sistema elettromeccanico costituito dal dispositivo e dal dito dell'utilizzatore. Sono state quindi effettuate analisi parametriche sulla Funzione di Trasferimento del dito umano e del dispositivo al variare del soggetto e delle condizioni di contatto, come la forza e l'angolo tra dito e superficie. Poiché l'analisi ha rivelato una ridotta variazione della Funzione di Trasferimento per i diversi volontari a parità di condizioni di contatto, la possibilità di utilizzare una Funzione di Trasferimento media per simulare le textures utilizzando il dispositivo PIEZOTACT è stata validata mediante campagne di discriminazione delle textures isotrope. I risultati ottenuti permettono di validare l'utilizzo di una Funzione di Trasferimento media, evitando quindi la necessità della caratterizzazione della risposta dinamica del dito del singolo utilizzatore del dispositivo.

Diversi gruppi di ricerca lavorano unendo le competenze di laboratori inerenti a diverse discipline per indagare sinergicamente la catena complessiva della percezione tattile, a partire dalla caratterizzazione superficiale, passando per gli stimoli meccanici, fino alla risposta cerebrale e alla percezione. In questa tesi, nell'ambito di una collaborazione multidisciplinare, il dispositivo PIEZOTACT è stato sfruttato per fornire un feedback tattile in uno studio volto a valutare la risposta cerebrale a stimoli meccanici generati dall'esplorazione di superfici reali e simulate, tenendo in conto anche i meccanismi di attenuazione dei segnali tattili dovuti ai movimenti eseguiti dal soggetto per l'esplorazione della superficie. L'utilizzo del dispositivo tattile ha permesso di mettere in luce le similitudini e le diversità nella risposta cerebrale in condizioni di tatto reale e simulazione tattile.

In generale, i risultati ottenuti hanno permesso di fornire importanti informazioni sul ruolo delle vibrazioni indotte dal contatto nella percezione tattile, e si è fornito altresì uno strumento affidabile di riproduzione degli stimoli meccanici associati a tali vibrazioni, che sarà in futuro utilizzato per ulteriormente investigare i fenomeni alla base della percezione tattile.

Questa tesi di Dottorato è stata sviluppata nell'ambito della cotutela di tesi fra il DIMA (Dipartimento di Ingegneria Meccanica e Aerospaziale) dell'Università La Sapienza di Roma, Italia, e il LaMCoS (Laboratoire de Mécanique des Contacts et des Structures) dell'INSA (Institut National des Sciences Appliquées) di Lione, Francia.



# **Analysis and rendering of contact vibrational stimuli for tactile perception**

*A mamma*



# Summary

---

Introduction .....	5
Chapter 1 .....	9
State of the art.....	9
1.1 Context of the Ph.D. work .....	10
1.2 Background on tactile perception .....	13
1.2.1 Physiology of tactile perception .....	13
1.2.2 Active and passive touch .....	14
1.2.3 Exploratory procedures in active touch.....	15
1.2.4 Duplex-Theory of texture perception and tactile mechanical stimuli .....	17
1.2.5 Friction-Induced Vibrations in tactile perception.....	17
1.2.6 Forces and friction in tactile perception .....	19
1.2.7 Mastering of tactile stimuli: an ongoing challenge .....	20
1.2.8 Tactile rendering of textures .....	21
1.3 Positioning of the Ph.D. Thesis .....	22
Chapter 2 .....	24
Materials and method .....	24
2.1 Work overview and overall approach.....	25
2.2 Surface samples .....	27
2.1.1 Periodic surface samples .....	27
2.1.2 Isotropic surface samples .....	29
2.3 Measurement of tactile mechanical stimuli.....	33
2.3.1 Active touch test bench (ActTouch) .....	34
2.3.2 Passive touch test bench (TriboAir) .....	36
2.4 Tactile rendering device PIEZOTACT .....	39
2.5 Characterization of finger Transfer Function .....	41
2.5.1 Theoretical bases on Transfer Function.....	41
2.5.2 Test bench for the characterization of the finger Transfer Function .....	43
2.5.3 Test bench for the characterization of the PIEZOTACT and user’s finger Transfer Function.....	44
2.6 Discrimination campaign protocols.....	47

2.6.1 Discrimination protocol of periodic textures.....	48
2.6.2 Discrimination of isotropic textures .....	50
2.6.3 Building of Association Matrices .....	53
2.6.4 Ethics Committee .....	54
Chapter 3 .....	56
Mechanical signals analysis .....	56
3.1 From measurement to processing of tactile mechanical stimuli .....	57
3.2 Analysis of isotropic textures .....	59
3.2.1 Mechanical stimuli by active touch.....	59
3.2.2 Mechanical stimuli by passive touch.....	60
3.2.3 Active vs passive touch FIV .....	66
3.3 Isotropic vs periodic textures .....	68
3.4 Concluding remarks .....	69
Chapter 4 .....	71
Texture rendering by FIV stimuli .....	71
4.1 FIV rendering methodology .....	72
4.2 Experimental validation of FIV rendering .....	77
4.3 Discrimination campaigns.....	80
4.3.1 Discrimination of periodic surfaces .....	80
4.3.2 Discrimination of isotropic surfaces.....	84
4.3.3 Discrimination of periodic textures vs discrimination of isotropic textures .....	90
4.4 Modifying texture perception by FIV rendering .....	91
4.4.1 Protocol of discrimination campaign with FIV amplitude inversions.....	91
4.4.2 Results of discrimination campaign with FIV amplitude inversions .....	93
4.5 Concluding remarks .....	98
Chapter 5 .....	100
Role of finger Transfer Function in vibrotactile rendering .....	100
5.1 Parametrical analysis of the Transfer Function .....	102
5.1.1 Parametric analysis of the finger Transfer Function .....	102
5.1.2 Characterization of the overall electro-mechanical Transfer Function (PIEZOTACT and user's finger) .....	106
5.2 FIV mimicking using the averaged Transfer Function.....	112
5.3 Discrimination of isotropic textures with the averaged Transfer Function.....	113
5.4 Concluding remarks .....	115

Chapter 6 .....	117
Investigation into the brain response to vibrational mechanical stimuli .....	117
6.1 Neuroscientific background and definition of the objective of the study .....	119
6.2 Tasks and experimental setups .....	122
6.3 Surface samples .....	125
6.4 Analysis of tactile mechanical stimuli .....	125
6.5 Main findings in brain response .....	131
6.6 Concluding remarks .....	133
Chapter 7 .....	135
General conclusions .....	135
7.1 Main findings .....	136
7.1.1 From surface textures to FIV stimuli .....	136
7.1.2 Vibrotactile rendering device: PIEZOTACT .....	136
7.1.3 From FIV stimuli to texture discrimination .....	137
7.1.4 Finger Transfer Function and tactile rendering .....	138
7.1.5 Spot into brain response to tactile mechanical stimuli .....	139
7.2 Future works .....	140
References .....	142



# Introduction

The sense of touch is one of the channels through which the human beings perceive, apprehend, and interact with the external environment. Touch is the most articulated among the 5 senses, involving a complex interplay of the musculoskeletal and proprioception systems, and encompassing a wide range of stimuli, including forces, friction, vibrations and temperature, which activates different types of receptors located in the skin. The mechanisms that lie at the origin of touch are still largely unknown. They need to be investigated with a multidisciplinary approach by mechanical and material engineers, physiologists, psychologists, neuroscientists, physiochemists and so on. The mechanical stimuli are detected by mechanoreceptors, transduced as electrical signals, carried by nerves, and then decoded by the brain, passing through the filter of the human psychology. Tribology and dynamics aim to investigate the mechanical stimuli arising from the finger/surface contact, as well as the phenomena which occurs at the interface, correlating such stimuli with the surface characteristics and texture topography. Understanding the relationship between mechanical stimuli and tactile perception needs the synergistic effort of tribology, neuroscience, and psychology. Research is largely pursuing this goal, aiming to reconstruct the entire chain of tactile perception, starting from the characteristics of the surface, passing through mechanical stimuli, up to the cerebral and psychological response, pushing the knowledge about touch processes by means of workgroups which combines the knowhow of laboratories from different disciplines.

Understanding how the different mechanical stimuli play their role in tactile perception is not only important for the basic understanding of touch, but pave the way as well to the possibility to render tactile stimuli and simulate perception by tactile devices. We are already able to artificially recreate sight and hearing trough visual and acoustic devices of every sort, which integrates our life from decades. Sight and acoustic stimuli, i.e. electromagnetic and pressure waves, are already well understood and mastered. Although in recent years the development of tactile devices, mimicking the different mechanical stimuli (friction, vibrations, forces, etc.), has surged, tactile rendering of textures is still an ongoing challenge, due to the variety and complexity of such stimuli. Tactile rendering technologies would find application in all fields of our everyday life such as augmented reality, virtual reality, e-commerce, sensory rehabilitation, tele-surgery, sensory substitution and beyond. Thus, replicating touch would have a strong social and technological impact. The development of different tactile devices based on different tactile stimuli would allow as well to decouple different mechanical signals as vibrations or forces in order to investigate their role in the tactile perception processes.

The present Ph.D. work is collocated into a recent line of research which investigates the relationship between tactile perception of surface textures and the Friction-Induced Vibrations (FIV) that are generated during the tactile exploration. In fact, whenever a sliding contact occurs, vibrations are generated at the interface. Texture induced vibrations stimulate specific classes of mechanoreceptors and are identified as one of the key stimuli, along with friction and forces, which mediate tactile perception. The approach of the present research is focused from one hand on a deeper comprehension of the role of FIV in tactile perception of textures and from another hand on the possibility to render tactile vibrational stimuli by a tactile device.

Different rigid textures, periodic and isotropic ones, have been tested in this work. Mechanical stimuli from surface exploration are measured and analysed in order to investigate the different

features of the FIV, such as acceleration amplitude and frequency distribution, which encode the texture characteristics. A vibrotactile texture rendering device, able to render the vibrational stimuli by means of a piezoelectric actuator and its driving chain, has been developed. The possibility to discern textures based on FIV has been then addressed. Perceptual and discrimination campaigns have been carried out on volunteers, both with the real textures and the ones simulated using the developed device, mimicking FIV. The aim is to correlate the FIV features both with the texture topography and the discriminative perception, up to spot into the brain response in a collaborative work where the multidisciplinary approach, needed to study touch-related phenomena, is expressed.

The thesis is structured as following: In the first instance, the context in which this work is collocated and an overview of the current literature in the field of tactile perception is outlined in Chapter 1, focusing on the mostly related aspects of literature to the present work. Chapter 2 (materials and method) provides a description of the tools, test benches and protocols that have been developed and exploited throughout all the thesis. Chapter 3 is then dedicated to analyses of FIV induced by active and passive exploration of isotropic and periodic surface samples. The main features of FIV induced by the scanning of both types of textures are identified and compared. In Chapter 4, the rendering methodology underlying the tactile rendering device is presented and verified; the device is then validated through discrimination campaigns of real and simulated periodic and isotropic textures, involving panels on volunteers. Chapter 5 is dedicated to address the interaction between the finger and the vibrotactile device, by parametrically characterising the Transfer Function of the finger and the one of the overall system, constituted by the tactile device and the user's finger, as a function of the contact boundary conditions and for panels of volunteers. Finally, Chapter 6 reports a collaborative work with the Cognitive Neuroscience Laboratory (LNC) of the Aix-Marseille University (France) aimed to correlate mechanical stimuli and electroencephalographic (EEG) signals during the exploration of real and simulated textures. Chapter 7 provides general conclusions and future perspectives of the thesis work.

This Ph.D. thesis has been developed in joint supervision between the DIMA (Dipartimento di Ingegneria Meccanica e Aerospaziale) of the Sapienza University of Rome, Italy, and the LaMCoS (Laboratoire de Mécanique des Contacts et des Structures, UMR CNRS 5259) of the INSA (Institut National des Sciences Appliquées) of Lyon, France.





# Chapter 1

## State of the art

This work is focused on the analysis and rendering of mechanical stimuli involved in the tactile perception of textures, with a particular focus on vibrational stimuli. This chapter provides an overview of the context and of the literature concerning the different aspects of tactile perception, which will be encountered in the manuscript. While the current literature on tactile perception, within the different disciplines, is extremely huge and variegate, this Chapter aims to overview the most relevant contributions on the specific fields and topics addressed by the Ph.D. work. The positioning of the work is then discussed.

# 1.1 Context of the Ph.D. work

---

The sense of touch is the least understood of the 5 senses. Despite the great advancement of research and knowledge that is moving forward, the mechanisms behind touch are still largely unknown. Touch originates with the exploration of the surface, from which static and dynamic mechanical signals are generated. Such signals, together with the motion of the body parts, i.e. the proprioception, contribute to stimulate the mechanoreceptors contained in the entire musculoskeletal system. These signals are then encoded into electrical signals that are transmitted to the brain, to be decoded and allowing the tactile sense. Unlike sight and hearing, touch requires physical interaction between the finger and the object to be explored, and this generates a series of complex phenomena related to the contact. For this reason, Tribology and Dynamics are between the disciplines suitable to address the study of touch mechanisms. To date, among the many questions that researchers have only partially managed to answer, there is the role of different mechanical stimuli (vibrations, friction, forces, etc.) in codifying the different characteristics of surfaces (roughness, periodicity, hairiness, compliance, hardness, and so on); as well, how these mechanical stimuli are related to the perception and discrimination of surface features. The challenge is made much more difficult by so many factors that come into play, such as nonlinearity of the mechanical contact interaction, proprioception, brain treatment of tactile stimuli, psychological response etc. Tactile perception is in itself a highly multidisciplinary problem, that needs to be investigated by different points of view, with the joint skills of Mechanics, Neurology, Neurosciences, Psychology, Material Science, Medicine, Biology, and so on. Specifically, being an interactive sense involving direct physical contact with the explored object, touch is affected by all those parameters that influence a contact between two bodies, and which is the subject of study of Tribology. Kinematics of surface exploration, contact boundary conditions (such as velocity, contact forces, finger/surface angle, etc.), physiochemical characteristics of the finger, etc., need to be investigated in order to understand their role in the encoding of stimuli that mediate perception. The coupled dynamics of the two bodies in contact, i.e. the finger and the explored surface, depends as well from all the boundary parameters. As discussed in the next section, dedicated to the related state of the art, vibrations, friction, and forces stand among the most important mechanical stimuli involved in tactile perception. The analysis of such mechanical stimuli hides many complexities and requires extensive dedicated lines of research aiming to investigate their role in perception. In this context, this Ph.D. thesis is focused on vibrational stimuli (namely Friction-Induced Vibrations) that arise from the contact between the finger and the surface during tactile exploration, aiming to contribute to the understanding of the relationship between the different features of such stimuli, the texture topography, and the texture perception.

As research proceeds into the mechanisms underlying tactile perception, investigating the mechanical stimuli that mediate it, another challenge arises from a social and technological point of view: the possibility of artificially recreating tactile sensation, as we already do with sight and hearing. In fact, we are already familiar with the stimuli that are the basis of sight and hearing, and we are able to capture and reproduce them through visual and acoustic devices. Given its complexity, tactile rendering is still an ongoing challenge. Artificially

recreating touch, through tactile rendering of surfaces, could enhance the existing technologies in a countless number of fields, such as online commerce, where we could feel the intricate details of fabrics and objects from a distance, virtual reality, augmented reality, videogaming, movies, multimedia contents, art, learning and development, teaching, tactile rehabilitation, teleoperation, remote surgery, sensory substitution (e.g. Braille displays for visually impairment), and beyond. Such advancements in haptics and tactile rendering could have a very strong social and technological impact (Figure 1). Because tactile stimuli are so varied and complex, a huge amount of different haptic devices are under development, based on haptic feedback generated by different tactile stimuli (vibrations, forces, friction, etc.). An overview of the main tactile rendering methods is given in the following sections. The future hope is to put together the various tactile feedback based on different mechanical stimuli to recreate the tactile sensation in a more faithful and comprehensive way. This Ph.D. thesis work deals as well with the development, and exploitation for research purposes, of a vibrotactile device capable of reproducing "the texture vibration". On the one hand, the development of tactile devices necessarily involves the understanding of the role of the different mechanical stimuli, and of the different features of mechanical stimuli, in tactile perception. On the other hand, the development of devices that reproduce specific mechanical stimuli is useful for research purposes to isolate and decouple the class of mechanical stimuli in question from other tactile stimuli, to investigate their actual role in perception. The development of tactile rendering devices is therefore a two-way challenge. Combining the direct investigation of mechanical stimuli underlying tactile perception, the development of a tactile device and the exploitation of such tactile device to study the role of stimuli in perception, is the philosophy behind this Ph.D. thesis.

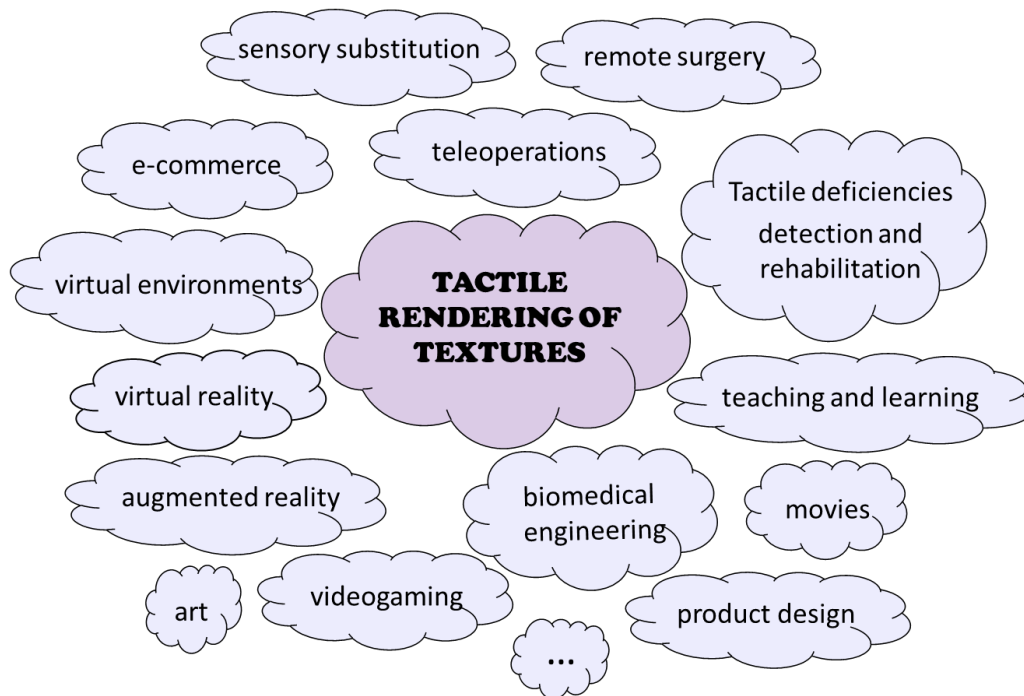
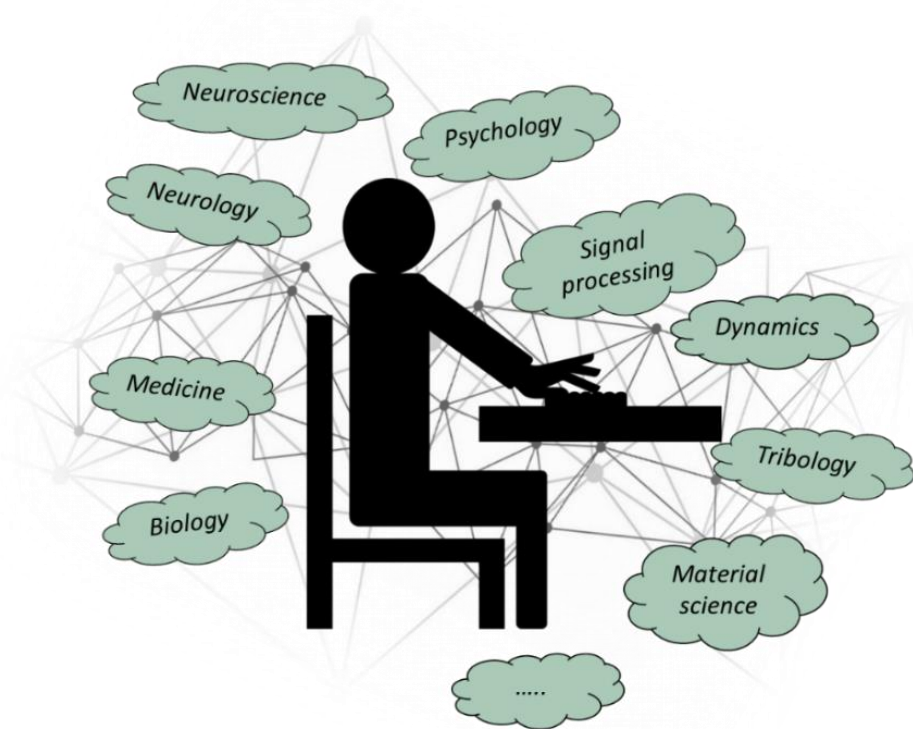


Figure 1: Fields of application of tactile rendering.

The present thesis is inscribed in a more general framework including different disciplines involved in the overall investigation and comprehension of touch (Figure 2). In fact, the sense of touch originates from the interaction between human body parts and the surface, generating mechanical stimuli of different types (concerning Tribology, Dynamics, Material Science, Physics etc.) that stimulate receptor's response (Physiology, Medicine, Biology), which are then processed by the peripheral and central nervous system and decoded by the brain (Neuroscience, Neurology), along with all the phenomena involved thank to proprioception. Tactile perception is then the result of the combination between brain processing of mechanical stimuli and Psychology of the human being. Derived social and technological applications involves a wide spectrum of disciplines as well, such as Engineering, Medicine, Neurology, Psychology, Economy, Informatics, Teaching and so on (Figure 1). In terms of research, it is clear that understanding the processes underlying touch needs the synergistic effort of different laboratories from different disciplines and a multidisciplinary overall view. In this context, the present Ph.D. thesis had the opportunity to collaborate with the laboratories involved in the framework of the “ANR CONTACT” project [1] and the “GDR TACT” workgroup [2].



*Figure 2: Touch: a multidisciplinary matter.*

## 1.2 Background on tactile perception

---

This section provides an overview of the literature in the field of tactile perception, focused on the aspects that concern the present Ph.D. work. The section begins with an introduction to the physiology of touch; Then, an overview of the literature concerning exploration procedures and kinematics is provided. Subsequently, the most important lines of research on the mechanical stimuli underlying tactile perception are presented, with a particular focus on vibrational stimuli. An overview of haptic and tactile rendering devices is finally provided, focusing in particular on the most exploited rendering methodologies in the literature.

### 1.2.1 Physiology of tactile perception

Human beings perceive, apprehend, and interact with the external world by means of different sensory channels that operate synergistically. The senses of sight, taste, smell, hearing and vestibular sense are called ‘special senses’[3]. Instead, the ‘general somatic senses’ are constituted by the exteroceptive senses, which detect the information coming from the body surface (touch, pressure, temperature...), the proprioceptive senses, that are related to the physical state of the body and the spatial and motor information (kinesthetic sense, mediated by joints and ligaments), and the viscerosceptive senses, that relate to the detection of the stimuli coming from the internal organs. The somatic senses can be divided in three different categories: the mechanoreceptive somatic sense (involving the mechanical stimuli on the tissues), the thermal sense, and the sense of pain. The sensory stimuli (afferences) are detected by different types of receptors, then the coded signals are carried by the nerves to the central nervous system and then decoded by the brain. Each receptor is a sort of transducer that generates a voltage and a flow of electricity on its nerve termination, when undergoes a physical or chemical variation of its structure. Different receptors can detect different stimuli. In the field of somaesthetic senses, the mechanoreceptors detect their mechanical deformation, the thermoreceptors the changes in temperature, the nociceptors pain or tissue damage etc. Sensory receptors are located also into the muscles, joints, tendons, ligaments and provide the kinesthetic sense (i.e. the perception of the relative motion of the body parts) [3].

The haptic perception is the process of recognizing and discriminating objects through touch. It involves both the kinesthetic sense (proprioception) and the cutaneous inputs, which arises when the contact between the skin and the surface of an object occurs, and the mechanical deformation of the skin stimulate the mechanoreceptors [4]. Each type of mechanoreceptor constitutes a specific channel able to decode a different information [5]. The mechanoreceptors (Table 1) are Pacinian corpuscles, Ruffini endings, Meissner’s corpuscles and Merkel disks, which can be divided into two categories based on their speed of adaptation with respect to the mechanical stimuli: slow adapting receptors (SA), able to detect constant mechanical stimuli (like pressure and skin stretch), and rapidly adapting receptors (RA), able to detect transient mechanical stimuli (vibrations). The skin is densely populated by mechanoreceptors,

in particular the hands and the fingertips. The spatial resolution of each type of mechanoreceptor is linked to the number and position of receptors that lie in a certain portion of tissue. The receptors located in the deeper layers of the skin show a larger receptive field, rather than the afferents located in the more superficial cutaneous layer. They are classified in type I (small receptive field) and type II (large receptive field).

Table 1: Mechanoreceptors classification and main characteristics [6].

Receptors	Merkel disk	Meissner's corpuscles	Pacinian corpuscle	Ruffini endings
<b>Adaptation</b>	Slow SA	Rapid RA	Rapid RA	Slow SA
<b>Perceptive field</b>	Small (11 mm <sup>2</sup> ) Type I	Small (9.4 mm <sup>2</sup> ) Type I	Large (100 mm <sup>2</sup> ) Type II	Large (60 mm <sup>2</sup> ) Type II
<b>Density</b>	70 units per cm <sup>2</sup>	140 units per cm <sup>2</sup>	20 units per cm <sup>2</sup>	10 units per cm <sup>2</sup>
<b>Frequency field</b>	2–16 Hz	3–40 Hz	40–500 Hz	100–500 Hz
<b>Perceptions</b>	Static Pressure, detection of object spatial structure and form	Transient pressure indentation, motion, grip control	Vibration sensations	Skin stretch sensation

## 1.2.2 Active and passive touch

The sense of touch has been strongly explored from a behavioural point of view, as well as from a physiological one. Gibson is among the first to emphasize the difference between touching and being touched [7], i.e. active and passive touch. Active touch couples both the kinesthetic sense and the proper sense of touch, and is the real way through which we perceive the external world. Quoting the words of Gibson [7], “*active touch is an exploratory rather than a merely receptive sense*”, with a purposive connotation, and the act of touching is a search for stimulation to obtain the desired information about the explored object, which is possible thank to the concomitant excitation of receptors contained in the skin but also in joints and tendons. In other words, it relates on inputs coming from the whole skeleto-muscular and vestibular system, providing a definite channel of information about the external environment, which can be seen as something much similar to a special sense organ [7]. Moreover, according to Gibson, the simple formula that the active touch consists of passive touch plus kinesthesia is insufficient and the hypothesis of two components of stimulation, one exterospecific and one propriospecific, contributing to generate a wholly unified sensory experience, is more promising [7].

In passive touch the object is perceived only by means of the passive stimulation of the skin, but no kinesthetic sense is involved, since the static or dynamic contact between the body and the object is caused by an outside system. Nevertheless, passive touch is very useful to study the mechanisms of stimulation of the mechanoreceptors and to decouple the influences of the

parameters involved in the contact pairs constituted by the body and explored object. According to some studies [8], [9], it does not necessarily determine a deficiency in tactile perception and in accuracy during a discrimination task; nevertheless, this point is still controversial.

### 1.2.3 Exploratory procedures in active touch

If the haptic mechanism is a purposive exploratory function [7], [10], it may be worthy to wonder what determines the sequence of exploratory activities when objects are haptically apprehended and how happens the choice of the next hand movement to be performed, that is the question that Lederman and Klatzky address in [7], [11], [12]. In the first instance, Lederman and Klatzky observed that we interact with objects using stereotyped hand movements, that they called exploratory procedures (EPs), which aim to obtain information on specific object properties. They observed that each fundamental property of an object (such as texture, hardness, temperature, weight, size, global shape) is instinctively explored by human being with an exploratory procedure that has certain invariants and typical features. For example, the EP that emerges spontaneously when testing the hardness of an object is pressure, thermal properties are explored with static contact, weight with unsupported holding, global shape and volume with enclosure, exact shape with a contour following. Lateral motion is the procedure used to inspect the texture of a surface, and its invariant is a repetitive lateral movement (tangential rubbing) between skin and surface.

The choice of the EPs to be used is strictly linked to the object properties and to the task. Moreover, Lederman and Klatzky classified the EPs in optimal (in terms of accuracy and time), necessary and sufficient, and they observed that in free exploration people tend to use a certain EP because it is optimal or even necessary and not because it is merely sufficient [10]. They observed also that the exploratory and manipulatory movements occur in consecutive stages (two-stages theory), first with more general EPs to obtain a coarse information about the object properties and then, if the information collected are judged insufficient for the task, with a deeper exploration involving more specific EPs. This means that the choice of the next exploration movement is driven by a step-by-step acquired knowledge, following a “bottom-up” logic as well as a “top-down” one [10], [12]. More recent studies [13]–[16] confirm Lederman’s and Klatzky’s observations.

A study [13] that investigates the interdependences between finger movement direction and haptic perception of oriented textures shows that freely chosen movements used in free active exploration aim for a maximization of perceptual information gain; in case of orientated texture (e.g. grating surface, composed of periodically repeating grooves with a clear orientation defined by the grooves), people are better in discriminating the spatial period of the texture as they move more orthogonal to the texture. In fact, the frequency of the temporal cues is maximized when finger movements are directed orthogonally to the texture orientation and decrease as the finger movements direction moves from the orthogonal, until the frequency associated to the spatial period of the texture becomes zero with the finger moving

parallel to the grooves [13]. This study highlights also that people optimize texture perception by adjusting their movements in directions that maximize the perceptual performance; this adjustments of the movements in course of exploration appear only in the final stages of the exploration but not in the earlier stages. Thus, exploratory movements are adjusted on the basis of previously accumulated perceptual signals. The adjustments occur only after enough signals related to texture orientation are available, so haptic perception becomes more accurate as long as the exploration proceeds. Moreover, since the movement adjustment is influenced by the task and the movement kinematics depends on both the task and the texture characteristics, sometimes the task provokes some people to use cognitive strategic decisions that lead to nonoptimal and unnecessary exploratory movements, rather than natural and optimal exploratory procedures.

Another study [16] enhances this concept investigating the “expectancy-driven” adjustment of the exploratory movements, comparing the movements in the first stage of the exploration in case of predictable perceptual situation (i.e. situations in which a previous knowledge of the object is available) and in case of unpredictable ones (i.e. unknown objects). The results remark that only when a prior knowledge of the objects is available the exploratory movements are already adjusted in the earlier stages of the exploration, while in unpredictable situations the exploration occurs following the logic of the two-stages theory. Furthermore, people do not always try to optimize the exploratory strategies, especially when a high differential sensitivity is not required by the task.

As highlighted by Lederman and Klatzky [10]–[12], the instinctive exploration procedure for the perception of surface textures is lateral motion, rubbing the surface texture. The work in [14] investigates the kinematics of unconstrained tactile texture exploration using samples large enough to better reflect each subject’s natural exploratory strategies, avoiding the movements to be constrained by the sample surfaces geometry, and confirms that the EPs are dependent by the perceptual task as well as the surface characteristics. The used samples cover a wide range of perceptual qualities. According to the study, people explore the texture most of all (70%) using simple linear movements of the finger like distal-proximal movements and lateral scanning (radial-ulnar movements) (Figure 3), followed by complex motion such as circular ones (22%), followed by stationary movements like pressure (8%). The exploratory kinematics depends on the task and on the surface characteristics. Moreover, according to the study, people tend to use different scanning speeds when scanning different textures. For example, subjects tends to scan surfaces that are judged to be slippery faster than surfaces that are judged to be sticky, regardless of the task. Subjects adjust their exploratory strategy during exploration, for example the scanning speed evolves over time increasing significantly as the trial progresses.

Moreover, in [17] it is evaluated if perception of roughness of texture is independent of the manner in which we touch the surface, by testing six scanning conditions, such as direct touch, where the finger is in contact with the surface, and indirect touch, where the surface is scanned with a hand-held probe, active (moving the hand across a stationary surface), passive (moving the surface across a stationary hand), and pseudo-passive (subject's hand is moved by the experimenter across a stationary surface). The study [17] highlights that roughness constancy



is preserved during active touch and pseudo-passive touch but not passive scanning, emphasizing the role of proprioception in tactile perception.

Considering these observations, during the thesis work, passive touch has been exploited to analyse mechanical tactile stimuli with fixed boundary conditions, while perception campaigns have been performed with active touch.

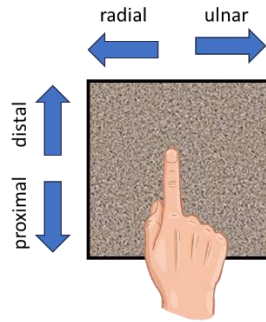


Figure 3: Sliding directions: proximal, distal, ulnar, radial.

## 1.2.4 Duplex-Theory of texture perception and tactile mechanical stimuli

The basic understanding of the mechanisms that lie at the origin of touch necessarily pass through the investigation of the mechanical stimuli that are detected by mechanoreceptors. Firstly Katz [18], and then Hollins and Risner [19], introduced the Duplex-Theory of tactile perception, which represent a turning point for researchers. According to the Duplex-Theory, the tactile perception of a surface texture is mediated by two coupled but different mechanisms: a "*spatial sense*" that allows the discrimination of coarse textures, and a "*vibration sense*" for the discernment of fine textures. Therefore, for discriminating the fine textures, a sliding contact between finger and surface is needed, generating transient cues (vibrations, transient skin deformations, mainly detected by RA II receptors). Instead, the coarse textures can be perceived with the sole static contact between fingers and surface (static pressure, skin stretch), and sliding contact is not necessary. Hollins and Risner [19] identified as coarse textures those having a spatial period  $> 200 \mu\text{m}$ , and as fine textures those with a spatial period  $< 100 \mu\text{m}$ . More recent studies confirm the theory and emphasize the main role of fingerprints in thresholding between coarse and fine textures [6], [20]–[25].

## 1.2.5 Friction-Induced Vibrations in tactile perception

From a mechanical point of view, sliding contacts involve presence of friction and vibrations. Whenever a sliding contact between two bodies occurs, Friction-Induced Vibrations (FIV) are generated at the contact (Figure 4) [26]. The interaction at the contact interface results in a

distribution of micro-impacts, local ruptures, 3<sup>rd</sup> body cracking and impacts that generate impulsive excitations and thus propagation of elastic waves that excite the system dynamics (FIV). According to the dynamic response of the system, the FIV may be stable or unstable (macroscopic stick-slip instability, negative friction-velocity slope instability, and modal instability) [27]–[33]. The FIV that occur at the contact between fingertip and surface of an object during a haptic process are mostly stable contact-induced vibrations: the system dynamics remain stable, and the vibrations excited by the contact are damped by either the material damping and the energy dissipation at the contact interface. Moreover, in an active free exploration of a surface, the brain is able to perceive the contact information in real time to adjust the boundary conditions to avoid possible stick-slip instabilities.

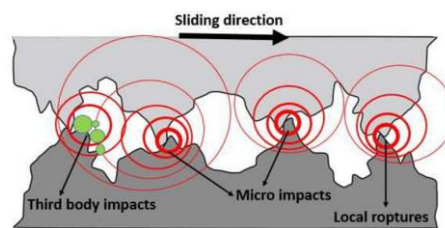


Figure 4: Friction-Induced Vibrations generation at the sliding contact pairs.

The Duplex-Theory enlighten the role of vibrational stimuli in fine texture discrimination [18], [34], [35], giving rise to a line of research investigating the role of FIV in tactile perception. Although we are still far from achieving a clear understanding of the phenomena underlying the texture perception, in the past two decades research in this field had significantly advanced. Several works investigate how Friction-Induced Vibrations encode the topographic characteristics of textures and mediate perception and discrimination of textures.

According to these studies, the acceleration RMS and frequency distribution of the FIV, originated by the fingertip scanning of a texture, show typical features depending on the surface topography, the exploration dynamics, the contact boundary conditions, the direction of exploration, and the fingerprints characteristics [6], [21], [22], [24], [25], [36]–[45]. Key features of the FIV stimuli (as well as friction and forces) have been investigated when exploring different kind of textures: textiles [22], [37], [40], [44],[22], [46]–[48], periodic [6], [22], [25], [36], [48], isotropic [36], [41], and common object’s surfaces [24], [38], [42], [49]. For example, FIV spectra associated to fabrics can show well-defined frequency peaks, linked to the spatial period of the texture, and a broadband frequency content, linked to the isotropic component of the fibre hairiness [22], [44]. In [37] induced vibrations are investigated in woven fabrics as a function of yarn density, yarn fineness, and number of yarns in unit pattern. In periodic textures, the fundamental frequency peak of the induced vibrations is given by the ratio between the sliding speed and the smaller wavelength between the one of the fingerprints and the one of the sample roughness [6], [20], [25], [36], [38], [43]. In fact, the fingerprints wavelength are found to play a fundamental role in filtering the FIV stimuli, affecting as well the threshold between coarse and fine textures perception fields [6], [21]–[24], [36]. It has been observed as well that sliding speed affects almost linearly the amplitude (RMS) of FIV

induced by the texture exploration, and implies as well a shift of the acceleration spectra towards higher frequency contents, independently from the texture [22]–[25], [36], [38], [42], [45]. Higher velocity means more energy exchanged at the contact. Studies focused as well on the FIV (and mechanical stimuli in general) dependence by the sliding direction [20], [41], [47], highlighting the proximal as the direction which maximizes tactile signals, while lateral scanning is characterized by more frequent occurrence finger instability and stick-slip phenomena. Moreover, in [41] mechanical stimuli and discriminative perception have been evaluated when sliding the finger both in proximal and distal direction, showing that distal direction is characterised by a high occurrence of stick-slip and discontinuous contact and a different fingerprint deformation, leading to a lower performance in discrimination than distal sliding. The role of stick-slip in altering the perceived surface roughness has been furtherly investigated in [48]. Moreover, the surface discrimination has been found to be less performing with lower scanning speed, because of occurrence of stick-slip instability [41] and lower power furnished at the contact. FIV features, such as amplitude and frequency distribution, have been found to mediate between texture topography and discriminative perception [6], [24], [50], since the tactile discrimination is found to be more linked to the characteristics of the mechanical stimuli rather than the texture topography. This is not surprising, since the coding of texture information passes through stimuli detected by mechanoreceptors and translated then into electric signals, sent to the brain. In particular, according to recent studies [6], [50] investigating the relation between the topographical characteristics of well-defined periodic textures and mechanical tactile stimuli, FIV mediation of the perception is well testified by a strong correlation with both the hedonistic feeling (such as ‘I like’, ‘I like a lot’, ‘I do not like’, ‘I do not like at all’) of the textures and surface perceptual descriptors (such as ‘smooth’, ‘rough’, ‘adhesive’, ‘textured’, ‘vibrating’).

The present thesis is collocated into the line of research investigating the role of FIV in tactile perception, giving continuity to the works discussed in this section.

## 1.2.6 Forces and friction in tactile perception

Sliding contact in surface exploration also means the presence of frictional forces: a broad line of research focuses on the role of contact forces and friction in surface perception, ranging from isotropic [41], [51]–[53] and periodic [22], [54] rigid textures, to textiles [47], [55],[22], [56] and beyond [57]. The investigation of the role of contact forces, and particularly friction, in mediating tactile perception is of extreme importance, but studded with complexities. As an example, the contact pairs between a finger and a rigid surface (i.e. rigid with respect to the finger) involves the finger with its fingerprints topography and sebum production, which provides a highly nonlinear behaviour with respect to the contact parameters. In fact, changes in finger/surface contact force provoke deformation in the skin relief constituting the fingerprints and the ejection of sebum, bringing to changes in the real contact area with respect to the theoretical one, altering the constraint between finger and surface; The same happens when changing other contact boundary conditions, such as the sliding speed, or direction of exploration, or the texture features [22], [41], [54]. Adhesion and stick-slip occurrence need

to be taken into account as well [26], [54]. When dealing with textiles, the investigation on friction and forces becomes even more complex, since both surfaces are deformable, with relating compliance and accommodation phenomena. Moreover, the variability of the friction coefficient for different subjects must to be taken into account [47], [53], [55]–[61], since the physiochemical and mechanical characteristics of the finger affect the friction behaviour.

Although its utmost importance in tactile perception, the role of friction is not deepened in this work, since the present thesis is focused on tactile vibrational stimuli.

### 1.2.7 Mastering of tactile stimuli: an ongoing challenge

In the vast panorama of sensory experiences that connect us to the external world, the sense of touch remains one of the most enigmatic and least comprehended. For decades, we have conquered the mastery of acoustic and sight stimuli, and the signals underlying them, i.e. pressure and electromagnetic waves, which can be well rendered by acoustic devices and visual displays. Acoustic and visual interfaces have been integrated into our daily lives, becoming indispensable companions in our modern world. On the contrary, understanding and replicating the intricate mechanisms of tactile perception continues to elude our complete grasp. The comprehension of tactile mechanical stimuli and the ability to render these stimuli (as we make for acoustic and visual ones) go hand in hand. However, differently from hearing and sight, touch involves a complex interplay of the musculoskeletal and proprioception systems, and it encompasses a wide range of mechanical stimuli, including forces, friction, vibrations and temperature, among others, activating numerous types of receptors. Mastering the world of haptics and tactile rendering is still an ongoing challenge. The so-called “surface haptics” (i.e. haptics for interactive surfaces [62]) represents a great enhancement of the current human-machine interface technologies and a new channel to interact with virtual environments. Haptics encompasses a wide range of different applications and types of haptic feedback, of varying complexity and very different goals. As an example, in our daily life we are all used to deal with devices like mobile phones, tablets, and videogame controllers, that are already able to deliver some simple haptic feedback, such as vibrations, pulses, bumping and buzzing effects. More recent research in the field of surface haptics aims to the possibility of rendering shapes, surface features and fine textures with computer interfaces, displays, handheld or wearable devices, creating the sensation of roughness, smoothness, softness, or hardness when users interact with virtual surfaces or objects.

The present work addresses the development of a tactile devices, specific to simulate surface textures, thus, in the following, literature more specifically related to texture rendering devices is provided.

## 1.2.8 Tactile rendering of textures

In the vast panorama of haptics, the focus of the present work is on the rendering of textures. In recent years, the development of tactile rendering devices is surging, exploring a variety of mechanisms whose tactile feedback is based on different mechanical signals such as friction, forces and vibrations [62]–[66]. The most commonly used approaches for rendering surface shapes and textures include vibrotactile [67]–[74], electrostatic [75]–[82], and ultrasonic [55], [59], [60], [83]–[86] devices. Some efforts are being made to combine multiple rendering modalities, such as vibrotactile and friction modulation, into a singular device to simulate touch in a more complete manner [87]–[90]. Electrostatic and ultrasonic devices are based on friction modulation [66], while vibrotactile rendering is achieved by evoking tactile sensations through vibrations generated by different actuators and dynamic exciters. In electrostatic devices, modulation of friction is achieved by generating electrostatic attraction forces between the user’s fingertip and the device’s surface. Ultrasonic devices are based on the air film that is generated between the user’s fingertip and the vibrating display, that is actuated at ultrasonic frequencies, which fall in the frequency range that can not be directly detected by mechanoreceptors. The vibrotactile rendering approach is already used to recreate some simple haptics effects or feedback, for example in mobile phones and videogame controllers. Recently the possibility of using it to obtain a vibrotactile rendering of textures and fine surface roughness has been explored [67]–[72]. For the three rendering modalities (vibrotactile, electrostatic, ultrasonic), a data-driven approach is often used: mechanical signals are acquired from real surface textures to be subsequently reproduced by the device [55], [67]–[71], [75]–[77], [83], [88]. Databases of mechanical signals, such as acceleration, velocity and friction forces, measured during real texture exploration, can be found in literature [91]–[93]. The most common approach in vibrotactile rendering consists in scanning the surface using an object or a rigid tool such as a stylus, equipped with vibration and force transducers, which mediates the contact between finger and texture, both in the measurement phase and in the tactile rendering one [67]–[71], [88], [93]. However, this approach ignores the primary role of the skin, and therefore the fingerprints, in the generation of the stimuli at the contact interface (see sections 1.2.4, 1.2.5, 1.2.6). Touch involves manipulation and physical interaction between the finger and the object to be perceived, and this is what happens when interacting with a tactile rendering device as well. In this regard, several studies investigate the interaction between fingertip and tactile device [25], [73], [94]–[97].

Within this broad framework of different tactile devices, working with different physical principle to modulate friction, induced vibration or both of them, a particular focus is here placed on the role of vibrational stimuli and the respective mimicking device.

## 1.3 Positioning of the Ph.D. Thesis

---

Although a considerable knowledge is being acquired in the field, much is still unknown about the path from surface texture, through mechanical stimuli, to tactile perception and discrimination. We are still far from mastering tactile stimuli, both in terms of basic understanding and in terms of development of haptic devices able to deliver a faithful and global reproduction of tactile sensation (section 1.2). As reported in the previous sections, different lines of research, all of main importance, focus on the role of different mechanical stimuli in touch processes.

The present Ph.D. thesis collocates in the line of research that investigates the role of vibrational stimuli (FIV) in the tactile perception of textures, of which an overview has been given in section 1.2.5. On one hand, needing to clarify the features of the stimuli that are strictly related with our perception of textures, analyses of mechanical vibrational stimuli are carried out on different rigid textures having different topographies (isotropic, periodic), in order to identify the main features of FIV stimuli (amplitude, frequency distribution) which encode the topographical characteristics and mediate their tactile perception. On the other, a vibrotactile device, able to reproduce the FIV stimuli, is developed. The approach is based on measuring, and then rendering by a vibrational actuator, the FIV stimuli generated by texture exploration, collocating it in the panorama of tactile devices presented in section 1.2.8 (vibrotactile, data-driven approach). Apart from possible technological applications, the developed vibrotactile device is used in this work to decouple mechanical stimuli from other tactile ones, as a tool to push over research on the role of different FIV features in tactile perception of textures. To achieve a correct simulation of the FIV stimuli, the dynamic response of the finger when interacting with both real surface textures and the device has been investigated as well. During the whole development of the Ph.D. work, the tribological and dynamic analyses have been accompanied by discrimination campaigns, on real and simulated textures, with the aim of deepen the relationship between mechanical vibrational stimuli and perception, up to a specific campaign (in collaboration with the Cognitive Neuroscience Laboratory (LNC) of the Aix-Marseille University) where the brain response has been monitored as well by EEG technics.



# Chapter 2

## Materials and method<sup>1</sup>

This chapter offers an overview of the approach and a comprehensive description of the test benches, protocols, and methodologies employed to carry on the presented work. The opening section provides an overview of the work and outlines the overall approach exploited for its execution. Then, the different sample surfaces, exhibiting either periodic or isotropic topography, are presented and the experimental setups are described. The tactile rendering device called “PIEZOTACT” used throughout this work, is introduced as well. Finally, details are provided on the protocols for the discrimination campaigns of real and simulated surfaces, by outlining the procedures and methodologies employed to assess participants' ability to discriminate different surfaces when interacting with various real and simulated textures.

It should be noticed that the test benches, presented in their reference configuration in this chapter, will be revisited and utilized, in the subsequent chapters, with slight variations as a function of the various experimental campaigns object of this work.

---

<sup>1</sup> The content of this chapter has been partially published in [98]–[100].



## 2.1 Work overview and overall approach

---

This PhD thesis aims to delve into the complex phenomenon of tactile perception, with a specific focus on exploring the relationship between surface topography, mechanical stimuli, perception and discrimination of different surface textures, up to the mimicking of significant mechanical stimuli by a tactile device, with a spot into the brain response. Within the multidisciplinary panorama of disciplines involved into touch (Figure 2), Figure 5 shows the areas of investigation and contributions involved in this PhD thesis, focused on biomechanics, with some bricks in psychology and neuroscience.

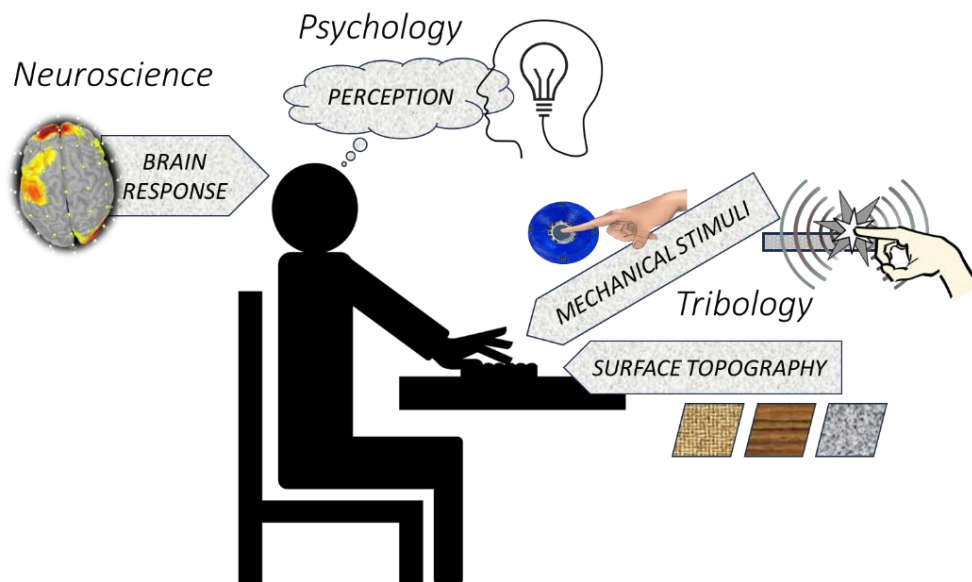


*Figure 5: Areas of investigation of the PhD thesis, within the several disciplines involved into tactile perception.*

From the interaction between finger and surface, tactile stimuli are generated when exploring a surface. In order to understand the correlation between mechanical stimuli and the perception of textures, both the analysis of mechanical stimuli and their mimicking by means of a tactile rendering device are treated in a synergistic way. Figure 6 shows a scheme of the overall approach.

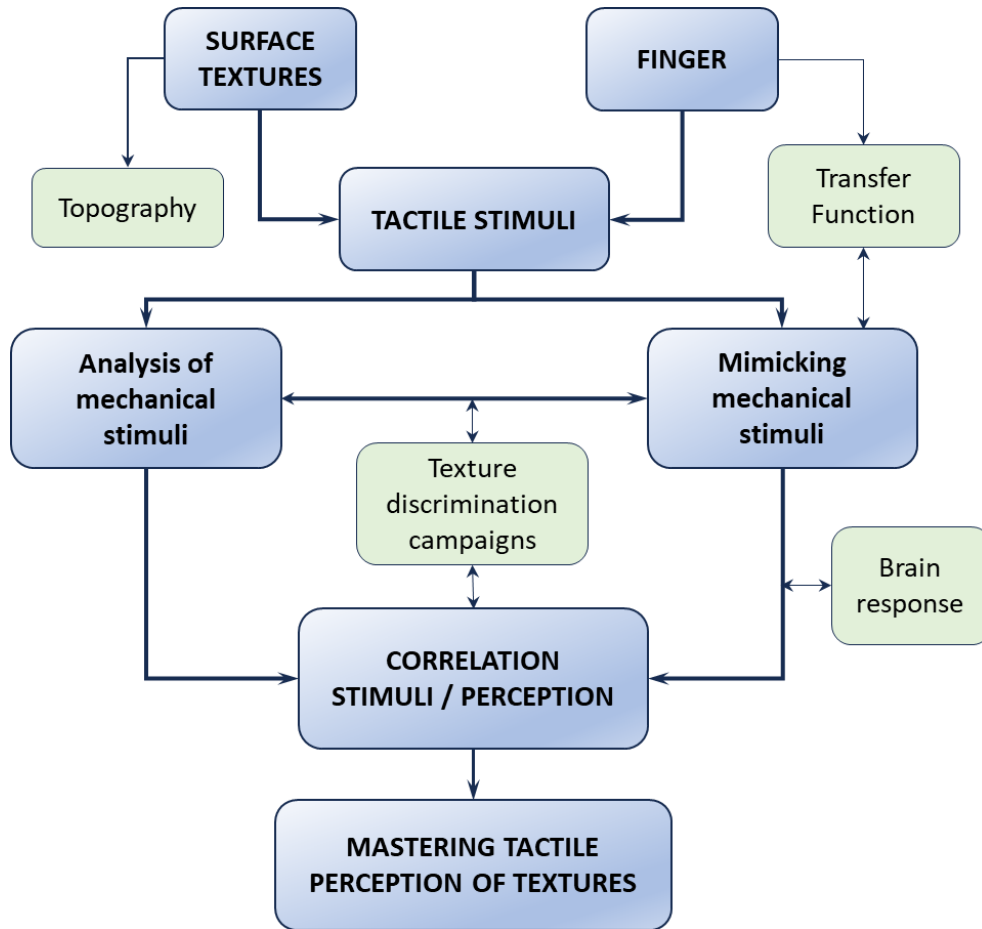


Figure 6: Flow block scheme of the overall approach.

In the first instance, the link between mechanical stimuli and texture topography has been investigated when the finger interacts with either periodic or isotropic textures. Mechanical stimuli (contact forces, friction, Friction-Induced Vibrations) have been measured and analysed using two different methods of exploration: active and passive touch. Particularly, the Friction-Induced Vibration (FIV) stimuli have been analysed to identify the key features of the signals (amplitude, frequency distribution), which encode the topographical and perceptual characteristics of the different textures (Chapter 3).

In parallel, the vibrotactile rendering device PIEZOTACT has been developed to mimic, by means of a dynamic actuator, the FIV measured during the exploration of the real surfaces. The developed rendering strategy, which allows to reproduce the vibrational stimuli, is based on the exploitation of the overall Transfer Function of the device, including the user's finger. The device, and the rendering methodology that underlies it, have been experimentally verified (by comparison between original and mimicked FIV) and then validated through texture (periodic and isotropic) discrimination campaigns, carried out on panels of participants involving both real and simulated surfaces (Chapter 4).

A special attention has been paid on the interaction between the finger and the tactile device as well. Being at the basis of the developed rendering device, the Transfer Function has been

extensively investigated through parametric analyses for different contact conditions and participants. An average Transfer Function among participants has been calculated to feed the tactile device. Discrimination campaigns on real and simulated isotropic textures have been conducted to validate the effectiveness of using the average Transfer Function to process the FIV signals for tactile rendering (Chapter 5).

A spot into the brain response arose from a collaboration with the Cognitive Neuroscience laboratory of the University of Marseille and the Cognitive Psychology laboratory of the University of Bourgogne, in which the mechanical stimuli and the electroencephalographic (EEG) signals have been contextually measured during the exploration of real surfaces and during the reproduction of such surfaces by the PIEZOTACT device, in different test conditions (Chapter 6).

The different bricks of the work have been developed in a complementary manner: while the analysis of the mechanical stimuli allowed for identify their role and features in tactile perception of texture, the rendering vibro-tactile device has been exploited to decouple the stimuli and to specifically modify their features for investigating their role in the discrimination of textures. In a similar way, thanks to the rendering device, the isolation of the FIV stimuli, from other mechanical stimuli arising from the contact interaction or the motion of the subject, allowed to depict some features in the brain response to texture exploration.

## 2.2 Surface samples

---

Although a particular emphasis given to isotropic textures, this work ranges between the analysis of periodic and isotropic surfaces and the comparison of the stimuli associated with them, aiming to a deeper understanding of the interplay between topography, mechanical stimuli, perception and discrimination of textures, with a look to the brain response. The periodic and isotropic surfaces, that will find ample space in this work, are accurately described in the following.

### 2.1.1 Periodic surface samples

A collection of 12 microtextured periodic surface samples, with well-controlled periodic topography, has been employed to generate tactile stimuli. These samples, provided by the FEMTO-ST Institute of Besançon, have been previously subjected to comprehensive psychological and mechanical analysis in prior studies [6], [50].

The samples consist of rectangular plates made of polyurethane resin (Rencast FC52), measuring  $25 \times 60 \text{ mm}^2$  and having a thickness of 3 mm. Their production involved a complex series of steps, encompassing photolithography and plasma etching of silicon wafers, followed

by a moulding and replication procedure [6], [50]. These samples present a surface topography characterized by cylindrical "dots" arranged in a hexagonal pattern (Figure 7). The characteristic dimensions defining them include the height of the dots (H), the diameter of the dots (D), and their spatial period (Sp), representing the distance between the dots. The surface periodicity (intended as the periodicity of the texture along a line parallel to the dot series) is quantified using the equivalent wavelength  $\lambda = D + Sp$  as a unique indicator.

In preceding research, these samples underwent psychological assessment to delineate perceptual descriptors [50], together with an extensive tribological investigation establishing strong links between their topographical characterization, mechanical stimuli (especially friction-induced vibrations) and their perceptual and hedonistic classification [6]. Table 2 furnishes the topographical data, acquired through a 3D variable focus microscope (Alicona InfiniteFocus), and their perceptual and hedonistic categorization [6], [50].

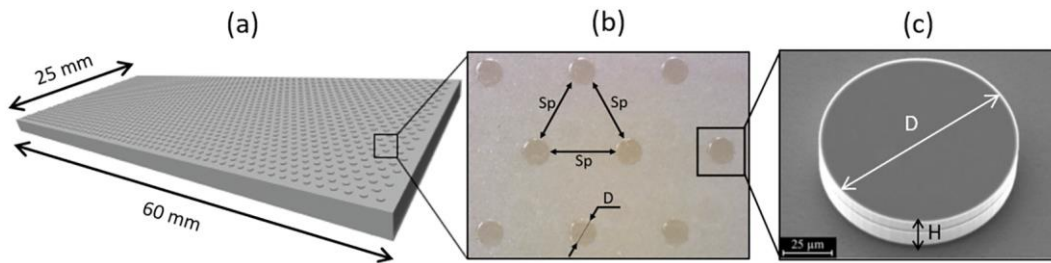


Figure 7: Periodic surface samples topography and geometric features: (a) scheme of an overall textured sample, (b) optical microscopic observation of a sample surface, (c) scanning electron microscopic observation of a cylindrical dot.

Table 2: Periodic samples topographical data and perceptual and hedonistic categorization.

Sample denomination	Height H [μm]	Diameter D [μm]	Spatial period Sp [μm]	Equivalent wavelength λ [μm]	Perceptual category	Hedonistic category	Uniformity of judgment
M1	27	107	13	120	smooth	I like a lot	✓
M2	24	107	53	160	smooth	I like a lot	✓
M3	19	22	28	50	smooth	I like a lot	✓
M4	38	108	111	218	textured	I like	✓
M5	55	208	109	317	textured	I like	✓
M6	18	71	113	184	textured	I do not like	✓
M7	14	207	111	318	textured	I do not like	✓
M8	18	106	607	716	rough	I do not like at all	✓
M9	14	207	318	524	rough		x
M10	27	502	114	616	adhesive		x
M11	29	797	116	913	adhesive		x
M12	15	12	126	138	textured		x

## 2.1.2 Isotropic surface samples

Aiming to investigate the link between surface topography, mechanical stimuli, tactile perception and discrimination of textures with isotropic (randomly rough) topography, a set of sample surfaces has been manufactured starting from sandpaper of different granulometry, by pouring epoxy resin into silicone moulds (Figure 8).

A detailed description of the production procedure follows below.

- A mould matrix has been designed and then produced by additive manufacturing out of PLA.
- A squared sample of sandpaper, having a 50 mm edge, has been glued on the mould matrix (Figure 8b).
- Bi-component silicone (ELKEM BLUESIL RTV 3428) has been prepared and poured in a container; then, the mould matrix has been immersed into the silicone (Figure 8c).
- Once the silicone solidified, the matrix has been extracted (Figure 8d) to obtain the silicone mould.
- Epoxy resin (Prochima E-30) has been poured into the obtained silicone mould.
- Once the resin solidified, it has been extracted, and squares having side of 50 mm and thickness of 4 mm have been obtained (Figure 8e).
- The sample identifier (i.e. the order of the corresponding sandpaper) have been engraved on the back of the sample.

The entire process described above has been replicated for each of the 13 samples, using sandpaper with varying granulometry, ranging from P40 to P4000. The selection of sandpaper with different grain sizes has been done purposefully to achieve a comprehensive set of samples covering a wide spectrum of textures, ranging from very coarse to very fine, all exhibiting isotropic randomly rough topography.

Additionally, an extra sample has been created as a reference, which did not have any specific applied texture. This reference sample has been obtained from the free surface of the epoxy resin and has been termed 'no texture.' However, it is worth noting that even the 'no texture' sample possessed its own texture, namely the surface topography resulting from the crystalline structure of the epoxy resin. In conclusion, the completion of the entire process yielded a collection of 14 sample surfaces (Figure 8a).

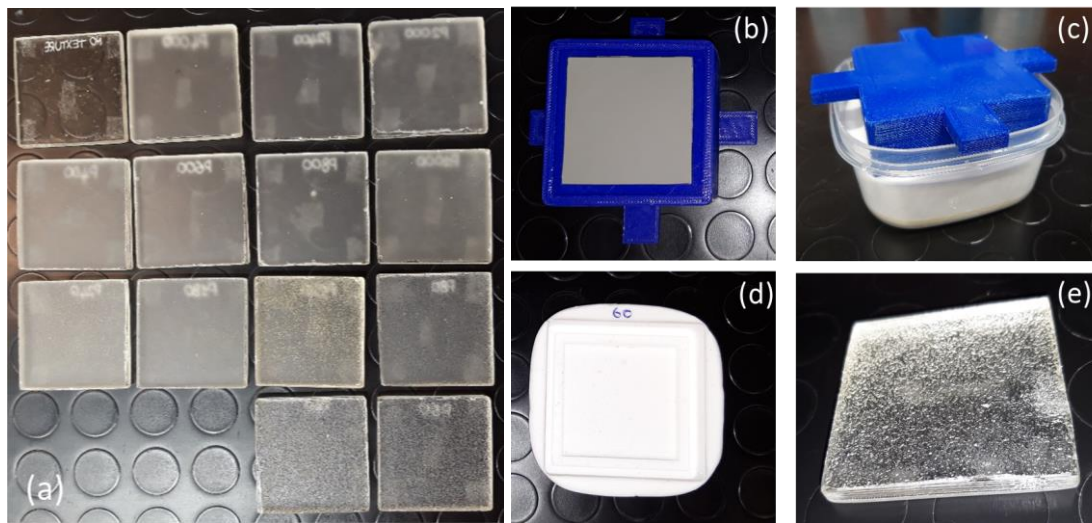


Figure 8: Manufacturing of isotropic samples: (a) the 14 isotropic epoxy resin surface samples; (b) mould matrix with the sandpaper glued on it; (c) mould matrix into the silicone; (d) obtained silicone mould; (e) obtained epoxy resin sample.

A topographic analysis has been conducted on the manufactured isotropic samples to obtain their topographical characteristics. The analysis has been carried out by a numerical microscope WHX-2000 Keyence (an example in Figure 9).

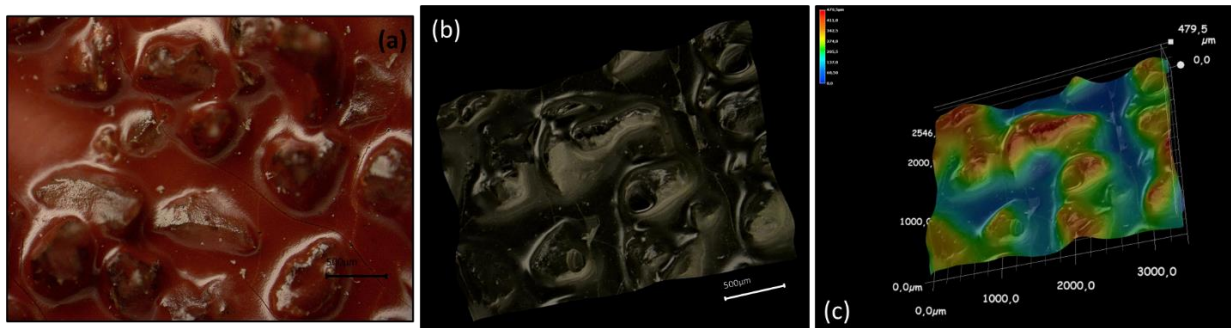


Figure 9: From sandpaper to epoxy resin sample (P40): observation with Keyence microscope of sandpaper (a), observation of epoxy resin sample (b) and its 3D topography colormap (c).

The data collected from the Keyence microscope have been then processed using the MountainsMap software, enabling the extraction of various roughness parameters (Figure 11) and the respective topographies (Figure 10).

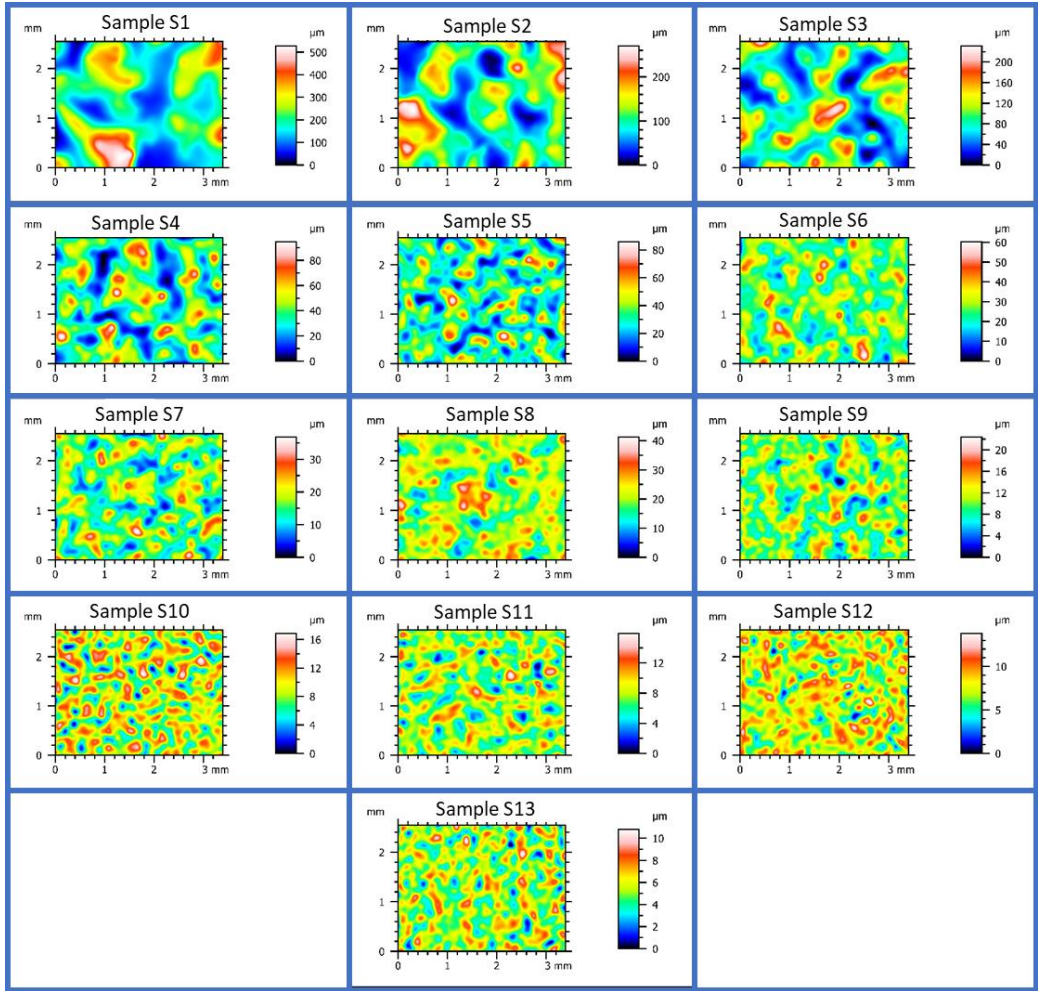


Figure 10: Isotropic sample topographies (VHX-2000 Keyence).

The trends of the three most common roughness parameters, Ra, Rz and Rq, exhibit a consistent pattern across the different samples. Their values are decreasing as the fineness of the texture increases, except for minor fluctuations in the samples with finer topography. Among these parameters, Ra has been deemed the most significant for this study, being the average of the absolute value of the profile. As it will be described in the following chapters, in this work, significant correlations have been identified between the roughness Ra and the perceptual and mechanical analysis of isotropic surfaces.

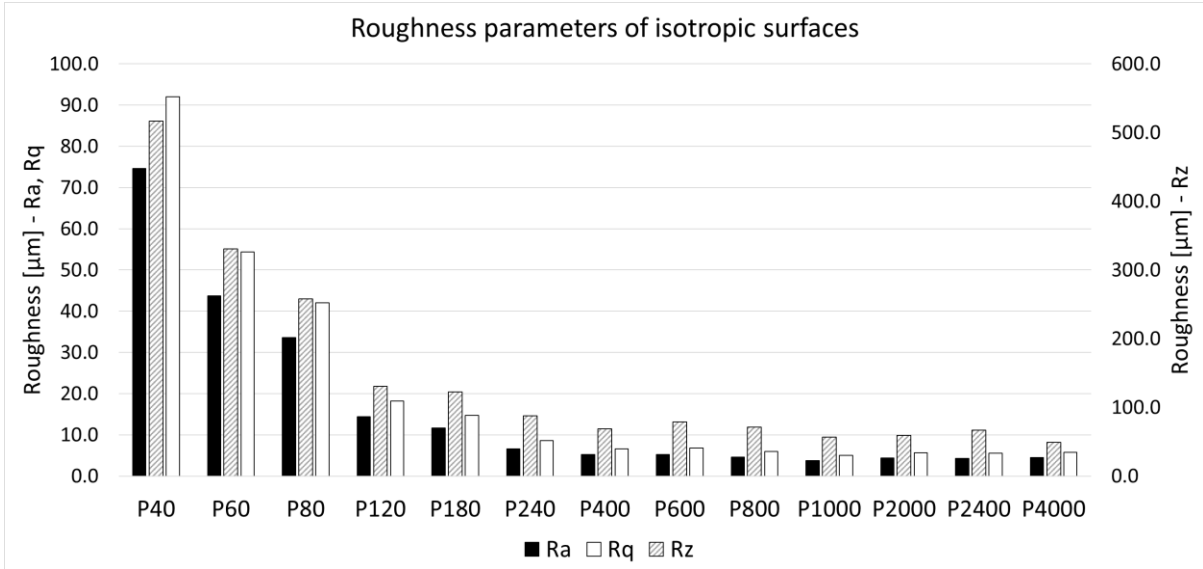


Figure 11: Isotropic sample roughness parameters obtained by the (WHX-2000 Keyence).

The samples have been then sorted according to the measured Ra roughness. Table 3 presents the roughness parameter Ra values for the manufactured samples, along with their corresponding original sandpaper grades. It should be noticed that samples S7 and S8, derived from P400 and P600 sandpapers, respectively, have been found to exhibit the same measured Ra, despite having distinct topographies (Figure 10). Therefore, it has been decided to order them based on their original sandpaper grades. The only inversion found in the Ra classification, with respect to the original sandpaper grade, has been obtained between samples P1000 and P4000 (denoted S10 and S13, respectively).

The roughness of the "no texture" surface, present in Table 3, has been obtained using a MarSurfPS10 mechanical profilometer, since it has not been possible to observe it under the microscope, due to excessive transparency.



Table 3: Isotropic sample roughness ( $R_a$ ) and original sandpaper grade.

Sample denomination	# Sandpaper	$R_a$ [ $\mu\text{m}$ ]
S1	P40	74.6
S2	P60	43.7
S3	P80	33.6
S4	P120	14.4
S5	P180	11.7
S6	P240	6.6
S7	P400	5.2
S8	P600	5.2
S9	P800	4.6
S10	P4000	4.5
S11	P2000	4.4
S12	P2400	4.3
S13	P1000	3.8
NO	/	0.1

## 2.3 Measurement of tactile mechanical stimuli

---

In this section, the experimental setups and the protocols used to measure the mechanical stimuli during the exploration of surface textures are described. Two distinct types of protocols have been employed: one based on active touch, and another one based on passive touch.

In active touch, the subject interactively and voluntarily explores the surface, imposing the contact boundary conditions (sliding speed, contact forces, exploratory movements, angle between finger and surface, etc.). Both the proper sense of touch and the kinesthetic sense are activated.

In passive touch, no kinesthetic sense is involved, the finger is kept fix, and the surface is set in motion by an external mechanical system, which partially controls the contact boundary conditions.

The approach based on active touch facilitates measurements with semi-controlled or free-exploratory protocols, enabling replication of more realistic touch conditions. On the other hand, the approach based on passive touch enables more deterministic measurements with controlled parameters, particularly sliding speed, allowing as well for the possibility of conducting parametric analyses, providing valuable insights into the influence of different parameters on the mechanical stimuli elicited by touch.

Throughout the present work, two test benches have been designed and then used synergistically to obtain combined and complementary information about the phenomena under investigation, i.e. a comprehensive understanding and replication of the mechanical stimuli associated with different surfaces, tactile perception and discrimination processes.

### 2.3.1 Active touch test bench (ActTouch)

A test bench (Figure 12) has been developed to measure the mechanical stimuli during active touch, which is the natural mode used to explore the surface textures. The sample surface is fixed with double sided tape on the top of a triaxial force transducer (Testwell K3D60) to recover the contact forces (normal and two tangential components, from which the friction coefficient is then obtained). To perform the active touch tests, the participant slides the finger on the surface sample, while an accelerometer (PCB 352A24, PCB Piezotronics, Inc.) is fixed by wax on the fingernail to measure the FIV (acceleration) signal originated by the finger scanning on the surface sample. This allows ample freedom of movements for the subject, who can freely explore the surface in various directions, in a circular motion, or in a completely free way, as in real conditions of tactile interaction with a rigid surface.

The active touch experimental setup, used to measure the forces and FIVs originated by the finger/surface sliding contact, is shown in Figure 12. The boundary conditions, such as sliding velocity, contact forces and finger/surface angle are imposed by the participant. The signals from the transducers are acquired by a SIRIUSi (DeweSoft) DAQ system at a 5kHz sampling frequency.

Although this test bench allows active touch measurements to be made with any exploratory movement, for the tests object of this work a semi-controlled measurement protocol has been opted for. The following constraints have been therefore introduced on the boundary conditions, imposed by the participant. It has been decided to explore the samples in proximal direction, by sliding the finger on the sample and then lifting it between subsequent strokes, so that a longitudinal (sliding velocity parallel to the finger axis) non-alternating proximal exploratory motion has been achieved, allowing for maximizing vibratory signals and reducing the occurrence of stick-slip phenomena (see section 1.2). It has been asked to the participant to maintain a normal contact load approximately around 0.2 N and a finger/surface angle of approximately 15-20 degrees. Moreover, the participant has been asked to maintain (autonomously or with the aid of a metronome) approximately the same exploration time during all the trials. For each surface, the protocol of the surface exploration has been repeated at least 15 times. The acquired data have been then exported to Matlab software to be post-processed.



Figure 12: Active touch test bench for measurement of tactile mechanical stimuli.

Through the active touch test bench ActTouch, it is possible to explore the samples by longitudinal, transversal, circular or completely free movements. The aim of this work is to test a procedure for measuring and reproducing FIV for a tactile rendering of surface textures. Therefore, for a preliminary approach, an exploration trajectory has been chosen to optimize vibrational signals for tactile rendering.

On the basis of the literature (Chapter 1) and a preliminary analysis [101] a proximal longitudinal exploratory movement has been opted for. Figure 13 shows an example of longitudinal and transversal exploration of a sample from [101]: the contact during the transversal sliding is characterized by a strong mechanical instability of the finger, leading to the occurrence of stick-slip and lower reliability of the measurements. Moreover, when stick-slip is avoided, the main frequency content can be recovered in both sliding directions, but the amplitude of vibration is lower in case of transversal sliding, with respect to the longitudinal one (in Figure 13 the Y-scale is different to facilitate the plot readability). The main frequency peaks are more defined and characterized by a smaller bandwidth in the longitudinal direction. These findings are in agreement with the literature [6], [41], [43], [45]. In the first instance, these observations suggested to prefer the longitudinal sliding, rather than the transversal one, for FIV analysis and rendering.

In [101], a circular exploration of the samples has been evaluated, as well, through FIV signal analysis and reproduction, and through a preliminary discrimination campaign of surfaces, which has shown that the discrimination performance was superior for longitudinal rather than circular exploration. Moreover, circular exploration has been observed to be strongly affected by a frequent occurrence of stick-slip instability as well (as transversal exploration), while the longitudinal sliding is characterized by a more stable frictional and dynamic response.

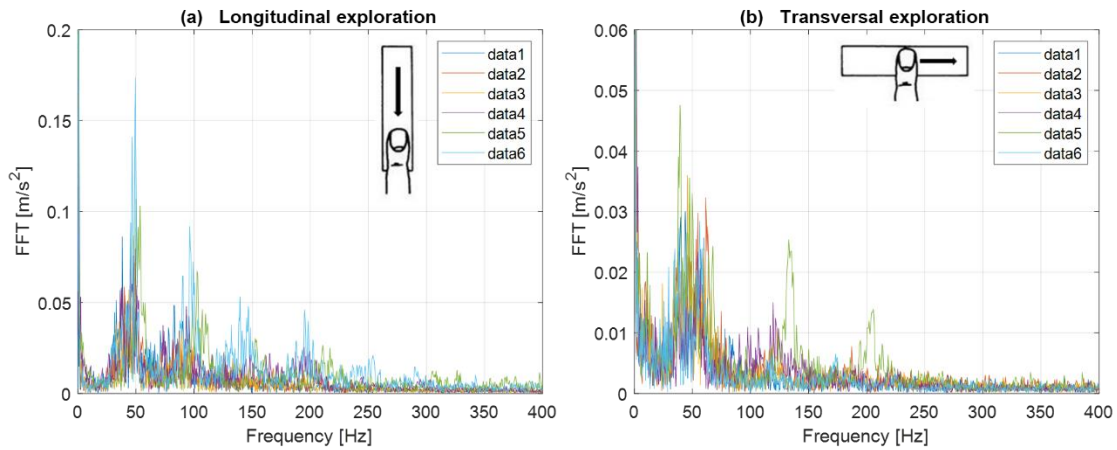


Figure 13: FIV from active longitudinal (a) and transversal (b) exploration of a periodic sample.

About the contact force to be exercised during the surface exploration, on the basis of FIV measurements and reproduction tests carried out in [101], it has been decided to set the normal force during surface exploration at 0.2N. In fact, from the literature [6], [102] the most used value for the force maintained during the surface exploration was 0.4N, but this value has been judged unnatural and associated with a strong occurrence of stick-slip and adhesion when exploring the samples used for this work, both the periodic [101] and the isotropic ones. In fact, it should be noticed that the contact force, exerted by a subject when exploring a surface, is strongly affected by the adhesion (sticking) between surface and fingertip skin. The more adhesive the surface is, the more easily stick-slip occurs, leading the subject to decrease the applied force. Preliminary tests [101] led to set a contact force of 0.2 N for the used samples. Finally, the finger/surface angle has been fixed at about 15 – 20 degrees, considering the data available in literature [6], [102].

### 2.3.2 Passive touch test bench (TriboAir)

The TriboAir test bench (Figure 14) is a linear tribometer that has been developed, before the current study, to investigate the mechanical signals arising from the sliding contact between two bodies, in particular the Friction-Induced Vibrations.

Since the FIV, induced by the finger/surface interaction, are generally characterised by low amplitudes, it is important to prevent parasitic vibration and noise coming from the mechanical system and other contact interfaces. The Triboair test bench allows to avoid parasitic vibrations thanks to the design of the moving platform (on which the surface sample has been mounted) driven by four air bearings, moving along two shafts, and a voice coil actuator. Thus, the platform is completely suspended on air, and the only contact originating FIV is the one under investigation. The controlled sliding motion is ensured by a linear voice coil actuator (BEI KIMCO LA30-75-001A) and a linear optical encoder (MicroE OPS-200-1-1), which allow to define the law of motion and the platform sliding velocity thanks to a PID controller (ELMO

Gold DC Whistle, G-DCWHI10/100EE). The contact forces are measured by two tri-axial force transducers (KISTLER 9017C) mounted on the platform.

It is a multi-purpose test bench, which has been developed and has found application in the investigation of various tribological phenomena (e.g. contact instability and stick-slip phenomena in dry and lubricated contacts) spanning from the aerospace engineering field, to applications in various kinds of braking systems, to tactile perception and beyond [25], [29]–[33], [99], [103]. In the present work, it has been exploited to investigate the mechanical stimuli associated with passive touch in controlled conditions, allowing parametric analyses with respect to the contact parameters and more deterministic and repeatable measurements. In particular, it is possible to control the sample sliding speed, in order to perform tests with a constant relative velocity between fingertip and surface.

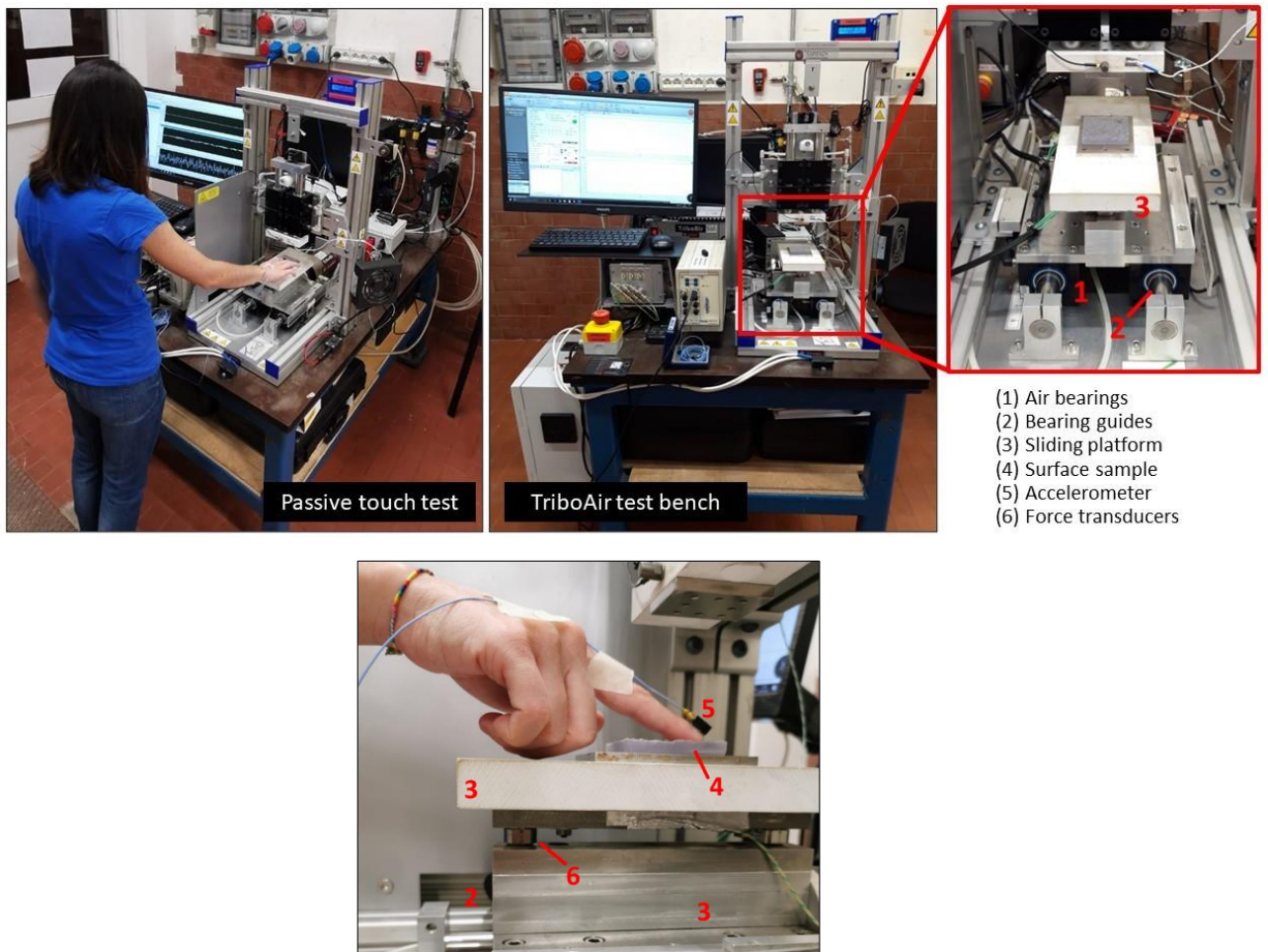


Figure 14: TriboAir test bench configuration for passive touch measurements of mechanical stimuli.

To perform the passive touch measurements, the participant is asked to place the finger on the surface sample, fixed on the top of the moving platform. A trapezoidal profile of the speed is imposed to assure a constant sliding speed of the platform within the measurement track (Figure 15). The normal contact force between finger and surface, which can be monitored during the test on the monitor, is imposed directly by the participant. The participant is asked to maintain a constant normal load of approximately 0.2 N, (consistently with the active touch protocol). The participant arm can be placed on a support to maintain a constant finger/surface inclination (about 15-20 degrees), and to help the participant to keep the finger stationary and the normal force constant. Before the platform motion starts, the participant places the finger on the surface sample. Since the finger is motionless and the Triboair platform slides in distal direction, with respect to the finger, the relative velocity of the finger with respect to the surface sample results to be in proximal direction. Then, after the surface sliding motion ends, the participant lifts the finger. The same test is repeated at least 6 times for each surface. The FIV (acceleration) signal is acquired by an accelerometer (PCB 352A24, PCB Piezotronics, Inc.) glued by wax on the fingernail of the participant. The data are acquired by a National Instruments (NI4472) acquisition board, at a sampling frequency of 5kHz. The acquired data are then exported to Matlab and post-processed.

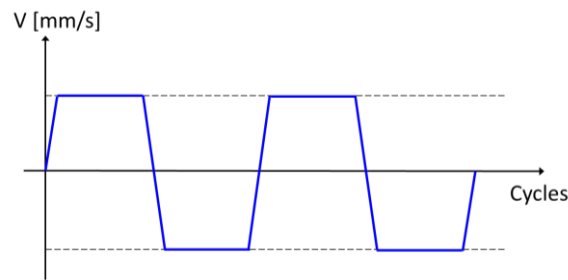


Figure 15: Trapezoidal sliding speed profile imposed to the TriboAir.

## 2.4 Tactile rendering device PIEZOTACT

This paragraph describes the tactile rendering device, named PIEZOTACT, that represents one of the highlights of this work. In this section it is introduced and detailed from the point of view of its components, while the actual tactile rendering methodology, its experimental verification and validation through discrimination campaigns on periodic and isotropic textures, will find ample space in the dedicated Chapter 4.

The purpose of the device is to reproduce by means of an actuator, the FIV previously measured from the exploration of real surfaces. The actuated vibration can be perceived by placing the fingertip in contact with the surface of the actuator. The used actuator is an electro-active polymer (EAP) piezoelectric actuator, supplied by CEA LITEN of Grenoble (France). It has been chosen because of its interesting characteristics from a technological point of view, such as its lightness, its small thickness and its flexibility (which therefore allows it to be integrated even in flexible surfaces); moreover, a certain degree of transparency can be achieved [104]–[107]. These characteristics make it suitable to be applied in wearable devices, such as tactile gloves, as well as in tactile display, touchscreens etc. The actuator is printed with a piezoelectric ink, constituted by the EAP vinylidene fluoride-trifluoroethylene (PVDF-TrFE) copolymers, on a flexible polyimide substrate. The printed piezo ink film expands when a voltage is applied, resulting in the bending of the actuator, and thus allowing out-of-plane vibrations. The used printed actuator has a typical actuation voltage up to 200Vpp in the frequency range from 1Hz to 10000 Hz, a capacitance of 80nF at 1000 Hz and a current consumption of 1mA at 200Vpp and 300Hz. The design, fabrication, and characterisation of the used PVDF-TrFE actuator are detailed in [104].

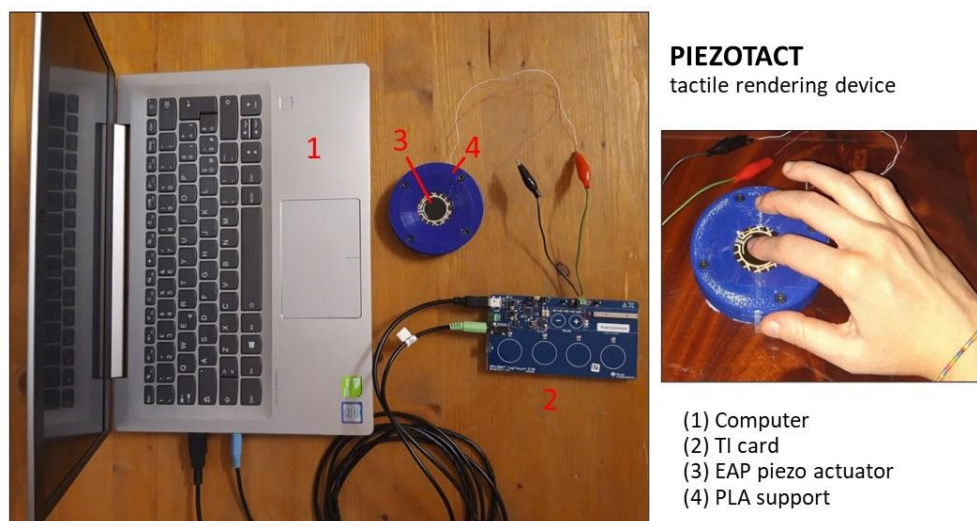
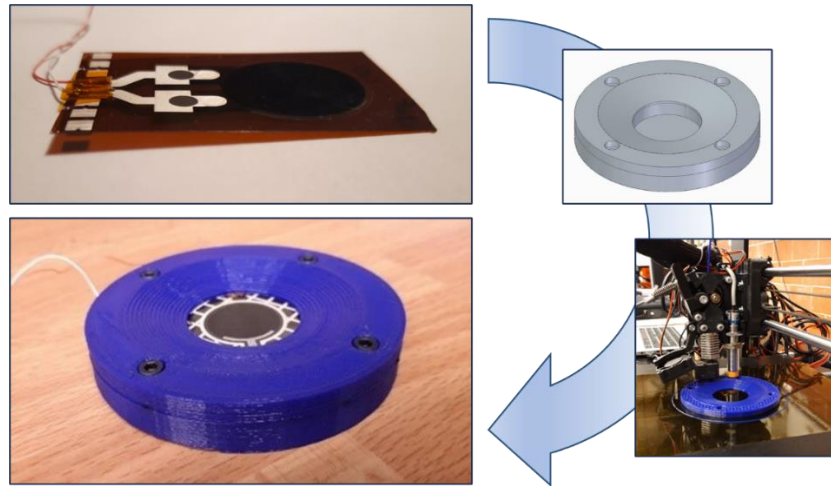


Figure 16: PIEZOTACT vibrotactile rendering device.

The actuator is held into an ergonomic support produced by additive manufacturing out of PLA (Figure 17). The actuator membrane is suspended over a central hole of the support, bounded along its circumference. The shape of the upper part of the support presents a sloped design to allow a comfortable placement of the finger on the actuator.



*Figure 17: The EAP piezoelectric actuator has been bounded into a PLA ergonomic support produced by additive manufacturing.*

An electronic card (Texas Instruments DRV2667EVM-CT) is used to drive the EAP piezo actuator. This electronic card integrates a boost converter that allows the amplification of the input signal according to 4 different gain levels, designated by the manufacturer as B1, B2, B3, B4. Starting from preliminary experiments [101], it has been decided to fix the gain on B3 for the tactile rendering protocol. The Texas Instruments (TI) board accepts as input an audio signal, which can be directly sent from a PC analogue output.

A commercial PC is therefore sufficient to send the analogue signal to the TI board, which drives the piezoelectric actuator EAP. This adds wide versatility to the device. During the course of this work, different commercial PCs have been tested, with similar performances (Lenovo Ideapad 520S-14IKB, HP Elitebook 830 G5 and Acer Nitro 5). The signal is sent by the PC audio card using the Matlab software.

The developed tactile rendering methodology will be discussed, verified and validated in the dedicated Chapter 4. The rendering method is essentially based on the preliminary characterization of the Transfer Function of the PIEZOTACT device, including the user's finger, and on its subsequent use in processing the FIV signals previously measured by exploring the real surfaces. This step is fundamental because it is not possible to send the FIV measured on real surfaces directly to the device: they would be strongly modified by the Transfer Function of the electro-mechanical system, so that the signal that would be reproduced by the actuator and perceived by the user would be a completely different one.



## 2.5 Characterization of finger Transfer Function

---

Therefore, the evaluation of the transfer function is crucial to process the input signals and to achieve the correct FIV signal by the device. This requires an in-depth analysis of the human finger transfer function and the transfer function of the overall system constituted by the PIEZOTACT and the finger. This section concisely describes the theoretical bases, the developed test benches used for the parametric analyses of the transfer function, which will then be presented in the dedicated Chapter.

### 2.5.1 Theoretical bases on Transfer Function

The Transfer Function characterization is a crucial point when investigating and mimicking FIV, and is at the basis of the tactile rendering technique underlying the PIEZOTACT device.

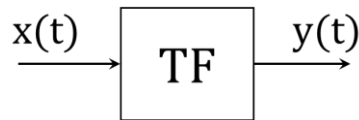


Figure 18: Transfer Function  $TF$ , input  $x$  and output  $y$ .

From a theoretical point of view, in case of deterministic signals (such as the FIV), in a dynamical LTI (linear time-invariant) system, the Transfer Function ( $TF(\omega)$ ) represents the ratio between the output signal  $Y(\omega)$  and the input signal  $X(\omega)$  in the frequency domain (Figure 18):

$$X(\omega)TF(\omega) = Y(\omega) \quad (1)$$

Where  $X(\omega)$  and  $Y(\omega)$  are, respectively, the Fourier Transform of the input time signal  $x(t)$  and the output time signal  $y(t)$ :

$$X(\omega) = \int_{-\infty}^{+\infty} x(t) e^{-j\omega t} dt \quad (2)$$

$$Y(\omega) = \int_{-\infty}^{+\infty} y(t) e^{-j\omega t} dt \quad (3)$$

It represents an intrinsic characteristic of the system.

A real system, such as the one under investigation, is generally non-linear, not time-invariant, and affected by measurement noise. In these cases, a statistical treatment is more appropriate.

In this optics, the Frequency Response Functions (FRF) (i.e. Transfer Functions) can be estimated on the basis of the following relations [108]:

$$H_1(\omega) = \frac{S_{yx}(\omega)}{S_{xx}(\omega)} \quad (4)$$

$$H_2(\omega) = \frac{S_{yy}(\omega)}{S_{yx}(\omega)} \quad (5)$$

$$Coherence(\omega) = \frac{|S_{yx}(\omega)|^2}{S_{xx}(\omega)S_{yy}(\omega)} = \frac{H_1(\omega)}{H_2(\omega)} \quad (6)$$

where  $S_{yx}$  estimates the Cross Power Spectral Density between the output and input signals, while  $S_{xx}$  and  $S_{yy}$  estimate the Power Spectral Densities of the input and output signals, respectively:

$$S_{yx}(\omega) = Y^*(\omega)X(\omega) = \int_{-\infty}^{+\infty} R_{yx}(\tau)e^{-j\omega\tau}d\tau \quad (7)$$

$$S_{xx}(\omega) = X^*(\omega)X(\omega) = |X(\omega)|^2 = \int_{-\infty}^{+\infty} R_{xx}(\tau)e^{-j\omega\tau}d\tau \quad (8)$$

$$S_{yy}(\omega) = Y^*(\omega)Y(\omega) = |Y(\omega)|^2 = \int_{-\infty}^{+\infty} R_{yy}(\tau)e^{-j\omega\tau}d\tau \quad (9)$$

where  $R_{yx}$  and  $R_{xx}$  are the Correlation Functions, which estimate how much two signals are correlated:

$$R_{yx}(\tau) = E \{y(t + \tau)x(t)^*\} \quad (10)$$

$$R_{xx}(\tau) = E \{x(t + \tau)x(t)^*\} \quad (11)$$

$$R_{yy}(\tau) = E \{y(t + \tau)y(t)^*\} \quad (12)$$

With  $E \{ \circ \}$  = expected value operator, which for a continuous signal  $c$ , having Probability Density Function  $p(c)$ , is defined as  $\int_{-\infty}^{+\infty} c p(c)dc$ .

The following relations insist, in frequency, between  $H_1$ , input  $X$  and output  $Y$ :

$$S_{xx}(\omega)H_1(\omega)^2 = S_{yy}(\omega) \quad (13)$$

$$X(\omega)H_1(\omega) = Y(\omega) \quad (14)$$

$H_1$  and  $H_2$  are used, in real systems, to estimate the FRF by reducing the effects of measurement noise: the  $H_1$  estimator reduces the effects of output noise, while the  $H_2$  estimator reduces the effects of input noise. In the absence of input or output noise it would be  $H_1=H_2$ .  $H_1$  tends to better estimates anti-resonances, while  $H_2$  tends to better estimates resonances.

The Coherence function estimates the signal/noise ratio and thus provides information on how consistent the system response is with the excitation.

The system under investigation (PIEZOTACT and finger) is highly non-linear, due to either the device nonlinearities and even more the finger and the contact nonlinearities. As example, different contact forces deform the finger and modifies the contact area. Therefore, in theory, it would not be suitable for a treatment by the Transfer Function. The effectiveness of the approach has been therefore directly verified through experimental tests and validations through tactile perception campaigns. In addition, parametric analyses of the transfer function, with respect to contact parameters and variation of the human finger, have been performed to manage the influence of such parameters on the transfer function and its use in mimicking FIV.

## 2.5.2 Test bench for the characterization of the finger Transfer Function

A test bench (Figure 19) has been developed to characterize the human finger transfer function, by means of an electrodynamic shaker (2075E The Modal Shop INC. A PCB Group CO., driven by the amplifier SmartAmp Power Amplifier 2100E21 The Modal Shop INC. A PCB Group CO.). The SIRIUSi DAQ and the Dewesoft software are used both to drive the shaker (via the power amplifier in open loop) and to acquire the signals from the transducers and, at a sampling frequency of 5KHz for all the input and output channels. An accelerometer (PCB PIEZOTRONICS 352A24) is fixed by wax on the fingernail of the participant to measure the acceleration. A piezoelectric charge force transducer (ENDEVCO 2321, driven by the amplifier Kistler KIAG SWISS Type 5001) is used to measure the contact force. This kind of force transducer allows to measure both the dynamic (AC) and the static (DC) component of the contact force, indispensable to perform the parametric analysis of the finger transfer function while monitoring the applied force. The force transducer is fixed on the top of the shaker. By its nature, this type of transducer is highly sensitive to temperature changes, which in this case are present due to the participant's finger temperature. To prevent temperature sensitivity, a ceramic plate is glued to the force transducer to thermally and electrically insulate the force transducer from the participant's finger. A support for the participant's arm is set up to maintain an angle of approximately 20 degrees between the participant's finger and the

contact surface. To experimentally characterize the finger transfer function, a random signal up to 1kHz is delivered while the participant holds his finger on the force transducer, with the accelerometer on the fingernail. The  $H_1$  transfer function between the force and the acceleration (Inertance) is then calculated. The transfer function calculated in this way also considers the ceramic plaque between the force transducer and the finger. Nevertheless, the transfer function of the ceramic plaque, characterized in a preliminary stage, is constant within the frequency range of interest, due to its high stiffness, and has no relevant effect on the results.

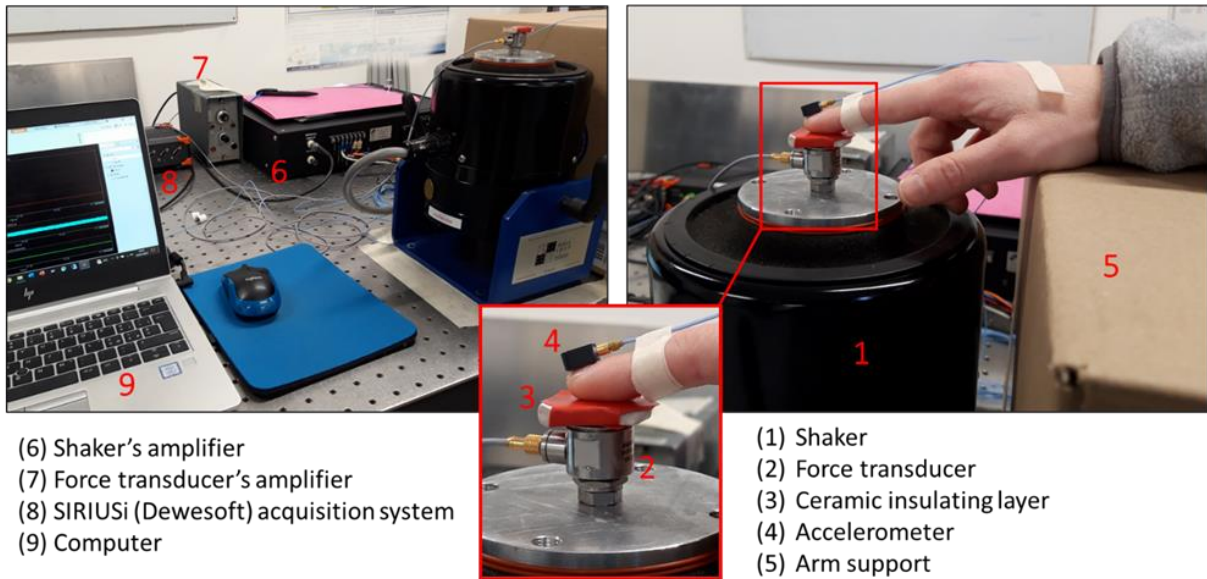


Figure 19: Shaker test bench for parametric analysis of the finger Transfer Function.

### 2.5.3 Test bench for the characterization of the PIEZOTACT and user's finger Transfer Function

The experimental setup to characterize the overall transfer function of the PIEZOTACT device (including the user's finger) is shown in Figure 20. The piezoelectric actuator, in its PLA support, is mounted on top of a triaxial force transducer (Testwell K3D60) to monitor the force exerted by the participant on the actuator membrane. The participant places his finger on the actuator to perceive the reproduced vibration (without touching the support, to avoid altering the force measurement between the finger and the actuator membrane). An accelerometer (PCB 352A24, PCB Piezotronics, Inc.) is glued by wax to the participant's fingernail to measure the acceleration. The transducer signals are acquired using a SIRIUSi (Dewesoft) acquisition system at a sampling rate of 5kHz. During the test, the participant can monitor the contact force exerted between finger and actuator on the PC screen, through the Dewesoft acquisition software.

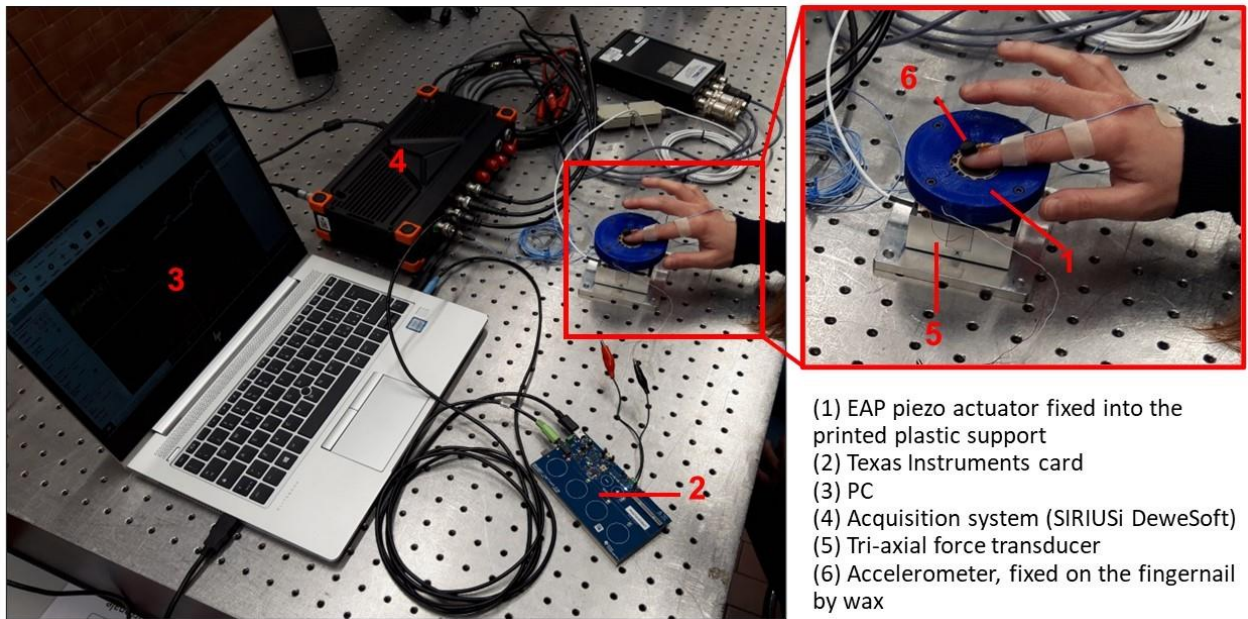


Figure 20: Experimental setup to characterize the overall PIEZOTACT and finger Transfer Function.

At the same time, the PC is used as a signal generator for the PIEZOTACT device. To characterize the transfer function, a random signal up to 1kHz (maximum receptivity range of the mechanoreceptors) is sent to the device using the Matlab software. The Transfer Function between the random signal (input) and the acceleration recovered by the accelerometer on the participant's fingernail (output) is calculated. The theoretical dissertation in section 2.5.1 is numerically implemented in Matlab (Figure 21). To calculate the Transfer Function for tactile rendering, an H1 estimator has been opted for, more appropriate in the case of measurement noise and nonlinearities at the output. The H2 estimator and Coherence have always been monitored as control parameters as well.

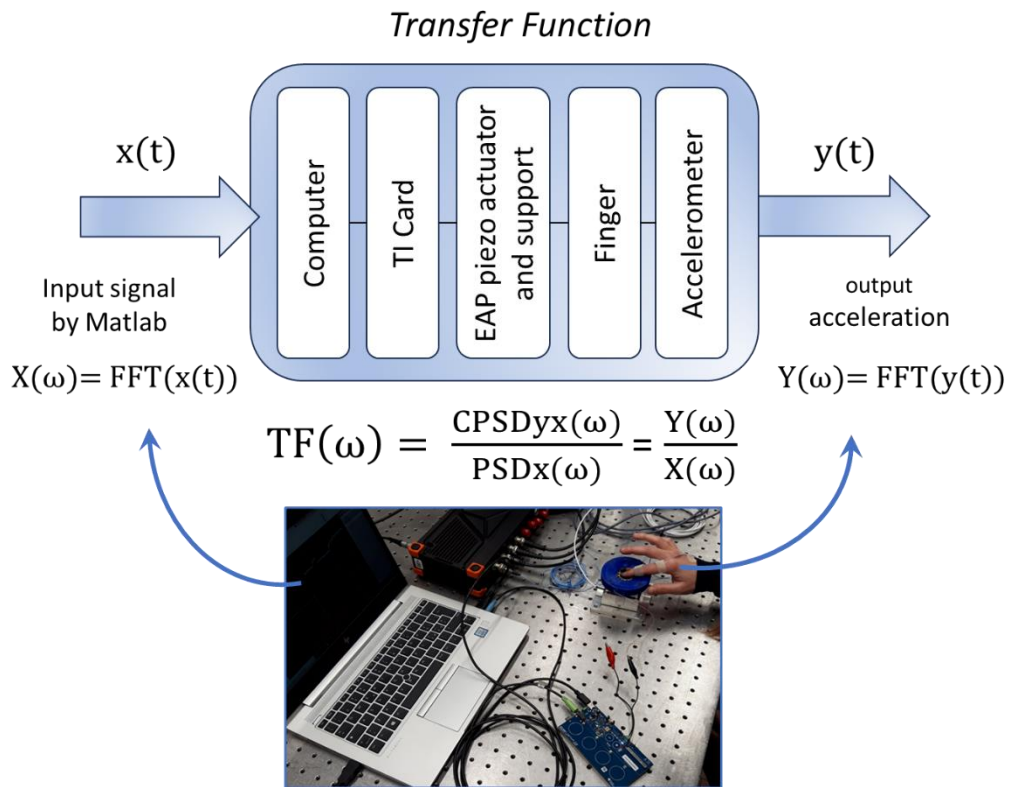


Figure 21: Scheme of the overall Transfer Function characterization between output acceleration measured on the fingernail and random signal sent by Matlab to the PIEZOTACT device.

Figure 22 shows an example of Transfer Function of the PIEZOTACT device including user's finger for normal finger/actuator contact force values selected in the range affected by tactile perception. An in-depth parametric characterization of the Transfer Function as the contact parameters vary will be discussed in Chapter 5.

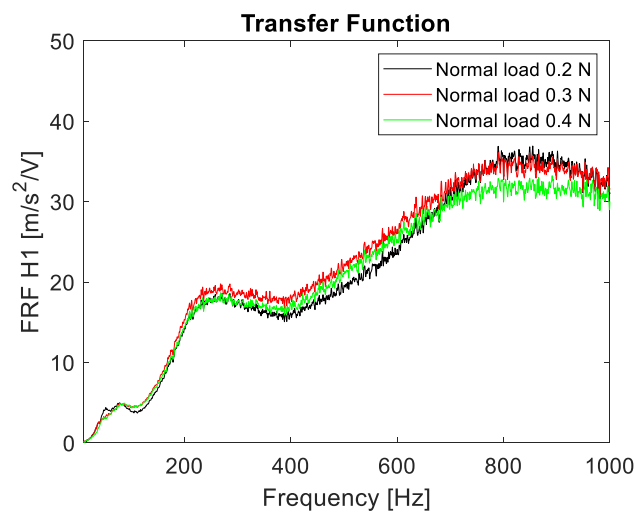


Figure 22: Example of Transfer Function of the PIEZOTACT device including the user's finger for different contact forces in the range interested in tactile perception.

## 2.6 Discrimination campaign protocols

---

This paragraph describes in detail the protocols used to carry out discrimination campaigns on participants. These campaigns are carried out both on the real surfaces (isotropic or periodic) and on the corresponding surfaces simulated by means of the PIEZOTACT device (i.e. FIV stimuli reproduced by means of the device).

In the case of discrimination campaigns on simulated textures, the aim is to investigate whether participants are able to associate to each of the surfaces simulated by PIEZOTACT to the corresponding real surface. It is important to take into account that the device reproduces only the FIV acting on the finger during the surface exploration, so the discrimination campaign provides interesting information on the role of FIV in the discrimination of textures. The device, in fact, allows to decouple the vibratory component of tactile stimuli and to study their role in the perception of textures. Moreover, the PIEZOTACT device allows as well to manipulate the FIV signal obtained from the scanning of real surfaces, for example by altering its amplitude and frequency content, to carry out tests specifically aimed at investigating the impact of the different features of the vibrational signals on tactile perception.

The discrimination of simulated surfaces is always accompanied by the discrimination of real surfaces. During this phase the participants are asked, in different ways (which will be detailed below), to recognize the real textures relying solely on the sense of touch. The phase of discrimination of real surfaces is important for two reasons:

- First of all, it allows to evaluate whether two samples are actually clearly discriminable in reality, before carrying out the test on the simulated surfaces. If two samples are not correctly discriminated in the case of simulated surfaces, it is essential to know whether the corresponding real samples are discernible.
- Moreover, the discrimination of real surfaces provides, in itself, very interesting information on the relationship between discriminative perception of textures and mechanical signals. By investigating the mechanical signals associated with errors in real texture discriminations, it is possible to advance more deeply in the understanding of which features of the mechanical stimuli are involved in the discrimination of textures. An example is provided by a previous work of [6], although the discrimination protocol and goal is completely different from the one used in the present work. In [6], it has been found that the periodic textures, classified from the psychological point of view in different perceptual and hedonistic descriptors, were markedly associated with mechanical signals having certain characteristics of FIV.

The present work provides further insights into the world of discrimination of real and simulated textures and the associated mechanical stimuli. The protocols used to carry out the campaigns of discrimination of real (periodic and isotropic) and simulated surfaces, by means of the PIEZOTACT device, are described in detail in the following paragraphs.

## 2.6.1 Discrimination protocol of periodic textures

This paragraph describes the protocol adopted to carry out the discrimination campaign of periodic samples.

The campaign consists in two different discrimination tasks, the first dealing with the discrimination of real sample surfaces (TASK 1) and the second one with the rendered textures by the PIEZOTACT device (TASK 2). To perform the campaign, the 12 periodic surface samples are regrouped into 18 sets, each constituted by either 3 or 4 randomly chosen samples (shown in Table 4); the sets are built such that each sample is compared at least once with all the other samples during the campaign. For each set of samples, first the discrimination of real surfaces is performed and then the one relating to the corresponding simulated surfaces. In order to obtain the simulated surfaces, starting from the original real ones, the FIV signals are previously acquired by the scanning of the real surfaces and then processed to be reproduced by the PIEZOTACT device:

- The participant undergoes first a measurement session in which the FIV, obtained during active touch, are measured; During this measurement session, the Transfer Function of the PIEZOTACT with the participant finger is as well measured by the test bench presented in section 2.5.3.
- Then, the signals are processed by the experimenter to obtain the simulated textures to be reproduced by the PIEZOTACT.
- Next, the participant is recalled to perform the discrimination test on real and simulated textures. The two discrimination task protocols are described in the following.

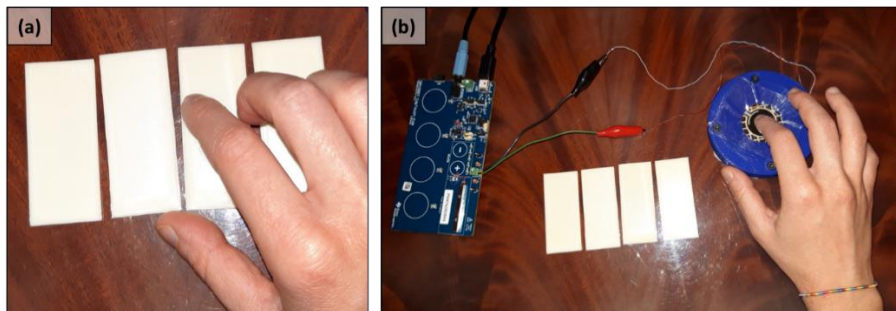


Figure 23: Discrimination campaign of periodic real (a) and simulated (b) textures.

### TASK 1

The TASK 1 consists in the discrimination of the real periodic surfaces (Figure 23a). In the first instance, for the subset of 3 (or 4) samples under investigation, the participant can freely explore the real textures to acquire familiarity with their tactile perception. In this phase, the participant can touch the surfaces and read the sample numbers (printed on the back side of



the samples), learning to associate to each perceived texture the corresponding number. Then, the participant is blindfolded and equipped with earmuff to avoid acoustic and visual feedback. The samples are then presented in a random order to the participant, who is asked to touch and discriminate the samples, by associating each sample to the correct number, entrusting only with the tactile sense. No time limit is imposed to the participant to perform the test.

## TASK 2

The TASK 2 involves the simulated surfaces (reproduced FIV signals) by the PIEZOTACT device (Figure 23b). For each set of samples in Table 4, a random sequence of 5 or 6 simulated textures is defined, also with repetitions of the same surface, in order to prevent the remaining samples to be recognized by exclusion by the participant. The random sequence of simulated textures is then presented to the participant, which is asked to touch the vibrating surface and to associate each simulated texture to the corresponding real one, declaring each surface number. During the test, the participant is let free to touch the set of real samples to compare the real and simulated textures. The participant is also allowed to perceive the sequence of simulated surfaces more than once, and the test is declared as finished when the participant is satisfied by its answers (no time limit is imposed to the participant to perform the discrimination task). The participant wear noise-cancelling earmuff to avoid the acoustic feedback by the actuator.

*Table 4: Sets of samples used for the discrimination campaign, each constituted by 3 or 4 periodic surfaces.*

<b>Set</b>	<b>Samples</b>	<b>Set</b>	<b>Samples</b>
A	M1, M8, M10	L	M3, M6, M1
B	M11, M9, M12	N	M1, M5, M9
C	M4, M2, M3	O	M8, M9, M7, M3
D	M6, M7, M5, M11	P	M12, M8, M4, M6
E	M1, M11, M4	Q	M6, M9, M2
F	M8, M11, M2	R	M2, M10, M5, M12
G	M10, M11, M3	S	M4, M7, M5
H	M10, M9, M4	T	M8, M5, M3, M12
I	M12, M7, M1, M2	U	M10, M7, M6

The protocol described above was the first protocol defined, after preliminary tests, for the discrimination campaign of the periodic textures. Nevertheless, during the overall campaign, some limitations in the procedure have been highlighted, which were then overcome in the discrimination protocols of subsequent campaigns:

- First of all, it has been realized that subsets composed of 4 samples (which sometimes corresponded to a sequence of 6 simulated surfaces) were too tiring for the participant.

In the following campaigns a maximum number of 3 surfaces per subset has been then fixed.

- Because of the difficulties in memorizing the sample number, in the subsequent campaigns, the participant has been avoided to remember the number associated with the sample, by providing position identifiers (example: A, B, C, as can be seen in the following paragraph on the isotropic textures discrimination protocol).
- Another intrinsic limitation to the methodology of discrimination of periodic textures is linked to the fact that it was not possible to define a definite order (a well-defined sequence), as they are associated with different tactile descriptors (smooth, textured, rough, adhesive) and topography, in which there is not a single parameter that varies. This means that in the discrimination of real surfaces (TASK 1) necessarily intervenes a component given by tactile memory (the participant, in fact, has to become familiar with the surfaces and has to memorize them, to discriminate them later). For this reason, when developing isotropic textures, similar textures with increasing average roughness have been chosen.

## 2.6.2 Discrimination of isotropic textures

This paragraph describes in detail the protocol adopted to carry out the campaign of discrimination of isotropic surfaces on panels of participants. The randomly rough isotropic surfaces are identified by a sequence of increasing roughness (as defined in section 2.1.2), according to which the surfaces have been ordered. This sequence is the one used as a reference when asking participants to sort samples from the roughest to the smoothest ones.

The discrimination campaign on participants is carried out for both the real and the simulated (reproduced FIV by the PIEZOTACT device) textures. The aim is to investigate the correlation between the mechanical stimuli, and particularly the FIV, and the capability of the participants to discriminate between the different isotropic randomly rough surfaces.

For each participant, the test is split into two sessions:

- During the first session (duration of approximately one hour), measurements of FIV and contact forces, according to the active touch protocol described in section 2.3.1, are performed for each of the 14 isotropic surfaces. The Transfer Function of the PIEZOTACT device with the participant finger is obtained as well, as described in section 2.5.3.
- Before moving on to the second session (i.e. the proper discrimination tests), the obtained signals are post-processed by the experimenter to be reproduced by the PIEZOTACT device.
- For the second session (duration of approximately one hour and a half), the participant performs the discrimination campaign on real and simulated surfaces. The discrimination campaign consists into 3 different tasks, described in the following.

The measurement session and the discrimination session do not take place on the same day, to avoid fatigue for the participants and to allow the experimenter to process the acquired data and obtain the signals needed to simulate the textures by the PIEZOTACT device. The participant undergoes first the measurement session, and he/she is then recalled in order to carry out the discrimination session.

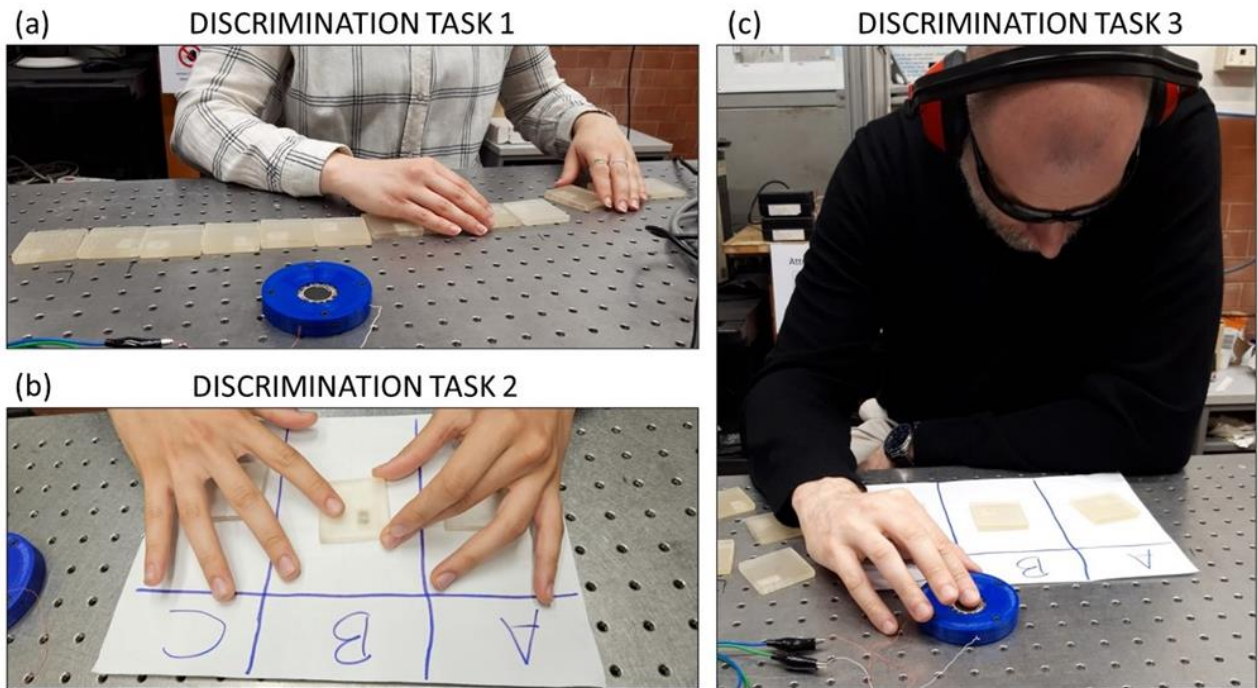


Figure 24: Discrimination campaign, articulated into 3 different tasks: (a) TASK 1; (b) TASK 2; (c) TASK 3.

### TASK 1

The first task consists into a preliminary test performed on all the 14 surface samples (Figure 24a). The samples are presented in a random order to the participant. The participant is blindfolded with scratched spectacles, allowing to distinguish the shape and position of the samples but not the surface textures. Before starting the test, the participant is asked to wash the hands with soap and water and then let them dry. He/She is then asked to touch and explore the 14 samples and to put them in order, from the roughest to the smoothest ones. No constraints concerning the used exploration procedure are imposed to the participant. No time limit is imposed to the participant to perform the task. This preliminary task allows to investigate if the participant put the 14 samples in the corresponding order of the physical surface roughness; moreover, the participant can acquire familiarity with the tactile perception of the 14 surfaces. The task is repeated 3 times and the declared sequences by the participant are annotated by the experimenter.

Then, to perform the second and third tasks, the surface samples are randomly divided into 12 groups, each constituted by 3 samples. The "no texture" sample has been excluded from the second and third tasks. In fact, being very smooth, the “no texture” sample gave rise to adhesion and stick-slip phenomena during the measurement phase, which resulted in high amplitude vibrations that could generate confusion for the participants. The used sets of samples are reported in Table 5.

After performing TASK 1, for each set (triplet) of samples, the second and the third task are consecutively performed. More specifically, for each subset of samples, the participant performs TASK 2 and immediately after performs TASK 3. Afterward, the next set of samples is presented to the participant. This protocol is performed consecutively for all sets of samples in Table 5.

*Table 5: Used sets of isotropic samples for discrimination TASK 2 and TASK 3.*

<b>Set</b>	<b>Samples</b>
A	S2, S4, S8
B	S5, S7, S9
C	S6, S11, S10
D	S1, S3, S13
E	S5, S8, S12
F	S5, S9, S10
G	S2, S3, S4
H	S1, S8, S13
I	S1, S7, S12
L	S4, S13, S10
M	S4, S8, S9
N	S13, S12, S10

## TASK 2

The second task consists into the discrimination of real surface samples. The participant is blindfolded with scratched spectacles, which allow to see the shape and position of the 3 tested samples but prevent the participant to see the surface textures. Before starting the test, the participant is asked to wash the hands with soap and water and then let them dry. The 3 surfaces belonging to the tested set are presented to the participant in a random order. The participant is then asked to touch and freely explore the 3 surfaces, and to put them in order, from the roughest to the smoothest, entrusting only with the tactile sense. The participant is suggested to explore the real surfaces with the index finger of the dominant hand in a proximal direction, in conditions similar to those used for measuring FIV. No time limit is imposed to the participant to perform the task. Then, an identifier A, B, C is assigned to the samples, which are left in the order chosen by the participant for the next task (Figure 24b). The declared sequence by the participant is annotated as well by the experimenter.

### TASK 3

The third task consists into the discrimination of the simulated textures, thanks to the vibrational signal (FIV) mimicked by the PIEZOTACT device. For each set of samples, a random sequence of 3 or 4 simulated textures (reproduced FIV by the PIEZOTACT), chosen between the surfaces belonging to the same set previously tested in TASK 2, is proposed to the participant. In the sequence there can be repetitions of the same signal, or a signal corresponding to one of the sample can not be reproduced in from the sequence. This prevented the participant to answer by exclusion. It is asked to the participant to perceive the sequence of signals by touching the vibrating actuator, and then to associate the reproduced signal to the corresponding real surface (A, B, C) (Figure 24c). The participant is allowed to perceive a reproduced signal, or the entire sequence, more than once and to touch the real samples to compare the real and simulated surfaces. The participant wear earmuffs to avoid acoustic feedback from the actuator. No time limit is imposed to the participant to perform the task. The declared sequence by the participant is then annotated by the experimenter.

### 2.6.3 Building of Association Matrices

This paragraph provides a concise overview of the methodology employed to present the results from all the discrimination campaigns conducted in this study.

The results of each discrimination campaign conducted in this work have been analysed by means of Association Matrices constructed as follows. On the horizontal plane of the matrix there are, on the abscissa axis  $x$ , the sample surfaces (real or simulated) presented to the participants, and on the ordinate axis  $y$ , the corresponding real sample sequence, so that each pairs  $\{x,y\}$  represents a sample association declared by the participant. With this structure, the correct associations of the samples lie on the main diagonal of the matrix, while the discrimination errors lie outside the diagonal. The vertical axis presents the association percentages. These percentages are calculated as the ratio between the number of times that a particular association is declared by the participants and the number of times that the sample is presented to the participants in the whole discrimination test, expressed as a percentage.

Figure 26 shows an example of how an Association Matrix is built. The chosen association values and axis tick labels are completely casual, as the aim is uniquely to show the matrix structure and how to build and to read it. Let's suppose to have 4 surface samples, named SA, SB, SC, SD. Let's suppose we have the results in Figure 25a from the discrimination campaign. The associated rough association matrix is reported in Figure 25b: from the first column in Figure 25a it is possible to observe that each sample has been presented 3 times to the participants in the entire campaign, so the denominator in the columns of the matrix in Figure 25b is always 3; then, the numerator is the number of times each association has been declared by the participants, kept from the second column in Figure 25a. For example, from the first column in Figure 25a, the presented sample SC has been confounded once with the declared sample SD, and thus a score of 1/3 of association is assigned in Figure 25b corresponding to

the row SC and the column SD, and so on. The resulting associations matrices are reported in Figure 26, in terms of percentages.

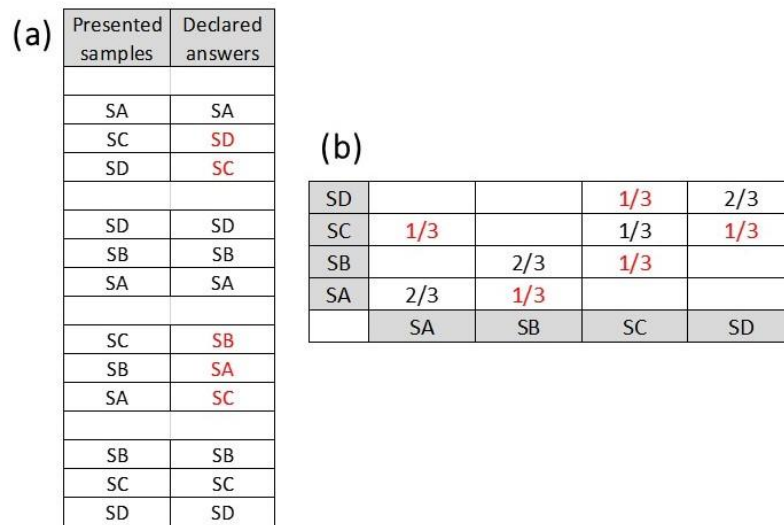


Figure 25: Example showing the logic of building of the association matrix (b) from the data obtained by the discrimination test (a). The discrimination errors are highlighted in red.

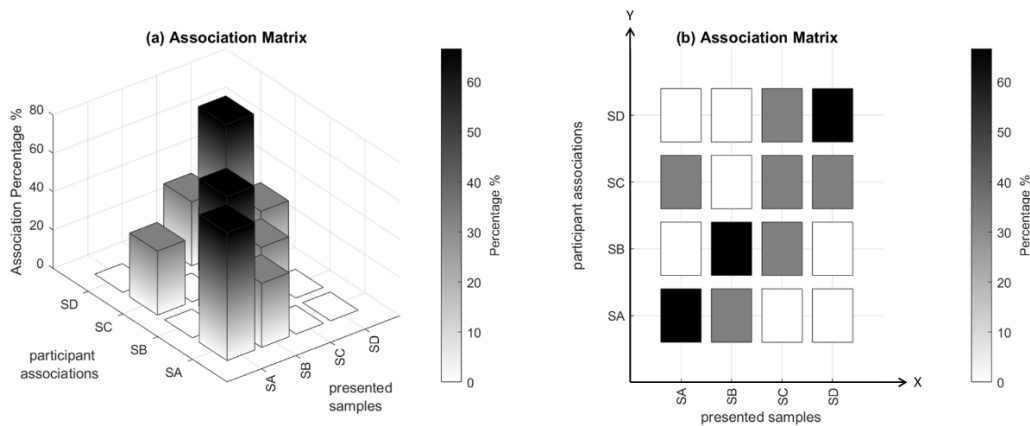


Figure 26: Schema of building of Association Matrix: 3D plot (a) and 2D plot (b).

## 2.6.4 Ethics Committee

Informed consent for experimentation was always obtained by all the involved participants in the campaigns and the privacy rights of human participants has been observed. All participants gave their written informed consent to take part in this study, which conformed to the ethical standards set out in the Declaration of Helsinki.



# Chapter 3

## Mechanical signals analysis<sup>2</sup>

This chapter presents the analysis of mechanical signals, with a particular focus on FIV, obtained from the active and passive exploration of the investigated surfaces. The analysis is carried out on the isotropic surfaces described in section 2.1.2. The results obtained are subsequently compared with those found in previous works [6], [101] involving periodic surfaces (described in section 2.1.1). The main purpose is to investigate what are the main features of FIV, and more in general, mechanical stimuli, that encode the perception and discrimination of surface textures.

---

<sup>2</sup> The content of this chapter has been partially published in [99].



### 3.1 From measurement to processing of tactile mechanical stimuli

---

The procedure used to analyse the data obtained from the measurements of the mechanical stimuli (contact forces and acceleration) is described below.

Figure 27 provides an example (4 proximal strokes during surface exploration) of the mechanical signals obtained from active touch, measured using the protocol described in section 2.3.1. Figure 28 shows the acceleration (FIV) and the three components (normal and tangential) of the contact force, as they result from the measurement, according to the active touch protocol. Since longitudinal exploration is in the Y direction, the tangential force is almost completely concentrated along the Y component.

The signals are then cut, as represented by the red rectangles in Figure 27, to isolate the part of the signal of interest, consisting in the exploration phases of the sample.

Figure 29 shows the selected signal related to a single stroke. For each sample exploration, a dynamic analysis of the FIV and contact forces is carried out. In Figure 29, an example of time and spectral (FFT) distributions of the FIV (acceleration) are presented. From the acceleration (time signal), the RMS amplitude is computed. The friction coefficient (COF) is calculated from the three components of the contact force, according to Coulomb's law.

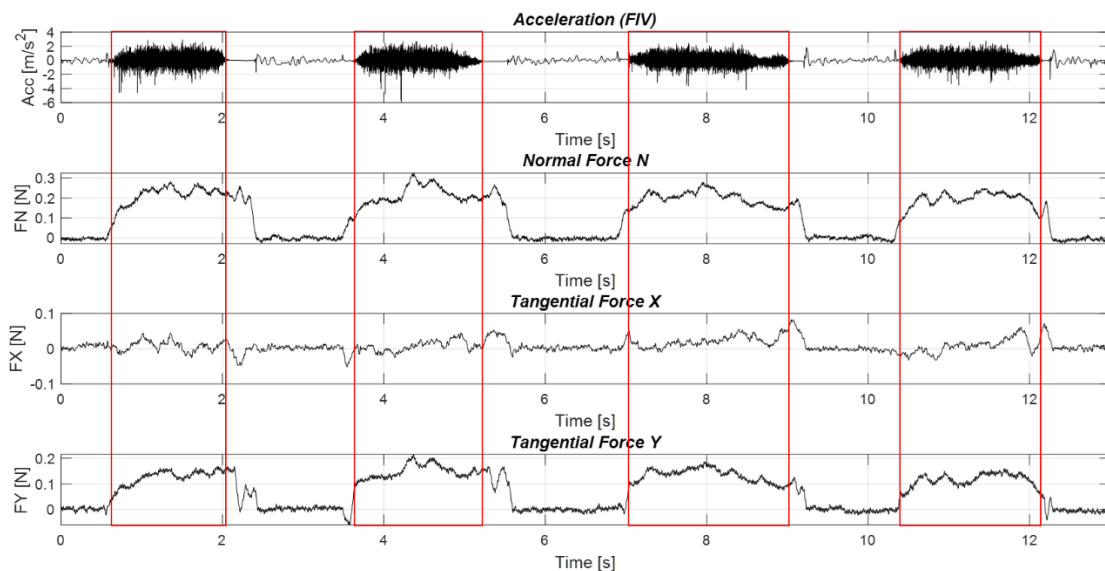


Figure 27: Example of measured mechanical signals (acceleration (FIV) and three components of contact force) for 4 active strokes on a sample; red rectangles highlight the signal selections postprocessed with Matlab for signal analysis.

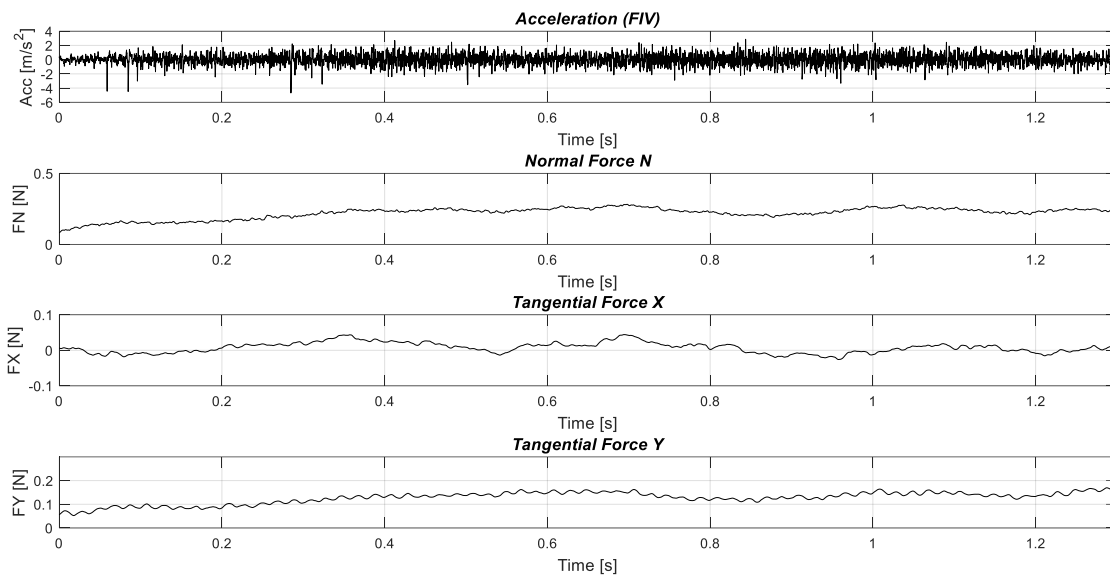


Figure 28: Example of selected mechanical signals for processing.

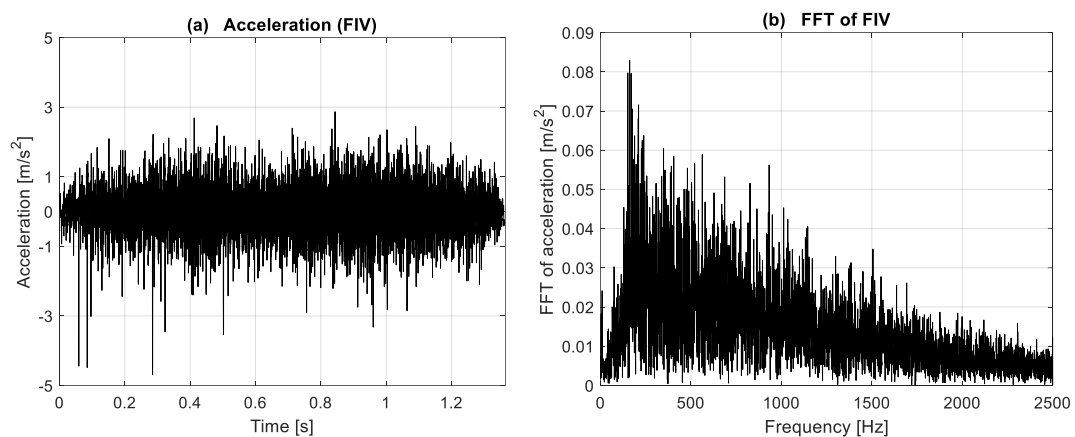


Figure 29: Acceleration (a) and its FFT (b), from the example of the cut signal in Figure 28.

Figure 30 shows an example of average FFT and PSD calculated on the 4 explorations of the surface sample shown in Figure 27, compared with the individual FFTs and PSDs of the individual strokes. For each exploration, the FFT (resp. PSD) is calculated, then the average spectrum is computed between the 4 FFT (resp. PSD). It should be noticed that the characteristic spectrum of the surface sample is well repeatable at each single stroke, despite it comes from active touch, where the velocity is not controlled. The frequency distribution stays the same and the amplitude is quite similar. These observations are valid for all the tested samples. Then, average spectra are used, as well as single spectra, to obtain information about the main features of the FIV stimuli.

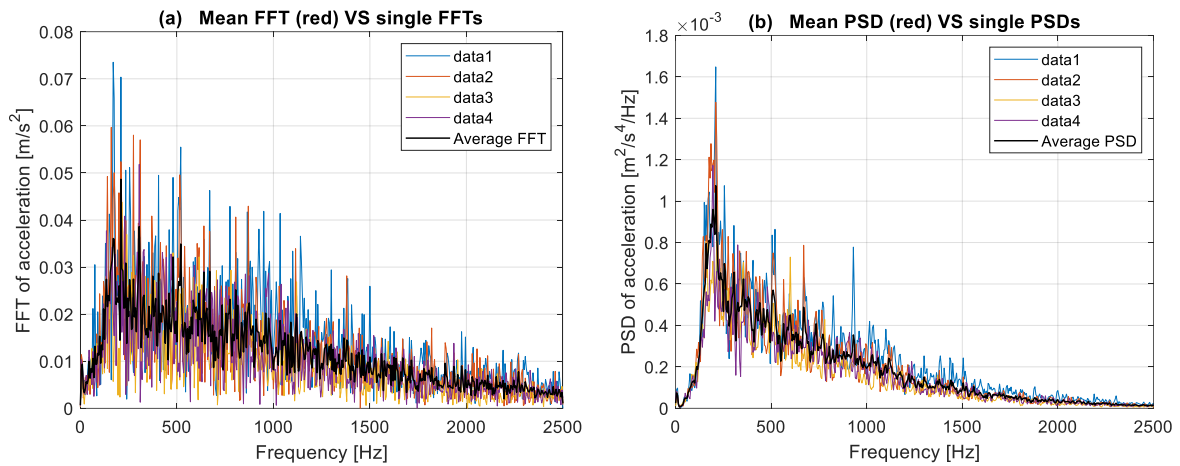


Figure 30: Average FFT (a) and PSD (b) between the 4 strokes in Figure 27, compared with the single FFTs and PSDs.

The shown example is extracted from measurements obtained from the exploration of the S8 sample by a participant. For each of the analysed surfaces and each participant, the average FFT and PSD spectra are calculated for at least 10 sample explorations.

## 3.2 Analysis of isotropic textures

This paragraph presents the analysis of the mechanical stimuli generated during the exploration of the isotropic surfaces (being periodic textures analysed in previous works [6], [101]), by active and passive touch, as well as the comparison of the results from the two approaches.

### 3.2.1 Mechanical stimuli by active touch

The FIV (acceleration) signals, obtained during active tactile exploration of the 14 isotropic samples, have been measured by the protocol presented in section 2.3.1.

The average Power Spectral Density (PSD), associated to 10 active touch measures (i.e. 10 strokes of the participant finger) on each isotropic sample, has been then computed by the MATLAB software. The PSD spectra associated to active touch of each of the 14 isotropic samples, by a participant, are compared in Figure 31.

The isotropic samples show an overall large band spectrum, within the frequency range of mechanoreceptor main sensitivity (10-600 Hz). Qualitatively, the FIV associated to the 14 tested samples show a very similar frequency distribution. What varies the most between samples is the FIV amplitude, that goes from higher FIV amplitudes for coarser textures

(higher roughness) to lower FIV amplitudes for smoother samples (lower roughness). Moreover, coarser textures show a relatively large frequency peak corresponding to the fingerprints width, as expected by the literature [6], [21], [22].

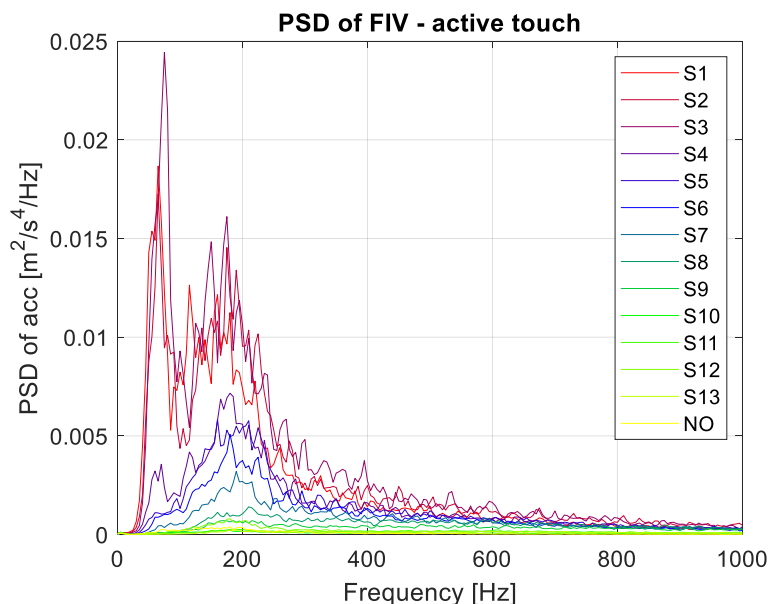


Figure 31: Comparison between the PSD spectra associated to the active touch of the 14 isotropic samples, for a participant.

The active touch measurements have been performed for each participant (with his/her own finger's characteristics) involved in the subsequent discrimination campaigns, to obtain the FIV signals to be mimicked by the PIEZOTACT device. The same overall qualitative trend has been recovered for all the participants. This qualitative trend suggests that, when considering isotropic textures, the most important feature of the FIV spectra, allowing to distinguish one texture from another, is the amplitude of vibration rather than the frequency distribution.

### 3.2.2 Mechanical stimuli by passive touch

A test campaign with controlled contact parameters has been carried out on a participant, in order to investigate the FIV spectrum when both the contact velocity and load are controlled (passive touch). To perform FIV measurements during finger/surface interaction in controlled conditions, the TriboAir test bench and the protocol described in section 2.3.2 have been used.

The campaign of measurements under controlled conditions, carried out on a participant, allows to obtain more deterministic and repeatable measurements, to investigate whether it is possible to identify indicators capable of explaining the relation between topography, mechanical stimuli, and discrimination of textures.

Figure 32 compares the average FIV spectra associated to each of the 14 isotropic samples, measured for the participant, with a constant sliding velocity of 30 mm/s, imposed by the test bench, and a contact force of 0.2N.

The analysis of the PSD, obtained with controlled sliding velocity, confirms the trend found in active touch (section 3.2.1, Figure 31). The 14 samples present large band spectra, with a similar FIV frequency distribution, and a variation in the FIV amplitude is recovered between samples. As well, the general qualitative trend shows that higher FIV amplitudes are associated to coarser textures, while lower FIV amplitudes are obtained for smoother samples. Also in this case, this qualitative trend suggests that the most important FIV feature to discriminate isotropic textures is the amplitude of vibration, rather than the frequency distribution.

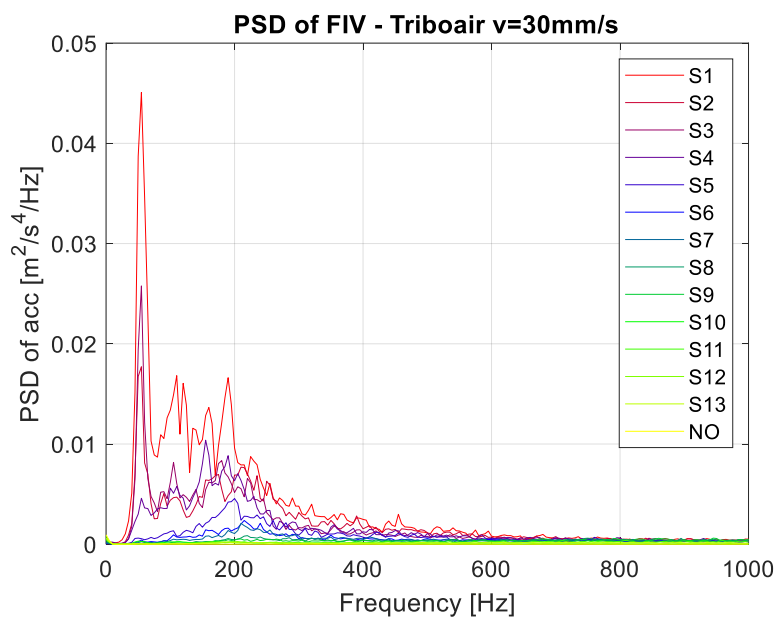


Figure 32: Comparison between the PSD spectra associated to the passive touch of the 14 isotropic samples for a participant.

Figure 33 shows the sample roughness (Ra) compared with the RMS of the FIV measured during passive touch (controlled velocity of 30mm/s and load 0.2N) for a reference participant. The Ra roughness is decreasing from S1 to S14, as defined in section 2.1.2. When considering the FIV amplitude, the RMS shows a decreasing trend with the physical roughness from sample S1 to sample S9, while, from sample S10 to sample S13, the trend of the FIV RMS starts to present some fluctuation characterised by similarities and inversions with respect to the roughness. Moreover, samples from S2 to S4 have close RMS values, even if the roughness are well differentiated.

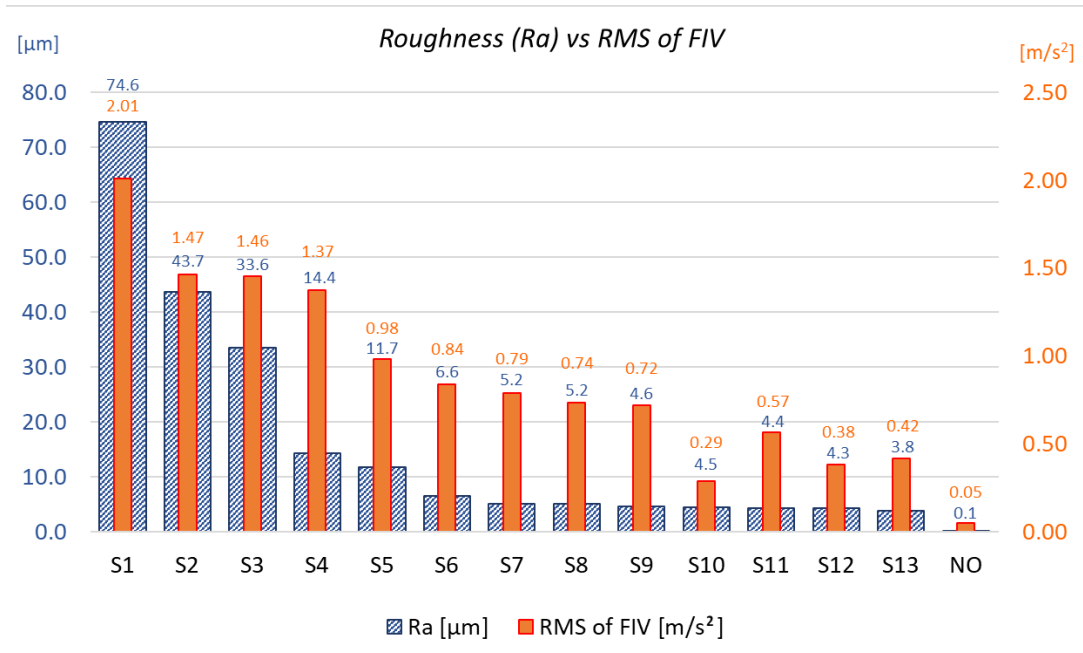


Figure 33: Ra roughness vs RMS of FIV (acceleration) for passive touch of the 14 isotropic samples for a reference participant.

Figure 34 shows the RMS of the acceleration (FIV) and the Friction Coefficient (COF) associated to the 14 isotropic samples, tested under controlled boundary conditions (load 0.2 N and velocity 30 mm/s) during passive touch. The friction coefficient shows an overall decreasing trend with respect to the decreasing of the physical roughness of the samples. This trend tends to follow the one of the FIV RMS, except for few fluctuations. In fact, higher friction means higher power exchanged at the contact, and consequently higher acoustic energy. As expected, the “NO TEXTURE” sample presents a very low FIV RMS amplitude and a very high friction coefficient, due to the higher adhesive resistance.

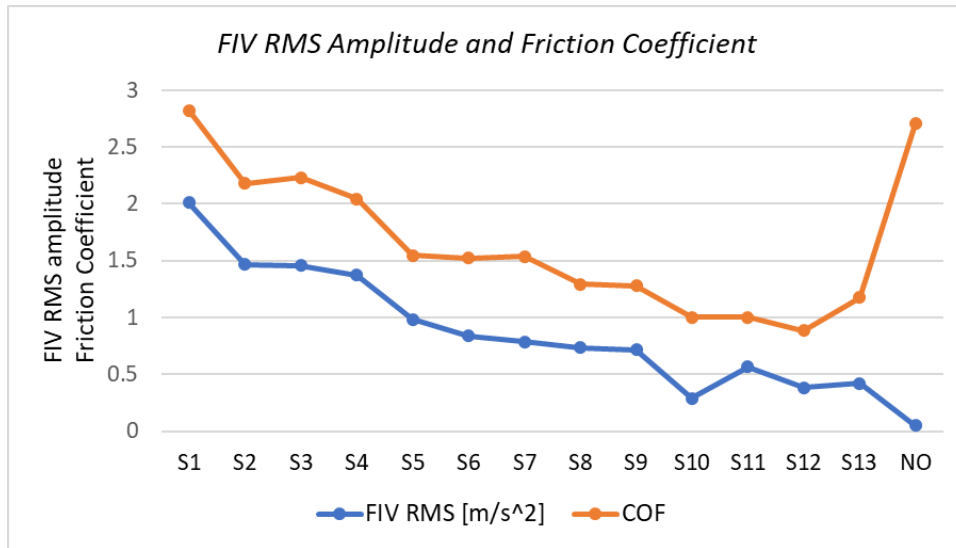


Figure 34: RMS of acceleration and friction coefficient for the 14 isotropic samples, measured with passive touch, for a reference participant.

The FIV analysis has been carried out for three different values of the sliding velocity, imposed by TriboAir: 10 mm/s, 20 mm/s and 30 mm/s. The same general behaviour has been found for each tested velocity. For the same sliding velocity, the FIV amplitude increases as the sample roughness increases. Nevertheless, some other considerations can be made from the FIV parametric analysis with respect to the sliding velocity.

In the first instance, as an example, Figure 35 shows the FIV PSD spectra associated with three different samples (S1, S2 and S3), obtained for the three tested velocities. For a given sample, a significant increase in the FIV amplitude with increasing sliding speed can be noticed, while the frequency distribution remains similar, with a slight shift toward high frequencies as the sliding speed increases, consistently with literature. For what concerns the frequency peak associated to the fingerprints, the shift toward higher frequency with increasing velocity is clearly evidenced.

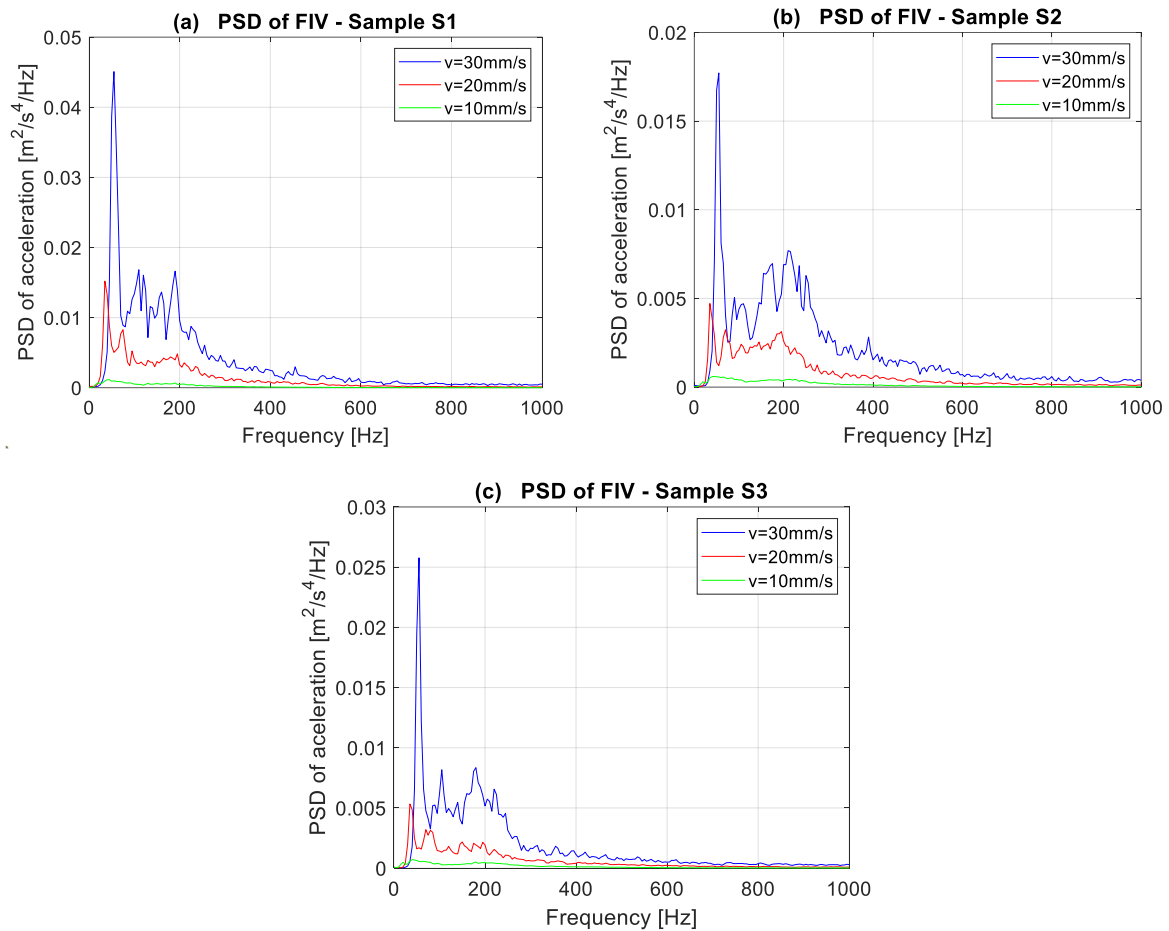


Figure 35: FIV PSD for the three tested sliding velocities for three test samples, S1 (a), S2 (b) and S3 (c).

Figure 36 reports, for each of the three tested velocities, the comparison between the FIV PSD spectra associated to the three samples S1, S2 and S3: for the same sliding velocity, the samples present the same frequency distribution, while the amplitude increases as the roughness of the sample increases. The first well defined frequency peak can be ascribed to the participant fingerprint period; in fact, the frequency value of the peaks (in Hz) corresponds to the ratio between the considered sliding velocity and the participant fingerprint wavelength [6], [21], [22], [24], [36].



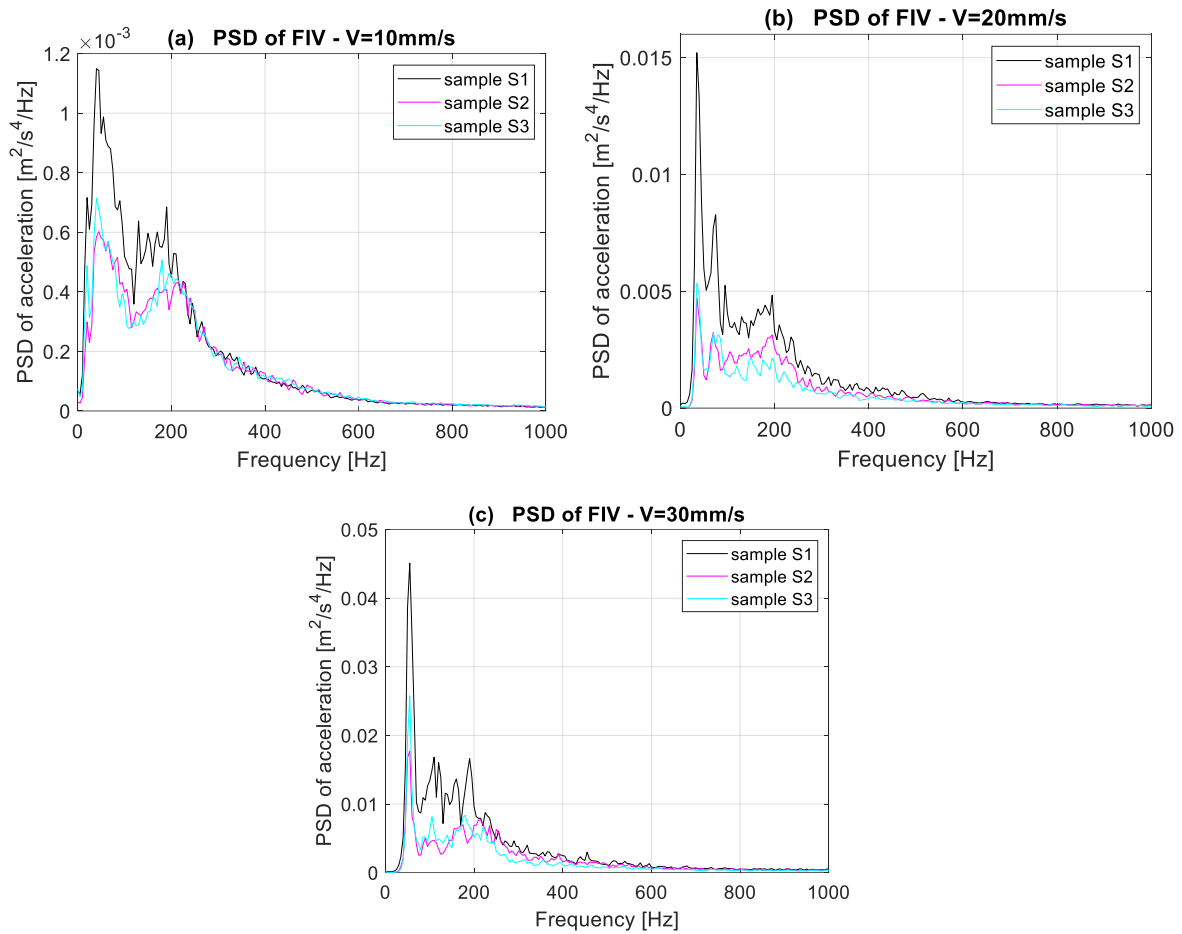


Figure 36: Comparison between the FIV PSD of 3 samples for a sliding velocity of (a) 10 mm/s, (b) 20 mm/s and (c) 30 mm/s.

Figure 37 reports the FIV RMS amplitude for the three tested velocities (10, 20 and 30 mm/s) for the 14 isotropic samples. In agreement with the example in Figure 35, for each sample the FIV RMS amplitude increases as the sliding speed increases. The same trend of FIV RMS with respect to sample roughness can be highlighted for the three tested velocities.

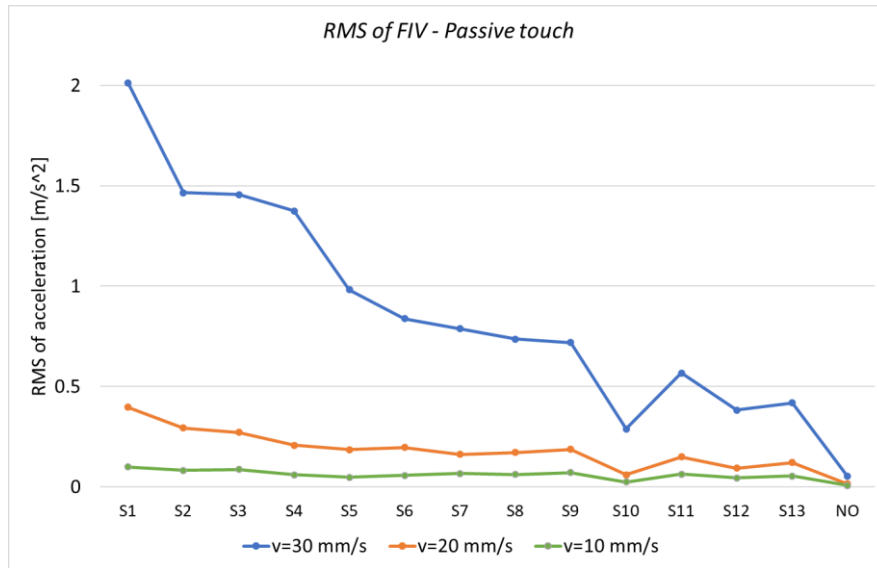


Figure 37: RMS amplitude of FIV for the tested sliding speeds of 10 mm/s, 20 mm/s and 30 mm/s.

### 3.2.3 Active vs passive touch FIV

The FIV spectra obtained by active and passive touch (Figure 31 and Figure 32), when exploring isotropic surface samples, show a similar overall trend with respect to the surface roughness.

The FIV spectra by passive touch (Figure 32) are obtained for a sliding velocity of 30mm/s, imposed by the TriboAir test bench. The spectra are grouped in subsets (for facilitating the comparison between FIV by active and passive touch) in (Figure 38, Figure 39, Figure 40). The same subsets will be discussed for the discrimination results in Chapter 4.

Even if, in active touch, the contact boundary conditions (e.g. sliding velocity) depends on the participant's movement, and therefore are not always constant during the stroke, the qualitative behaviour of FIV in active conditions and in passive conditions is in a very good agreement. In particular, the same trend of the FIV amplitude with the samples is observed. The overall trend of the amplitude of the FIV spectra increase with the increase of the surface roughness, and the frequency distribution are consistent in both cases. The vibrational energy is recovered in the same frequency range, with a large band profile.

Moreover, for FIV measured from both passive and active touch, a main frequency peak can be distinguished at about 55 Hz for the coarser textures (from S1 to S4 in particular), which is due to the fingerprints width of the reference participant for a sliding velocity of 30 mm/s, in agreement with previous results [6], [21], [22] for coarse textures.

This overall agreement is of main relevance because it allows to validate using active touch, which reflects the natural surface exploration, to measure and mimic the FIV signals.

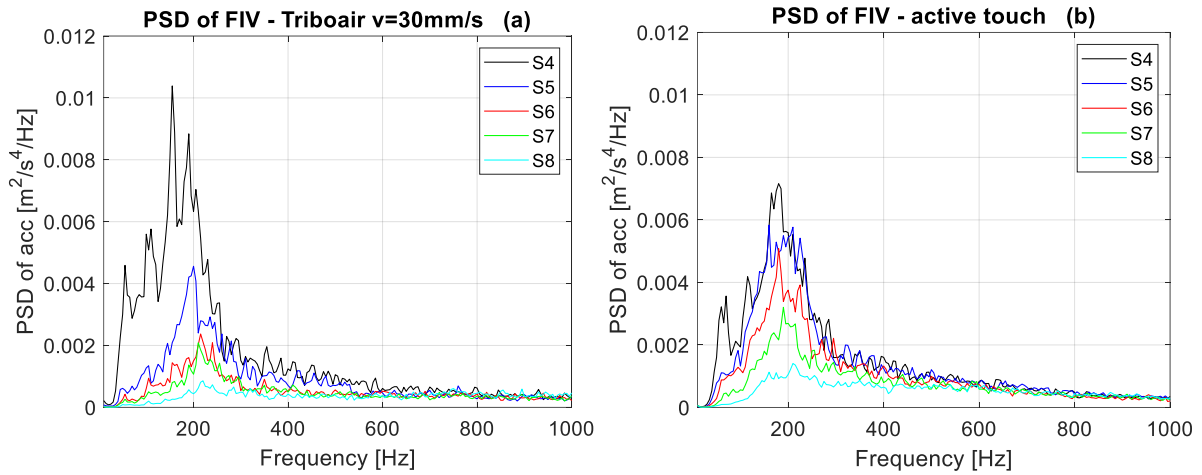


Figure 38: Comparison between FIV spectra by passive touch (a) and active touch (b), for 4 test samples, from S4 to S8 (for the same reference participant).

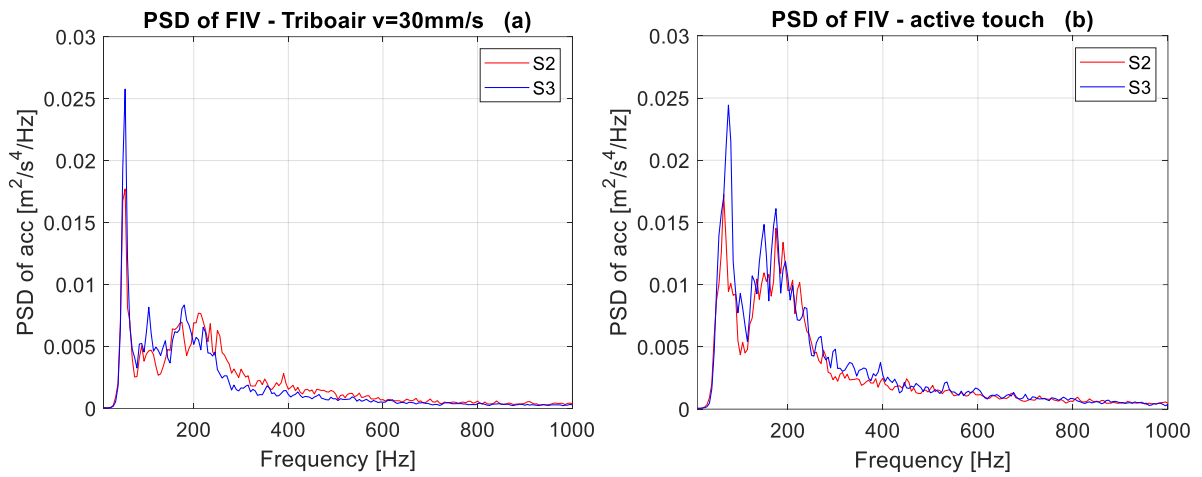


Figure 39: Comparison between FIV spectra by passive touch (a) and active touch (b), for the samples S2 and S3 (for the same reference participant).

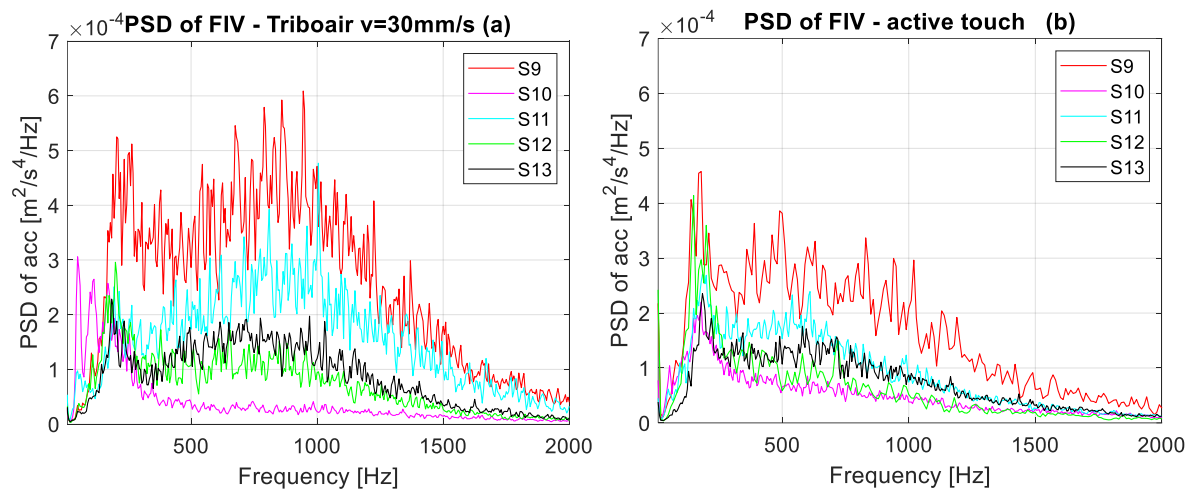


Figure 40: Comparison between FIV spectra by passive touch (a) and active touch (b), for 5 test samples, from S9 to S13 (for the same reference participant).

### 3.3 Isotropic vs periodic textures

---

When comparing the trend observed for the tested isotropic randomly rough surfaces with the results of a previous study [6], related to periodic textures, different key features of the FIV mechanical stimuli can be highlighted to discriminate the textures.

In periodic textures [6], the frequency distribution of the induced vibrations showed clearly different FIV frequency distributions, with well-defined frequency peaks which could be associated both a “descriptive” and a “hedonistic” perception of the textures; in particular, their frequency distribution was well correlated to the clustering of the surfaces with different perceptual descriptors, such as “rough” or “adhesive”, “textured” and “smooth”. The FIV amplitude played a role only in the perception of the coarser periodic textures, for which the FIV had a similar frequency distribution, and the surfaces were clustered, on the basis of the FIV amplitude, in either “rough” or “adhesive”. Thus, for the periodic textures, finer textures were well clustered by the frequency distribution, while the amplitude of the induced vibrations played a role only in discriminating the coarser textures. More detailed information on the referred previous study on periodic surfaces can be found in [6].

Isotropic textures, object of this work, show FIV spectra characterized by a similar wide frequency band, with no significant differences in the frequency distribution between samples, independently from the roughness associated to each sample. On the contrary, the vibration amplitude varies significantly between the 14 samples, quite consistently with the trend of the sample roughness. Therefore, for isotropic random textures, the most important FIV feature, distinguishing between the surface samples, seems to be the amplitude of the induced vibrations.

For what concerns the friction coefficient, in periodic textures [6], for the tested samples, no correlation was found between friction coefficient and perceptual clustering of the surfaces. Indeed, the focus of the present work is mostly of the Friction-Induced Vibrations and their role in tactile perception, so the role of the friction coefficient in the discrimination of textures has not been deeply investigated.

This finding will be tested and corroborated by discrimination campaigns of real and simulated isotropic textures in chapters 4 and 5.

## 3.4 Concluding remarks

---

In this chapter, Friction-Induced Vibrations associated to active and passive exploration of isotropic surface textures have been investigated. FIV amplitude has been highlighted as a key feature to discriminate isotropic textures, in opposition to what was found in previous works [6] for periodic textures.

The parametric FIV analysis of isotropic samples by passive touch confirmed that the RMS amplitude increases as the sliding velocity increases, while the frequency distribution remains consistent.

Moreover, a decreasing trend of the friction coefficient and FIV RMS amplitude has been found with respect to the physical surface roughness.

Isotropic textures turn out to be characterized by different FIV amplitudes, with a similar wide band frequency distribution. The FIV amplitude increases as the physical surface roughness increases for the coarser textures, while similarities and inversions between roughness and FIV amplitude have been observed for the finer textures.

The results on the FIV analysis suggest that the main FIV feature to discriminate isotropic textures is the amplitude of the signal, rather than its frequency distribution. This finding has been corroborated by the following discrimination campaigns of real and simulated isotropic surfaces (see chapters 4 and 5). Contrarily, periodic textures were perceived and discriminated by the FIV frequency distribution, characterized by well-defined frequency peaks according to the surface and fingerprint topography and sliding contact boundary conditions [6].

A strong agreement has been found as well in the FIV spectra recovered by active and passive touch, allowing to validate the use of active touch, which is the natural way to explore textures, in FIV reproduction for tactile rendering, which will be presented in the following Chapter.



# Chapter 4

## Texture rendering by FIV stimuli<sup>3</sup>

This chapter presents the development and exploitation of a tactile rendering device based on the reproduction of Friction-Induced Vibrations. The tactile device, named PIEZOTACT, already introduced in section 2.4, is based on the idea of reproducing the FIV, previously measured during the exploration of real surfaces, by means of a piezoelectric actuator and its driving chain. To achieve a correct mimicking of the vibrational stimuli through the device, a tactile rendering strategy is developed and is presented in detail in this chapter. An experimental verification, by comparing the spectra of the acceleration measured on the real surface and the one reproduced by the actuator, is therefore presented. Subsequently, the validation of the PIEZOTACT device and rendering methodology is obtained by means of discrimination campaigns of real and simulated textures. In addition, a discrimination campaign carried out by generating fake textures through PIEZOTACT, by inverting the FIV amplitudes, is carried out to further investigate the role of FIV amplitude in the perception of the isotropic textures under examination.

---

<sup>3</sup> The content of this chapter has been partially published in [98], [99].

## 4.1 FIV rendering methodology

A tactile rendering device based on Friction-Induced Vibrations has been developed. The aim is to reproduce, by means of an actuator, the FIV previously measured during the exploration of real surface textures. The idea is to return the same tactile vibrational stimuli, coming from real textures, on the user's fingertip, placed on the vibrating actuator. This approach allows to decouple the vibrational part of the mechanical stimuli (friction, forces etc.) generated at the contact during the exploration of the surfaces. The decoupling of the vibrational stimuli, from other mechanical tactile stimuli, is very useful to investigate and better understand their role in the tactile perception, which a particular focus to perception of textures. In addition, this approach allows to insert another brick in the development of tactile rendering devices: in the future, the goal is to synergistically combine different types of tactile feedback (such as vibrational, frictional and/or temperature feedback) in the same device to obtain truly immersive haptic technologies that faithfully reproduce tactile perception. While the device used in this work, called PIEZOTACT, has been presented in section 2.4, the respective rendering strategy is detailed in the following.

The goal is to faithfully reproduce the FIV, measured with the accelerometer during the exploration of real surfaces, by means of the actuator. The first important observation that must be made is that, to achieve this, it is not possible to simply send the FIV signal directly in input to the tactile device: this signal would in fact be strongly modified by the Transfer Function of the system. This would be a wrong rendering strategy (Figure 41 and Figure 42), which would lead to have in output of the device the FIV transformed by the Transfer Function. An example of signal resulting from this wrong strategy is presented in Figure 42, where the target FIV signal (Figure 42a) and the one obtained by the device (Figure 42b) would be definitely different. In Figure 42 the two signals are not compared on the same plot because of the different order of magnitude.

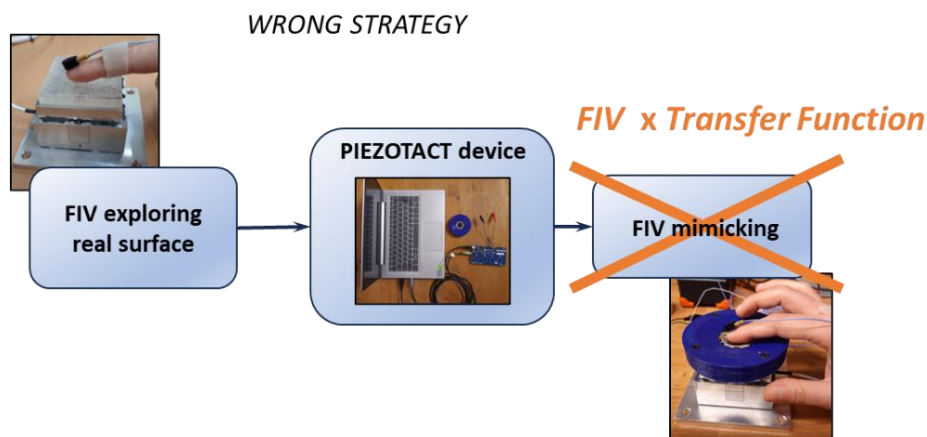


*Figure 41: Wrong rendering strategy: the FIV signal cannot be directly sent to the device since it is modified by the device's Transfer Function.*



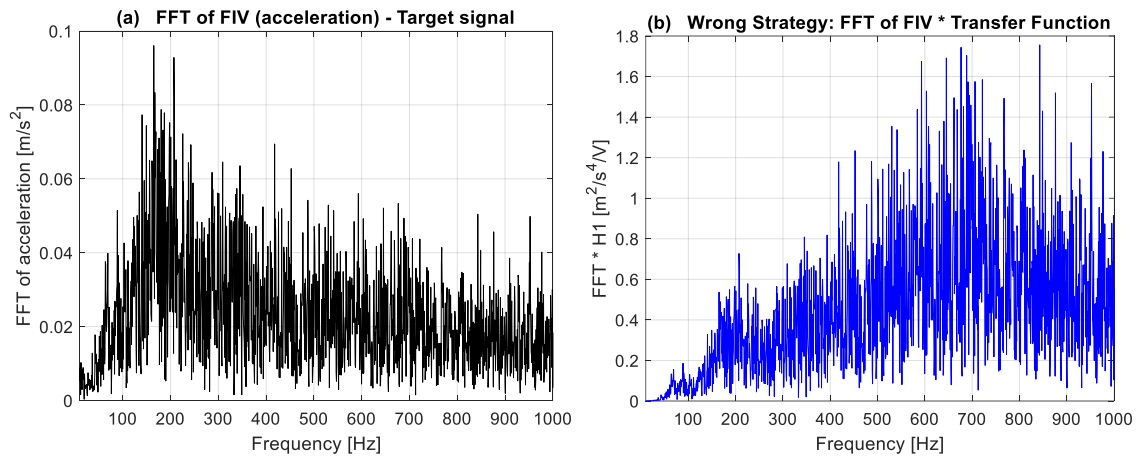


Figure 42: Example of result when applying the wrong strategy: (a) FFT of FIV measured when exploring a surface (target signal to be reproduced by the device) and (b) FFT of FIV modified by the Transfer Function of the device, which would be the result of sending the FIV target signal directly as input to the device.

In order to obtain the correct reproduction of the signal it is therefore necessary to take into account the Transfer Function of the overall electro-mechanical system constituted by the device and the user's finger. The overall Transfer Function has been characterized as explained in detail in section 2.5 and in particular in section 2.5.3, starting from a random signal sent by the computer, and recovering the acceleration on the fingernail, while the finger is maintained on the device.

The Transfer Function is then used to process the FIV signals measured when exploring real textures (i.e. the signals that we want to faithfully reproduce) and obtain a signal that, given as input to the device, allows to achieve the correct reproduction of the FIV by the device. Figure 43 shows a scheme of the developed rendering strategy, which will be described in detail below.

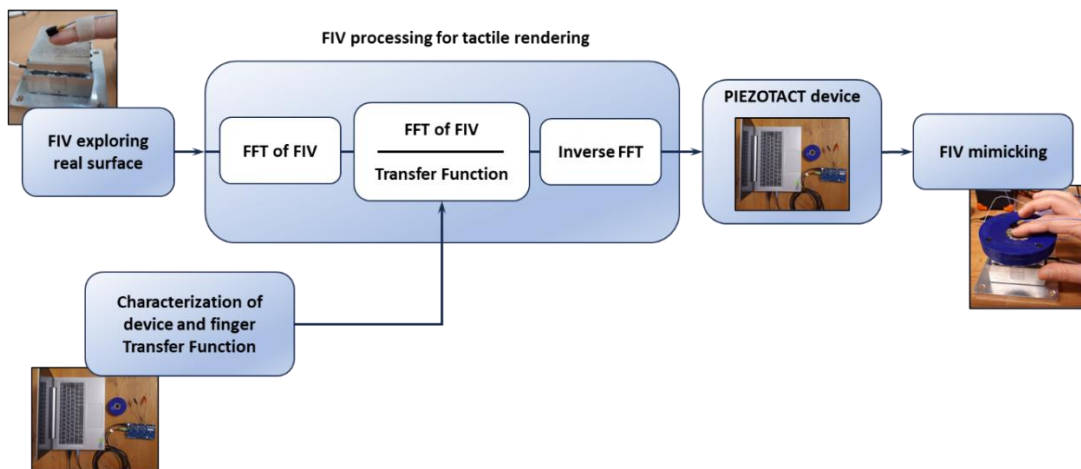


Figure 43: Scheme of the tactile rendering strategy to correctly mimic FIV by the PIEZOTACT device.

In the following the theoretical signal processing to render the FIV is reported. This theoretical approach will be then implemented in MATLAB.

Let's define  $FIV(t)$  the acceleration signal to be reproduced (i.e. the FIV measured when exploring a real surface), while  $FIV(\omega)$  is its Fourier Transform (Eq. 15), and  $TF(\omega)$  is the Transfer Function (Eq. 4), defined in section 2.5.1.

$$FIV(\omega) = \int_{-\infty}^{+\infty} FIV(t) e^{-j\omega t} dt \quad (15)$$

To obtain the desired input to the tactile device, let's define a new frequency signal  $Z(\omega)$  as the ratio between the signal  $FIV(\omega)$  and the Transfer Function  $TF(\omega)$ :

$$Z(\omega) = \frac{FIV(\omega)}{TF(\omega)} \quad (16)$$

Then, the Inverse Fourier Transform of  $Z(\omega)$  can be calculated as:

$$z(t) = \frac{1}{2\pi} \int_{-\infty}^{+\infty} Z(\omega) e^{j\omega t} d\omega \quad (17)$$

The calculated  $z(t)$  is then the input time signal to be sent to the tactile device.

According to the definition of  $TF(\omega)$ , when  $z(t)$  is sent as input to the system (tactile rendering device and user's finger) the following relation is satisfied in frequency:

$$W(\omega) = Z(\omega) TF(\omega) = \left( \frac{FIV(\omega)}{TF(\omega)} \right) TF(\omega) = FIV(\omega) \quad (18)$$

Figure 44 shows the role of the terms in Eq. 18 in the rendering strategy.

At the end, the obtained output signal  $W(\omega)$ , i.e. the Fourier Transform of the acceleration measured on the fingernail touching the tactile device, must be equal to the one ( $FIV(\omega)$ ) measured on the fingernail when exploring the real surface. This is the basis of the experimental verification proposed in section 4.2.

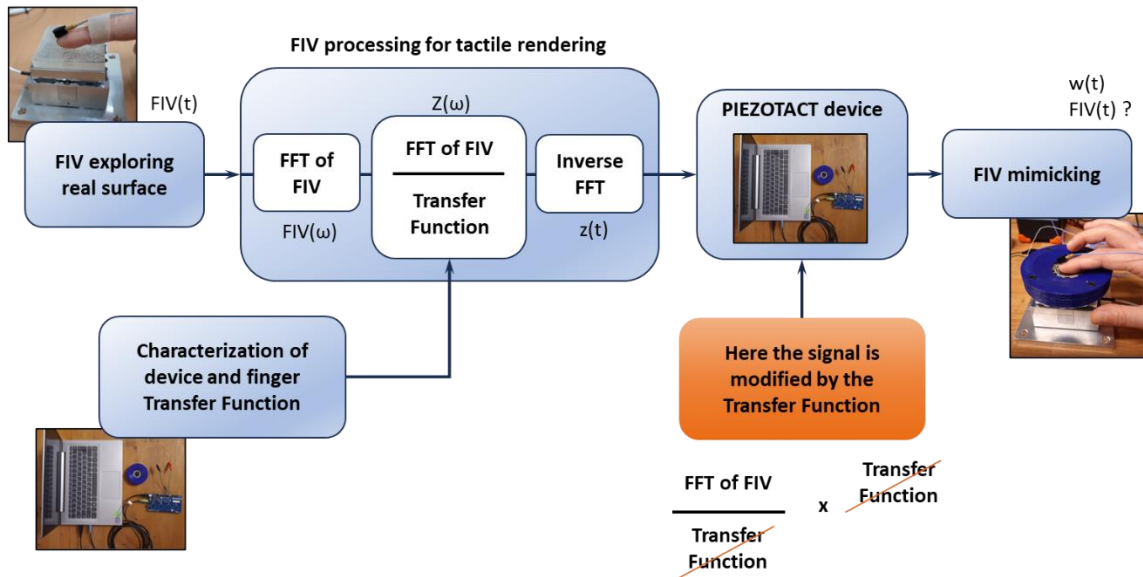


Figure 44: Scheme of the rendering strategy highlighting the terms in Eq. 18.

Figure 45 shows an example of signal processing according to the described rendering strategy: Figure 45a shows the frequency signal  $FIV(\omega)$  and the new signal  $Z(\omega)$  obtained by dividing  $FIV(\omega)$  by the Transfer Function (Eq. 16); Figure 45b show the acceleration signal  $FIV(t)$  in the time domain, measured by exploring the real surface, and the new time input signal  $z(t)$  obtained by performing the Inverse FFT of the signal  $Z(\omega)$ , which is the input to be given to the device (voltage); Figure 45c shows the Transfer Function used to process the signal. The signals represented in Figure 45 obviously have different units of measurement, but they have been equally overlapped on the same plot to show the diversity of the shape of the signals.

As highlighted in Figure 45a, the input signal for the tactile device is modified according to the shape of the system's Transfer Function (Figure 45c). For frequencies where the Transfer Function increase, the input for rendering amplitude decrease, with respect to the measured one, and vice versa. The input time signal  $z(t)$ , green curve in Figure 45b, is then sent to the tactile device in order to obtain the reproduction of the FIV on the fingernail.

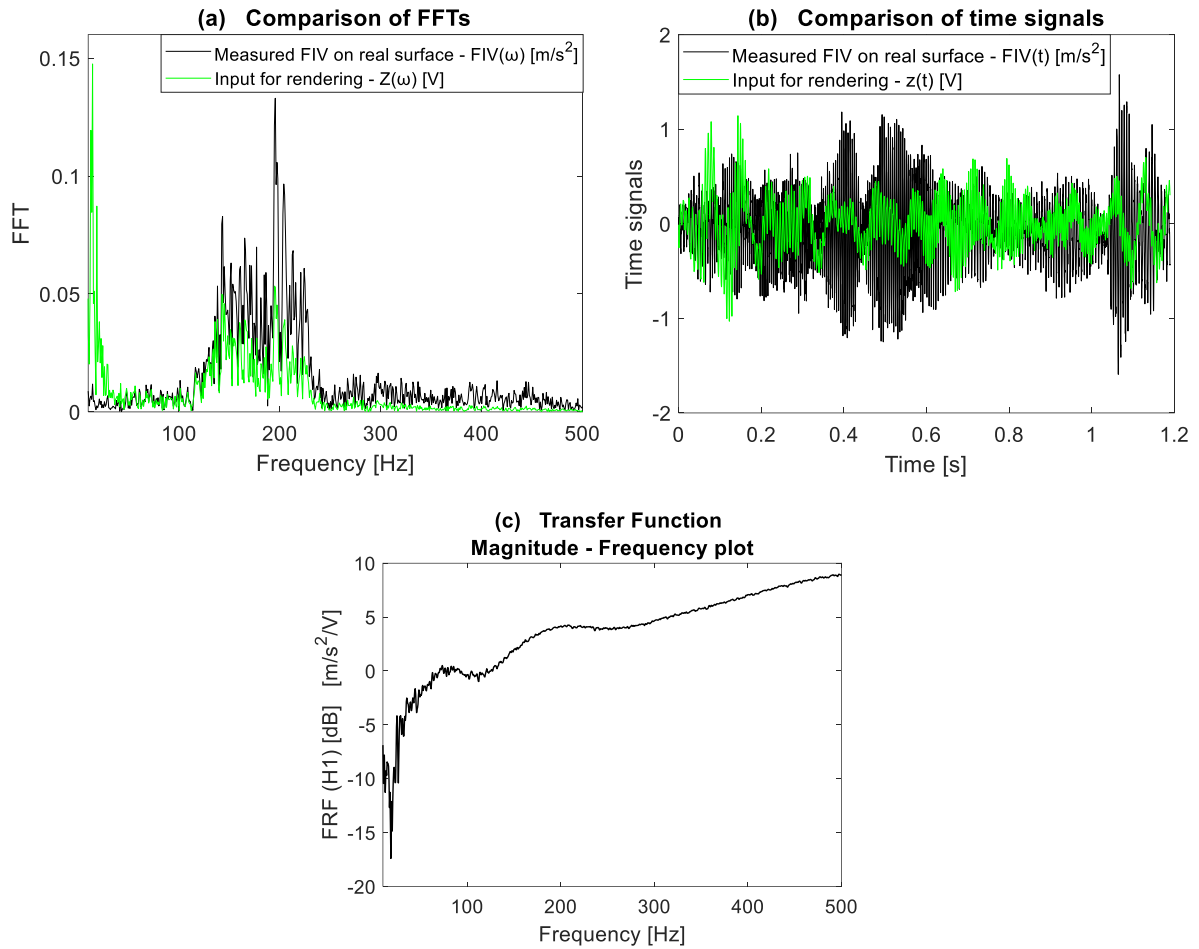


Figure 45: (a) comparison between the spectrum of the FIV measured when touching the real surface and the spectrum of the input signal to drive the tactile device. (b) comparison between the respective time signals. (c) the used Transfer Function to process the signal.

It is interesting to notice that this strategy has a more general validity: whatever a transient signal to be reproduced (not necessarily FIV), and whatever the Transfer Function of the system is known, the signal processing remains valid. The only precaution is to correctly characterize the Transfer Function. In fact, since the Transfer Function is defined for linear and time-invariant (LTI) systems, it is still necessary to appropriately characterize the specific system under investigation to evaluate the influence of the different parameters involved on the response of the system, to verify the appropriateness of the characterization of the Transfer Function.

The system under investigation (PIEZOTACT device and user's finger), as already highlighted in section 2.5.1, is strongly non-linear because of the non-linearities arising from the contact, the finger, and the device, so it is necessary to verify the approach through experimental verifications and perception campaigns, which are described in the next sections. Instead, a parametric characterization of the Transfer Function, as a function of the involved parameters (participant, applied force, finger angle with respect to the device, etc.), will be discussed in chapter 5.

## 4.2 Experimental validation of FIV rendering

The correct FIV rendering has been experimentally verified by comparing the original FIV signal, measured by exploring the real texture, and the one rendered by the PIEZOTACT device (Figure 46). The FIV have been measured using the active touch protocol described in section 2.3.1, and then reproduced using the rendering methodology presented in section 4.1.

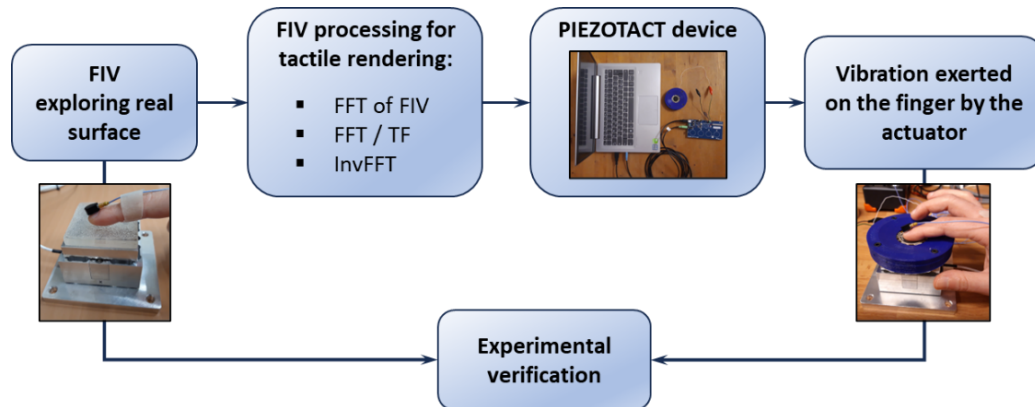


Figure 46: Scheme of the approach to verify the correct FIV mimicking by the PIEZOTACT device and rendering strategy.

Figure 47 and Figure 48 show examples of the achieved FIV reproduction, by the PIEZOTACT device and the developed rendering strategy. Figure 47 shows an example using a periodic texture, while Figure 48 using an isotropic one. The FFT and PSD spectra of the accelerations measured during the exploration of the real surfaces and the ones recovered when the finger is placed on the actuator are compared. In both examples, the spectra of the acceleration are very similar, almost overlapping, for the real (black curves) and simulated (green curves) textures. These results testify that the device can correctly reproduce the target FIV signal, and experimentally validate the device and rendering methodology.

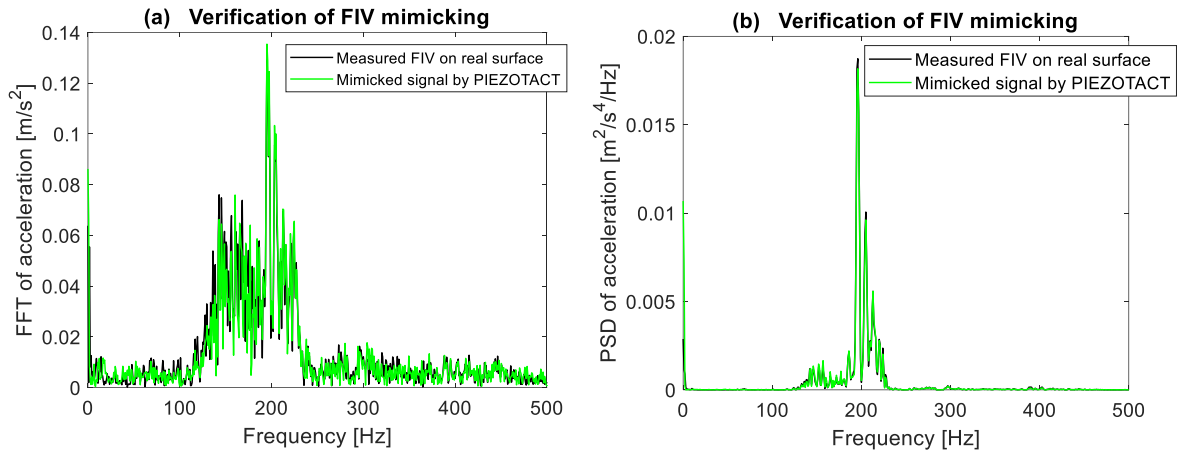


Figure 47: Verification of FIV mimicking through the comparison of the FFT (a) and PSD (B) spectra obtained by a real and simulated periodic sample (up to 500 Hz where the significant FIV content is located).

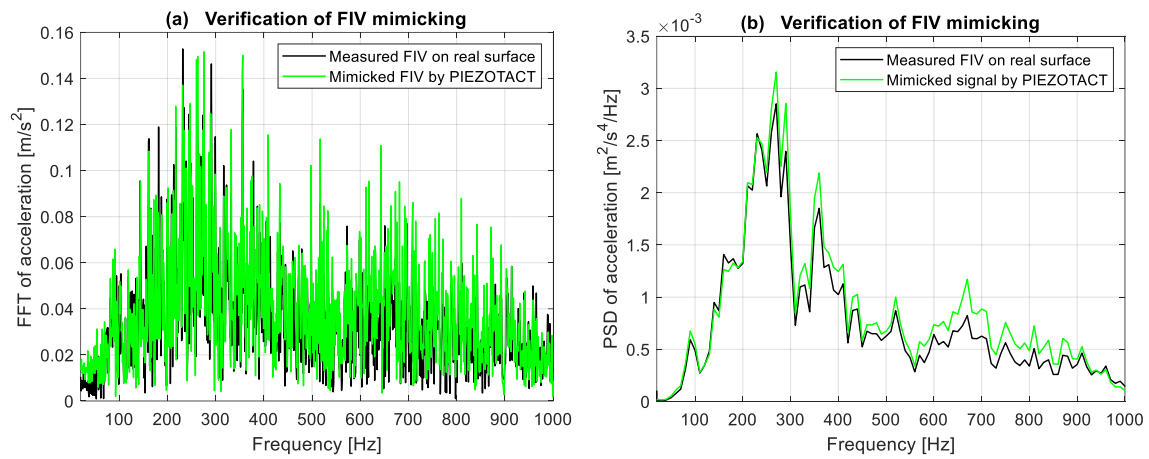


Figure 48: Verification of FIV mimicking through the comparison of the FFT (a) and PSD (B) spectra obtained by a real and simulated isotropic sample.

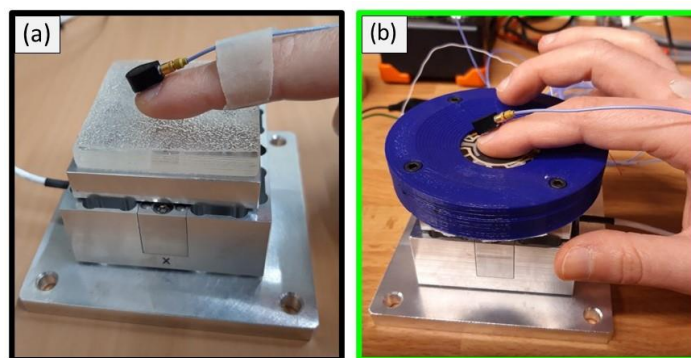


Figure 49: Comparison of finger configuration and experimental measurement setup in the exploration of the real surface (a) and during the perception of mimicked FIV by the PIEZOTACT(b).

The correct signal reproduction assures the possibility to simulate a target signal by processing it by the Transfer Function, with the presented rendering strategy, whatever the target signal is. It should be noticed that, in the case of real textures, the vibrational stimulation of the mechanoreceptors in the fingertip comes from the dynamic interaction between skin and surface, due to the sliding of the fingertip on the surface. On the other hand, in the case of the mimicked signal, the vibrational stimuli come from the actuator, without any motion of the finger, by the normal vibration of the contact surface (Figure 49).

Moreover, in terms of tactile rendering, an important consideration must be made. The acceleration (FIV) is measured during the exploration of real surfaces with the configuration in Figure 49a. On the other hand, the acceleration, when touching the actuator surface vibrating with the mimicked FIV, is measured with the configuration in Figure 49b. The similarity of the two configurations can be easily noticed in Figure 49.

In both cases (real and mimicked FIV), the acceleration is measured by the accelerometer fixed by wax on the fingernail of the participant. The underlying hypothesis is that, being the finger configuration (as is shown in Figure 49) the same for the two cases, having a similar spectrum of the vibrations measured at the fingernail means having similar excitation of the mechanoreceptors at the fingertip for a subject. This assumption would lead to similar perceptive response when touching real and simulated textures. To verify such hypothesis, and to verify the key role played by the FIV in the discrimination of textures, perception campaigns on real and simulated surfaces have been performed, and reported in the following sections.

## 4.3 Discrimination campaigns

---

Texture discrimination campaigns on volunteers have been conducted in order to validate the tactile device, using both periodic and isotropic textures. The goal is to investigate the ability of participants to discriminate (recognize) the simulated textures by PIEZOTACT, associating them with the corresponding real surfaces. The results of the campaigns have been analysed through the Association Matrices discussed in section 2.6.3. Following the first experimental validation described in section 4.2, the discrimination campaigns on real and simulated textures allow to validate the device from a point of view of the tactile perception.

Moreover, for both periodic and isotropic textures, the results of the discrimination have been interpreted in the light of the most important features of FIV (amplitude and frequency distribution) to investigate the role of such features in the discriminative perception of real and simulated textures.

### 4.3.1 Discrimination of periodic surfaces

A preliminary pilot discrimination campaign on a participant (male, 41 years old) has been conducted using the periodic textures described in section 2.1.1. The protocol detailed in section 2.6.1 has been operated. The protocol involves the measurement of FIV and the characterization of the Transfer Function of the participant, followed by the proper discrimination campaign on both real and simulated surfaces (Figure 50). The FIV have been measured using the active touch protocol described in section 2.3.1 for all the involved periodic surfaces, and then reproduced using the rendering methodology presented in section 4.1.

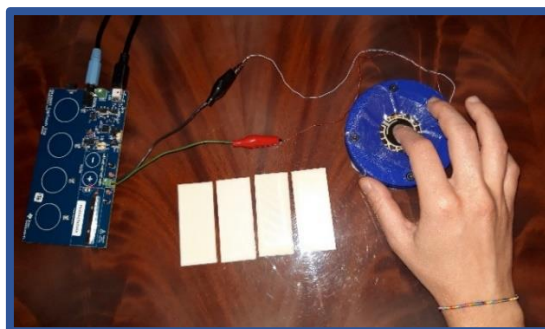


*Figure 50: Discrimination of periodic textures.*



The overall result of the campaign is reported in Figure 51 and Figure 52. Figure 51a and Figure 52a show the result of the discrimination of the real periodic surfaces, while Figure 51b and Figure 52b present the results of the discrimination of the simulated textures by the PIEZOTACT device.

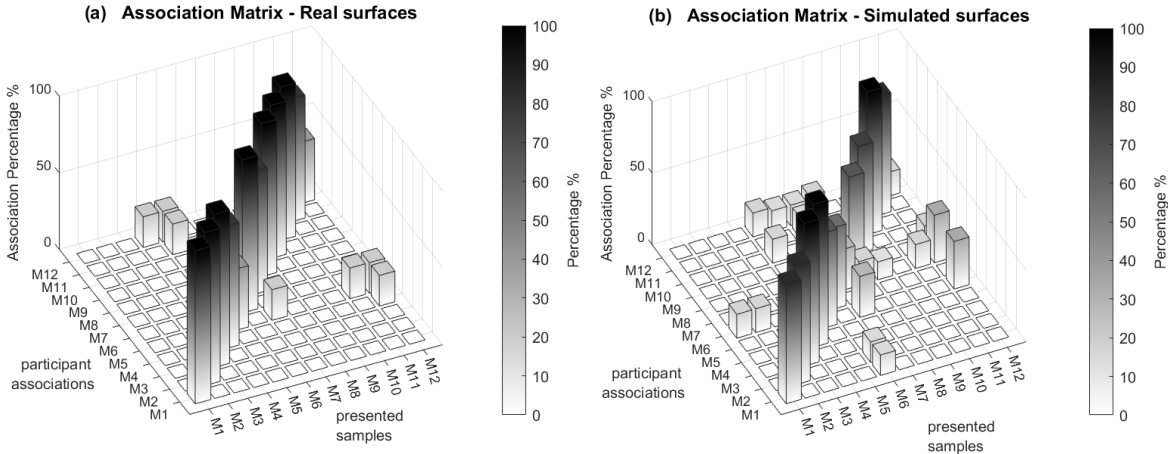


Figure 51: Results of discrimination campaign on real (a) and simulated (b) periodic textures (3D Association Matrices).

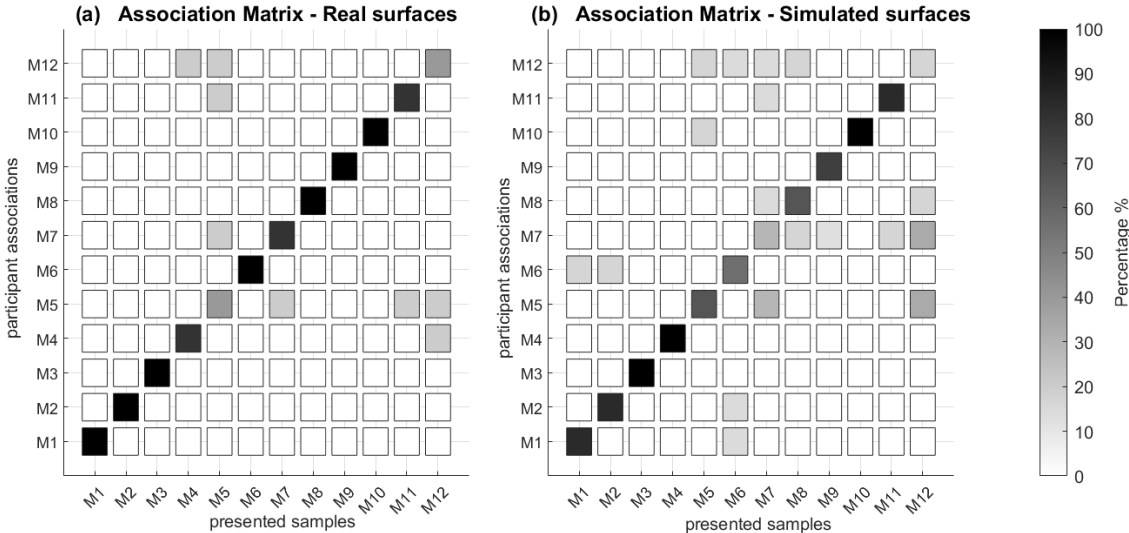


Figure 52: Results of discrimination campaign on real (a) and simulated (b) periodic textures (2D Association Matrices).

As shown in Figure 51 and Figure 52, the participant achieved a very good performance in discriminating both the real and simulated textures. In fact, very high percentages of association can be localized on the principal diagonal of both the matrices for all the tested samples. Let's recall that on the main diagonal there are the correct discrimination of the samples.

Moreover, the results in the discrimination of the simulated textures (by mimicking FIV) can be compared to those in the discrimination of the real samples. The matrix related to the simulated surfaces presents few more discrimination errors, but overall, a good agreement is found between the results obtained when discriminating real and simulated surfaces. The most frequent discrimination errors, which occurred in the tests with the simulated textures, have been recovered in the case of the real ones too. As an example, samples M5, M7, M11 and M12 have been frequently confused in both campaigns, and they present the lowest percentages on the main diagonal of both the matrices.

The results of the discrimination campaign have been then interpreted by means of the FIV. In the cases of the most occurred wrong discriminations, the FIV spectra, measured when touching the real surfaces (which have been then reproduced by the tactile device), are very close each other, justifying the errors in the discrimination of both the real and the simulated surfaces.

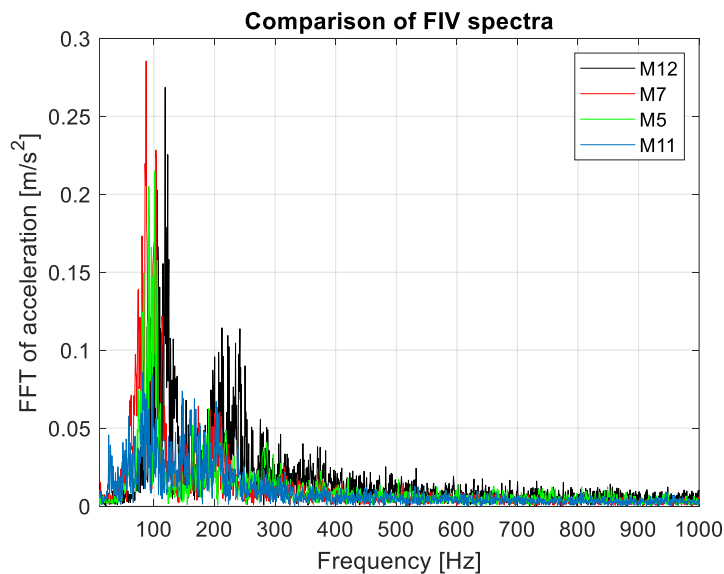


Figure 53: Spectra of FIV associated to the samples that have been mostly confused in the discrimination of both real and simulated textures (M5, M7, M11, M12).

As an example, Figure 53 reports the compared FIV spectra of the 4 most confused samples in the discrimination campaigns of both real and simulated textures, M5, M7, M11, M12. The 3 samples M7, M5 and M12, are characterized by very similar FIV spectra both in terms of FIV amplitude and frequency distribution. These samples have been frequently confused. In particular, the samples M7 and M5 have very similar topographic parameters (Table 2) and FIV characteristic spectra, and they resulted always hard to discriminate. Sample M11 show a lower FIV amplitude with respect to samples M5, M7 and M12, but the same frequency distribution. This emphasizes the importance of the frequency distribution, rather than the amplitude, of FIV signals in the perception and discrimination of fine periodic textures, in agreement with [6].

On the contrary, as an example, samples M8 and M4 show different FIV spectral distributions (Figure 54) and they never got confused during the campaign. More examples and discussions on this pilot discrimination campaign on periodic textures can be found in [101].

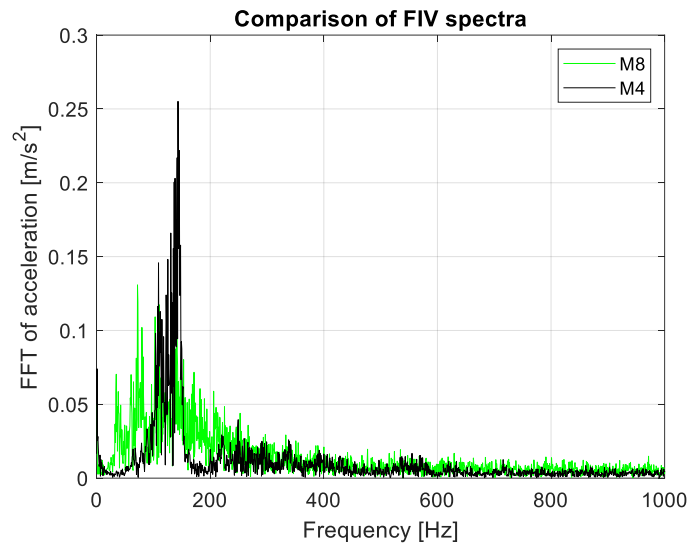


Figure 54: Example of FIV associated to sample that have been always well discriminated both in case of real and simulated textures (M4, M8).

The implications of such results are very interesting. First of all, the high discrimination success highlights the main role played by FIV in the discrimination of textures, especially fine ones. This also testifies the effectiveness of the PIEZOTACT device in vibrotactile rendering, and, moreover, its usefulness in being used as a tool to decouple and mimic the vibrational part of tactile stimuli and to better understand the link between vibrational tactile stimuli (FIV) and texture perception. Moreover, good and wrong discrimination of real periodic samples, as well as the simulated ones by FIV, have been linked to their associated FIV, especially in terms of frequency distribution (in agreement with [6]).

A further validation of the device has been then provided by the discrimination campaign on isotropic textures presented in the following section.

### 4.3.2 Discrimination of isotropic surfaces

A discrimination campaign has been conducted on 10 participants (1 female and 9 males, with age ranging between 21 and 44 years, 1 lefthander and 9 righthanders) using the isotropic textures described in section 2.1.2. The FIV have been measured using the active touch protocol described in section 2.3.1, for all the involved periodic surfaces, and then reproduced using the rendering methodology presented in section 4.1. The specific Transfer Function of the PIEZOTACT device, with each participant’s finger, has been measured as well.

The protocol detailed in section 2.6.2 has been followed. For each of the 3 discrimination tasks, described in section 2.6.2, the results related to the 10 participants are presented in the following section. The results have been represented and analysed by means of the association matrices described in section 2.6.3.

Figure 55 reports the results of the campaign.

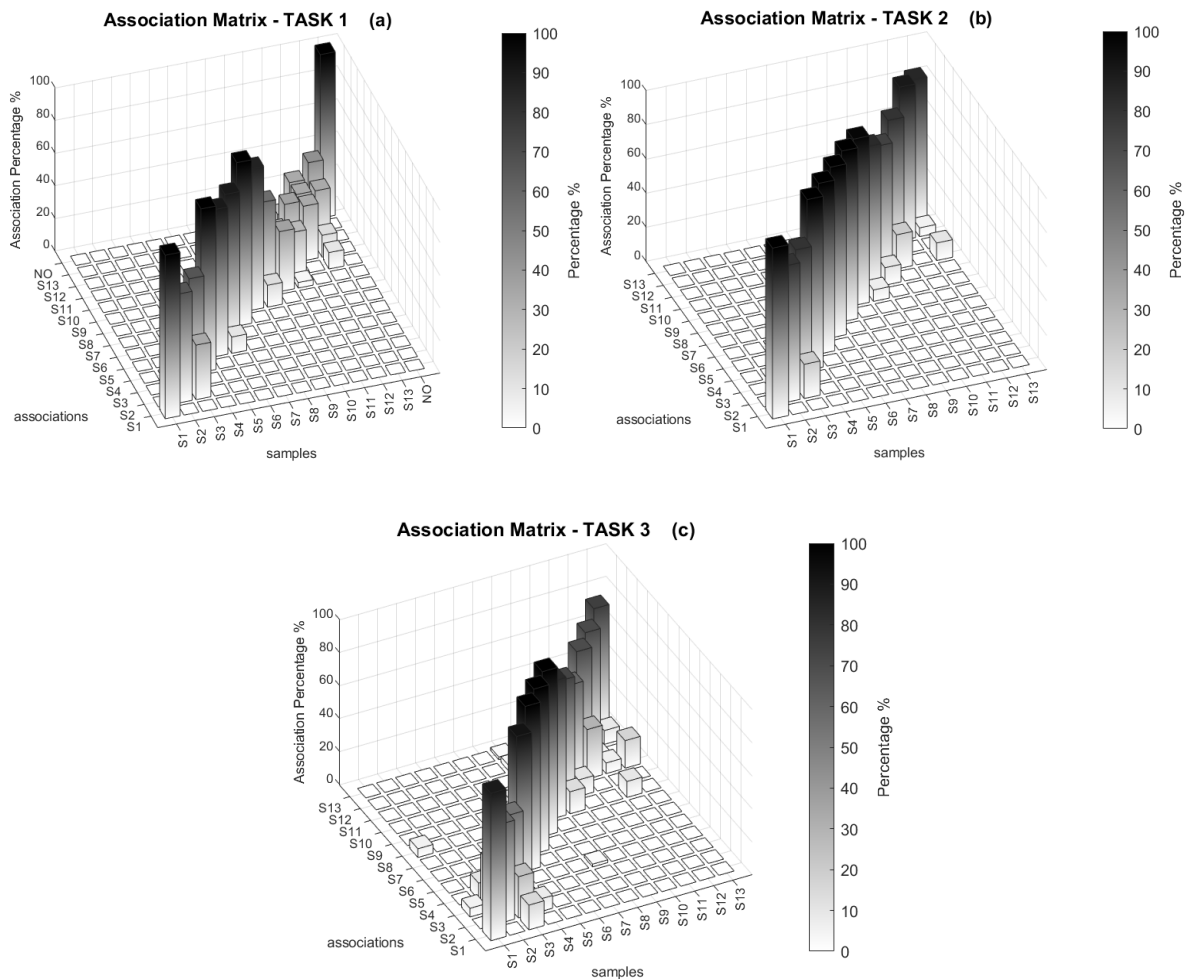
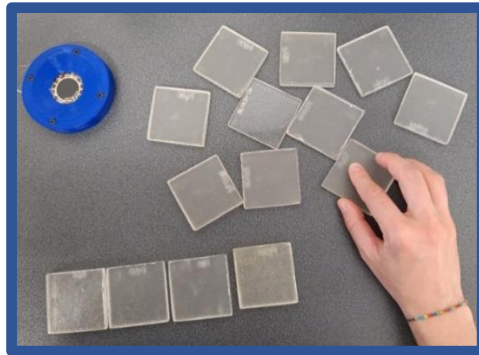


Figure 55: Results of discrimination campaign: results of the preliminary TASK 1 (a) on real surfaces; results of TASK 2 (b) on subsets of real textures; results of TASK 3 (c) on the simulated textures by the PIEZOTACT.

## RESULTS OF TASK 1

Figure 55a shows the results of the discrimination task 1. In this task (Figure 56), the participants dealt with the sorting of the entire set of 14 samples (real surfaces), from the roughest to the smoothest one. High percentage of association are localized on the main diagonal of the matrix, testifying a good performance of the participants to identify the sequence of the explored textures. On the other hand, discrimination errors interested in particular the samples S2 and S3, which have been often confused. As well, discrimination errors occurred for the group of samples from S9 to S13. The “no texture” sample was always correctly positioned in the sequence by all the participants.



*Figure 56: the Task 1 involves the discrimination of the entire set of 14 surfaces, by sorting them from the roughest to the smoothest one.*

## RESULTS OF TASK 2

Figure 55b shows the results of the task 2 of the discrimination campaign. The task (Figure 57) was related to the discrimination of the real surface samples, divided into sets, each constituted by 3 samples. The results related to all the sets are reported in the matrix. High percentages of association are localized on the main diagonal of the matrix, testifying an overall good performance of the participants to discriminate the real samples. Some discrimination errors interested again the samples S2 and S3, and most of the errors have been registered for the group of samples from S9 to S13, confirming the results obtained for the preliminary task 1.

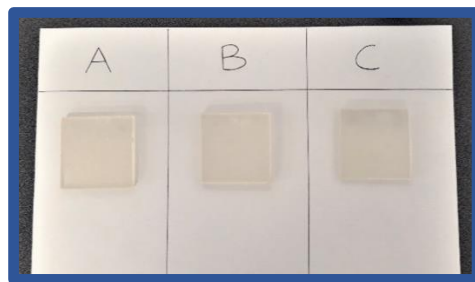


*Figure 57: The Task 2 involves the discrimination of isotropic samples divided into triplets, by sorting them from the roughest to the smoothest.*

### RESULTS OF TASK 3

Figure 55c shows the results of the discrimination task 3, related to the simulated textures (reproduced FIV), by the PIEZOTACT device (Figure 58). High percentage of association are localized on the main diagonal of the matrix, testifying a good performance of the participants to discriminate the textures mimicked by the device, thanks to the reproduced FIV stimuli. Again, some discrimination errors are related to the samples S2 and S3, confused with each other, while most of the errors have been registered again between samples from S9 to S13.

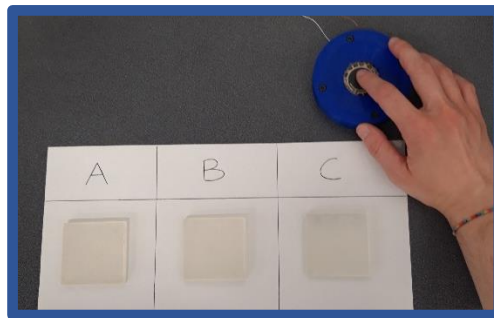


*Figure 58: The Task 3 involves the simulated textured by mimicking the FIV with the PIEZOTACT.*

### RESULT DISCUSSION

The resulting matrices have been compared in Figure 59, highlighting the areas of the matrices where the discrimination errors are localized for each task.

Let's recall that the first task was related to the ordering of the entire sequence of 14 isotropic samples, the second task to the discrimination of the real isotropic samples, arbitrary divided into sets (each constituted by 3 samples), and the third tasks concerned the simulated surfaces, mimicking the FIV by the PIEZOTACT device.

Figure 59 highlights that there is a clear agreement between the results of the 3 discrimination tasks. The overall discrimination campaign shows good results for all the tasks, either with real or simulated textures, with high percentages of association on the main diagonal of the matrices. In all the 3 tasks the main discrimination errors are localized into the same areas of the matrices. In particular, the samples S2 and S3 have been confused during all the 3 tasks, both with real and simulated textures. Moreover, the group of samples, from S9 to S13, underwent to highest percentages of discrimination errors in the all the 3 tasks. On the contrary, the group of samples from S4 to S8 have always been correctly discriminated in the 3 tasks.

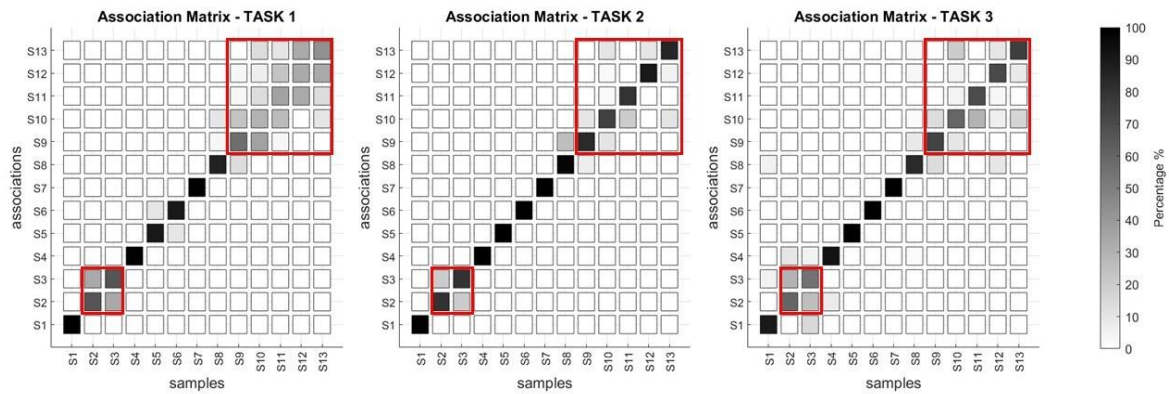


Figure 59: Comparison between the matrices associated to the 3 tasks constituting the discrimination campaign. In all the matrices, the groups of samples that have been confused the most are highlighted.

The agreement between the results found for the real textures (Task 1 and Task 2) and for the discrimination of the simulated textures by mimicking the FIV by the PIEZOTACT device (Task 3) testifies the good rendering performance of the device and the developed rendering methodology. Moreover, while touch is a very complex sense, which involves many stimuli (vibrations, pressure, contact stresses, friction, temperature, humidity, etc.), the PIEZOTACT device and the underlying signal processing allow the rendering of textures, decoupling the FIV stimuli by the other stimuli involved into the overall tactile perception. The results obtained by the discrimination tasks, with the good correlation in discriminating real and simulated surfaces (by only FIV), allows thus to emphasize once more the main role played by the FIV stimuli in the perception and discrimination of fine textures.

The found correlation between the FIV spectra and the results of the entire discrimination campaign (composed by the 3 tasks) is here discussed in detail.

Figure 60a and Figure 60b show examples of FIV spectra associated to the groups of confused samples into the entire discrimination campaign, for both real and simulated textures, while Figure 60c shows an always correctly discriminated group of samples.

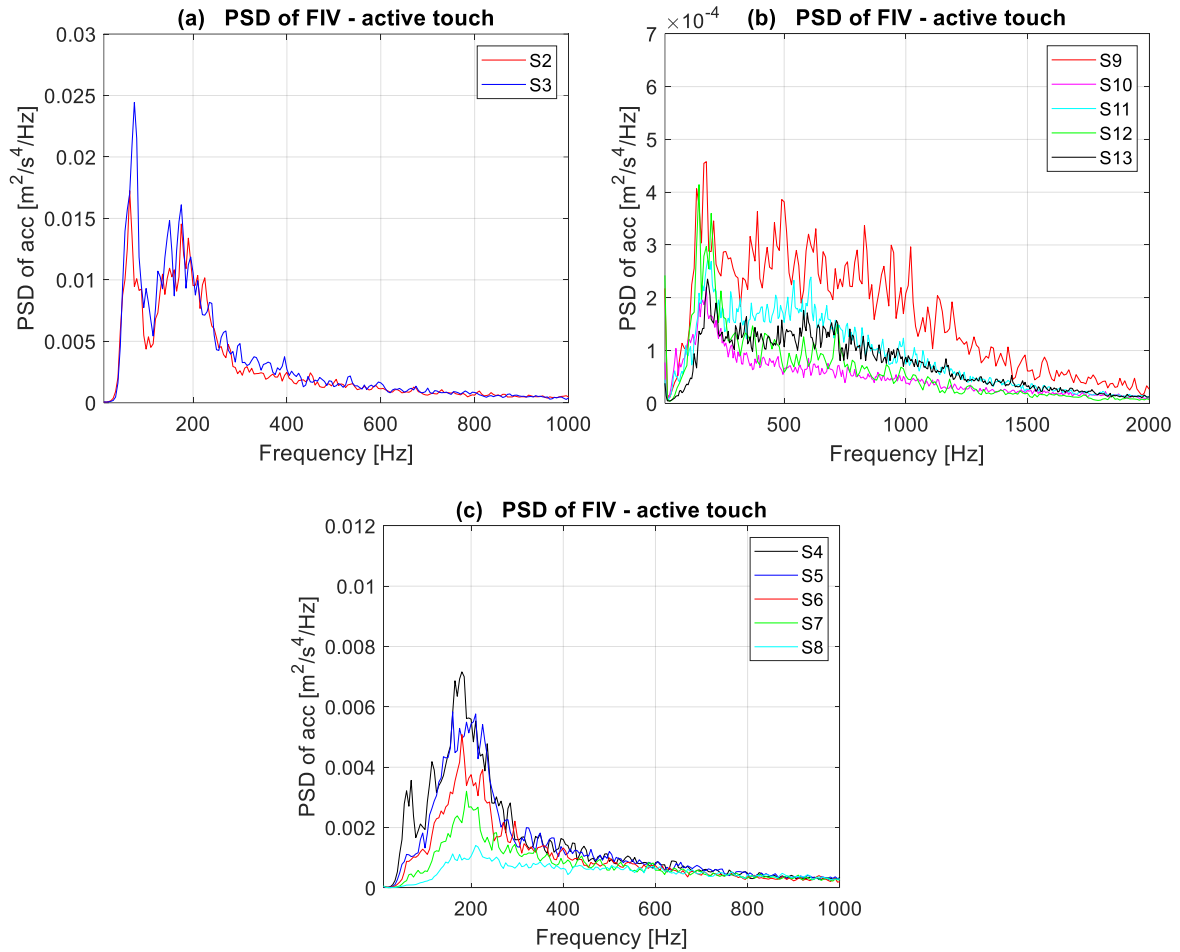


Figure 60: Examples of FIV spectra associated to confused groups of samples in (a) and (b) and correctly discriminated samples in (c).

The following observations can be then highlighted by comparing the discrimination and the FIV spectra:

- The samples S2 and S3, which have been often confused in the 3 tasks, show FIV with very similar amplitude and frequency distribution (Figure 60a).
- Similarly, the group of samples from S9 to S13 undergone to confusion in the entire campaign. The 10 participants had difficult to discriminate this group of samples both in the case of the real samples and in the one related to the mimicked FIV. During the task 1, related to the entire sequence of 14 real samples, the percentages of error were very high for the considered group of samples. Again, the FIV spectra, associated to these samples (Figure 60b), show similar amplitudes, and inversions of amplitudes with respect to the surface roughness.
- On the contrary, by observing the FIV spectra related to the samples from S4 to S8 (Figure 60c), which have been always correctly discriminated during the 3 tasks, it turns out that they show clearly different amplitudes of the FIV spectra.



The results of the discrimination campaign have been analysed in the light of the RMS of FIV acceleration as well. Figure 61 shows the sample roughness (Ra) compared with the RMS of the FIV, measured during passive touch (controlled velocity of 30 mm/s) for a reference participant, where the roughness is decreasing from S1 to S13.

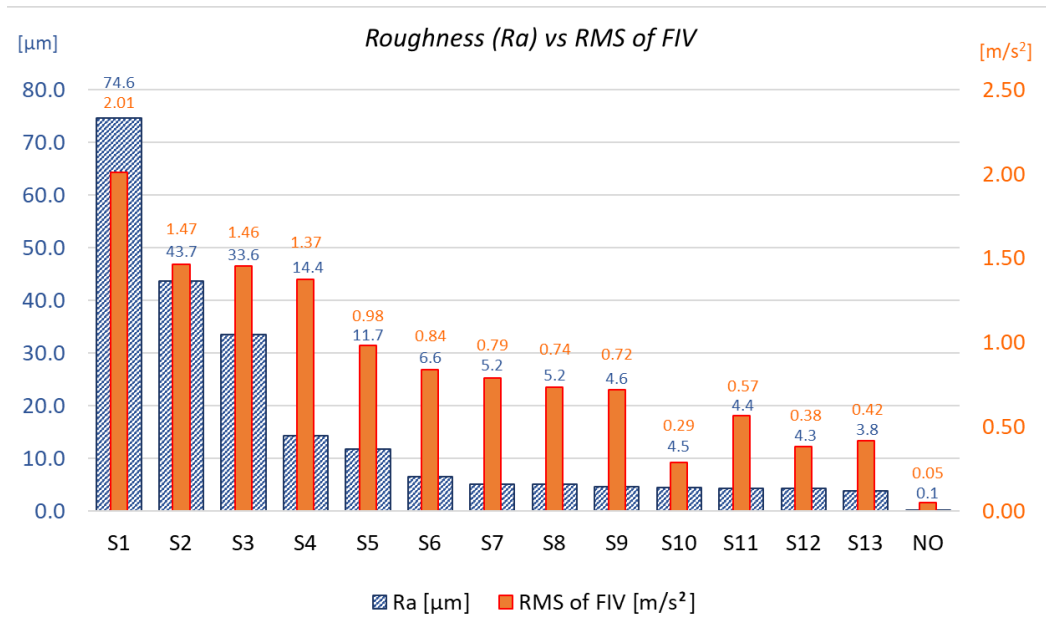


Figure 61: Ra roughness vs RMS of FIV for passive touch of the 14 isotropic samples for a reference participant.

When considering the FIV amplitude, from sample S1 to sample S9, the RMS decreases with the roughness, while, from sample S10 to sample S13, the trend of the RMS of the FIV presents inversions with respects to the roughness. When considering the results from the discrimination campaigns, the following considerations can be made:

- Samples from S1 to S9 have been generally well discriminated, with the following exceptions:
  - The samples S2 and S3, which have been confused in the entire discrimination campaign, present very similar RMS of induced vibrations, although they present clearly different Ra.
  - As well, the samples S8 and S9 present a very similar RMS but a different Ra and, in some cases, the samples have been confused in the discrimination campaigns.
- On the contrary, the samples from S10 to S13 underwent the highest percentage of errors in the entire discrimination campaign, both on real and simulated textures. In accordance, their RMS present similarities and inversions with to respect to the sample roughness.

- Moreover, samples S7 and S8 present similar values of Ra, but they have been always well discriminated in the entire campaign. In accordance, the associated RMS of FIV and the FIV spectra (Figure 61 and Figure 60c) are clearly different.

Summarising, the trend of the FIV (RMS and spectral distribution) agrees with the results obtained in the discrimination campaign on real and simulated textures. For isotropic textures, the discrimination errors occurred each time the FIV amplitude were similar or reversed, with respect to the roughness.

The FIV, and in particular the RMS amplitude of FIV, have been then directly correlated the perception and discrimination of the textures under examination, while the surface roughness (Ra) did not prove to be a good indicator. Effectively, it should be kept in mind that the mechanical signal directly received by the mechanoreceptor is the skin transient deformation (vibrations) and not the topography.

From Figure 61 it can be noticed as well that the samples with higher difficulty to be discriminated are the ones under a certain level of FIV amplitude (about  $0.7 \text{ m/s}^2$  in Figure 61). In future works it would be interesting to investigate if there is a sensitivity threshold below which the vibrations, induced by the tactile exploration of the surface, are too low to allow the clear discrimination of textures. For the reference participant, presented in Figure 61, this threshold could be identified by an RMS value of about  $0.7 \text{ m/s}^2$ .

### 4.3.3 Discrimination of periodic textures vs discrimination of isotropic textures

The results of the discrimination campaign on isotropic randomly rough samples presented in section 4.3.2 agree with the results obtained for periodic textures in section 4.3.1:

- In both cases, for periodic and random textures, the participants have been able to associate the simulated textures (reproduced FIV) by the PIEZOTACT device to the real ones, with very good percentages of success. This good discrimination performance found for two different types of textures, periodic and isotropic, validates the developed PIEZOTACT device and texture rendering methodology.
- Moreover, in both cases (periodic and isotropic textures), it has been possible to well correlate the results of the discrimination campaign with the FIV spectra, despite the discrimination of periodic textures turned out to be mainly driven by the FIV frequency distribution, while the isotropic textures resulted to be discriminated by the FIV amplitude. Moreover, this shows how useful the PIEZOTACT device is as a tool to investigate the effect of the different features of vibrational tactile stimuli (amplitude, frequency distribution) in the perception and discrimination of textures.

## 4.4 Modifying texture perception by FIV rendering

---

The developed PIEZOTACT device holds not only technological applications, in which the hope is to be able to merge a rendering of textures by FIV with that based on other mechanical stimuli, such as friction, to obtain a faithful reproduction of surface perception. The primary purpose behind the development of PIEZOTACT is to serve as a research tool, specifically for exploring the influence of various features of tactile vibrational stimuli on the perception and discrimination of textures. In this perspective, the device is capable of isolating and decoupling vibrational stimuli (FIV) from other tactile stimuli, enabling an in-depth investigation into their role in perception. Moreover, it can also be used to appropriately manipulate signals, alter their features (e.g. amplitude and frequency distribution of FIV), and create fake textures that allow to deepen the investigation into the relationship between surface topography, mechanical stimuli and tactile perception.

Since the present work already emphasized the important role of the amplitude of the vibrational stimuli in the discrimination of isotropic textures, a further discrimination campaign on textures simulated by the tactile device has been conducted here by inverting the amplitude of the measured FIV, to evaluate whether participants consistently discriminated textures in accordance with this inversion.

The used protocol and the results of the discrimination campaign are reported in the following sections.

### 4.4.1 Protocol of discrimination campaign with FIV amplitude inversions

A discrimination campaign has been performed on a panel of 5 participants (1 female and 4 males, with ages ranging between 23 and 45 years). Fake textures, simulated by the PIEZOTACT device, have been built by inverting the amplitude of the FIV measured on the real surfaces, to investigate whether this amplitude inversion is followed by the participants during the discrimination tests.

Two sets of surface samples have been selected: a first set constituted by the samples S2, S6, S13, and a second set constituted by the samples S5, S8, S11. For each of the sets, the FIV signals corresponding to 2 surfaces have been inverted in terms of amplitude on the basis of their RMS ratios. An example is reported in Figure 62, related to the first sample set. Figure 62a shows the FIV signals measured when exploring the real surface samples S2 and S13. Figure 62b shows the same FIV, but inverted on the basis of their RMS ratio, as the ‘S2 INVERTED’ has the same RMS amplitude of the ‘S13’ and the ‘S13 INVERTED’ has the same RMS of the ‘S2’. As an example, ‘S2 INVERTED’ is obtained by dividing the

acceleration signal (FIV) of ‘S2’ by the ratio between the RMS acceleration of ‘S13’ and the RMS acceleration of ‘S2’. Figure 62c and Figure 62d show the corresponding PSD spectra: the FIV PSD of the inverted samples (Figure 62d) maintain the same frequency distribution with respect to their corresponding originals (Figure 62c), although the RMS amplitudes are inverted. Then, the obtained signals have been processed to be rendered by the PIEZOTACT device.

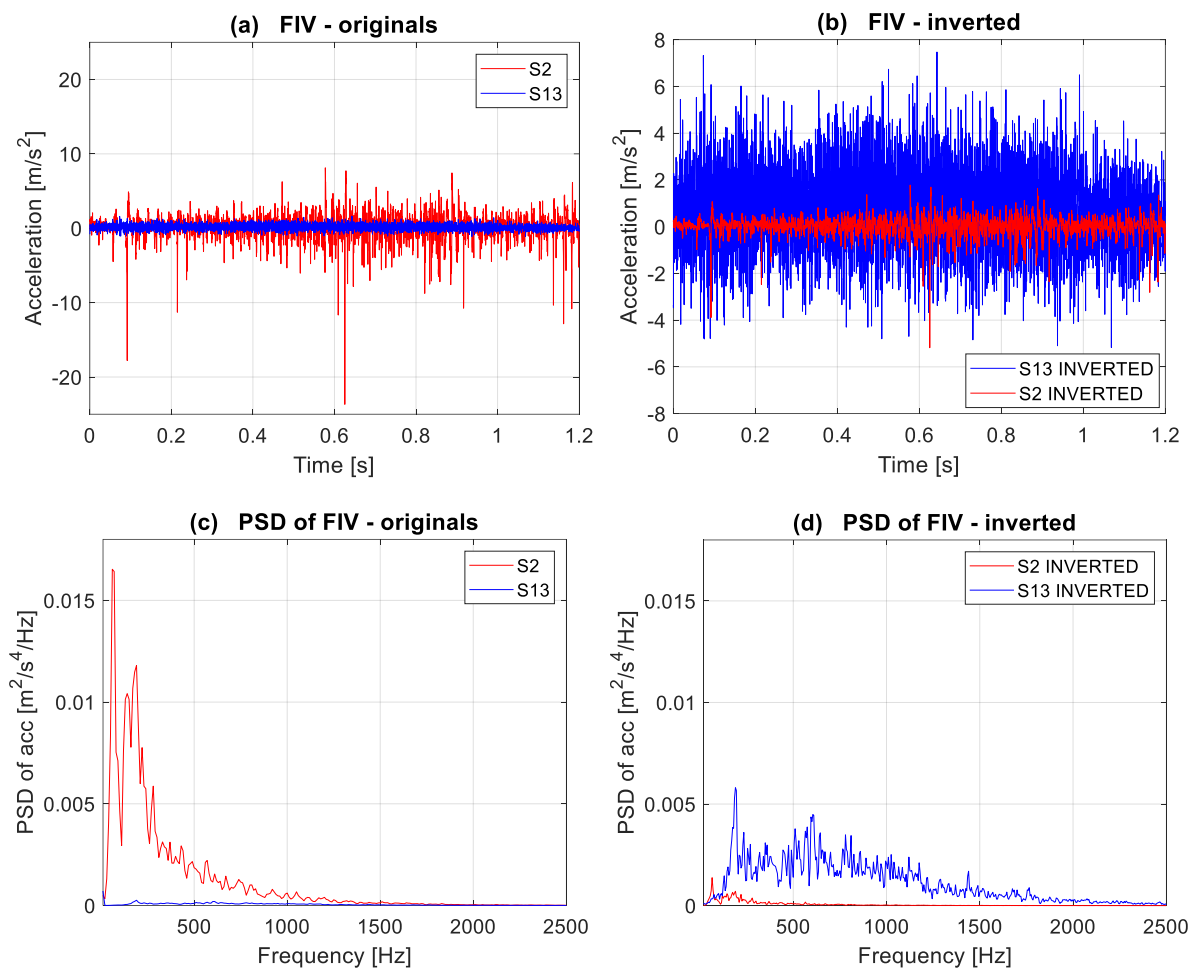


Figure 62: Example of inversion of FIV spectra of two surfaces based on FIV RMS amplitude: (a) FIV measured on the real surfaces; (b) FIV with amplitude inversion; (c) PSD of FIV measured on the real surfaces; (d) PSD of FIV with amplitude inversion.

For each set of samples, a discrimination test has been performed on the real surfaces according to the protocol of TASK 2 (see section 2.6.2), which involves the discrimination of the real samples, sorting them from the roughest to the smoothest. Then, for each set of samples, 4 discrimination tests with the simulated textures by the PIEZOTACT have been carried on, according to the protocol of TASK 3 (see section 2.6.2). For each of the sample sets, 2 tests have been conducted with 2 out of the 3 simulated textures inverted in terms of RMS FIV amplitude, and 2 tests with the 3 textures simulated with their original FIV

amplitude. The discrimination campaign is resumed in Table 6, where the simulated textures by the PIEZOTACT, starting from the FIV signals inverted in terms of RMS amplitude, have been conventionally named as ‘S2 INVERTED’, ‘S13 INVERTED’, ‘S5 INVERTED’ and ‘S11 INVERTED’. Each of the 5 participants underwent to the same discrimination test.

*Table 6: Resume of discrimination campaign of simulated textures by the PIEZOTACT with inversions of FIV RMS amplitude.*

<b>Set of samples (triplets)</b>	<b>Discrimination test: presented simulated textures to participants</b>
SET #1: samples S2, S6, S13	S2 INVERTED, S6, S13 INVERTED
	S6, S13, S2
	S13 INVERTED, S2 INVERTED, S6
	S2, S13, S6
SET #2: samples S5, S8, S11	S11, S8, S5
	S5 INVERTED, S8, S11 INVERTED
	S8, S5, S11
	S8, S5 INVERTED, S11 INVERTED

#### 4.4.2 Results of discrimination campaign with FIV amplitude inversions

The results, relating to the 5 participants, have been analysed by means of association matrices constructed with the same logic used for the matrices in section 2.6.3, but with some modifications, explained in the following.

For each of the 2 sets of samples (see section 4.4.1), 3 matrices have been constructed (Figure 63): one for the discrimination of the real surfaces (Figure 63a and Figure 63b), one for the discrimination of the simulated textures starting from the original FIV, without inversions, (Figure 63c and Figure 63d), and one for the discrimination of the simulated textures with inversion of the FIV amplitude (Figure 63e and Figure 63f).

The matrices in Figure 63a and Figure 63b, relating to the discrimination of real surfaces, have, as usual, on the abscissa  $x$  the real samples presented to the participants, and, on the ordinate  $y$ , the same sequence of real samples. In such a way, the pairs  $\{x,y\}$  represent the participants' associations, and the correct sample discrimination lie on the main diagonal. The obtained matrices show that all the real surfaces have always been correctly discriminated.

The matrices in Figure 63c and Figure 63d, relating to the discrimination of the simulated textures, starting from the original FIV, have, as usual, on the abscissa x the textures simulated by the PIEZOTACT (exactly reproducing the original FIV) presented to the participants, and, on the ordinate y, the associated real samples. Figure 63c and Figure 63d show that all the simulated textures have been correctly discriminated (except for an error that occurred only once by a participant in set #2).

Figure 63e and Figure 63f present the results of the discrimination of the textures simulated with inversion of the FIV amplitude. The matrices are constructed as follows. They are built by placing on the abscissa x the simulated textures by the PIEZOTACT (built with inversions according to the FIV RMS) presented to the participants. On the ordinate y there are the real surfaces arranged so that each simulated texture with inverted FIV RMS is associated with the real sample having the corresponding FIV RMS (example: the simulated texture 'S2 INVERTED' is arranged in correspondence with the real surface which has the same FIV RMS, i.e. surface S13, instead of the original S2 sample). This arrangement ensures that on the main diagonal of the matrix there are the expected associations, i.e. the associations which confirm the hypothesis that, by inverting the FIV RMS amplitude, the participants invert the original surfaces in the discrimination test. In this case, the results will therefore be referred, in the following, as 'expected results' ('expected associations') and 'unexpected results' ('unexpected associations') instead of 'correct/incorrect discriminations'. High association percentages are located on the main diagonal, testifying that the participants discriminated the textures, constructed with inversion of the FIV RMS amplitude, according to the expectation (Figure 63e and Figure 63f). As hypothesized, by inverting the FIV amplitude of two samples, the participants were misled to invert them in the discrimination.

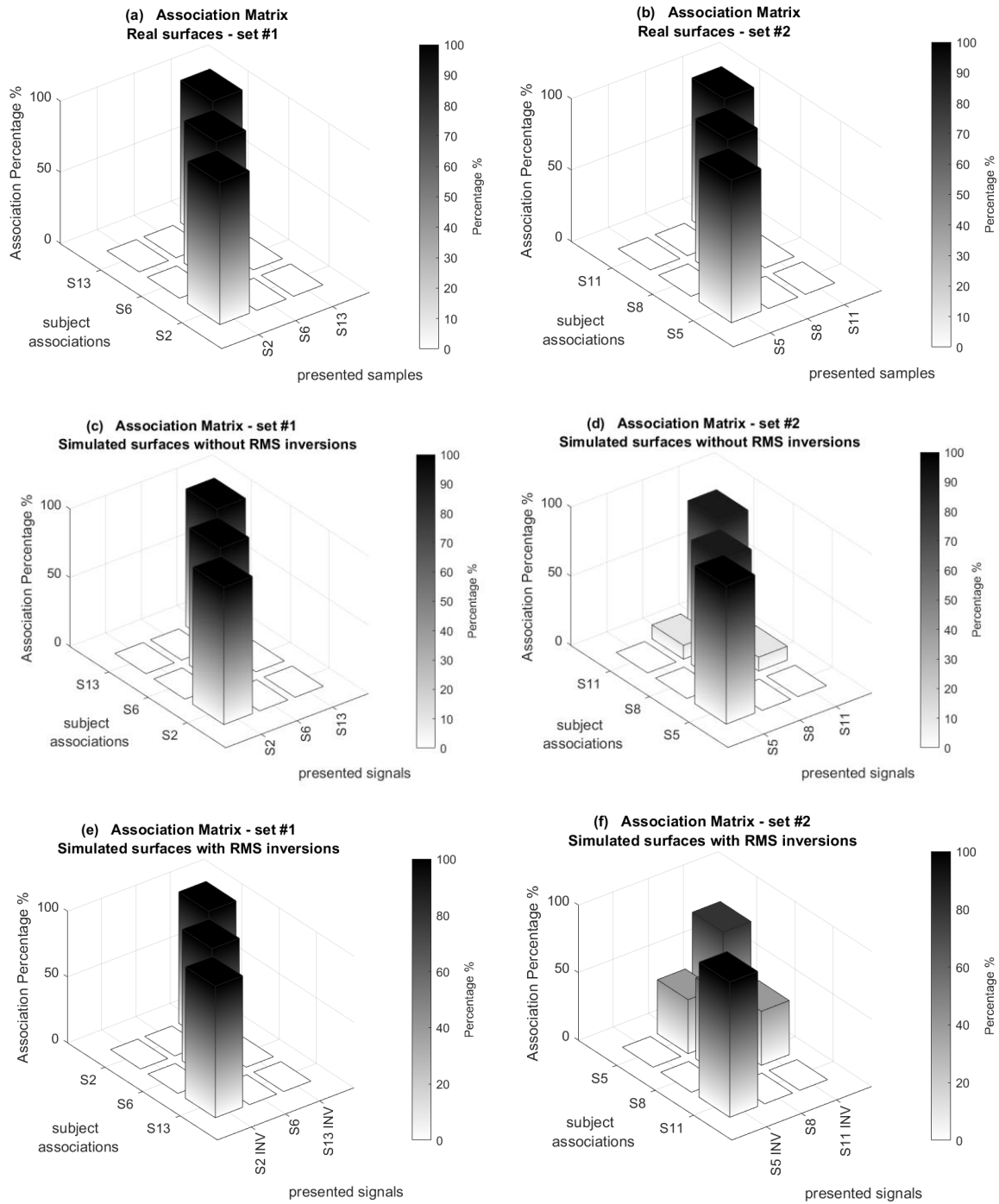


Figure 63: Results of discrimination tests for real samples ((a) and (b)), for textures simulated without amplitude inversions ((c) and (d)), and for simulated textures with RMS FIV amplitude inversions ((d) and (e)). On the left ((a), (c), (e)) the results related to set#1 and on the right ((b), (d), (f)) the results related to set#2.

The correct and incorrect discriminations (or expected and unexpected results) of the textures have been then analysed in the light of the FIV RMS amplitudes (Figure 64) and the FIV spectra (Figure 65).

The real samples present well distinct RMS and spectra of FIV and have been always correctly discriminated. When the simulated samples, presenting inversions in FIV RMS amplitude (see Table 6), have well distinguished amplitudes (Figure 64a and Figure 64b) and spectra (Figure 65a and Figure 65b), they led to the expected results in the discrimination.

Nevertheless, in the association matrix in Figure 63f it is possible to find some not negligible unexpected associations, which came from 2 different participants. Observations in the analysis of the FIV spectra (Figure 65c) and the relative RMS (Figure 64c), associated to those 2 participants, explain the obtained unexpected results. In fact, the 2 participants associated the simulated texture S11 INVERTED with the real sample S8. Let's keep in mind that S11 INVERTED was constructed having the same RMS FIV as sample S5, but maintaining the original spectral distribution of the sample S11. In this case, for 2 participants, this made the S11 INVERTED and S8 spectra very similar, as can be seen in Figure 65c. Their RMS of FIV are quite similar as well, as can be seen in Figure 64c. This explain the found unexpected result in the discrimination task (matrix in Figure 63f). It should be kept in mind that FIV results from the interaction between the surface and fingertip topographies, and different subject will generate different spectra for the same surface.

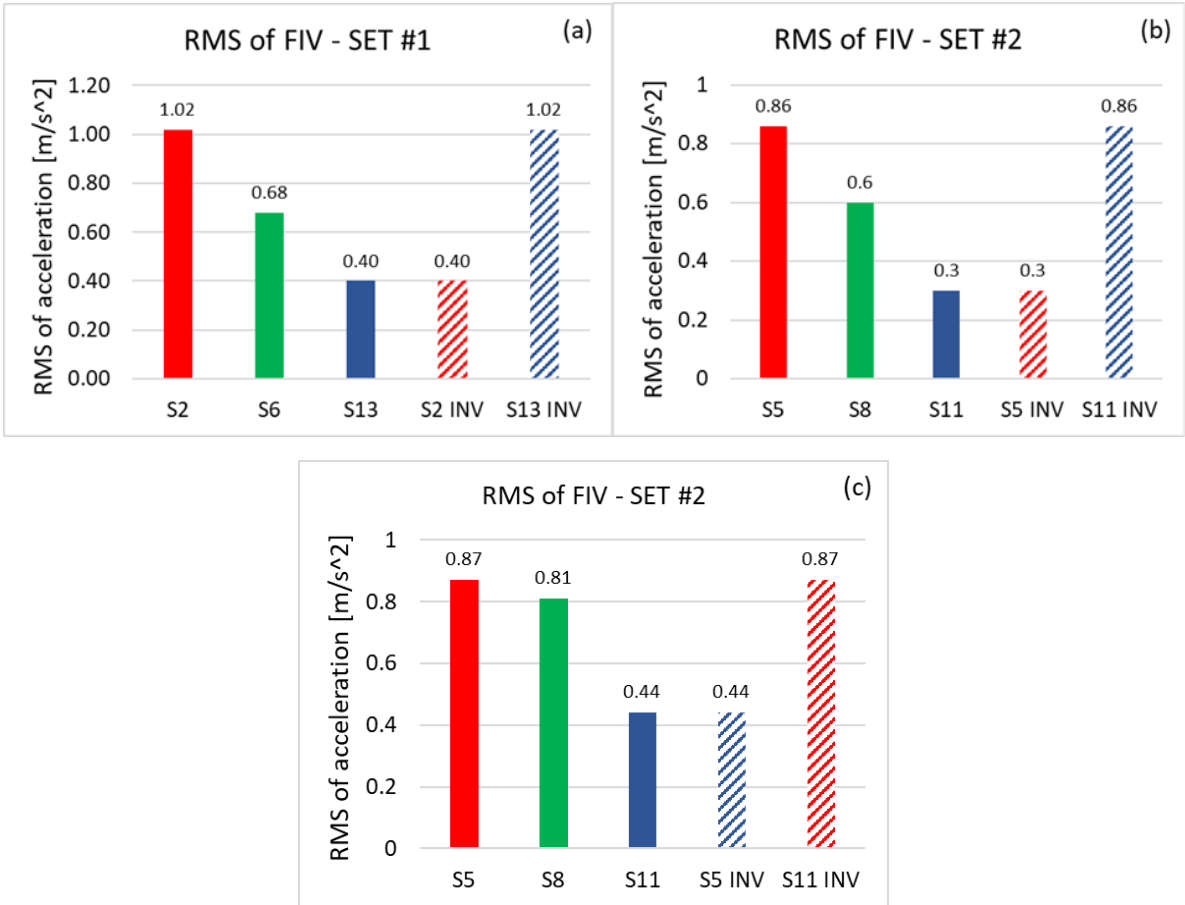


Figure 64: Examples of FIV RMS for different real and simulated textures. In (a) and (b) FIV RMS associated to expected associations/correct discriminations for SET #1 and SET #2 respectively, for a representative participant. In (c) FIV RMS associated to unexpected associations (SET #2), for a representative participant between the two who confused the samples S11 INV and S8.



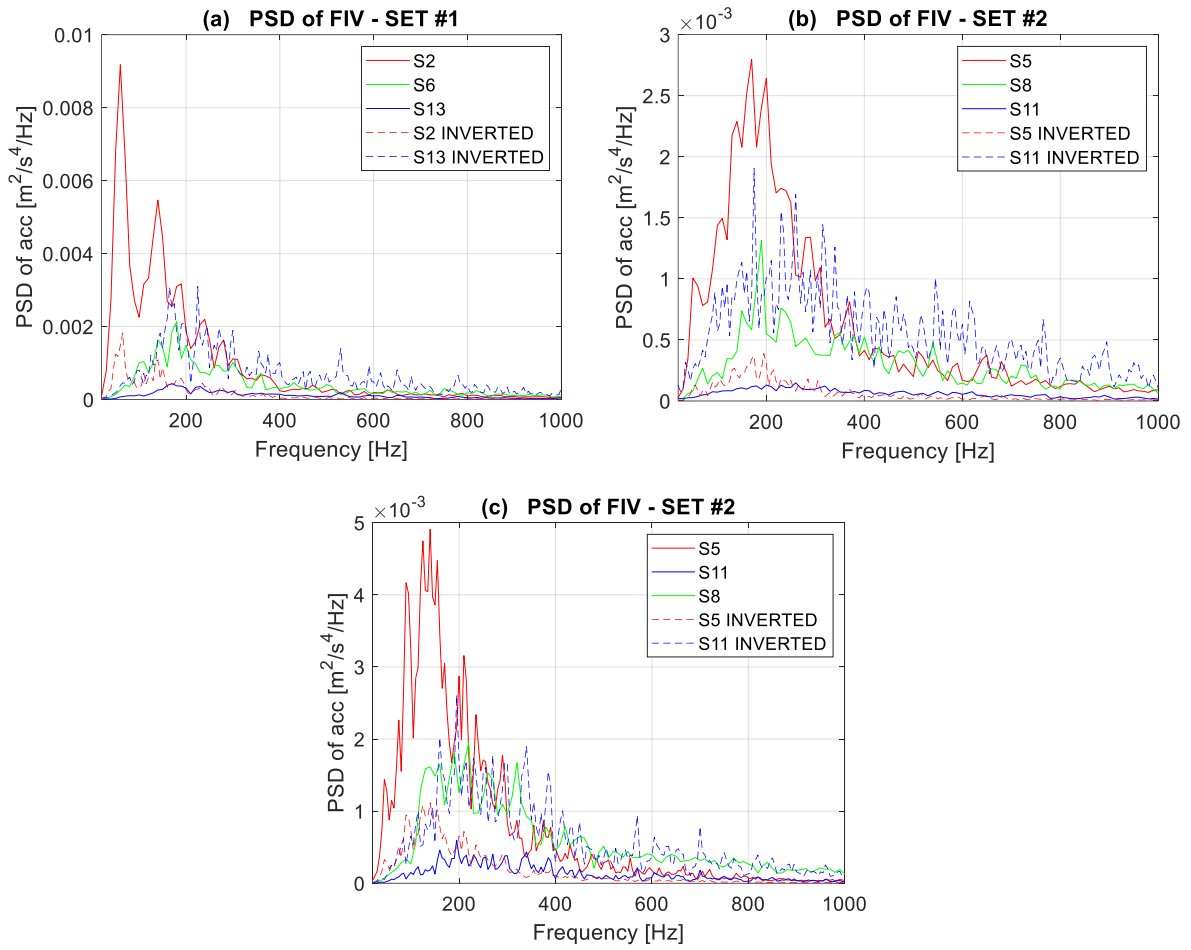


Figure 65: Examples of FIV spectra associated to real and simulated textures. In (a) and (b) spectra related to expected associations/correct discriminations for SET#1 and SET#2 respectively, for a representative participant. In (c) spectra related to unexpected associations (SET #2), for a representative participant between the two who confused the samples S11 INV and S8.

## 4.5 Concluding remarks

---

In this chapter, a vibrotactile rendering methodology based on Friction-Induced Vibrations has been presented, experimentally verified, and validated by perceptual campaigns.

In the first instance, a tactile rendering strategy has been presented that allows to faithfully mimic the FIV measured during the exploration of real surface textures. This methodology is based on the characterization and exploitation of the Transfer Function of the whole system consisting of the device, including the user's finger.

Therefore, the methodology has been experimentally verified by comparing the original FIV measured when exploring the real textures and the FIV mimicked by the developed device.

The rendering method has been then validated through tactile perception campaigns. Different textures, both periodic and isotropic, have been simulated by the device. Excellent performances in the discrimination of real and simulated textures have been achieved in the discrimination campaigns. Agreement has been found as well between the results in discriminating real and simulated textures. In both cases, the correct and incorrect discriminations for real and simulated textures have been interpreted and explained by means of the FIV, emphasizing a fundamental link between FIV and texture perception.

Moreover, a discrimination campaign on isotropic textures involving pairs of samples with inverted RMS amplitudes of the induced vibrations, when rendered by the PIEZOTACT, has been performed. The textures with FIV amplitude inversions were coherently discriminated by participants, as expected, emphasizing once more the role of FIV amplitude in the discrimination of isotropic textures. This campaign has shown as well how the PIEZOTACT device is a useful tool to study the impact of each feature of the vibrational signal generated by the exploration of textures in tactile perception. In fact, it allows to “play” with the different features of the FIV signal (amplitude, frequency distribution) and create artificially fake textures to investigate more deeply the relationship between FIV features and perception of textures. In the next future, other campaigns will be conducted, for example, on periodic textures, reversing and modifying the frequency distribution, with an approach similar to that used in this work.

Due to its main role in the FIV rendering methodology, the dynamic response of the system, consisting of the device and the user's finger, has been investigated more in detail in the following Chapter.



## Chapter 5

# Role of finger Transfer Function in vibrotactile rendering<sup>4</sup>

When dealing with the design of tactile devices, the interaction between the device and the user's finger becomes crucial and is worth to be deeply investigated. The sense of touch, by its nature, relies on the physical interaction with the object being explored. This principle holds true for tactile rendering devices as well; the interaction between the touched surface and the user's finger plays a key role in designing effective systems. In this context, when mimicking the vibrational stimuli, it is of utmost importance to consider the dynamic response of the finger during its interaction with the device/surface.

More specifically, since the texture rendering methodology proposed in section 4.1 is based on the processing of the target FIV signal, by the Transfer Function of the whole electro-mechanical system, its characterization is fundamental for mimicking the FIV signals with accuracy.

Different users mean different fingers, placed on the actuator, with their proper Transfer Function. Furthermore, being the system nonlinear, a role is also played by the contact parameters between the user's finger and the surface, such as the normal contact force and the finger/surface angle. In chapter 4 the Transfer Function was re-characterized for each individual user to perform discrimination campaigns and to validate the device. Moreover, the contact boundary conditions between finger and actuator were maintained fixed for all users.

---

<sup>4</sup> The content of this chapter has been partially published in [100].

In this Chapter, with a view to optimize the tactile device and the rendering methodology, a parametric analysis of the Transfer Function of the human finger, and then of the vibrotactile device including the user's finger, has been carried out on panels of participants.

Subsequently, the possibility of using an average Transfer Function between participants, to process the FIV signals, has been evaluated. The exploitation of the average Transfer Function to simulate textures using the PIEZOTACT device has been validated by discrimination campaigns on isotropic textures. The results obtained from the discrimination campaign carried out with the average Transfer Function have also been compared with the results obtained in section 4.3.2, where the individual Transfer Functions of each user of the device were exploited.

## 5.1 Parametrical analysis of the Transfer Function

A “step by step” approach has been exploited to first investigate the dynamics of the finger alone, and then the overall Transfer Function of the overall system constituted by the PIEZOTACT device and the finger. First a preliminary campaign of the finger Transfer Function has been carried out using a dynamic exciter (shaker), with the test bench described in section 2.5.2 on 5 participants. In the light of the encouraging results of this preliminary campaign, a broader parametric analysis has been then performed directly on the vibrotactile rendering device (with the setup in section 2.5.3), which is of interest for the processing of the FIV signals. In the campaign conducted on the device, the analysis has been extended to 20 participants, and further contact configurations.

### 5.1.1 Parametric analysis of the finger Transfer Function

The parametric campaign on the finger Transfer Function has been carried out using the test bench described in section 2.5.2 (Figure 66). The parametric study has been carried out on 5 participants (2 females and 3 males, with ages ranging between 21 and 55 years, 1 lefthander and 4 righthanders).

For the parametric analysis, the angle between the finger and the ceramic surface on the top of the shaker has been set at 20 degrees, maintained thanks to an arm support. For each participant, measurements have been performed with a contact load of 0.2N, 0.4N and 0.6N. The participant could hold the target contact load by observing the mean load displayed on the monitor.

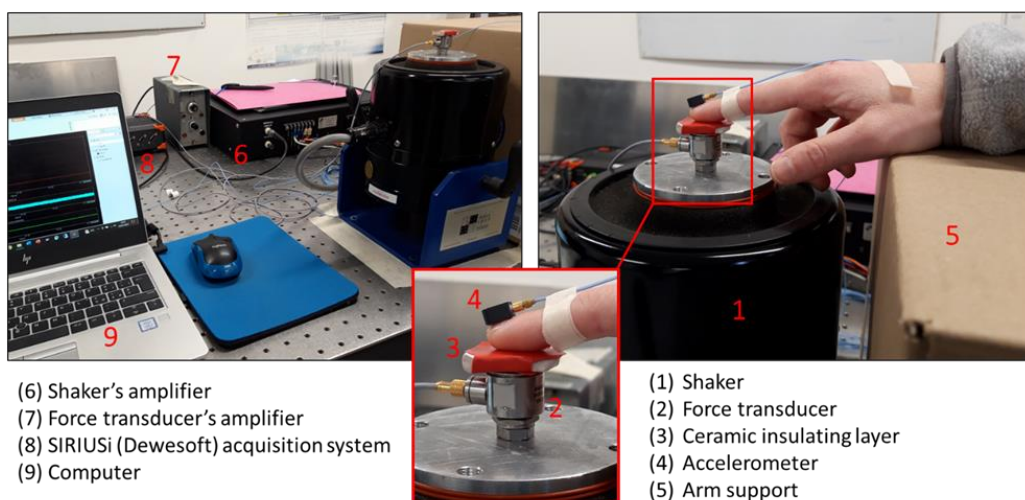


Figure 66: Test bench for parametric analysis of the finger transfer function.

The parametric analysis has been then articulated in two points:

- For a single participant, the comparison of the finger Transfer Functions, by varying the contact load between finger and vibrating surface, has been carried on.
- For a given contact load, the comparison of the finger Transfer Function of different participants has been performed.

The results of the parametric campaign are reported in the following.

Figure 67 shows the comparison of the finger Transfer Functions of all participants in the same test conditions: Figure 67a reports the finger Transfer Function of all the participants with a normal contact load of 0.2N, Figure 67b with a contact load of 0.4N and Figure 67c with a contact load of 0.6N. In all cases, the Transfer Functions of the participants are similar in trend and generate a bundle of curves of few dB of maximum deviation. Figure 67d presents all the curves relating to all participants and all test conditions (0.2N, 0.4N, 0.6N), superimposed on the same graph: they form a bundle of curves with a similar trend and a maximum deviation of 8dB.

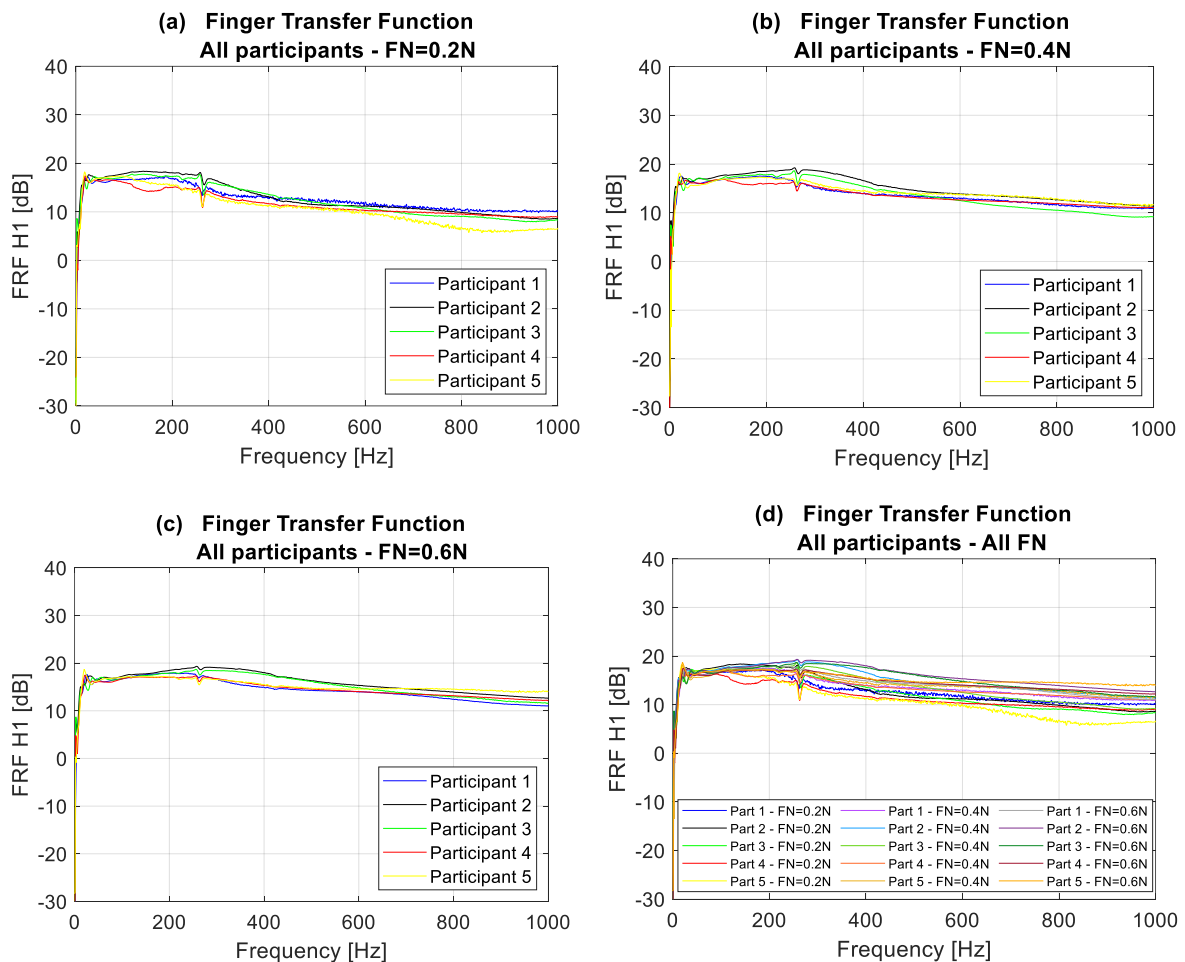


Figure 67: Comparison, among all participants, of the finger transfer function in the same test conditions: (a) contact load of 0.2N, (b) contact load of 0.4N, (c) contact load of 0.6N. In (d) the comparison of the finger transfer functions of all participants in all load conditions (0.2N, 0.4N, 0.6N).

Figure 68 presents the evolution of the maximum deviation as a function of the normal contact load. Increasing the contact load, the deviation of the Transfer Functions with the participants decreases. This may be explained by the increasing of the contact area and dynamic coupling of the subsystems, due to a larger load, decreasing the variability of the results. Lower loads can increase the variability in the effective contact area as the fingertip is less deformed.

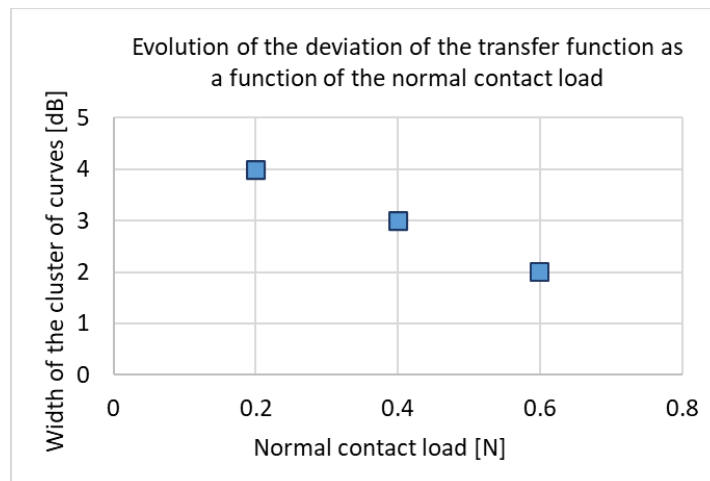


Figure 68: Maximum deviation of the transfer functions as a function of the normal contact load between the finger and the ceramic plate.

In light of these results, an average Transfer Function among participants has been then calculated for each test condition (normal load): an example of the average Transfer Function, superposed on the specific ones of the participants, is presented in Figure 69, for the case of a contact load of 0.2N.

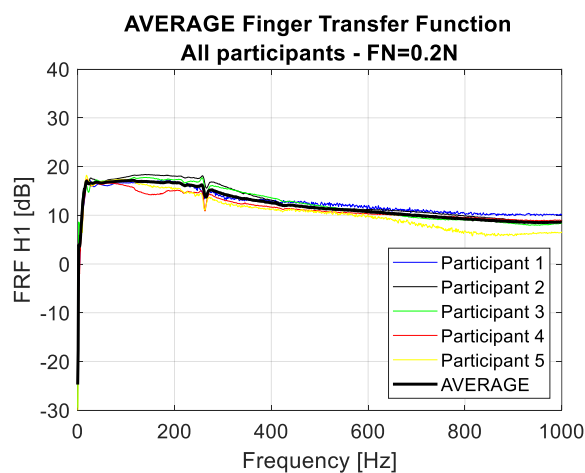


Figure 69: Example of calculated average transfer function among participants (for a load of 0.2N) together with the specific participant curves.



Moreover, for each participant, the gain of the finger Transfer Function increases as the contact load increases; an example, referred to one participant, is reported in Figure 70a. The same behaviour has been found for all participants.

For each test condition (0.2N, 0.4N, 0.6N) the average Transfer Function among all participants has been computed. Figure 70b shows the comparison between the average Transfer Functions, among participants, for the three test conditions (0.2N, 0.4N, 0.6N). The trend of the average Transfer Function reflects the trend of the singular Transfer Function of each participant: as the normal contact load increases, the gain of the Transfer Function increases, due to the increase of the contact surface and mechanical coupling between fingertip and actuator.

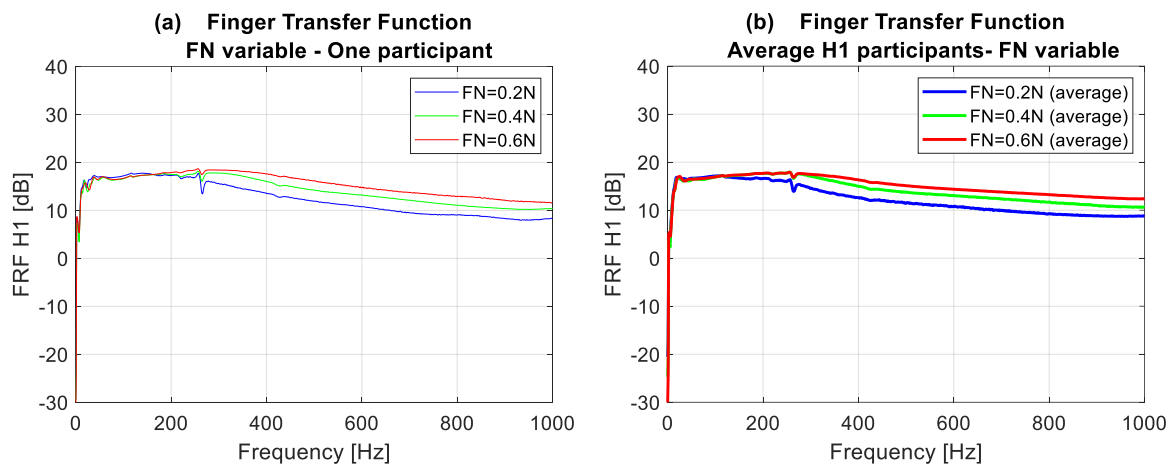


Figure 70: (a) For one participant, the finger transfer function increases as the contact load increases. (b) average finger transfer functions, calculated among all participants, for each test conditions (0.2N, 0.4N, 0.6N): the transfer function increases as the contact load increases.

It should be noticed that the antiresonance at about 265 Hz, present in all Figures, is characteristic of the used electrodynamic shaker. As proof, Figure 71a shows the Control Transfer Function obtained by fixing the accelerometer with wax directly on the ceramic plate. The Transfer Function has been obtained between the acceleration ( $[m/s^2]$ ) and the random signal ( $[V]$ ) sent through the acquisition system, to consider for the overall electro-mechanics of the system consisting of the shaker, the force transducer, and the ceramic plate. Figure 71a clearly highlights that the antiresonance at 265Hz was already present in the electro-dynamic shaker, and it is recovered in the participants' Transfer Functions (Figure 71b).

Being the aim of the study the comparison of the finger Transfer Functions of different participants and in different boundary conditions, always maintaining the same experimental setup, this antiresonance, due to the dynamics of the excitation system, has been neglected.

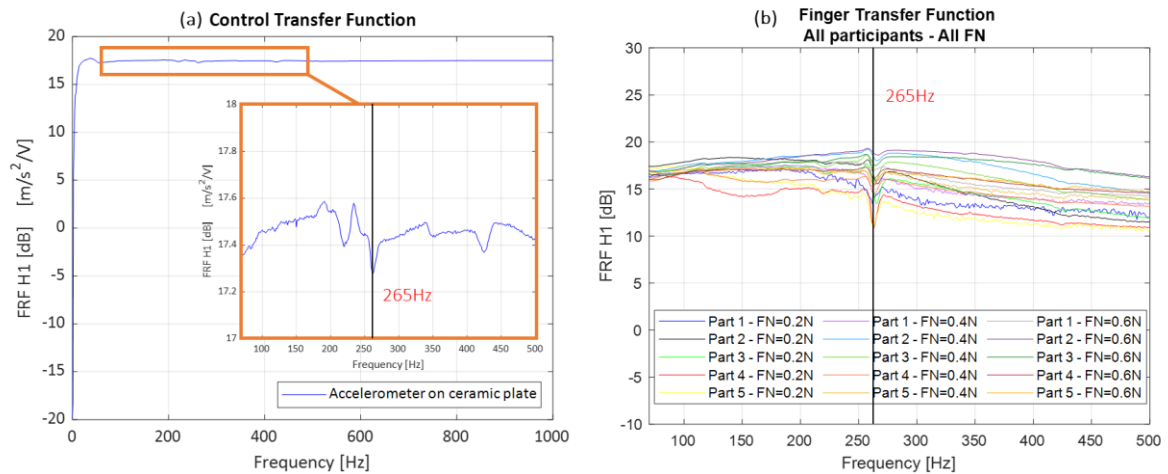


Figure 71: The antiresonance at 265Hz is characteristic of the dynamic shaker (a), and can be recovered in all the finger Transfer Functions for all participants and all test conditions (b).

The parametric analysis of the finger Transfer Function has been then extended to the study of the overall system consisting of the PIEZOTACT device and the user's finger, which is of primary interest in the present work.

### 5.1.2 Characterization of the overall electro-mechanical Transfer Function (PIEZOTACT and user's finger)

Given the encouraging results of the parametric analysis of the finger Transfer Function reported in section 5.1.1, it has been decided to carry out a wider campaign directly using the PIEZOTACT device including the participants' finger.

The parametric study has been carried out on 20 participants (10 females and 10 males, with ages ranging between 20 and 55 years). It is important to notice that the panel of participants who performed this campaign was composed by different participants with respect to the panel who performed the campaign in section 5.1.1 for the Transfer Function of the Finger alone, incrementing the robustness of the results.

The used experimental test bench is described in section 2.5.3 (Figure 72).

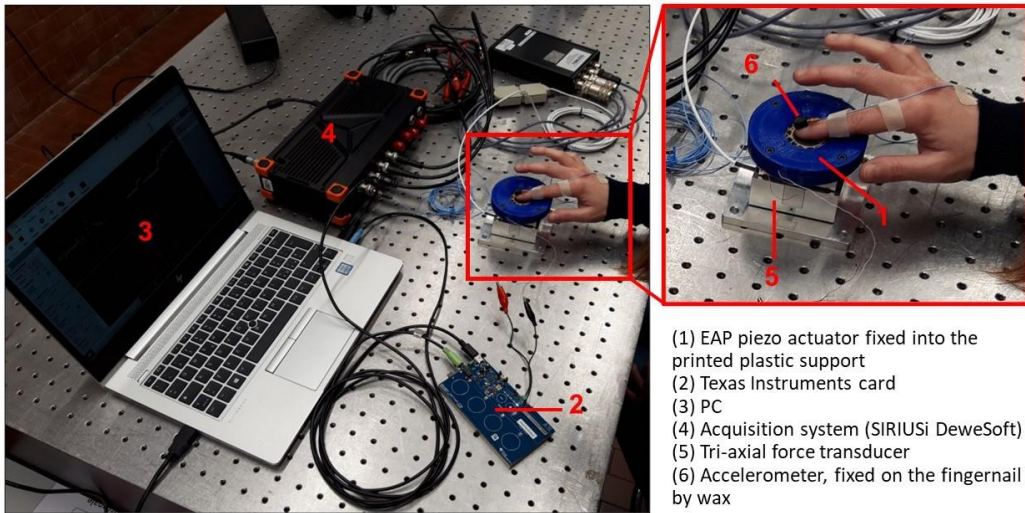


Figure 72: Experimental setup to characterize the overall PIEZOTACT and finger Transfer Function.

The parametric analysis has been conducted by varying the participant, the finger/actuator contact force and the finger/actuator inclination angle. As regards the contact force, the values of 0.2N, 0.4N and 0.6N have been maintained (values in the range involved in tactile exploration). For the finger/actuator contact angle, the values of 20° and 40° have been selected, with the same criterion. To assist the participant in maintaining the designated finger/actuator angle, the arm support has been conveniently arranged. Figure 73 resumes the tests performed by each participant to carry on the parametrical analysis.

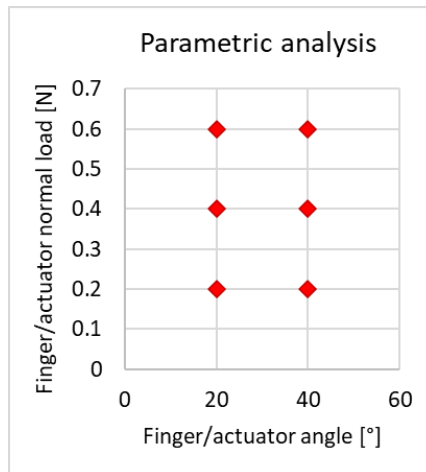


Figure 73: Resume of the tests performed by each participant to carry on the parametric analysis of the transfer function of the PIEZOTACT device including the participant's finger.

The parametric analysis has been articulated in two points:

- For a single participant, the comparison of the device and finger Transfer Function by varying different contact parameters between finger and vibrating surface (normal contact load and finger/surface angle), has been carried on.
- For a given choice of contact parameters (normal contact load and finger/surface angle), the comparison of the device and finger Transfer Function of different participants has been performed.

Firstly, the device and finger Transfer Function for a single participant is discussed by varying the contact parameters between finger and vibrating surface.

As found for the finger alone, for each participant, fixed the finger/actuator angle, the gain of the Transfer Function increases as the contact force increases. The same trend is found for all the participants and for both the tested values of the finger/actuator angle ( $20^\circ$  and  $40^\circ$ ). Figure 74 shows an example for a participant.

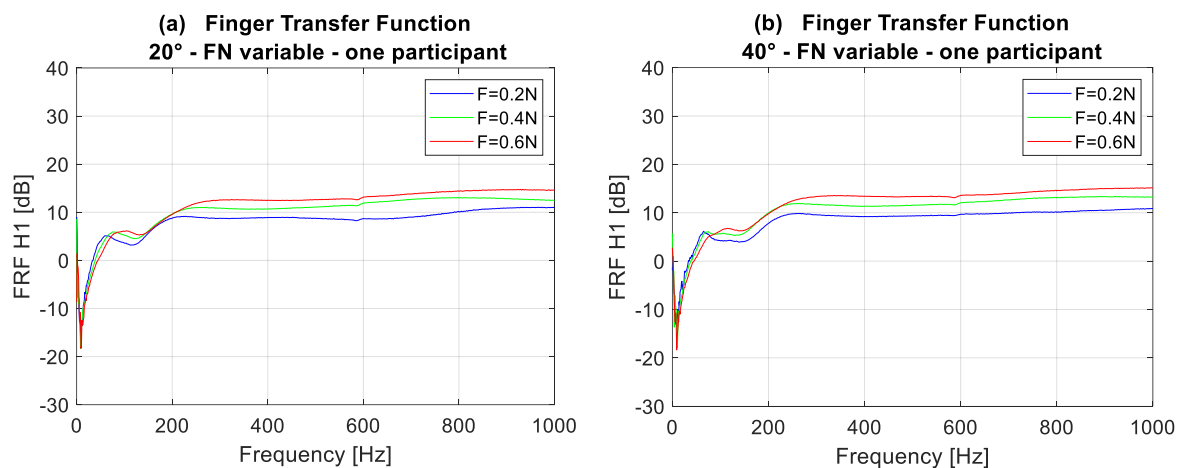


Figure 74: Example of transfer function for a participant as the contact load varies, for an angle of  $20^\circ$  (a) and  $40^\circ$  (b).

For each participant, fixed the value of the contact force, the Transfer Function referred to the two values of the finger/actuator angle ( $20^\circ$  and  $40^\circ$ ) are compared. The variation of the angle causes a slight variation of the shape of the Transfer Function, but without a significant deviation and without a definite trend. This behaviour is found for all the contact forces and for all the participants. Figure 75 reports an example for a participant.

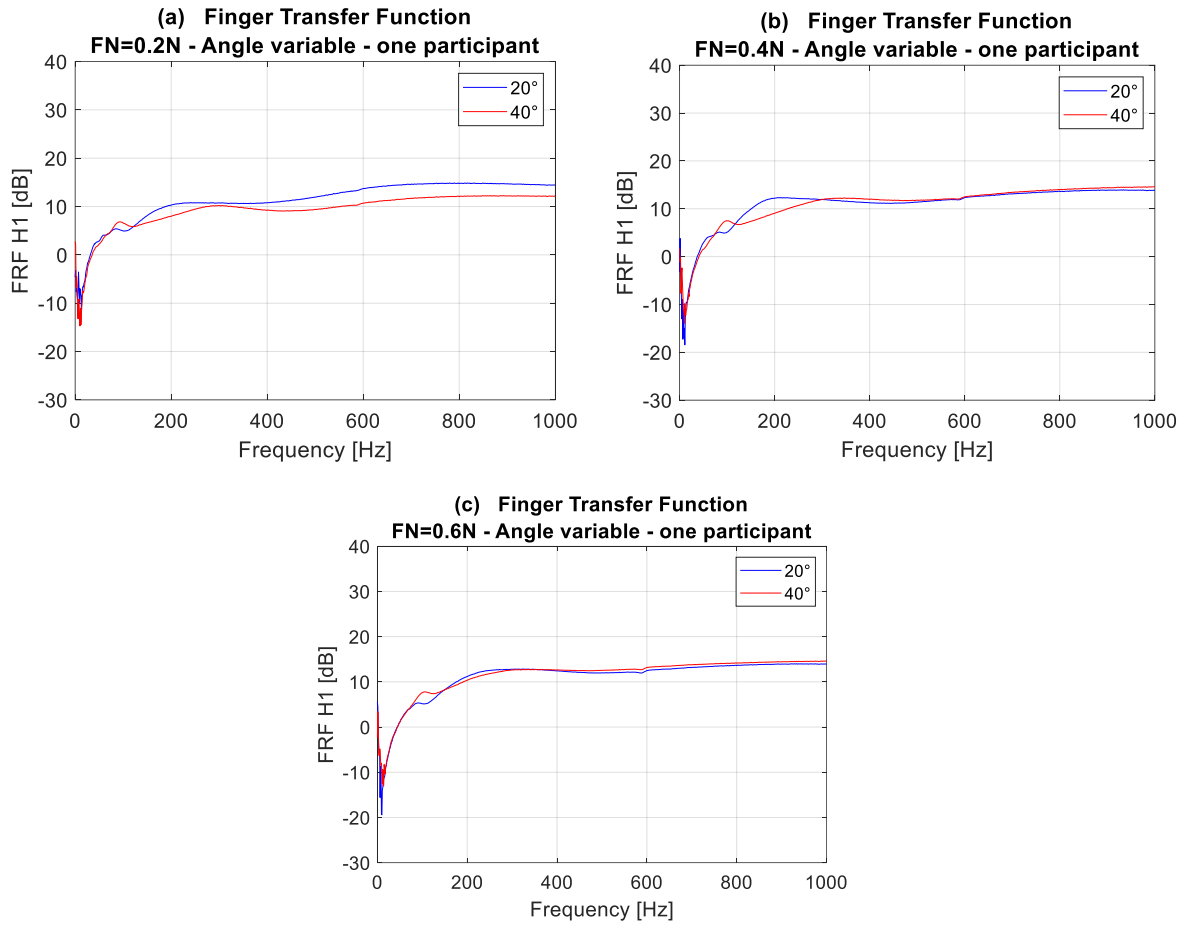


Figure 75: Example of comparison, for a participant, between the transfer function for angles of 20° and 40° with a load of 0.2N (a), 0.4N (b), 0.6N (c).

Then, for each tested condition {angle, force}, the Transfer Functions of the 20 participants are compared.

Figure 76 shows an example for the condition {20°, 0.2N}. As in section 5.1.1, the Transfer Functions of all the participants form a bundle of curves with a few dB of maximum deviation, with a well-defined and repetitive trend. The average Transfer Function of all the curves is computed as well (Figure 76). The same behaviour is found for all test conditions {angle, force}. Figure 77 reports the maximum deviation of the Transfer Functions of all participants for each test condition {angle, force}. Having fixed the finger/surface angle, as for the finger alone, the maximum deviation shows a decreasing trend as the contact force increases, for both 20° and 40°.

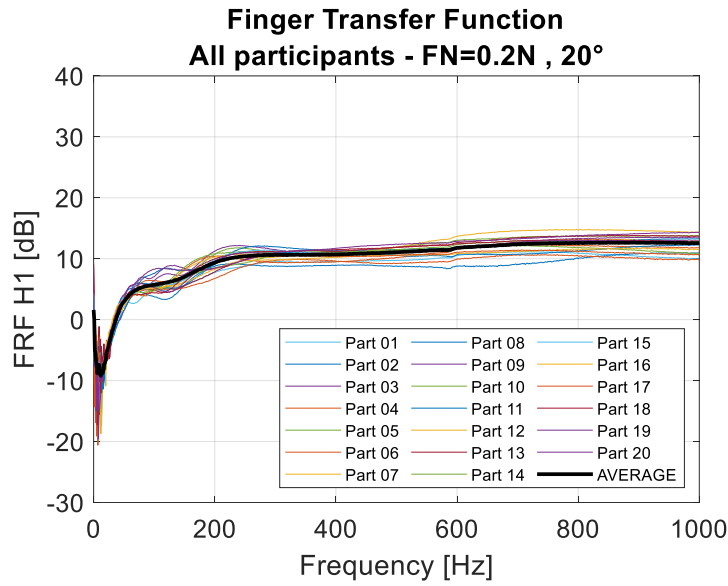


Figure 76: Superposition of the transfer functions of all the participants for the condition  $\{20^\circ, 0.2N\}$  and the average transfer function.

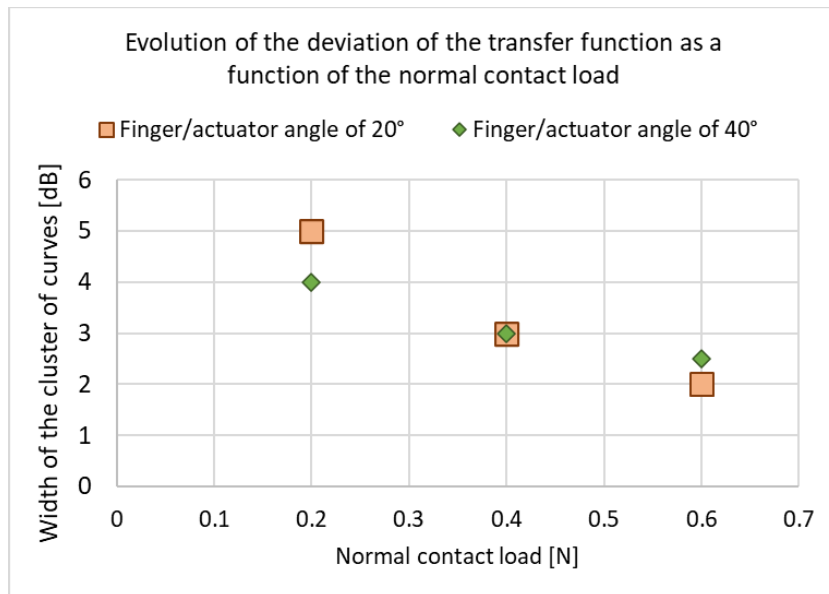


Figure 77: Maximum deviation of curves, representing the transfer function of the system (PIEZOTACT device and user's finger) of all participants, as a function of the finger/actuator normal contact load and the finger/surface angle.

For each participant, each measurement for each test condition  $\{\text{angle, force}\}$  has been repeated 3 times consecutively, without repositioning the finger. Then, a repeatability test has been performed, for each participant, for the condition  $\{20^\circ, 0.2N\}$ , which is the condition associated with the greatest variability (greater deviation of the bundle of curves) of the Transfer Function, and therefore represents “the worst case”. For the condition  $\{20^\circ, 0.2N\}$ ,

the participant has been asked to repeat the measurement of the Transfer Function 3 times, withdrawing the finger and repositioning it between one measurement and another. Figure 78a shows the superimposition (for a participant taken as an example) of the 6 tests performed by the participant for the condition  $\{20^\circ, 0.2N\}$ : the 6 measurements, either with or without repositioning the finger, present a very high repeatability, with negligible variations. Moreover, Figure 78b shows the associated Coherence Functions, which are always very close to 1 (except for very low frequencies, which the actuator cannot handle); a Coherence close to 1 and stable in frequency has always been found for all measurements under all the conditions.

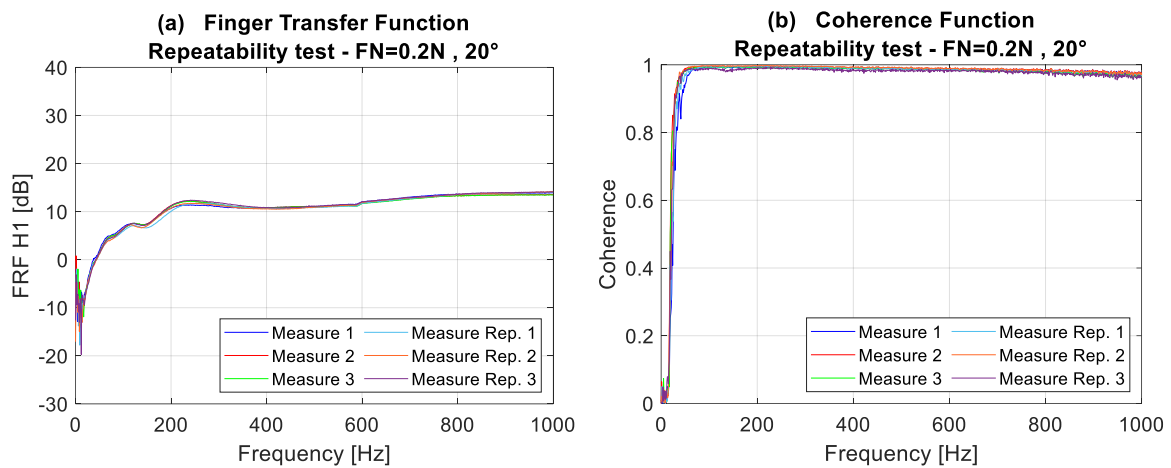


Figure 78: Example of Repeatability test: (a) Transfer Functions and (b) Coherence Functions for the 6 measures performed by the participant, 3 consecutive measurements without repositioning the finger and 3 measures withdrawing and then repositioning the finger; all showing high repeatability and high Coherence.

In conclusion, all the obtained Transfer Functions differ slightly between participants and within the tested ranges of contact boundary conditions.

The real question lies on the effect of such slight variations on the mimicking of the FIV stimuli and on their perception by a subject, mediated by the stimuli transmission and elaboration by the brain. In the light of these results, it has been decided to use the average Transfer Function, calculated on the panel of participants, to simulate (mimic) the set of isotropic textures. A discrimination campaign on the real and simulated isotropic textures has been then carried out. The average Transfer Function among 20 participants calculated for the combination  $\{20^\circ, 0.2N\}$  has been used (Figure 76), as it reflects the choice of parameters with which the FIV were measured during the exploration of the real surfaces (see section 2.3.1). Moreover, as shown in Figure 77, the condition  $\{20^\circ, 0.2N\}$  represents the condition with the greatest deviation of the curves, therefore the "worst case" in terms of variability of the Transfer Function.

## 5.2 FIV mimicking using the averaged Transfer Function

---

Before performing the discrimination campaign, the reproduction of the FIV stimuli using the PIEZOTACT device has been compared when using either the specific Transfer Function of a participant or the averaged one. The FIV signal measured by exploring the real texture has been processed and sent to the device; the participant placed the finger on the vibrating actuator and the acceleration has been measured on the fingernail with the accelerometer. Figure 79 shows the comparison between the PSD of the original FIV (red line), measured when the finger explores the real surface (S7), and the PSD of the signals measured during the mimicking of the signal by the vibrotactile device. The same original FIV signal has been processed in one case with the specific Transfer Function of one participant (blue line), and in the other case with the averaged Transfer Function (green line). When considering the specific Transfer Functions, the acceleration measured on the fingernail when exploring the surface are perfectly reproduced by the tactile device. In the case of the signal reproduced with the averaged Transfer Function, the reproduction is slightly less performing, but still well mimicking the main trend and amplitude distribution of the spectrum.

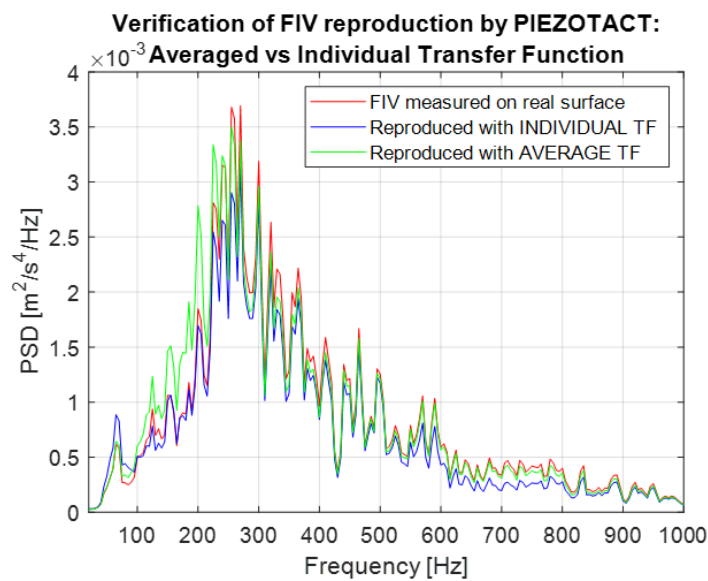


Figure 79: Verification of mimicked FIV by PIEZOTACT device with individual and averaged Transfer Function.



## 5.3 Discrimination of isotropic textures with the averaged Transfer Function

---

The feasibility and effectiveness of using an averaged Transfer Function to simulate the surface textures by the PIEZOTACT device has been tested directly through a discrimination campaign.

The discrimination campaign has been carried out on 10 participants, on both the real and simulated textures, according to the protocol described in section 2.6.2. The panel of 10 participants (1 female and 9 males, with ages ranging between 24 and 45 years) who performed this campaign was composed by different participants with respect to the panels who performed the campaigns for the characterization of the Transfer Function, described in sections 5.1.1 and 5.1.2, and was as well different to the one who performed the discrimination campaign in section 4.3.2, increasing the robustness of the conclusions.

The results are analysed by means of association matrices constructed as explained in section 2.6.3. Each matrix is cumulative of the associations declared by the full panel of participants. Figure 80 shows the results of the discrimination campaign on both real and simulated textures: TASK 1 in Figure 80a, TASK 2 in Figure 80b and TASK 3 in Figure 80c. In all the three discrimination tasks, the association percentage on the main diagonal is very high for all the sample surfaces, which testifies the excellent performance in the discrimination of both real and simulated textures, simulated using the PIEZOTACT device from the averaged Transfer Function. The use of the averaged Transfer Function is therefore validated for the isotropic textures under investigation.

Moreover, it should be recalled that the panel of participants used for calculating the averaged Transfer Function was different from the one used for the discrimination tasks, further validating the possibility to use a mean Transfer Function, previously calculated on an arbitrary panel of participants, for mimicking the FIV stimuli by the vibrotactile device.

The results of the discrimination campaign with the average Transfer Function can be as well compared with those obtained from the discrimination campaign in section 4.3.2, in which the simulated textures were obtained using the specific Transfer Function of the participants. The used discrimination protocol is exactly the same, allowing comparison between the two campaigns. The discrimination campaigns, both of real and simulated textures, have comparably good results. This means that the use of an average Transfer Function is equally effective than using, for each participant, its own specific Transfer Function for the tested textures.

The variability of the Finger Transfer Function among participants and contact conditions seems to be sufficiently reduced not to significantly affect the discrimination of the textures simulated by the device, at least as regards the textures tested in this work.

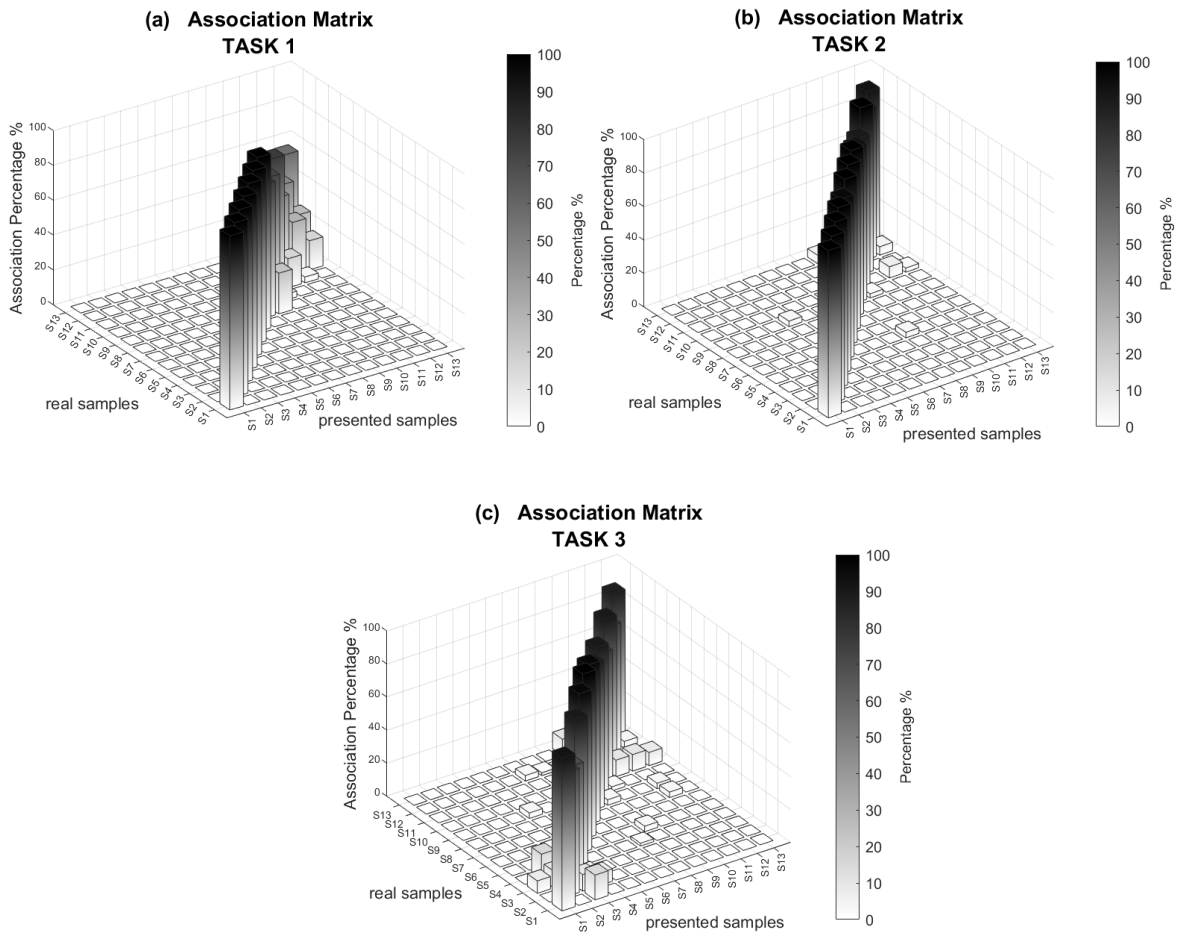


Figure 80: Results of the discrimination campaign: (a) TASK 1, sorting of the full set of real surfaces; (b) TASK 2, discrimination task on sets of real surfaces; (c) TASK 3, discrimination task on simulated textures.

## 5.4 Concluding remarks

---

With the objective of investigating the individual finger Transfer Function, an analysis of the dynamic response of the human finger, and its role in rendering FIV stimuli, has been conducted.

The overall parametric analysis on the finger's Transfer Function revealed that the gain of the Transfer Function increases as the contact force between the finger and the vibrating surface increases, while the angle between the finger and the surface slightly influenced the Transfer Function's shape, but no significant variations were identified.

More in general, the Transfer Functions obtained for different participants, under varying conditions of contact force and angle, were found to present a quite similar trend in frequency and low deviation in amplitude. An averaged Transfer Function has been then calculated among the participants and has been employed to process FIV stimuli induced by the exploration of real isotropic textures, subsequently reproduced by the PIEZOTACT device, to be directly tested in a discrimination campaign.

The discrimination campaigns yield excellent discrimination results, comparable to the previous campaign (see section 4.3.2) that utilized individual participant Transfer Functions. Such results highlighted a negligible impact of the variability of individual finger dynamic responses (Transfer Functions) on the simulation of the tested textures by vibrational stimuli.

The possibility of using an averaged Transfer Function in the rendering of the vibrational tactile stimuli makes it possible to get rid from having to recharacterize the finger Transfer Function for each individual user of the device, making this technology more versatile.



# Chapter 6

## Investigation into the brain response to vibrational mechanical stimuli<sup>5</sup>

This chapter reports an investigation conducted in the framework of the ANR CONTACT project [1]. This study is the result of a collaboration between the LNC (Laboratory of Cognitive Neuroscience) of the Aix-Marseille University (France), the DIMA (Department of Mechanical and Aerospace Engineering) of the Sapienza University of Rome (Italy), the LaMCoS Laboratory (Laboratory of Contacts and Structures Mechanics) of INSA Lyon and CNRS (France), the LEAD (Learning and Development Studies Laboratory) Laboratory of the University of Bourgogne (France), and the FEMTO-ST Institute of Besançon (France) (Figure 81).

This study is inserted in a general framework (Figure 81) that aims to reconstruct the overall process of tactile perception, beginning with surface texture, progressing through mechanical stimuli, their associated perception and the brain's response.

The study evaluates the brain response to mechanical stimuli obtained during the active exploration of the surfaces and compare it with the brain response obtained during the rendering of vibrational stimuli by the PIEZOTACT device, with and without mental imagery.

The following sections explain the purpose of the study, the adopted protocol and the results. Some neuroscientific background that led to the definition of the objective of the investigation and the adopted protocol is provided. Then, the setup and results of the tribological analyses are detailed. The main neuroscientific findings (brain response) [109], [110] are reported (resumed) as well.

---

<sup>5</sup> The content of this chapter will be partially published in [109].

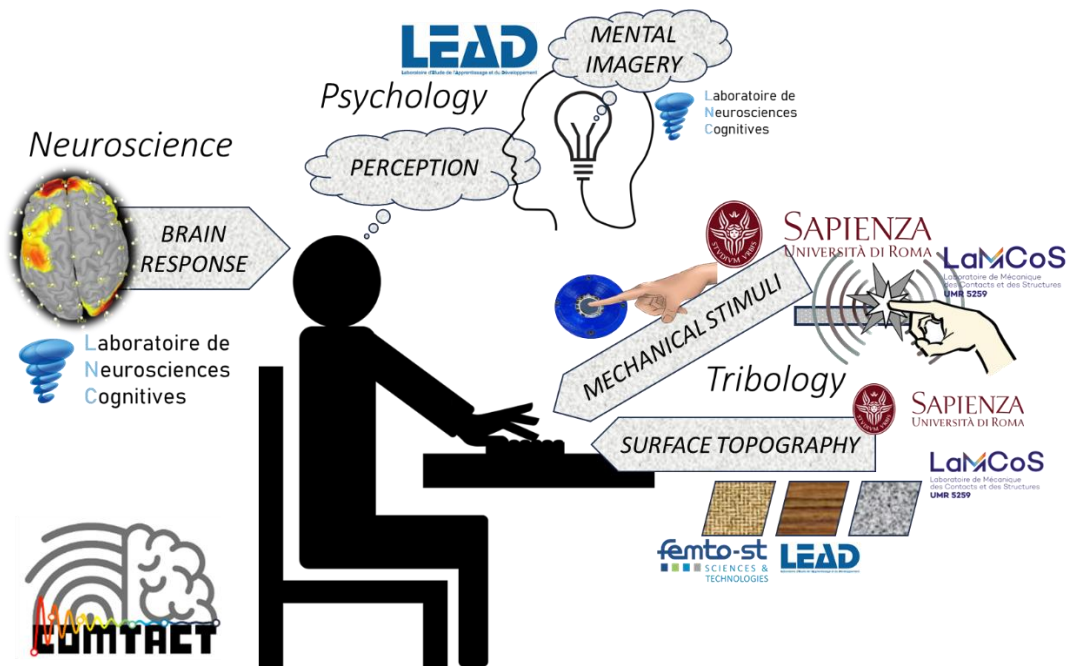


Figure 81: In the framework of the ANR CONTACT [1] project, the study aims to investigate the brain response to natural touch and rendered vibrational stimuli with and without mental motor imagery [109], [110].

## 6.1 Neuroscientific background and definition of the objective of the study

---

The tactile afferents respond to transient deformations of skin that occurs when the skin interacts with the object being touched, and then convey sensory information to the brain. The brain not only decodes mechanical stimuli, but also implements several strategies to improve the process of perception. One of these is sensory attenuation which, according to what has been demonstrated, is put in place when a voluntary exploration movement is operated to self-generate tactile stimuli (active touch) [111]–[113]. Under such conditions, the brain operates a suppression of some sensory inputs. This sensory attenuation is operated by the brain to reduce the massive and excessive flow of information that reach the brain during the execution of the movement. The sensory suppression occurs both during the execution of the movement and during the preparatory phase for voluntary movement [114].

The sensory attenuation (also called ‘sensory gating phenomenon’) is linked to the efferent copy that is generated when the motor command is produced [112], [115], [116]. While an afference is a sensory input (tactile feedback) that is received by sensory receptors from the peripheral nervous system to the central nervous system, an efference is a motor signal that is sent from the central nervous system (CNS) to the periphery. When a motor command is generated by the brain, efferences flow, through the efferent nerves (i.e. nerves that transmit signal from the CNS to the periphery) to the motor system to produce the movement. At the same time, an efferent copy is created. An efferent copy is an internal copy of the efferent (outflowing) signal, which is then used to feed the internal forward model which predicts the sensory effects of the movement. So, when the motor command is created, a prediction of the movement’s sensory consequences is produced as well (Figure 82). Thus, when performing the movement, the brain compares the tactile feedback with the sensory predictions emerging from the forward model. The most they are similar, the most the sensory attenuation occurs. On the contrary, discrepancy between the sensory effects of the movement and the internal prediction reduces the sensory attenuation, i.e. reduces the suppression of afferent inputs [111]–[113], [116], [117], and the tactile feedback is more treated by the brain. During the tactile process a continuous exchange of information between the internal forward model and the tactile feedback occurs [118]. Sensory feedback is thus essential to update internal prediction [112]. This process is controlled by specific areas of the brain, the premotor cortices (i.e., supplementary motor area, SMA), which is responsible for the planification of the movement.

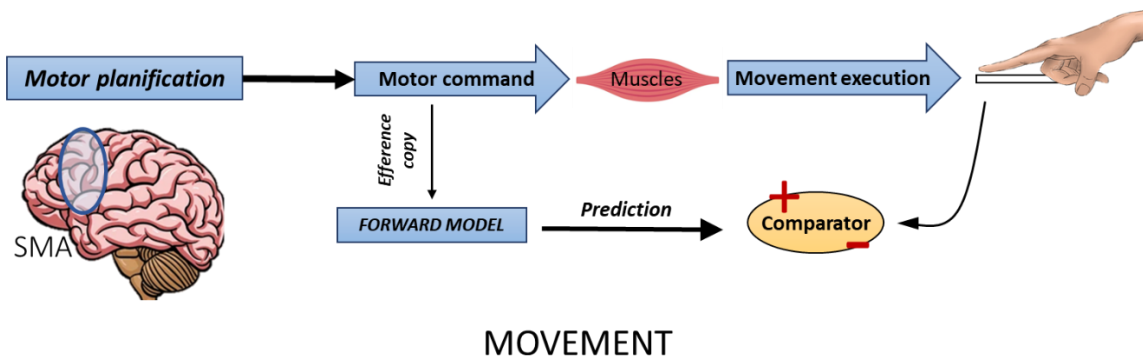


Figure 82: From planification to movement execution [109], [110].

Motor imagery consists into imagining to perform actions without their execution (Figure 83). Different studies on motor imagery have revealed that there are similarities between the real performed movements and the imagined ones, without any motor output, at the behavioural, physiological and neuronal levels [119]–[121]. When investigating into the sensory gating phenomenon, motor imagery has been evidenced as particularly suitable to access to the sensorimotor predictions at the origin of the sensory attenuation [122]. In fact, mental imagery of a movement involves all the processes related to the planning of the movement by the premotor areas of the brain, but the motor outputs are absent. Among these processes, mental imagery of a movement gives rise to the same sensory suppression elicited by overt movement [123], [124].

During motor imagery, in fact, movement planning occurs in the premotor areas of the brain, and a motor command is sent to the peripheral system. During this phase, efferences and efferences copies are generated as well, and the latter feed an internal forward model. Therefore, during motor imagery, there is a prediction of the consequences of the movement as in the case of the execution of the real movement. During motor imagery, the motor command, which is generated, is subsequently inhibited by the brain to avoid producing the execution of the movement.

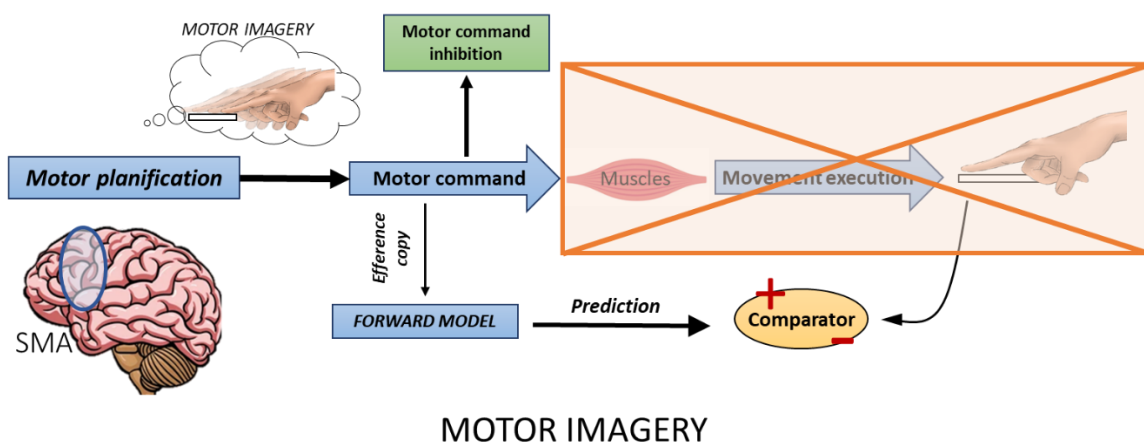


Figure 83: Motor Imagery mechanism.



To date, no previous studies have directly tested the hypothesis of whether imagined movement of exploring a surface, during a motor imagery task, engages the same central sensorimotor mechanisms as overt touch movements do, when benefiting of the participants' tactile feedback replay. To test this hypothesis, tactile feedback has been provided by the PIEZOTACT tactile device, introducing supplementary sensory information associated with vibrations induced by surface exploration (Figure 84). Because internal prediction needs to be updated by the current sensory (and motor) signals [115], [116], providing to the participants their own tactile replay during mental imagery, as if they were actually exploring the surface with their finger, might help to prevent the internal prediction from fading. The originality of this investigation in motor imagery is related to the fact that it is free from everything purely related to the motor output of movement, while having access to the processing of vibrational tactile feedback by using the PIEZOTACT device [109], [110].

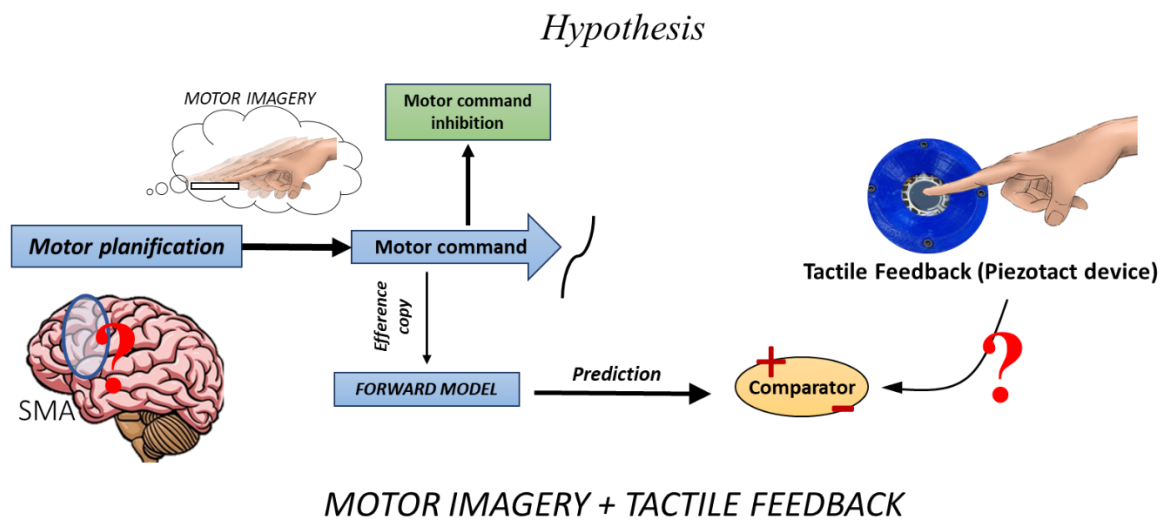


Figure 84: Hypothesis: restitution of tactile feedback during motor imagery task.

The collaborative work presented in this Chapter aims to answer two main questions:

- Does sensory processing differ between the actual touch produced by the exploration movement of a surface and the mimicked tactile stimuli by the vibrotactile device?
- Would motor imagery combined with tactile feedback related to real movement make it possible to get closer to the sensory processing of natural exploration movement?

The PIEZOTACT device has been here exploited to provide the tactile feedback.

## 6.2 Tasks and experimental setups

Three tasks (Figure 85) have been performed by 10 participants (6 women and 4 men, ages ranging between 21 and 27 years), while the 3 surfaces described in section 6.3 have been used.

- TASK 1 - Natural touch task: active exploration of real surface texture.
- TASK 2 - Control task: tactile feedback by PIEZOTACT device without any motor action, (i.e., no movement and no mental imagery).
- TASK 3 - Mental Imagery task: motor imagery of the finger movement (without the movement execution) adding tactile feedback by the PIEZOTACT device.

The second and third tasks were counterbalanced across participants, which means that half of the participants performed first the Task 2 and then the Task 3, while the others performed first the Task 3 and then the Task 2: this prevent the results to be task dependent. The surfaces were presented as well in different order to the participants, to prevent the results to be dependent by the order of the textures. The tasks and experimental protocol are detailed in the following.

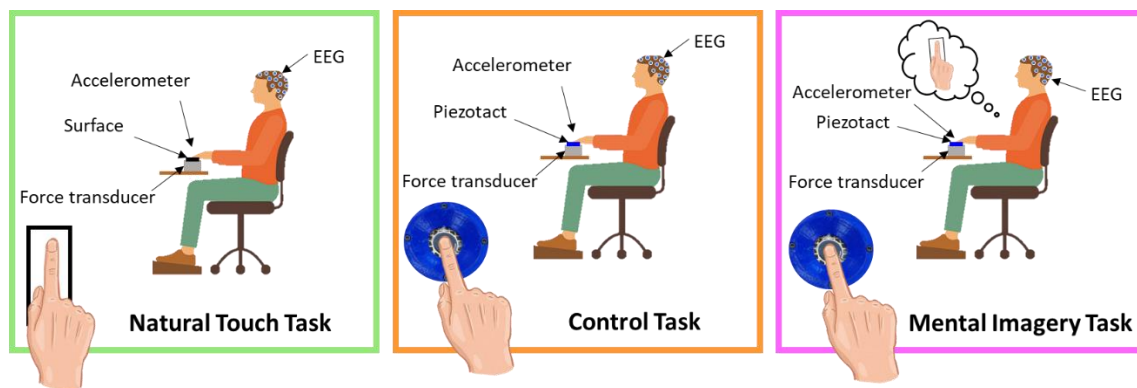


Figure 85: Schema of the 3 tasks performed by each participant [109], [110].

### TASK 1: Natural touch

For each tested surface (section 6.3), it has been asked to the participant to actively explore the surface with proximal longitudinal movements, lifting the finger between strokes. The participant, with closed eyes, has been left free to impose the contact boundary conditions: contact force, sliding speed and the finger/surface angle. The participant has been instructed to freely explore the textures focusing the attention on the perceived tactile sensation.

During the performance of this task, mechanical stimuli (acceleration and forces) have been measured using the usual active touch experimental setup described in section 2.3.1. The surface has been fixed on a triaxial force transducer to measure the contact forces and the

fingernail of the participant has been equipped with an accelerometer to measure the FIV (Figure 86a).

Electroencephalographic (EEG) signals have been measured and processed (by the LNC Laboratory [109], [110]) to recover the brain response (Figure 86b).

At the end of the task, the overall Transfer Function of the PIEZOTACT device, including the user's finger, has been measured as well, so that the FIV could subsequently be processed for rendering the vibrational stimuli (section 4.1).

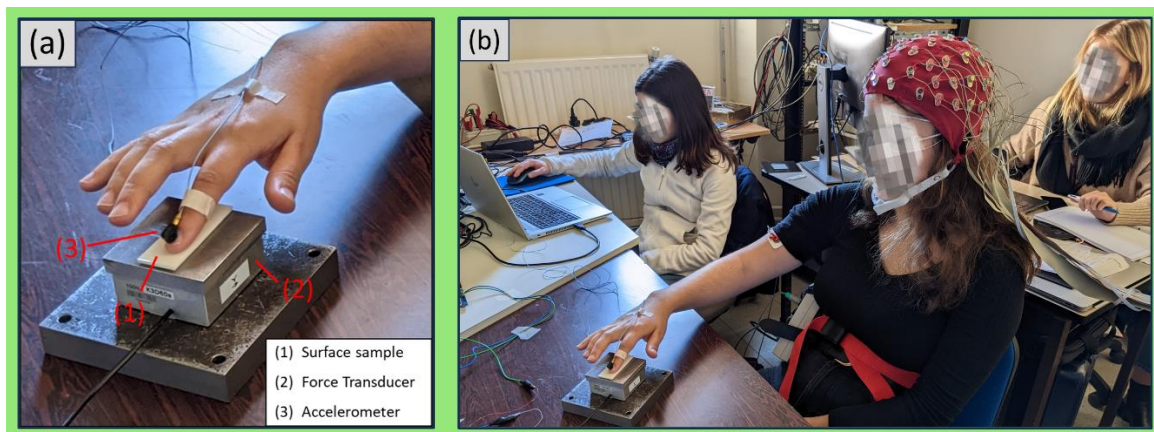


*Figure 86: Experimental setup for Task 1. In (a) the setup for measurement of mechanical stimuli during the active exploration of the surfaces. In (b) the entire experimental setup involving mechanical stimuli and EEG signals.*

### TASK 2: Control Task (tactile feedback)

This task 2 involved only the tactile feedback produced by the PIEZOTACT device, without movement and without motor imagery.

The participant has been asked to statically place his finger on the PIEZOTACT device, which reproduced the FIV previously measured in task 1, during the exploration of real surfaces. No constraint has been imposed on the contact force between finger and actuator to the participant. The participant has been asked to focus the attention on the perception of tactile sensation delivered by the device's feedback. The 3 rendered textures have been proposed in random order to the participant. At the end of the test, the participant has been asked to discriminate the textures, i.e. declare the real textures associated with the signals reproduced through the device.

To measure the mechanical stimuli, the setup detailed in section 2.3.1 and shown in Figure 87a, has been used. The actuator has been fixed on the force transducer and the accelerometer has been fixed to the participant's fingernail. An arm support has been provided to help the participant keep the finger static on the actuator.

EEG signals have been recorded (LNC Lab) to subsequently derive the brain response (Figure 87b).

### TASK 3: Mental Imagery (and tactile feedback)

During this third task it has been asked to the participant to engage mental motor imagery while tactile feedback was delivered via the PIEZOTACT device.

For the motor imagery, it has been emphasized to the participant the importance of envisioning themselves performing the movement from their own perspective and to fully immerse themselves in the sensations related to the movement, to make them actor of the movement, looking for kinesthetic mental imagery (KMI). A kinesthetic image, in which the task is experienced from the inside, seems to be a better representation than a visual image for acquiring the characteristic duration of a movement [125].

As in task 2, the participant has been asked to statically place his finger on the PIEZOTACT device, which reproduced the FIV previously measured during task 1. No constraint has been imposed on the contact force between finger and actuator to the participant. The 3 rendered textures have been proposed in random order to the participant. At the end of the test, the participant has been asked to discriminate the textures.

To measure the mechanical stimuli, the setup detailed in section 2.3.1, and shown in Figure 87a, has been used, as in task 2.

EEG signals have been recorded (LNC Lab) to subsequently derive the brain response (Figure 87b).

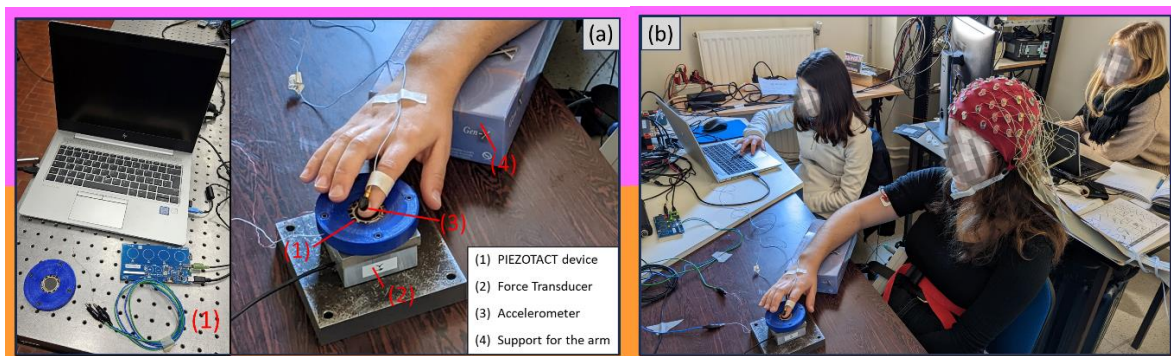


*Figure 87: Experimental setup for Task 2 and Task 3. In (a) the setup for measurement of mechanical stimuli during the reproduction of FIV by the PIEZOACT. In (b) the entire experimental setup involving mechanical stimuli and EEG signals.*

## 6.3 Surface samples

---

Three sample surfaces have been tested in this study, by selecting samples showing markedly different topographical characteristic and associated mechanical stimuli.

- A ‘biomimetic’ sample (Figure 88) whose characteristics proved to facilitate the sensory cortical process [126]. It has been manufactured with a 3D printer (Ultimaker 2+) using a thermoplastic biopolymer (Polylactic acid, PLA), by appropriately selecting three bioinspired characteristics: shape, spatial period, and depth of the ridges [110], [126], [127].
- Two microtextured surfaces with periodic isotropic topography (Figure 88), selected from the set of samples in Table 2, as representative of the groups of textures classified as ‘rough’ and ‘smooth’, respectively: the surfaces S08 and S03. Thus, in the following, sample S08 is referred as ‘rough’ and sample S03 is referred as ‘smooth’.

Figure 88 shows the three surfaces, observed at the VHX-2000 Keyence Digital Microscope.

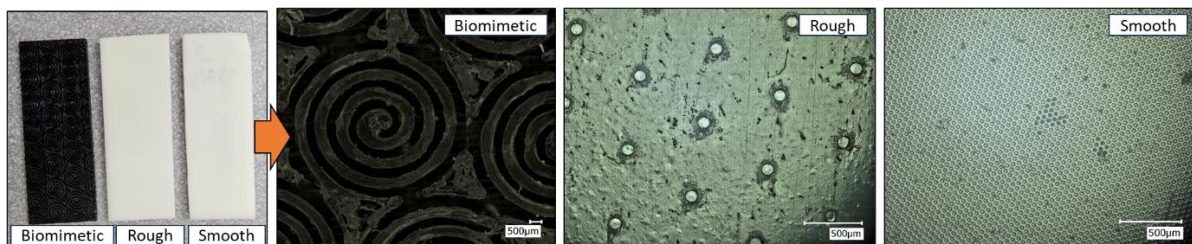


*Figure 88: The 3 tested surfaces (biomimetic, rough, smooth) observed with the VHX-2000 Keyence Digital Microscope.*

## 6.4 Analysis of tactile mechanical stimuli

---

The FIV measured during the active exploration of the surface samples have been analysed. Figure 89 shows examples of the FIV spectra obtained for the three textures, for 3 different participants. The three surfaces present different FIV spectra both in term of amplitude and frequency distribution. In terms of FIV amplitudes, for some participants the ‘biomimetic’ surface is characterised by higher amplitudes with respect to the ‘rough’ one (Figure 89a), while for other participants the inverse behaviour is observed (Figure 89b and Figure 89c). In some cases (Figure 89c), the amplitudes reached by the ‘biomimetic’ and ‘rough’ surfaces are quite similar. For all participants, the ‘smooth’ surface shows a significant frequency distribution that extends to higher frequencies and markedly lower amplitudes, with respect to the other two textures.

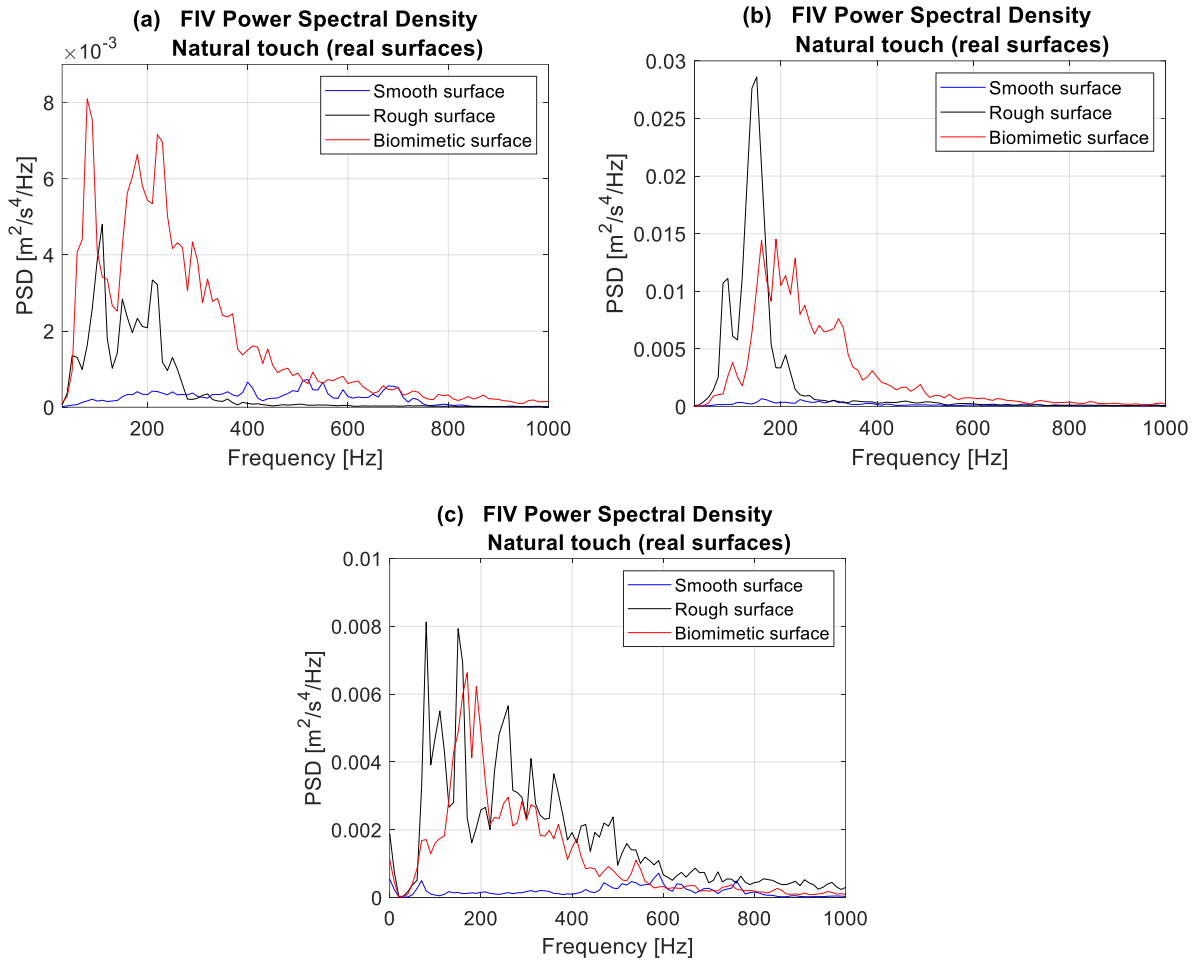


Figure 89: Examples of FIV spectra associated to the 3 tested surfaces during Task 1 (natural touch task), involving the active exploration of the textures, for three (a,b,c) different participants.

When comparing the FIV by active touch, obtained for all the participants for each surface, some observations can be made (Figure 90), in particular in terms of frequency distribution. It needs to be recalled that the FIV were recorded by active touch without any constraints on the sliding speed, contact force and finger/surface angle. Despite this, some features of the FIV signals are common for all participants. The most interesting case is represented by the ‘rough’ surface (Figure 90a). For all participants, the FIV frequency distribution presents well defined harmonics, mainly contained in a range between 50 and 400 Hz. In other words, a particular signature seems to be associated to the rough texture, despite the not controlled contact parameters during active touch tests. Examples are reported in Figure 91, for a better visualization. The frequencies peaks are consistent with an average sliding velocity in the range between 10 and 50 mm/s for the rough texture having an equivalent wavelength of 0.716 mm (see Table 2). This agrees with the FIV analysis by passive touch performed in a previous work [6]. The ‘biomimetic’ surface shows, for almost all participants, a large band frequency content localised between 50 and 450 Hz (Figure 90b). The spectra are very similar in terms of frequency distributions, with a first more definite frequency peak located, according to the participant, in the range between 70 and 110 Hz, and a larger band content, with a quite similar shape between participants, up to 450-500 Hz. The first definite frequency peak

(approximately between 70 and 110 Hz depending on the participant), found both in the 'rough' surface and in the 'biomimetic' one (i.e. the 'coarse' textures), but not in the 'smooth' one, may be linked to participant's fingerprints, in agreement with results in [6], [21], [22], [36] The 'smooth' surface show mainly a large band content, with very low amplitudes compared to the other surfaces.

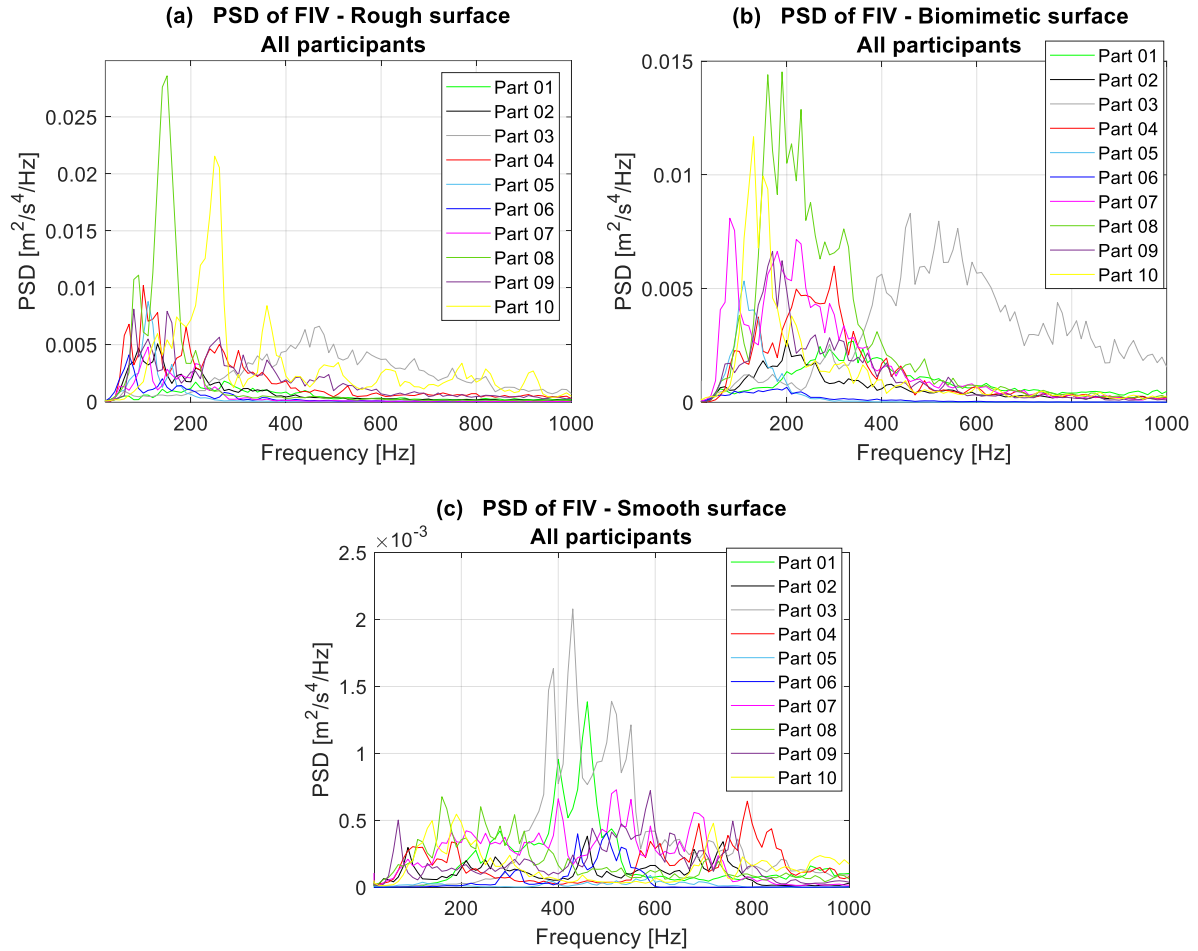


Figure 90: The PSD of FIV by active touch (Natural Touch Task) are compared for all participants for each surface: (a) rough, (b) biomimetic, (c) smooth.

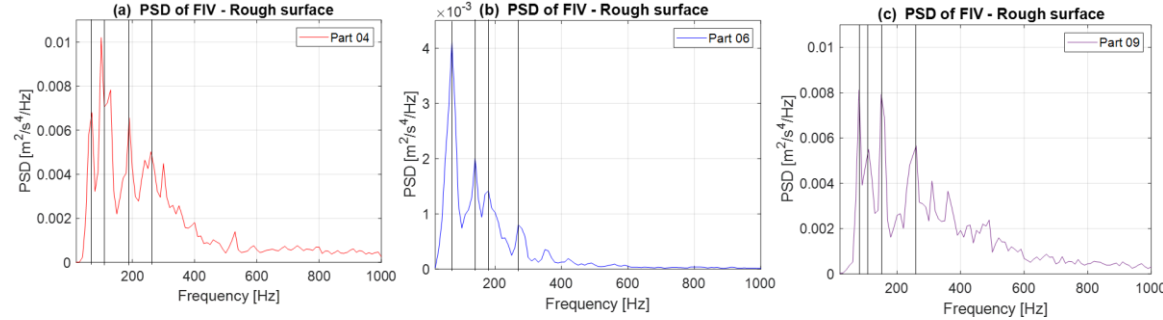
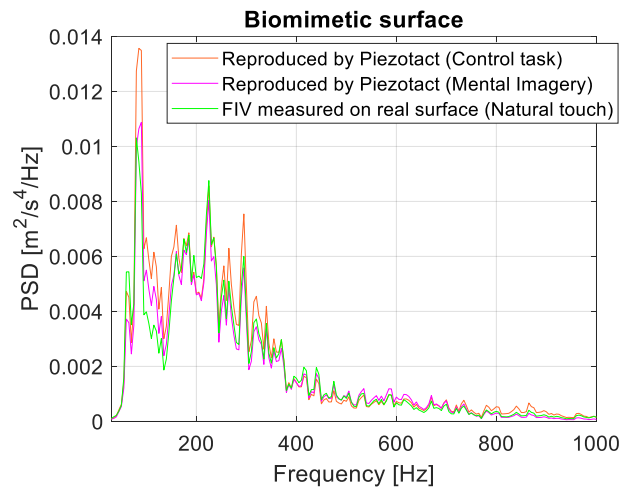


Figure 91: Examples of FIV associated to the 'rough' texture, showing a common trend characterised by main harmonics.

Figure 92 shows an example of the PIEZOTACT device's effectiveness in reproducing, on the user's finger, the same vibrational signals previously measured during the active exploration of the surfaces (the usual verification protocol in section 4.2 has been exploited). The PSD spectra associated with the natural touch (Task 1), and those recovered during the Tasks 2 and 3, in which the vibrations are rendered by the PIEZOTACT, are very similar, almost overlapping. Therefore, from a mechanical point of view, the vibration signal that globally reached the participant's finger, when touching the PIEZOTACT device, was supposed to be almost the same to the one that has been previously measured during the natural exploration of the surfaces. The same has been found for all textures and participants.



*Figure 92: Example of correct FIV signal rendering by the PIEZOTACT device, by comparing the spectra of the measured FIV during natural touch and the acceleration recovered during the control and imagined touch tasks.*

The contact forces have been analysed as well for the three tasks. Figure 93a shows the average normal contact force exerted by all participants in all trials during the 3 tasks, for each surface. No significant differences have been found in the normal force obtained for the different surfaces and during the different tasks involving the tactile feedback by the PIEZOTACT, i.e., control task (task 2) and the mental imagery task (task 3). Therefore, no differences in the load at the finger/actuator contact have been found, which could have affected the results on the sensory attenuation experienced in the mental imagery task, compared to the control task.

Instead, by analysing the normal forces associated with natural exploration, a difference in behaviour has been observed between the biomimetic surface and the others (Figure 93a). In fact, in the natural touch task, the participants explored, on average, the biomimetic surface with a higher force than the two periodic microtextured surfaces (rough and smooth). The friction coefficient has been then analysed for each surface (Figure 93b), averaged among all participants and all trials (in task 1). From the analysis (Figure 93b), it turns out that the periodic surfaces (rough and smooth) exhibit a similar friction coefficient, which is markedly higher than the friction coefficient associated to the biomimetic surface.



It seems that participants, let free to choose the contact force in the natural exploration (task 1), explored the periodic textures, characterised by a higher friction coefficient, with a lower contact force, in order to avoid adhesion and stick-slip phenomena [27], [28], [41], [128]. The biomimetic surface, which presents a lower friction coefficient, has been explored with a higher normal force. This difference in the friction coefficient between the periodic surfaces and the biomimetic one could be due to both the different material, (polyurethane resin for the periodic surfaces and PLA for the biomimetic one) and the different topography. Furthermore, being the biomimetic surface coarser than the two microtextured periodic surfaces (see Figure 88), the exerted contact force in natural exploration may depend on the coarseness of the texture topography, as already highlighted in literature [6]. Recognition of texture properties requires sliding contact between finger and object surface. Although it is well known that vibrations stimulate the tactile afferents, the mechanism by which Friction-Induced Vibrations (FIVs) interfere with tactile perception is still unknown. As well, the role of mechanical stimuli on hedonistic feedback from the touched surface is unknown. Correlations between surface features and perception are here examined, while the analysis of the mechanical stimuli, which are the direct elements of activation of the human receptors, is performed. Two different sensory analyses are exploited: hedonistic perception and perception dimension categorization. The analysis of the frequency and amplitude of the FIV, allowed for explaining the correlations between the perception analyses and the topography characteristics of the samples [6], [19], [129]. This point is open to future investigations.

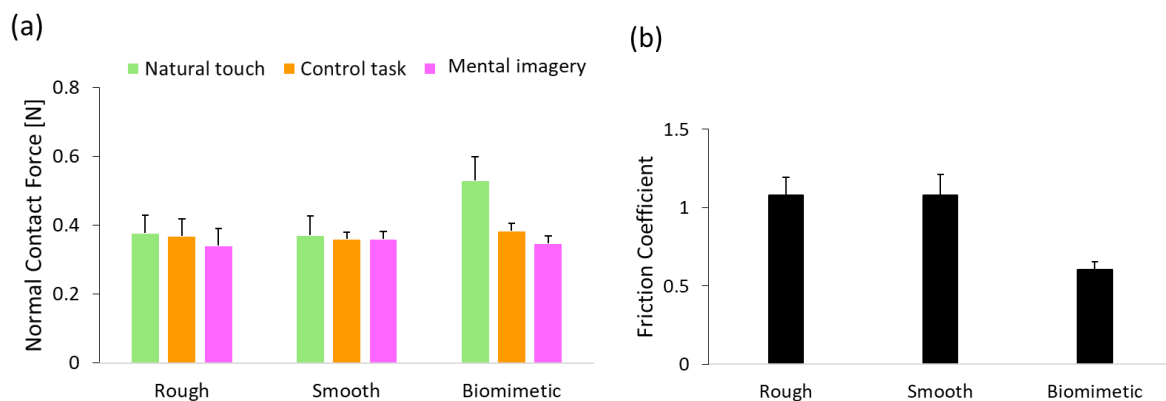


Figure 93: Normal contact forces measured during the 3 tasks (a) and friction coefficient (b) measured during the Natural Touch Tasks.

The samples discrimination performed at the end of the trials in task 2 and task 3 have been analysed by means of association matrices, built as usual (section 2.6.3). Let's recall that the tasks 2 and 3 were counterbalanced between participants, in order to avoid error arising from the tasks' ordering. The results are presented in Figure 94 and Figure 95, respectively referred to the simulated textures by the device with tactile feedback only (Figure 94a and Figure 94a) and with mental imagery (Figure 94b and Figure 94b).

When dealing with the sole tactile feedback (Figure 94a and Figure 94a), the 'smooth' textures have been always correctly discriminated with a 100% of association, while the 'rough' and 'biomimetic' simulated textures have been often confused. This is in accordance with the FIV

spectra in Figure 89 and Figure 90, showing that the FIV associated to the ‘smooth’ texture present markedly lower amplitudes and higher frequency content compared to the other two textures, while the ‘biomimetic’ and ‘rough’ surfaces present more similar FIV spectra, both in terms of frequency distribution and amplitude.

Referring to the mental imagery task, higher percentages of association can be found on the diagonal of the matrices for all samples (Figure 94b and Figure 94b), testifying an overall good discrimination performance, although errors are more dispersed and few of them involve also the ‘smooth’ texture.

Globally, the discrimination performance in the mental imagery task is found to be better than in control task (task 2), although the errors occurred in the control task can be more easily linked to FIV spectra than the ones occurred in the mental imagery one.

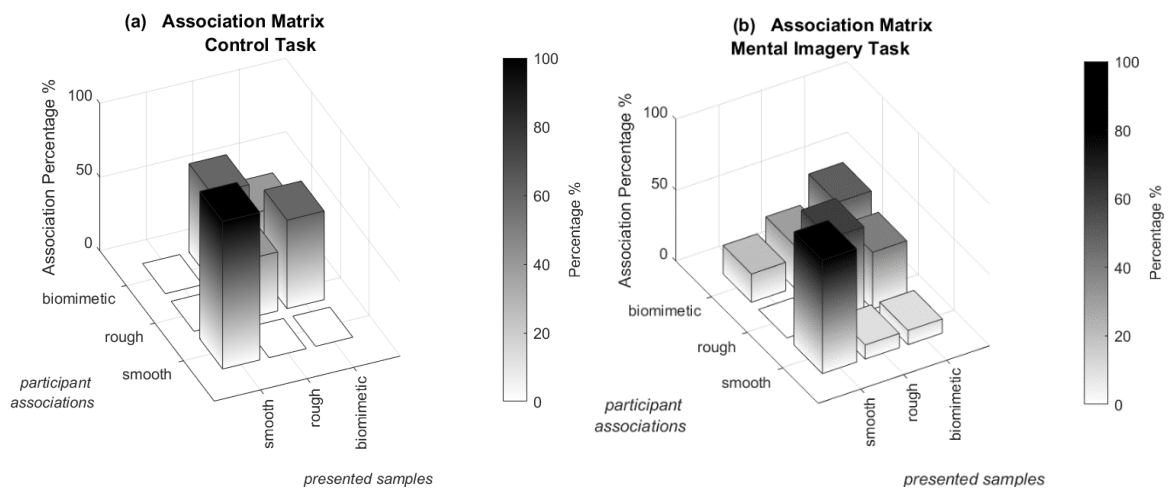


Figure 94: Results of samples discrimination in task 2 (a) and task 3 (b), as 3D association matrices.

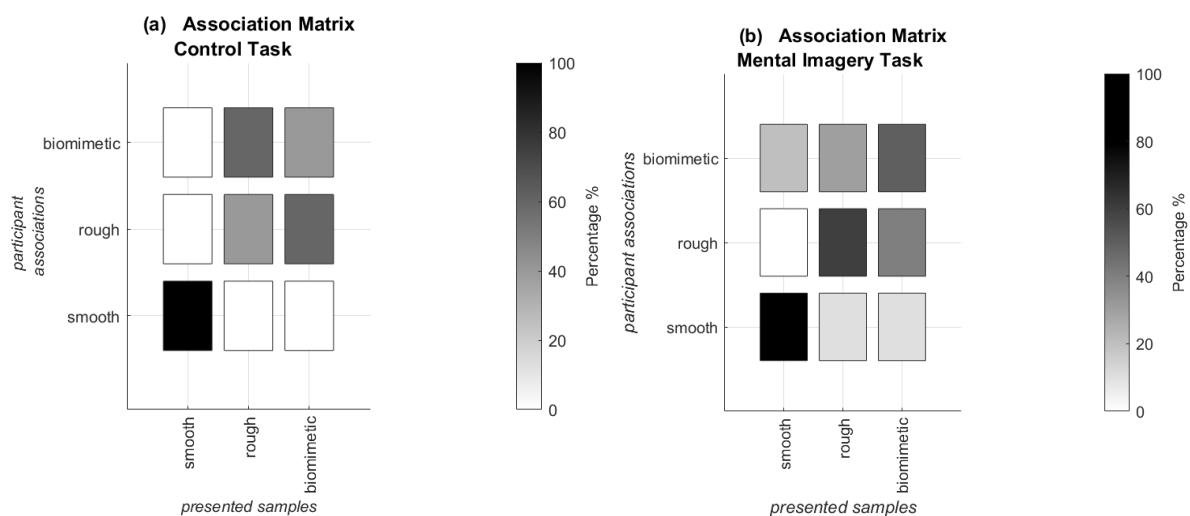


Figure 95: Results of samples discrimination in task 2 (a) and task 3 (b), as 2D association matrices.

## 6.5 Main findings in brain response

The main neuroscience findings, outcome from the analyses performed by the LNC group [109], [110], are resumed in this section.

The analysis particularly focused on the area of the sensorimotor cortex specifically responsible for processing tactile information, highlighted in yellow in Figure 96.

Figure 96 show statistical maps that highlight activation contrasts between tasks, related to cortical activity. When comparing the cortical activation between tasks it emerges that:

- In Control Task the SMA (sensorimotor cortex area) is more activated than in Natural Touch Task.
- In Control Task the SMA is more activated than in Mental Imagery Task.
- In Mental Imagery Task the SMA is more activated than in Natural Touch Task.

Instead, the Extrastriate body areas (EBA) and the Tempoparietal junctions (TPj) (Figure 96) are brain areas linked to the movement and the spatial representation of the body, so they are activated only when dealing with natural touch task.

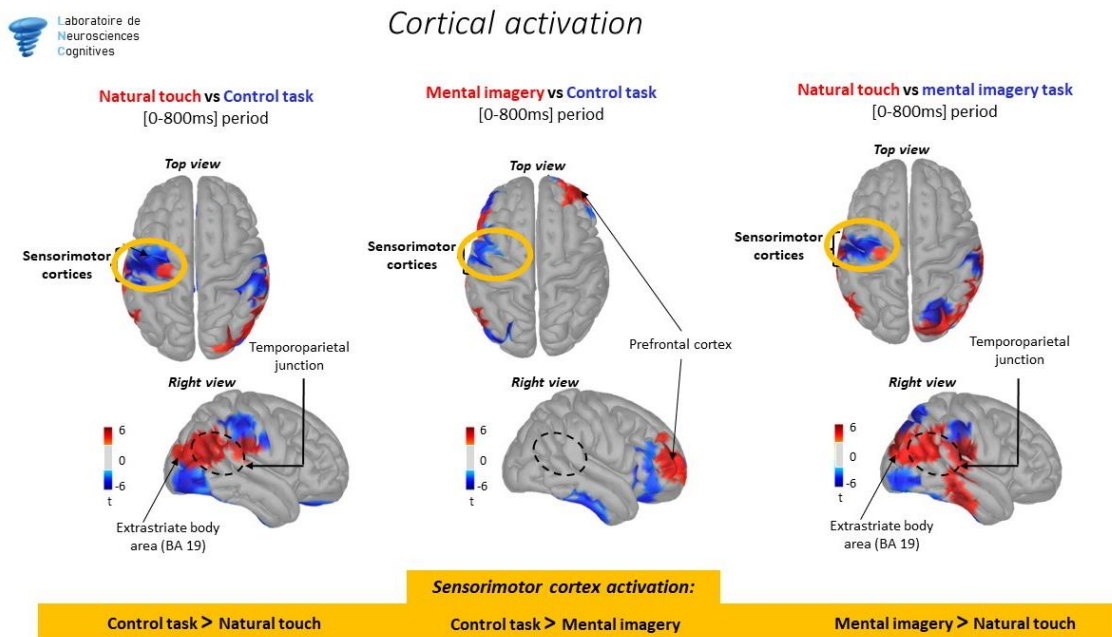


Figure 96: Sensorimotor cortex activation (LNC Lab) [109], [110].

Then, a time-frequency analysis has been performed to evaluate the temporal evolution of EEG signal power (Figure 97). Time-frequency analysis allows to evaluate signal event-related desynchronization (ERD) and synchronization for different frequency bands. The frequency band of interest, associated with treatment of tactile information, is the alpha band ([8-12 Hz]) [130], [131]. Synchronization is represented by red in Figure 97, while

desynchronization is highlighted in blue. Greater desynchronization of the alpha band is associated with greater cortical signal treatment (and thus lower sensory inputs suppression). The analysis in Figure 97 has been carried out by selecting as a baseline a time interval prior to the tactile event (when the participant was resting and before the movement planning phase) and comparing it with the first 800ms of the tactile exploration. Figure 97 shows a sensory processing (power in alpha band) gradient between the 3 tasks. Greater treatment of tactile information is associated with the Control Task, an intermediate situation is represented by the Mental Imagery Task, while the lower desynchronization is associated with the Natural Touch Task. Decreased desynchronization is associated with increased sensory attenuation operated by the brain. The same trend has been found for all the surfaces (Figure 97).

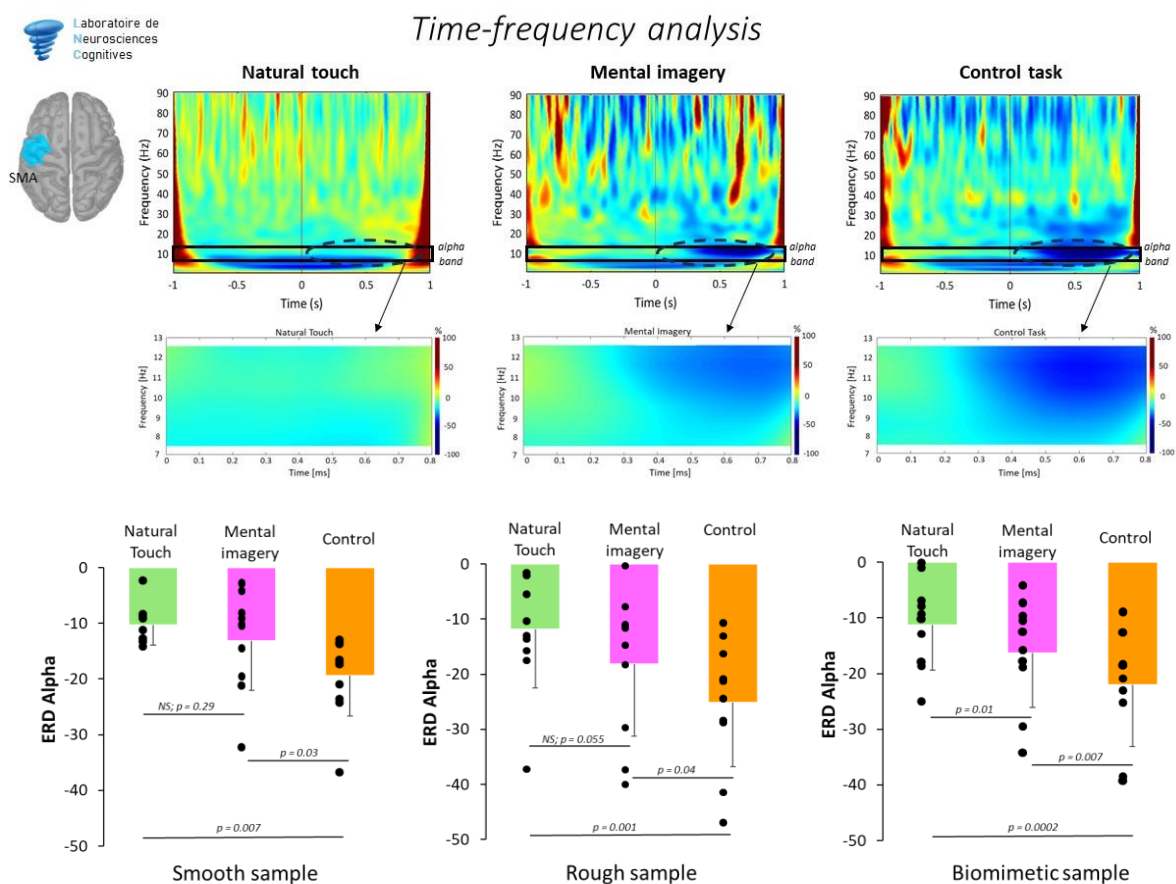


Figure 97: Time-frequency analysis on ERD alpha band (LNC Lab) [109], [110]. The black points represents the ERD alpha for each participant.

The overall analysis suggests that motor imagery associated to tactile feedback approaches the condition of natural touch, as attenuation phenomena occur more than when dealing with the sole tactile feedback by the PIEZOTACT.

## 6.6 Concluding remarks

---

Brain response has been evaluated when, during a motor imagery task, tactile feedback, matching the imagined movement, was provided. The cortical activity has been compared to the one recovered during a task of active exploration of surfaces and a task where only tactile feedback was provided (control task), without any motor action. The tactile feedback has been delivered to participants by means of the PIEZOTACT device, faithfully reproducing the vibrations originated during the active touch exploration of 3 tested textures.

The time-frequency analysis of the alpha band in the sensorimotor areas showed a decreasing gradient of desynchronization, thus decreasing processing of tactile signals, from the control task, to the motor imagery task, to the active exploration of textures. The decreasing of desynchronization of alpha band is linked to occurrence of sensory attenuation, highlighting that motor imagery associated to tactile feedback approaches the condition of natural touch more than the sole tactile feedback.

From the analysis of FIV by natural exploration of the 3 involved surfaces, common features (amplitudes and in particular, frequency distribution) have emerged for all participants, despite the choice of the test conditions (sliding speed, force and angle between finger and surfaces) was left completely free to the participants.

Interestingly, when discriminating the simulated textures with the PIEZOTACT, it turned out that better discrimination performances were achieved by the participants when engaging mental imagery than when dealing with the sole tactile feedback. At the same time, the discrimination errors in the control task could be more easily related to the features of the FIV spectra than the errors occurred during the mental imagery task.

Relating to the tactile rendering techniques, the results of this study may be useful to optimize future configurations of the device, for example by implementing a larger actuator surface that allows to mimic the exploration movement during the reproduction of vibrational stimuli or to engage motor mental imagery when perceiving the simulated textures by the device.



# Chapter 7

## General conclusions

By its nature, touch process involves the direct interaction between the human body and the object to be explored. As a result, touch is triggered by phenomena that occur at the contact interface, that produce stimulation of mechanoreceptors in the skin. The different mechanical stimuli, such as vibrations, forces, friction, represent different channels carrying fundamental information, which mediate between the characteristics of both the explored surface and the finger, the perception arising from their interaction. Tribological and dynamic investigation tools are thus essential to understand the contact phenomena underlying touch. In this context, this Ph.D. Thesis is focused specifically on deepening the understanding of the role of the vibrational stimuli (Friction-Induced Vibrations) in mediating between texture topographic characteristics and texture perception. This goal has been pursued by measuring, analysing and reproducing vibrational stimuli generated from texture exploration, thanks to different test benches and experimental protocols. Among the exploited tools, a tactile rendering device (PIEZOTACT), able to reproduce the measured FIV, has been developed, which, apart from technological applications, allows to isolate the vibrational component of the tactile mechanical stimuli. Discrimination campaigns on volunteers have been conducted to correlate FIV stimuli and perception, with different surface textures, both real and simulated by the vibrotactile device, taking into account as well the finger/device dynamic coupling. This chapter outlines the main findings and the perspectives of the work.

## 7.1 Main findings

---

The main original outcomes of the work are reported following the thesis structure, which ranges from surface textures, to tactile stimuli, rendering of tactile stimuli, up to a spot in the brain response.

### 7.1.1 From surface textures to FIV stimuli

The relationship between surface topography and tactile vibrational stimuli has been analysed. Two different types of rigid (with respect to skin) textures have been used: a set of periodic textures (see section 2.1.1 and [6]) and a set of isotropic textures (section 2.1.2). The main characteristics (amplitude and frequency distribution) of FIV, induced by the exploration of such textures have been analysed by active and passive touch, revealing the following main results:

- Qualitatively, the FIV analyses conducted by the active and passive touches agree for both isotropic and periodic textures.
- The tested isotropic textures present similar FIV frequency distribution, while the FIV feature that changes the most between samples is the amplitude. This leads to the hypothesis that the main FIV feature to discriminate isotropic textures is the amplitude.
- For the tested periodic textures, a previous work [6] identified, by passive touch measurements, the frequency distribution as the key characteristic of FIV; in the present work the same periodic textures have been analysed by active touch, revealing results qualitatively in agreement with [6].
- By comparing the FIV associated with periodic and isotropic textures, periodic textures are more characterized by the frequency distribution of FIV, while isotropic textures are more characterized by FIV amplitude.

### 7.1.2 Vibrotactile rendering device: PIEZOTACT

A tactile device, called PIEZOTACT, has been developed for the purpose of rendering FIV stimuli previously measured during the exploration of real textures. The device consists of a piezoelectric actuator and its driving chain; the rendering methodology is based on the exploitation of the Transfer Function of the overall system, consisting of the device and including the user's finger, to process the previously measured FIV signals. The developed rendering methodology has been verified by comparing the FIV spectra measured on real surfaces and those reproduced by the device. The verification revealed that the device is able to faithfully reproduce the overall FIV accelerations measured on the fingernail of the participant. The tactile rendering device has been then used to simulate the FIV corresponding



to periodic and isotropic textures. Then, the developed methodology has been validated by texture discrimination campaigns.

### 7.1.3 From FIV stimuli to texture discrimination

Several discrimination campaigns with real and simulated textures, using the PIEZOTACT device, have been conducted on groups of volunteers to evaluate the correlation between vibrational stimuli and perception. For both periodic and isotropic textures, discrimination tests have been conducted first on real textures the errors and the correct discriminations have been then analysed with respect to their associated FIV. Then, tests have been carried out on periodic and isotropic textures simulated by rendering the FIV stimuli by means of the PIEZOTACT device. The advantage is that the device is able to isolate the vibrational part (FIV) of tactile mechanical stimuli (such as friction, forces, etc.) and therefore to study their role in texture discrimination. Again, the errors and the correct associations have been then analysed through the FIV.

The main obtained results are the following:

- For both periodic and isotropic textures, good performances have been achieved by the participants in discriminating both the real textures and the simulated ones by the PIEZOTACT device.
- This result allows to underline the role of FIV in texture perception.
- Moreover, for both periodic and isotropic textures, the most occurred discrimination errors for real and simulated textures have been explained by the FIV analysis: samples that were often confounded in the discrimination campaigns (real and simulated) were associated with FIV having similar spectra, while samples presenting more markedly different FIV spectra were generally well discriminated.
- The previous results have been highlighted for the two different set of textures, despite the FIV for periodic textures are more characterised by the frequency distribution, while for isotropic textures the most important FIV feature turned out to be the amplitude.
- Overall, the most common errors in the discrimination of simulated (periodic and isotropic) textures was consistent with those found in the discrimination of real textures, highlighting a good agreement between the two campaigns, and emphasizing the important role of FIV in texture discrimination and the good performance of the device.
- In order to furtherly confirm the role of FIV amplitude in the discrimination of isotropic textures, fake textures have been built by inverting pairs of samples in terms of FIV RMS amplitude. Discrimination test conducted on these fake textures, simulated by the PIEZOTACT, revealed that volunteers discriminated the samples consistently with the FIV amplitude inversion.

## 7.1.4 Finger Transfer Function and tactile rendering

The Transfer Function of the overall system consisting of the PIEZOTACT device and the user's finger is the basis of the developed texture rendering methodology. The finger of each user of the device has different mechanical characteristics, size, skin moisture, compliance, etc. Moreover, the contact nonlinearities affect the finger dynamics as a function of the contact boundary conditions. It is therefore essential to study the dynamic response of the finger to the contact excitation and the overall dynamic Transfer Function of the overall finger and device system. In the first instance, the dynamic response (Transfer Function) of the human finger alone has been characterised by means of a dynamic exciter (shaker) delivering a random signal in the frequency range of interest of touch (between 0 and 1 kHz). Then, the overall Transfer Function (PIEZOTACT device + finger) has been characterized. Parametric analyses have been carried out on groups of volunteers by varying different contact parameters between the finger and the vibrating surface (contact load, angle).

The main outcomes are the following:

- For a single participant:
  - Once the finger/actuator angle is fixed, the gain of the Transfer Function increases as the normal load increases throughout the interested frequency range.
  - Once the finger/actuator contact load is fixed, the shape of the Transfer Function changes slightly as the angle between the finger and the actuator changes, without a well-defined trend. However, the changes in the Transfer Function shape and gain are negligible.
- When comparing different participants with the same contact boundary conditions (load, angle):
  - The Transfer Functions present a similar trend for all the subjects and form a bundle of curves of few dB of deviation.
  - The deviation of the bundle of Transfer Functions decreases as the contact load increases.

An average Transfer Function has been computed among participants to subsequently process FIV and then perform a discrimination campaign on isotropic textures, both with the real and the simulated textures. The performance of the volunteers in the discrimination campaign with the averaged Transfer Function turned out to be good and comparable with respect to the campaign performed using the specific finger Transfer Functions of each individual participant.

This, in addition to the basic understanding related to the dynamics of the finger in the finger/device coupling, makes the developed rendering technology more versatile, getting rid of the need to recharacterize the Transfer Function for each user of the device.

The approach will be validated on other types of textures in future works.

## 7.1.5 Spot into brain response to tactile mechanical stimuli

A multidisciplinary experimental campaign has been carried out thanks to the collaboration between the LNC (Laboratory of Cognitive Neuroscience) of the Aix-Marseille University (France), the DIMA (Department of Mechanical and Aerospace Engineering) of the Sapienza University of Rome (Italy), the LaMCoS Laboratory (Laboratory of Contacts and Structures Mechanics) of the INSA of Lyon (France), the LEAD (Learning and Development Studies Laboratory) Laboratory of the University of Bourgogne (France), and the FEMTO-ST Institute of Besançon (France), in the framework of the ANR CONTACT project [1], which aimed to reconstruct the overall process of tactile perception, beginning with surface texture, progressing through mechanical stimuli, their associated perception and the brain's response.

The study aimed to investigate the role of the exploration movement or the motor imagery on the sensory processing of touch. The PIEZOTACT device has been here exploited to provide the tactile feedback.

The main outcomes are resumed in the following:

- From a neuroscience point of view (LNC Laboratory), it has been found that motor imagery associated to tactile feedback approaches the condition of natural touch; in fact, attenuation phenomena, in general associated with the preparation of the movement, occur as well when the tactile stimuli are provided in a motionless contact but with motor imagery. When dealing with the sole tactile feedback, without movement and without imagery of movement, no attenuation occurs [109], [110].
- From an overall point of view, better discrimination performances were achieved by the participants when engaging mental imagery than when dealing with the sole tactile feedback; nevertheless, the discrimination errors could be more easily related to the features of the FIV spectra when dealing with the sole feedback by the PIEZOTACT, without mental imagery.

This study highlights how tactile devices such as PIEZOTACT can be very useful tools not only from the point of view of direct applications, but as well for investigating the overall touch chain, from the mechanical stimuli arising from the surface, up to the brain response and the perception.

From a neuroscience point of view, the questions this study aim to investigate are fundamental not only for basic understanding on the tactile mechanisms but also for applications that seek to use motor imagery in neurorehabilitation and even for the recovery of motor function after a stroke [132], [133].

## 7.2 Future works

---

Relating to the development of a tactile rendering device of textures by FIV stimuli, several perspectives are open for future works. In the first instance, despite the use of a specific electro-active polymer actuator in this Ph.D. thesis, different versions of the device are under development with different dynamic actuators.

In particular, a new version of the PIEZOTACT device with a larger active surface is under development. This would make it possible to mimic the movement of tactile exploration on the surface of the device during the reproduction of the FIV signal, introducing proprioception and sensory attenuation.

Moreover, it would be possible to implement a system for monitoring the kinematics of the finger during exploration, both during the measurement of the mechanical stimuli by active touch, and during the movement of the finger on the larger surface of the device. It would therefore be possible to return the stimuli in an active way, modifying them in real time according to force, speed, direction, etc.

In the future, the device (or other versions of the device) will be exploited to continue investigating the role of FIV features in tactile perception, with the same philosophy. Campaigns will be conducted in future works on larger groups of participants and on different types of textures, isotropic, periodic, textiles, common objects, etc. involving analyses, reproduction, and discrimination of tactile FIV stimuli. The physiochemistry of the finger will be considered as well, to have a more global view of the variability of stimuli ad perception for different subjects.

In a longer time perspective, the hope is to be able to couple different tactile feedback based on different mechanical signals, such as vibrations, friction, forces, temperature, to deepen the understanding and artificially recreate the tactile sensation in its entirety. This could only be achieved passing through the understanding of the complex phenomena involved in touch.



# References

---

- [1] ““ANR CONTACT” Project, ANR 2020-CE28-0010-03, funded by the “Agence Nationale de la Recherche” (France).’ [Online]. Available: <https://anr.fr/Projet-ANR-20-CE28-0010>
- [2] ‘Group de Recherche (GDR) “TACT: Le Toucher, Analyse, Connaissance, simulaTion”, Workgroup’. [Online]. Available: <https://www.gdr.tact.uha.fr/>
- [3] A. G. Guyton, “*Trattato di fisiologia medica*”, translated by A. Curatolo, Padova, Italia, Piccin Editore, 1978, pp. 572-591.
- [4] S. J. Lederman and R. L. Klatzky, ‘Haptic perception: A tutorial’, *Atten. Percept. Psychophys.*, vol. 71, no. 7, pp. 1439–1459, Oct. 2009, doi: 10.3758/APP.71.7.1439.
- [5] D. Purves *et al.*, ‘Mechanoreceptors Specialized to Receive Tactile Information’, in *Neuroscience. 2nd edition*, Sinauer Associates, 2001. Accessed: Oct. 05, 2023. [Online]. Available: <https://www.ncbi.nlm.nih.gov/books/NBK10895/>
- [6] V. Massimiani, B. Weiland, E. Chatelet, P.-H. Cornuault, J. Faucheu, and F. Massi, ‘The role of mechanical stimuli on hedonistic and topographical discrimination of textures’, *Tribol. Int.*, vol. 143, p. 106082, Mar. 2020, doi: 10.1016/j.triboint.2019.106082.
- [7] J. J. Gibson, ‘Observations on active touch’, *Psychol. Rev.*, vol. 69, no. 6, pp. 477–491, 1962, doi: 10.1037/h0046962.
- [8] A. S. Schwartz, A. J. Perey, and A. Azulay, ‘Further analysis of active and passive touch in pattern discrimination’, *Bull. Psychon. Soc.*, vol. 6, no. 1, pp. 7–9, Jul. 1975, doi: 10.3758/BF03333128.
- [9] G. D. Lamb, ‘Tactile discrimination of textured surfaces: psychophysical performance measurements in humans’, *J. Physiol.*, vol. 338, pp. 551–565, May 1983, doi: 10.1113/jphysiol.1983.sp014689.
- [10] S. J. Lederman and R. L. Klatzky, ‘Hand movements: A window into haptic object recognition’, *Cognit. Psychol.*, vol. 19, no. 3, pp. 342–368, Jul. 1987, doi: 10.1016/0010-0285(87)90008-9.
- [11] R. L. Klatzky and S. J. Lederman, ‘Stages of manual exploration in haptic object identification’, *Percept. Psychophys.*, vol. 52, no. 6, pp. 661–670, Nov. 1992, doi: 10.3758/BF03211702.
- [12] R. L. Klatzky and S. Lederman, ‘Intelligent Exploration by the Human Hand’, in *Dextrous Robot Hands*, S. T. Venkataraman and T. Iberall, Eds., New York, NY: Springer, 1990, pp. 66–81. doi: 10.1007/978-1-4613-8974-3\_4.
- [13] A. Lezkan and K. Drewing, ‘Interdependences between finger movement direction and haptic perception of oriented textures’, *PLOS ONE*, vol. 13, no. 12, p. e0208988, Dec. 2018, doi: 10.1371/journal.pone.0208988.
- [14] T. Callier, H. P. Saal, E. C. Davis-Berg, and S. J. Bensmaia, ‘Kinematics of unconstrained tactile texture exploration’, *J. Neurophysiol.*, vol. 113, no. 7, pp. 3013–3020, Apr. 2015, doi: 10.1152/jn.00703.2014.
- [15] T. Yokosaka, S. Kuroki, J. Watanabe, and S. Nishida, ‘Linkage between Free Exploratory Movements and Subjective Tactile Ratings’, *IEEE Trans. Haptics*, vol. 10, no. 2, pp. 217–225, Apr. 2017, doi: 10.1109/TOH.2016.2613055.
- [16] L. Kaim and K. Drewing, ‘Exploratory Strategies in Haptic Softness Discrimination Are Tuned to Achieve High Levels of Task Performance’, *IEEE Trans. Haptics*, vol. 4, no. 4, pp. 242–252, Oct. 2011, doi: 10.1109/TOH.2011.19.

- [17] ‘Perceptual Constancy of Texture Roughness in the Tactile System | Journal of Neuroscience’. Accessed: Oct. 11, 2023. [Online]. Available: <https://www.jneurosci.org/content/31/48/17603>
- [18] D. Katz, ‘The world of touch’, L. Erlbaum, 1989.
- [19] M. Hollins and S. R. Risner, ‘Evidence for the duplex theory of tactile texture perception’, *Percept. Psychophys.*, vol. 62, no. 4, pp. 695–705, Jan. 2000, doi: 10.3758/BF03206916.
- [20] J. Scheibert, S. Leurent, A. Prevost, and G. Debrégeas, ‘The Role of Fingerprints in the Coding of Tactile Information Probed with a Biomimetic Sensor’, *Science*, vol. 323, no. 5920, pp. 1503–1506, Mar. 2009, doi: 10.1126/science.1166467.
- [21] R. Fagiani, F. Massi, E. Chatelet, Y. Berthier, and A. Akay, ‘Tactile perception by friction induced vibrations’, *Tribol. Int.*, vol. 44, no. 10, pp. 1100–1110, Sep. 2011, doi: 10.1016/j.triboint.2011.03.019.
- [22] R. Fagiani, F. Massi, E. Chatelet, J. P. Costes, and Y. Berthier, ‘Contact of a Finger on Rigid Surfaces and Textiles: Friction Coefficient and Induced Vibrations’, *Tribol. Lett.*, vol. 48, no. 2, pp. 145–158, Nov. 2012, doi: 10.1007/s11249-012-0010-0.
- [23] R. Fagiani, F. Massi, E. Chatelet, Y. Berthier, and A. Sestieri, ‘Experimental analysis of friction-induced vibrations at the finger contact surface’, *Proc. Inst. Mech. Eng. Part J J. Eng. Tribol.*, vol. 224, no. 9, pp. 1027–1035, Sep. 2010, doi: 10.1243/13506501JET722.
- [24] J. Dacleu Ndengue *et al.*, ‘Tactile Perception and Friction-Induced Vibrations: Discrimination of Similarly Patterned Wood-Like Surfaces’, *IEEE Trans. Haptics*, vol. 10, no. 3, pp. 409–417, Jul. 2017, doi: 10.1109/TOH.2016.2643662.
- [25] M. D. Di Bartolomeo, F. Morelli, D. Tonazzi, F. Massi, and Y. Berthier, ‘Investigation of the role of contact-induced vibrations in tactile discrimination of textures’, *Mech. Ind.*, vol. 18, no. 4, Art. no. 4, 2017, doi: 10.1051/meca/2017027.
- [26] G. Lacerra, M. Di Bartolomeo, S. Milana, L. Baillet, E. Chatelet, and F. Massi, ‘Validation of a new frictional law for simulating friction-induced vibrations of rough surfaces’, *Tribol. Int.*, vol. 121, pp. 468–480, May 2018, doi: 10.1016/j.triboint.2018.01.052.
- [27] D. Tonazzi, F. Massi, L. Baillet, J. Brunetti, and Y. Berthier, ‘Interaction between contact behaviour and vibrational response for dry contact system’, *Mech. Syst. Signal Process.*, vol. 110, pp. 110–121, Sep. 2018, doi: 10.1016/j.ymsp.2018.03.020.
- [28] D. Tonazzi, M. Passafiume, A. Papangelo, N. Hoffmann, and F. Massi, ‘Numerical and experimental analysis of the bi-stable state for frictional continuous system’, *Nonlinear Dyn.*, vol. 102, no. 3, pp. 1361–1374, Nov. 2020, doi: 10.1007/s11071-020-05983-y.
- [29] A. Lazzari, D. Tonazzi, J. Brunetti, A. Saulot, and F. Massi, ‘Contact instability identification by phase shift on C/C friction materials’, *Mech. Syst. Signal Process.*, vol. 171, p. 108902, May 2022, doi: 10.1016/j.ymsp.2022.108902.
- [30] M. Di Bartolomeo, A. Lazzari, M. Stender, Y. Berthier, A. Saulot, and F. Massi, ‘Experimental observation of thermally-driven frictional instabilities on C/C materials’, *Tribol. Int.*, vol. 154, p. 106724, Feb. 2021, doi: 10.1016/j.triboint.2020.106724.
- [31] A. Lazzari, D. Tonazzi, and F. Massi, ‘Squeal propensity characterization of brake lining materials through friction noise measurements’, *Mech. Syst. Signal Process.*, vol. 128, pp. 216–228, Aug. 2019, doi: 10.1016/j.ymsp.2019.03.034.

- [32] I. Ghezzi, D. Tonazzi, M. Rovere, C. Le Coeur, Y. Berthier, and F. Massi, ‘Frictional behaviour of a greased contact under low sliding velocity condition’, *Tribol. Int.*, vol. 155, p. 106788, Mar. 2021, doi: 10.1016/j.triboint.2020.106788.
- [33] I. Ghezzi, D. Tonazzi, M. Rovere, C. Le Coeur, Y. Berthier, and F. Massi, ‘Tribological investigation of a greased contact subjected to contact dynamic instability’, *Tribol. Int.*, vol. 143, p. 106085, Mar. 2020, doi: 10.1016/j.triboint.2019.106085.
- [34] S. Bensmaïa and M. Hollins, ‘Pacini representations of fine surface texture’, *Percept. Psychophys.*, vol. 67, no. 5, pp. 842–854, Jul. 2005, doi: 10.3758/BF03193537.
- [35] S. J. Bensmaïa and M. Hollins, ‘The vibrations of texture’, *Somatosens. Mot. Res.*, vol. 20, no. 1, pp. 33–43, Jan. 2003, doi: 10.1080/0899022031000083825.
- [36] I. Cesini, J. D. Ndengue, E. Chatelet, J. Faucheu, and F. Massi, ‘Correlation between friction-induced vibrations and tactile perception during exploration tasks of isotropic and periodic textures’, *Tribol. Int.*, vol. 120, pp. 330–339, Apr. 2018, doi: 10.1016/j.triboint.2017.12.041.
- [37] J. Hu, X. Zhang, X. Yang, R. Jiang, X. Ding, and R. Wang, ‘Analysis of fingertip/fabric friction-induced vibration signals toward vibrotactile rendering’, *J. Text. Inst.*, vol. 107, no. 8, pp. 967–975, Aug. 2016, doi: 10.1080/00405000.2015.1077011.
- [38] C. M. Greenspon, K. R. McLellan, J. D. Lieber, and S. J. Bensmaïa, ‘Effect of scanning speed on texture-elicited vibrations’, *J. R. Soc. Interface*, vol. 17, no. 167, p. 20190892, Jun. 2020, doi: 10.1098/rsif.2019.0892.
- [39] B. Delhaye, V. Hayward, P. Lefèvre, and J.-L. Thonnard, ‘Texture-induced vibrations in the forearm during tactile exploration’, *Front. Behav. Neurosci.*, vol. 6, p. 37, 2012, doi: 10.3389/fnbeh.2012.00037.
- [40] R. Jiang, J. Hu, X. Yang, and X. Ding, ‘Analysis of fingertip/textile friction-induced vibration by time-frequency method’, *Fibers Polym.*, vol. 17, no. 4, pp. 630–636, Apr. 2016, doi: 10.1007/s12221-016-5913-1.
- [41] X. Zhou *et al.*, ‘Effect of Finger Sliding Direction on Tactile Perception, Friction and Dynamics’, *Tribol. Lett.*, vol. 68, Aug. 2020, doi: 10.1007/s11249-020-01325-6.
- [42] L. R. Manfredi *et al.*, ‘Natural scenes in tactile texture’, *J. Neurophysiol.*, vol. 111, no. 9, pp. 1792–1802, May 2014, doi: 10.1152/jn.00680.2013.
- [43] A. Prevost, J. Scheibert, and G. Debrégeas, ‘Effect of fingerprints orientation on skin vibrations during tactile exploration of textured surfaces’, *Commun. Integr. Biol.*, vol. 2, no. 5, pp. 422–424, Sep. 2009, doi: 10.4161/cib.2.5.9052.
- [44] İ. M. Koç and C. Aksu, ‘Tactile sensing of constructional differences in fabrics with a polymeric finger tip’, *Tribol. Int.*, vol. 59, pp. 339–349, Mar. 2013, doi: 10.1016/j.triboint.2012.04.021.
- [45] X. Zhou *et al.*, ‘Correlation between tactile perception and tribological and dynamical properties for human finger under different sliding speeds’, *Tribol. Int.*, vol. 123, pp. 286–295, Jul. 2018, doi: 10.1016/j.triboint.2018.03.012.
- [46] S. Ding, Y. Pan, and X. Zhao, ‘Humanoid Identification of Fabric Material Properties by Vibration Spectrum Analysis’, *Sensors*, vol. 18, no. 6, Art. no. 6, Jun. 2018, doi: 10.3390/s18061820.
- [47] B. Camillieri and M.-A. Bueno, ‘Influence of Finger Movement Direction and fingerprints Orientation on Friction and Induced Vibrations with Textile Fabrics’, *Tribol. Lett.*, vol. 69, no. 4, p. 143, Sep. 2021, doi: 10.1007/s11249-021-01517-8.
- [48] M. Natsume, Y. Tanaka, and A. Sano, ‘Skin-propagated vibration for roughness and textures’, in *2016 World Automation Congress (WAC)*, Jul. 2016, pp. 1–6. doi: 10.1109/WAC.2016.7583001.



- [49] S. Ding, Y. Pan, M. Tong, and X. Zhao, ‘Tactile Perception of Roughness and Hardness to Discriminate Materials by Friction-Induced Vibration’, *Sensors*, vol. 17, no. 12, Art. no. 12, Dec. 2017, doi: 10.3390/s17122748.
- [50] J. Faucheu, B. Weiland, M. Juganaru-Mathieu, A. Witt, and P.-H. Cornuault, ‘Tactile aesthetics: Textures that we like or hate to touch’, *Acta Psychol. (Amst.)*, vol. 201, p. 102950, Oct. 2019, doi: 10.1016/j.actpsy.2019.102950.
- [51] R. Sahli *et al.*, ‘Tactile perception of randomly rough surfaces’, *Sci. Rep.*, vol. 10, no. 1, Art. no. 1, Sep. 2020, doi: 10.1038/s41598-020-72890-y.
- [52] G. P. Chimata and C. J. Schwartz, ‘Tactile Discrimination of Randomly Textured Surfaces: Effect of Friction and Surface Parameters’, *Biotribology*, vol. 11, pp. 102–109, Sep. 2017, doi: 10.1016/j.biotri.2017.01.004.
- [53] M. Natsume, Y. Tanaka, and A. M. L. Kappers, ‘Individual differences in cognitive processing for roughness rating of fine and coarse textures’, *PLOS ONE*, vol. 14, no. 1, p. e0211407, Jan. 2019, doi: 10.1371/journal.pone.0211407.
- [54] N. Özgün, D. J. Strauss, and R. Bennewitz, ‘Tribology of a Braille Display and EEG Correlates’, *Tribol. Lett.*, vol. 66, no. 1, p. 16, Dec. 2017, doi: 10.1007/s11249-017-0969-7.
- [55] B. Camillieri, M.-A. Bueno, M. Fabre, B. Juan, B. Lemaire-Semail, and L. Mouchnino, ‘From finger friction and induced vibrations to brain activation: Tactile comparison between real and virtual textile fabrics’, *Tribol. Int.*, vol. 126, pp. 283–296, Oct. 2018, doi: 10.1016/j.triboint.2018.05.031.
- [56] K. Peyre, M. Tournalias, M.-A. Bueno, F. Spano, and R. M. Rossi, ‘Tactile perception of textile surfaces from an artificial finger instrumented by a polymeric optical fibre’, *Tribol. Int.*, vol. 130, pp. 155–169, Feb. 2019, doi: 10.1016/j.triboint.2018.09.017.
- [57] P.-H. Cornuault, L. Carpentier, M.-A. Bueno, J.-M. Cote, and G. Monteil, ‘Influence of physico-chemical, mechanical and morphological fingerpad properties on the frictional distinction of sticky/slippery surfaces’, *J. R. Soc. Interface*, vol. 12, no. 110, p. 20150495, Sep. 2015, doi: 10.1098/rsif.2015.0495.
- [58] D. Gueorguiev, E. Vezzoli, A. Mouraux, B. Lemaire-Semail, and J.-L. Thonnard, ‘The tactile perception of transient changes in friction’, *J. R. Soc. Interface*, vol. 14, no. 137, p. 20170641, Dec. 2017, doi: 10.1098/rsif.2017.0641.
- [59] W. B. Messaoud, M.-A. Bueno, and B. Lemaire-Semail, ‘Relation between human perceived friction and finger friction characteristics’, *Tribol. Int.*, vol. 98, pp. 261–269, Jun. 2016, doi: 10.1016/j.triboint.2016.02.031.
- [60] D. A. Torres *et al.*, ‘PCA Model of Fundamental Acoustic Finger Force for Out-of-Plane Ultrasonic Vibration and its Correlation with Friction Reduction’, *IEEE Trans. Haptics*, vol. 14, no. 3, pp. 551–563, 2021, doi: 10.1109/TOH.2021.3060108.
- [61] L. Skedung *et al.*, ‘Mechanisms of tactile sensory deterioration amongst the elderly’, *Sci. Rep.*, vol. 8, no. 1, Art. no. 1, Apr. 2018, doi: 10.1038/s41598-018-23688-6.
- [62] C. Basdogan, F. Giraud, V. Levesque, and S. Choi, ‘A Review of Surface Haptics: Enabling Tactile Effects on Touch Surfaces’, *IEEE Trans. Haptics*, vol. 13, no. 3, pp. 450–470, Jul. 2020, doi: 10.1109/TOH.2020.2990712.
- [63] S. Choi and K. J. Kuchenbecker, ‘Vibrotactile Display: Perception, Technology, and Applications’, *Proc. IEEE*, vol. 101, no. 9, pp. 2093–2104, Sep. 2013, doi: 10.1109/JPROC.2012.2221071.

- [64] A. Costes, F. Danieau, F. Argelaguet, P. Guillotel, and A. Lécuyer, ‘Towards Haptic Images: A Survey on Touchscreen-Based Surface Haptics’, *IEEE Trans. Haptics*, vol. 13, no. 3, pp. 530–541, Jul. 2020, doi: 10.1109/TOH.2020.2984754.
- [65] L. A. Jones and N. B. Sarter, ‘Tactile Displays: Guidance for Their Design and Application’, *Hum. Factors*, vol. 50, no. 1, pp. 90–111, Feb. 2008, doi: 10.1518/001872008X250638.
- [66] R. H. Osgouei, ‘Electrostatic Friction Displays to Enhance Touchscreen Experience’, in *Modern Applications of Electrostatics and Dielectrics*, IntechOpen, 2020. doi: 10.5772/intechopen.91056.
- [67] J. M. Romano and K. J. Kuchenbecker, ‘Creating Realistic Virtual Textures from Contact Acceleration Data’, *IEEE Trans. Haptics*, vol. 5, no. 2, pp. 109–119, Jun. 2012, doi: 10.1109/TOH.2011.38.
- [68] H. Culbertson, J. Unwin, and K. J. Kuchenbecker, ‘Modeling and Rendering Realistic Textures from Unconstrained Tool-Surface Interactions’, *IEEE Trans. Haptics*, vol. 7, no. 3, pp. 381–393, Sep. 2014, doi: 10.1109/TOH.2014.2316797.
- [69] A. Abdulali and S. Jeon, ‘Data-Driven Rendering of Anisotropic Haptic Textures’, in *Haptic Interaction*, S. Hasegawa, M. Konyo, K.-U. Kyung, T. Nojima, and H. Kajimoto, Eds., in *Lecture Notes in Electrical Engineering*. Singapore: Springer, 2018, pp. 401–407. doi: 10.1007/978-981-10-4157-0\_67.
- [70] A. M. Okamura, J. T. Dennerlein, and R. D. Howe, ‘Vibration feedback models for virtual environments’, in *Proceedings. 1998 IEEE International Conference on Robotics and Automation (Cat. No.98CH36146)*, May 1998, pp. 674–679 vol.1. doi: 10.1109/ROBOT.1998.677050.
- [71] S. Shin, R. H. Osgouei, K. -D. Kim, and S. Choi, ‘Data-driven modeling of isotropic haptic textures using frequency-decomposed neural networks’, in *2015 IEEE World Haptics Conference (WHC)*, Jun. 2015, pp. 131–138. doi: 10.1109/WHC.2015.7177703.
- [72] P. Strohmeier and K. Hornbæk, ‘Generating Haptic Textures with a Vibrotactile Actuator’, in *Proceedings of the 2017 CHI Conference on Human Factors in Computing Systems*, in CHI ’17. New York, NY, USA: Association for Computing Machinery, May 2017, pp. 4994–5005. doi: 10.1145/3025453.3025812.
- [73] S. Asano, S. Okamoto, Y. Matsuura, H. Nagano, and Y. Yamada, ‘Vibrotactile display approach that modifies roughness sensations of real textures’, in *2012 IEEE ROMAN: The 21st IEEE International Symposium on Robot and Human Interactive Communication*, Sep. 2012, pp. 1001–1006. doi: 10.1109/ROMAN.2012.6343880.
- [74] V. L. Guruswamy, J. Lang, and W.-S. Lee, ‘IIR Filter Models of Haptic Vibration Textures’, *IEEE Trans. Instrum. Meas.*, vol. 60, no. 1, pp. 93–103, Jan. 2011, doi: 10.1109/TIM.2010.2065751.
- [75] J. Jiao *et al.*, ‘Data-driven rendering of fabric textures on electrostatic tactile displays’, in *2018 IEEE Haptics Symposium (HAPTICS)*, Mar. 2018, pp. 169–174. doi: 10.1109/HAPTICS.2018.8357171.
- [76] R. H. Osgouei, J. R. Kim, and S. Choi, ‘Data-Driven Texture Modeling and Rendering on Electrostatic Display’, *IEEE Trans. Haptics*, vol. 13, no. 2, pp. 298–311, Jun. 2020, doi: 10.1109/TOH.2019.2932990.
- [77] R. H. Osgouei, S. Shin, J. R. Kim, and S. Choi, ‘An inverse neural network model for data-driven texture rendering on electrostatic display’, in *2018 IEEE Haptics Symposium (HAPTICS)*, Mar. 2018, pp. 270–277. doi: 10.1109/HAPTICS.2018.8357187.

- [78] S. Rasool and A. Sourin, ‘Image-Driven Haptic Rendering in Virtual Environments’, in *2013 International Conference on Cyberworlds*, Oct. 2013, pp. 286–293. doi: 10.1109/CW.2013.28.
- [79] S. Wu, X. Sun, Q. Wang, and J. Chen, ‘Tactile modeling and rendering image-textures based on electrovibration’, *Vis. Comput.*, vol. 33, no. 5, pp. 637–646, May 2017, doi: 10.1007/s00371-016-1214-3.
- [80] O. Bau, I. Poupyrev, A. Israr, and C. Harrison, ‘TeslaTouch: electrovibration for touch surfaces’, in *Proceedings of the 23rd annual ACM symposium on User interface software and technology*, in *UIST ’10*. New York, NY, USA: Association for Computing Machinery, Oct. 2010, pp. 283–292. doi: 10.1145/1866029.1866074.
- [81] T. Vodlak, Z. Vidrih, E. Vezzoli, B. Lemaire-Semail, and D. Peric, ‘Multi-physics modelling and experimental validation of electrovibration based haptic devices’, *Biotribology*, vol. 8, pp. 12–25, Dec. 2016, doi: 10.1016/j.biotri.2016.09.001.
- [82] T. Fiedler and Y. Vardar, ‘A Novel Texture Rendering Approach for Electrostatic Displays’, in *International Workshop on Haptic and Audio Interaction Design - HAID2019*, Lille, France, Mar. 2019. Accessed: Oct. 20, 2023. [Online]. Available: <https://hal.science/hal-02011782>
- [83] M.-A. Bueno, B. Lemaire-Semail, M. Amberg, and F. Giraud, ‘A simulation from a tactile device to render the touch of textile fabrics: a preliminary study on velvet’, *Text. Res. J.*, vol. 84, no. 13, pp. 1428–1440, Aug. 2014, doi: 10.1177/0040517514521116.
- [84] T. Watanabe and S. Fukui, ‘A method for controlling tactile sensation of surface roughness using ultrasonic vibration’, in *Proceedings of 1995 IEEE International Conference on Robotics and Automation*, May 1995, pp. 1134–1139 vol.1. doi: 10.1109/ROBOT.1995.525433.
- [85] M. Wiertelwski, R. Fenton Friesen, and J. E. Colgate, ‘Partial squeeze film levitation modulates fingertip friction’, *Proc. Natl. Acad. Sci.*, vol. 113, no. 33, pp. 9210–9215, Aug. 2016, doi: 10.1073/pnas.1603908113.
- [86] M. Wiertelwski, D. Leonardis, D. J. Meyer, M. A. Peshkin, and J. E. Colgate, ‘A High-Fidelity Surface-Haptic Device for Texture Rendering on Bare Finger’, in *Haptics: Neuroscience, Devices, Modeling, and Applications*, M. Auvray and C. Duriez, Eds., in *Lecture Notes in Computer Science*. Berlin, Heidelberg: Springer, 2014, pp. 241–248. doi: 10.1007/978-3-662-44196-1\_30.
- [87] G. Liu, C. Zhang, and X. Sun, ‘Tri-Modal Tactile Display and Its Application Into Tactile Perception of Visualized Surfaces’, *IEEE Trans. Haptics*, vol. 13, no. 4, pp. 733–744, Dec. 2020, doi: 10.1109/TOH.2020.2979182.
- [88] H. Culbertson and K. J. Kuchenbecker, ‘Importance of Matching Physical Friction, Hardness, and Texture in Creating Realistic Haptic Virtual Surfaces’, *IEEE Trans. Haptics*, vol. 10, no. 1, pp. 63–74, Mar. 2017, doi: 10.1109/TOH.2016.2598751.
- [89] S. Ryu, D. Pyo, S.-C. Lim, and D.-S. Kwon, ‘Mechanical Vibration Influences the Perception of Electro vibration’, *Sci. Rep.*, vol. 8, no. 1, Art. no. 1, Mar. 2018, doi: 10.1038/s41598-018-22865-x.
- [90] S. Shin and S. Choi, ‘Effects of haptic texture rendering modalities on realism’, in *Proceedings of the 24th ACM Symposium on Virtual Reality Software and Technology*, in *VRST ’18*. New York, NY, USA: Association for Computing Machinery, Nov. 2018, pp. 1–5. doi: 10.1145/3281505.3281520.
- [91] J. Jiao, Y. Zhang, D. Wang, X. Guo, and X. Sun, ‘HapTex: A Database of Fabric Textures for Surface Tactile Display’, in *2019 IEEE World Haptics Conference (WHC)*, Jul. 2019, pp. 331–336. doi: 10.1109/WHC.2019.8816167.

- [92] H. Culbertson, J. J. López Delgado, and K. J. Kuchenbecker, ‘One hundred data-driven haptic texture models and open-source methods for rendering on 3D objects’, in *2014 IEEE Haptics Symposium (HAPTICS)*, Feb. 2014, pp. 319–325. doi: 10.1109/HAPTICS.2014.6775475.
- [93] M. Strese, J.-Y. Lee, C. Schuwerk, Q. Han, H.-G. Kim, and E. Steinbach, ‘A haptic texture database for tool-mediated texture recognition and classification’, in *2014 IEEE International Symposium on Haptic, Audio and Visual Environments and Games (HAVE) Proceedings*, Oct. 2014, pp. 118–123. doi: 10.1109/HAVE.2014.6954342.
- [94] L. Knez, J. Slavič, and M. Boltežar, ‘A Sequential Approach to the Biodynamic Modeling of a Human Finger’, *Shock Vib.*, vol. 2017, p. e8791406, Aug. 2017, doi: 10.1155/2017/8791406.
- [95] D. L. Jindrich, Y. Zhou, T. Becker, and J. T. Dennerlein, ‘Non-linear viscoelastic models predict fingertip pulp force-displacement characteristics during voluntary tapping’, *J. Biomech.*, vol. 36, no. 4, pp. 497–503, Apr. 2003, doi: 10.1016/S0021-9290(02)00438-4.
- [96] S. Sato, S. Okamoto, Y. Matsuura, and Y. Yamada, ‘Wearable finger pad deformation sensor for tactile textures in frequency domain by using accelerometer on finger side’, *ROBOMECH J.*, vol. 4, no. 1, p. 19, Aug. 2017, doi: 10.1186/s40648-017-0087-1.
- [97] C. Basdogan, M. R. A. Sormoli, and O. Sirin, ‘Modeling Sliding Friction Between Human Finger and Touchscreen Under Electroadhesion’, *IEEE Trans. Haptics*, vol. 13, no. 3, pp. 511–521, Sep. 2020, doi: 10.1109/TOH.2020.2989221.
- [98] L. Felicetti, E. Chatelet, A. Latour, P.-H. Cornuault, and F. Massi, ‘Tactile rendering of textures by an Electro-Active Polymer piezoelectric device: mimicking Friction-Induced Vibrations’, *Biotribology*, vol. 31, p. 100211, Sep. 2022, doi: 10.1016/j.biotri.2022.100211.
- [99] L. Felicetti, C. Sutter, E. Chatelet, A. Latour, L. Mouchnino, and F. Massi, ‘Tactile discrimination of real and simulated isotropic textures by Friction-Induced Vibrations’, *Tribol. Int.*, vol. 184, p. 108443, Jun. 2023, doi: 10.1016/j.triboint.2023.108443.
- [100] L. Felicetti, E. Chatelet, B. Bou-Saïd, A. Latour, and F. Massi, ‘Investigation on the role of the finger Transfer Function in tactile rendering by Friction-Induced-Vibrations’, *Tribol. Int.*, vol. 190, p. 109018, Dec. 2023, doi: 10.1016/j.triboint.2023.109018.
- [101] L. Felicetti, *Tactile simulation of surface textures from haptic vibrational stimuli with electro-active polymer piezoelectric actuators*, Master Thesis, Sapienza University of Rome. 2020.
- [102] S. J. Lederman and M. M. Taylor, ‘Fingertip force, surface geometry, and the perception of roughness by active touch’, *Percept. Psychophys.*, vol. 12, no. 5, pp. 401–408, Sep. 1972, doi: 10.3758/BF03205850.
- [103] S. Ciprari, V. Ripard, A. Saulot, and F. Massi, ‘Investigation of third body role in dry contacts: Experimental procedure to dissociate the effects of substrate and interface layer on the contact pair frictional response’, *Tribol. Int.*, vol. 190, p. 109047, Dec. 2023, doi: 10.1016/j.triboint.2023.109047.
- [104] N. Godard *et al.*, ‘1-mW Vibration Energy Harvester Based on a Cantilever with Printed Polymer Multilayers’, *Cell Rep. Phys. Sci.*, vol. 1, no. 6, p. 100068, Jun. 2020, doi: 10.1016/j.xcrp.2020.100068.
- [105] P. Poncet *et al.*, ‘Static and Dynamic Studies of Electro-Active Polymer Actuators and Integration in a Demonstrator’, *Actuators*, vol. 6, no. 2, Art. no. 2, Jun. 2017, doi: 10.3390/act6020018.

- [106] P. Poncet *et al.*, ‘Design and realization of electroactive polymer actuators for transparent and flexible haptic feedback interfaces’, in *2016 17th International Conference on Thermal, Mechanical and Multi-Physics Simulation and Experiments in Microelectronics and Microsystems (EuroSimE)*, Apr. 2016, pp. 1–5. doi: 10.1109/EuroSimE.2016.7463310.
- [107] ‘Designing Vibrotactile Widgets with Printed Actuators and Sensors | Adjunct Proceedings of the 30th Annual ACM Symposium on User Interface Software and Technology’. Accessed: Nov. 09, 2023. [Online]. Available: <https://dl.acm.org/doi/abs/10.1145/3131785.3131800>
- [108] P. Avitabile, *Modal Testing: A Practitioner’s Guide*. John Wiley & Sons, 2017.
- [109] C. Sutter *et al.*, ‘Reconnecting mental imagery with our own touch-related feedback alleviates sensory gating’, *UNDER REDACTION*, 2023.
- [110] C. Sutter, *Sous nos pieds le cerveau. Surface biomimétique comme techniques pour agir sur les mécanismes corticaux de contrôle du mouvement et l’équilibre*, Ph.D. Thesis, Aix-Marseille Université. 2024.
- [111] S.-J. Blakemore, D. M. Wolpert, and C. D. Frith, ‘Central cancellation of self-produced tickle sensation’, *Nat. Neurosci.*, vol. 1, no. 7, Art. no. 7, Nov. 1998, doi: 10.1038/2870.
- [112] P. M. Bays, J. R. Flanagan, and D. M. Wolpert, ‘Attenuation of Self-Generated Tactile Sensations Is Predictive, not Postdictive’, *PLOS Biol.*, vol. 4, no. 2, p. e28, Jan. 2006, doi: 10.1371/journal.pbio.0040028.
- [113] P. M. Bays, D. M. Wolpert, and J. R. Flanagan, ‘Perception of the Consequences of Self-Action Is Temporally Tuned and Event Driven’, *Curr. Biol.*, vol. 15, no. 12, pp. 1125–1128, Jun. 2005, doi: 10.1016/j.cub.2005.05.023.
- [114] P. Haggard and B. Whitford, ‘Supplementary motor area provides an efferent signal for sensory suppression’, *Brain Res. Cogn. Brain Res.*, vol. 19, no. 1, pp. 52–58, Mar. 2004, doi: 10.1016/j.cogbrainres.2003.10.018.
- [115] D. M. Wolpert and R. C. Miall, ‘Forward Models for Physiological Motor Control’, *Neural Netw. Off. J. Int. Neural Netw. Soc.*, vol. 9, no. 8, pp. 1265–1279, Nov. 1996, doi: 10.1016/s0893-6080(96)00035-4.
- [116] D. M. Wolpert, Z. Ghahramani, and M. I. Jordan, ‘An internal model for sensorimotor integration’, *Science*, vol. 269, no. 5232, pp. 1880–1882, Sep. 1995, doi: 10.1126/science.7569931.
- [117] D. E. Angelaki and K. E. Cullen, ‘Vestibular system: the many facets of a multimodal sense’, *Annu. Rev. Neurosci.*, vol. 31, pp. 125–150, 2008, doi: 10.1146/annurev.neuro.31.060407.125555.
- [118] E. Fuehrer, D. Voudouris, A. Lezkan, K. Drewing, and K. Fiehler, ‘Tactile suppression stems from specific sensorimotor predictions’, *Proc. Natl. Acad. Sci.*, vol. 119, no. 20, p. e2118445119, May 2022, doi: 10.1073/pnas.2118445119.
- [119] Y. Höller *et al.*, ‘Real movement vs. motor imagery in healthy subjects’, *Int. J. Psychophysiol.*, vol. 87, no. 1, pp. 35–41, Jan. 2013, doi: 10.1016/j.ijpsycho.2012.10.015.
- [120] R. M. Hardwick, S. Caspers, S. B. Eickhoff, and S. P. Swinnen, ‘Neural correlates of action: Comparing meta-analyses of imagery, observation, and execution’, *Neurosci. Biobehav. Rev.*, vol. 94, pp. 31–44, Nov. 2018, doi: 10.1016/j.neubiorev.2018.08.003.
- [121] S. M. Kosslyn, G. Ganis, and W. L. Thompson, ‘Neural foundations of imagery’, *Nat. Rev. Neurosci.*, vol. 2, no. 9, Art. no. 9, Sep. 2001, doi: 10.1038/35090055.

- [122] J. Decety, 'The neurophysiological basis of motor imagery', *Behav. Brain Res.*, vol. 77, no. 1, pp. 45–52, May 1996, doi: 10.1016/0166-4328(95)00225-1.
- [123] K. Kilteni, B. J. Andersson, C. Houborg, and H. H. Ehrsson, 'Motor imagery involves predicting the sensory consequences of the imagined movement', *Nat. Commun.*, vol. 9, no. 1, Art. no. 1, Apr. 2018, doi: 10.1038/s41467-018-03989-0.
- [124] K. Kilteni and H. H. Ehrsson, 'Predictive attenuation of touch and tactile gating are distinct perceptual phenomena', *iScience*, vol. 25, no. 4, p. 104077, Apr. 2022, doi: 10.1016/j.isci.2022.104077.
- [125] Y.-A. Féry, 'Differentiating visual and kinesthetic imagery in mental practice', *Can. J. Exp. Psychol. Rev. Can. Psychol. Exp.*, vol. 57, no. 1, pp. 1–10, Mar. 2003, doi: 10.1037/h0087408.
- [126] C. Sutter, A. Moinon, L. Felicetti, F. Massi, J. Blouin, and L. Mouchnino, 'Cortical facilitation of tactile afferents during the preparation of a body weight transfer when standing on a biomimetic surface', *Front. Neurol.*, vol. 14, 2023, doi: 10.3389/fneur.2023.1175667.
- [127] M. Fabre, P. Sainton, C. Sutter, L. Mouchnino, and P. Chavet, 'Partial Unweighting in Obese Persons Enhances Tactile Transmission From the Periphery to Cortical Areas: Impact on Postural Adjustments', *Front. Hum. Neurosci.*, vol. 16, 2022, doi: 10.3389/fnhum.2022.782028.
- [128] D. Noura, D. Tonazzi, A. Meziane, L. Baillet, and F. Massi, 'Numerical and Experimental Analysis of Nonlinear Vibrational Response due to Pressure-Dependent Interface Stiffness', *Lubricants*, vol. 8, no. 7, Art. no. 7, Jul. 2020, doi: 10.3390/lubricants8070073.
- [129] R. D. Roberts, A. R. Loomes, H. A. Allen, M. Di Luca, and A. M. Wing, 'Contact forces in roughness discrimination', *Sci. Rep.*, vol. 10, no. 1, Art. no. 1, Mar. 2020, doi: 10.1038/s41598-020-61943-x.
- [130] G. Pfurtscheller and A. Aranibar, 'Event-related cortical desynchronization detected by power measurements of scalp EEG', *Electroencephalogr. Clin. Neurophysiol.*, vol. 42, no. 6, pp. 817–826, Jun. 1977, doi: 10.1016/0013-4694(77)90235-8.
- [131] C. Neuper, A. Schlögl, and G. Pfurtscheller, 'Enhancement of left-right sensorimotor EEG differences during feedback-regulated motor imagery', *J. Clin. Neurophysiol. Off. Publ. Am. Electroencephalogr. Soc.*, vol. 16, no. 4, pp. 373–382, Jul. 1999, doi: 10.1097/00004691-199907000-00010.
- [132] A. Pascual-Leone, D. Nguyet, L. G. Cohen, J. P. Brasil-Neto, A. Cammarota, and M. Hallett, 'Modulation of muscle responses evoked by transcranial magnetic stimulation during the acquisition of new fine motor skills', *J. Neurophysiol.*, vol. 74, no. 3, pp. 1037–1045, Sep. 1995, doi: 10.1152/jn.1995.74.3.1037.
- [133] J. A. Stevens and M. E. P. Stoykov, 'Using motor imagery in the rehabilitation of hemiparesis', *Arch. Phys. Med. Rehabil.*, vol. 84, no. 7, pp. 1090–1092, Jul. 2003, doi: 10.1016/s0003-9993(03)00042-x.



# ACKNOWLEDGMENTS

---

This PhD thesis has been carried out in joint supervision by the Department of Mechanical and Aerospace Engineering (DIMA) of the Sapienza University of Rome and the Laboratory of Contacts and Structures Mechanics (LaMCoS) of the National Institute of Applied Sciences (INSA) of Lyon, member of the University of Lyon. First of all, I would like to thank the two institutions, without which this PhD would not have been possible, and the research groups that have supported me in this journey into research.

My most sincere gratitude goes in particular to my PhD supervisors, Francesco Massi, Eric Chatelet, and Benyebka Bou-Saïd, for their immense professional but also human support. Davide Tonazzi deserves my heartfelt gratitude as well.

I sincerely thank all my PhD committee members, and in particular my PhD thesis reviewers, Professor Marie-Ange Bueno and Professor Ilker Murat Koç, for their comments, valuable insights, and constructive exchanges.

A great thank you goes to the members and institutions involved in the ANR CONTACT workgroup, with whom I have had the opportunity and pleasure to collaborate on many occasions, with immense human and professional benefit. A heartfelt thank you goes to the Cognitive Neuroscience Laboratory of the Aix-Marseille University, where I was a guest for our collaboration in the ANR CONTACT project, and in particular to Laurence Mouchnino, Jean Blouin and Chloé Sutter, for their support and supervision, for their hospitality, and for the professional and human enrichment deriving from our collaboration.

I would also like to thank the GDR TACT workgroup, with whom I had the opportunity to collaborate, and which has been an immense source of fruitful exchanges and enrichment within my research topic.

An immense thank you to my family, friends, colleagues, who have supported me in this journey, as well as to all the volunteers who have lent themselves for my experiments, without whom part of this work would not have been possible.

Last but not least, I want to express my most sincere gratitude to the Council of Mechanical Engineering of the DIMA for having providentially rejected my first Master's Degree Planning of Exams in 2018, in which I accurately excluded all the exams concerning the mechanical vibrations and tribology fields. Life is surprising!







## FOLIO ADMINISTRATIF

### THESE DE L'INSA LYON, MEMBRE DE L'UNIVERSITE DE LYON.

NOM : Felicetti

DATE de SOUTENANCE : 19/02/2024

Prénom : Livia

TITRE : Analysis and rendering of contact vibrational stimuli for tactile perception

NATURE : Doctorat

Numéro d'ordre : TH1076

Ecole doctorale : MEGA

Spécialité : Génie Mécanique

RESUME :

Among the 5 senses, the sense of touch is between the most articulated and the least understood. While we are able to master the signals that underlie sight and hearing, rendering them using loudspeakers and visual interfaces, the mechanisms underlying the sense of touch are still largely unknown. Touch, originating by the contact between the skin and the explored surface and involving several types of stimuli, requires a strongly multidisciplinary approach and involves a wide range of disciplines, such as Medicine, Neurosciences, Psychology, Dynamics, Tribology, Materials Sciences, and beyond. Tribology and Dynamics are involved in the study of all those complex phenomena that occur at the contact and that generate mechanical stimuli such as Friction-Induced Vibrations and contact forces, at the origin of the stimulation of skin's mechanoreceptors. This Ph.D. thesis is collocated into a research line closely dedicated to the investigation of the role of Friction-Induced Vibrations (FIV) in mediating between the characteristics of surface textures and the way in which textures are perceived and discriminated. Analyses of vibrational stimuli originating from the exploration of periodic and isotropic textures have been carried out in the present work, revealing different key features in the discrimination of such textures. A tactile rendering device, named PIEZOTACT, has been developed to reproduce/mimic the FIV previously measured during the exploration of real surfaces, conducting as well campaigns on groups of volunteers, to evaluate their ability to discriminate real and simulated textures starting from the sole vibrational tactile stimuli. Finally, a multi-disciplinary collaboration with laboratories from Neurosciences and Psychology has been performed to evaluate the brain's response to the mechanical stimuli generated by the exploration of real and simulated surfaces.

MOTS-CLÉS : Friction-Induced Vibrations, tactile perception, texture rendering device

Laboratoires de recherche :

- Laboratoire de Mécanique de Contact et des Structures (LaMCoS), UMR CNRS 5259-INSA de Lyon, France
- Dipartimento di Ingegneria Meccanica e Aerospaziale (DIMA), Sapienza Università di Roma, Rome, Italy

Directeurs de thèse :

BOU-SAID Benyebka, Professeur des Universités, INSA de Lyon  
MASSI Francesco, Professeur des Universités, Sapienza Università di Roma

Président de jury :

Meziane Anissa, Professeure des Universités, Université de Bordeaux

Composition du jury :

Meziane Anissa, Professeure des Universités, Université de Bordeaux, Président  
Bueno Marie-Ange, Professeure des Universités, Université de Haute-Alsace, Rapporteur  
Koç Ilker Murat, Professeur des Universités, Istanbul Technical University, Rapporteur  
Fregolent Annalisa, Professeure des Universités, Sapienza Università di Roma, Examinatrice  
Mouchnino Laurence, Professeure des Universités, Aix-Marseille Université, Examinatrice  
Chatelet Eric, Maître de Conférences HDR, INSA de Lyon, Examineur  
Bou-Saïd Benyebka, Professeur des Universités, INSA de Lyon, Directeur de thèse  
Massi Francesco, Professeur des Universités, Sapienza Università di Roma, Directeur de thèse  
Akay Adnan, Full Professor Emeritus, Carnegie Mellon University, Invité